Economic Assessment Service

IEA COAL RESEARCH

THE ECONOMICS OF GAS FROM COAL

A report by
Economic Assessment Service
established under the auspices of the
INTERNATIONAL ENERGY AGENCY

EAS Report E2/80
January 1983

ECONOMIC ASSESSMENT SERVICE
Head of Service – A. Baker

14/15 Lower Grosvenor Place,
London SW1W 0EX
England

Telephone: London 828 4661
Telex: 917624

THE ECONOMICS OF GAS FROM COAL

by
M. Teper
D. F. Hemming
W. C. Ulrich

EAS Report E2/80
January 1983

This Report has been produced by the Economic Assessment Service (EAS) of IEA Coal Research.

The expansion of coal as an energy source will require a change in the pattern of coal production, transport and utilisation. This was the reason for the establishment of EAS in 1975. Its purpose is to pursue economic studies that support the development of the international coal industry, and to help in identifying areas in which new research projects should be undertaken. It is one of the four projects that make up IEA Coal Research, together with the Technical Information Service, the World Coal Resources and Reserves Data Bank, and the Mining Technology Clearing House. IEA Coal Research was set up in 1975 under the auspices of the International Energy Agency (IEA) which had itself been founded in 1974 by member countries of the Organisation for Economic Cooperation and Development (OECD).

EAS is supported by twelve countries: Australia, Canada, Denmark, the Federal Republic of Germany, Ireland, Italy, Japan, the Netherlands, Spain, Sweden, the United Kingdom and the United States of America.

This report is based on an EAS survey and analysis of published literature, and on information gathered in discussions with interested organisations and individuals. Their assistance is gratefully acknowledged. It should be understood that the views expressed in this report are our own, and are not necessarily shared by those who supplied the information, nor by our member countries. Any queries or comments should be addressed to the first-named author.

ISBN 92-9029-072-2

ACKNOWLEDGEMENTS

The analysis in this report was carried out using a modification of the Discounted Cash Flow program developed at the Oak Ridge National Laboratory by Royes Salmon.

The data presented on the Texaco process have been derived from process yield data obtained using a development of the ARACHNE computer model of the National Coal Board (UK), with assistance from Peter van Cooten of Dutch State Mines (DSM).

The data presented on the British Gas, Exxon Catalytic and Shell Coal Gasification processes have been derived from information supplied by the relevant process developers.

Many other organisations and individuals have helped us during the preparation of this report and we thank all the above organisations and individuals for their assistance. However the Economic Assessment Service is responsible for the accuracy of calculations produced from the data supplied and for any interpretations made from them.

CONTENTS

CONTENTS (Cont'd)

TABLES

FIGURES

ACRONYMS AND ABBREVIATIONS

AGA	American Gas Association
atm	atmospheres absolute
BCR	Bituminous Coal Research, Inc.
BTU	British Thermal Unit
CO	carbon monoxide
CO_2	carbon dioxide
d	day
DCF	discounted cash-flow
DM	Deutsche Mark
DOE	Dept. of Energy
DSM	Dutch State Mines
EAS	Economic Assessment Service
EMR	Energy, Mines and Resources, Canada
EPRI	Electric Power Research Institute
ERDA	US Energy Research & Development Administration (currently US DOE)
Gcal	giga (10^9) calories
GJ	giga (10^9) joules
GRI	Gas Research Institute
h	hour
HCM	High Carbon Monoxide process (British Gas combined shift-methanation process)
H_2	hydrogen
HHV	higher heating value
IDC	interest during construction
IEA	International Energy Agency
IFP	Institut Français du Pétrole
IGT	Institute of Gas Technology
kcal	kilo (10^3) calories
LNG	liquefied natural gas
kWh	kilowatt-hour electrical
LNG	liquefied natural gas
m^3	cubic metre
maf	moisture and ash-free

ACRONYMS AND ABBREVIATIONS (cont'd)

MCG	medium calorific value gas (10-16 MJ/Nm^3 or 250-400 BTU/SCF)
MJ	mega (10^6) joules
MWe	megawatts electrical
MWt	megawatts thermal
NEDO	National Economic Development Office (UK)
Nm^3	normal cubic metres of gas measured at 0°C and 760 mm Hg absolute pressure.
PG & E	Pacific Gas & Electric Company
PJ	Peta (10^{15}) joules
ppm	parts per million
SCF	standard cubic feet of gas measured at 60°F and 760 mm Hg absolute pressure.
SCF/d	SCF per stream day
SD	stream day
SNG	substitute natural gas
SOYD	sum-of-years digits
t	metric tons
TJ	Tera (10^{12}) joules
UK	United Kingdom
y	year
US	United States
$	US dollar
¢	US cent
£	pound sterling

USEFUL CONVERSION FACTORS

1.0 metric ton (t)=2205 lb=1.102 short tons
1 x 10^6 SCF=26800 Nm^3
1 x 10^6 BTU=1.0546 GJ=252016 kcal
1 x 10^6 BTU/h=0.293 MW
1000 BTU/SCF=39.35 MJ/Nm^3=9404 kcal/Nm^3
1.0 $/GJ=1.0546 $/$10^6$ BTU=4.1947 $/$10^6$ kcal

0. SUMMARY

This report forms part of a study in the Economic Assessment Service (EAS) work programme entitled 'The Economics of Coal Conversion'. It deals with the production of both substitute natural gas (SNG) and medium calorific value gas (MCG) – (10-16 MJ/Nm^3 or 250-400 BTU/SCF). The following processes were selected for evaluation, primarily on the basis of availability of data. A later report will cover more advanced gasification processes.

SNG production

- BCR BI-GAS (Entrained)
- British Gas/Lurgi (Moving bed[1] – slagging)
- Exxon Catalytic (Fluidized bed)
- IGT HYGAS (Fluidized bed)
- Lurgi (Moving bed[1] – dry ash)
- Shell Coal (Entrained)
- Texaco (Entrained)

MCG production

- British Gas/Lurgi (Moving bed[1] – slagging)
- Lurgi (Moving bed[1] – dry ash)
- Shell Coal (Entrained)
- Texaco (Entrained)

Both SNG & MCG production were examined at the 3000 MWt (250 x 10^9 BTU/SD) level, and MCG was also evaluated at the 500 MWt (40 x 10^9 BTU/SD) level and at a load-factor of 0.85. The sensitivity of the results to changes in capital investment, load factor, and by-product values was examined. A discounted cash-flow analysis was carried out to derive gas costs in $/GJ[2]. The analysis was carried out in constant mid-1979 dollars **(no inflation)** for a range of coal prices and DCF rates-of-return. Two financial conventions were used: no-tax and no depreciation, which is representative of European public-sector investment; and 48% tax, 10% investment tax-credit and accelerated depreciation, which represents typical North American conditions. Some typical results are presented in Tables 1 & 2 for each of the two financial conventions.

Gas costs have been calculated on the basis of mature technology, and will be substantially higher for 'pioneer' plants. Gas distribution costs have not been examined in this report.

A significant conclusion is that for a given type of gas – SNG or MCG – the choice of process (but **not** the absolute level of gas costs) is unaffected by most economic parameters, such as, DCF rate-of-return, debt/equity ratio, taxation, load-factor and price of coal. This conclusion also holds for a given set of by-product values. These conclusions will not hold, of course, if the make-up of gas costs is very different, as for example, with in-situ gasification. Obviously, as will be discussed below, the type of coal available does have a significant impact on the choice of process. Our unpublished work suggests that the differences in the cost of constructing large SNG plants on a normal site in the member countries are

1 Also known as fixed bed – the coal moves slowly down the gasifier.
2 $1.0/GJ=$1.05/10^6 BTU=5.3 pence/therm ($2.0=£1)=8.4 DM/Gcal (DM 2.0=$1).

generally less than the uncertainty in the capital cost in any one country. Hence, we conclude that, in general, the choice of gasification process is very largely independent of whichever country one is considering. International co-operation in this field is, therefore, likely to be of mutual benefit to all the countries concerned.

There is a close relationship between gasifier process parameters, such as carbon conversion, oxygen and steam consumption, and the cost of the plant. Changes in these parameters will generally have a much greater effect on total plant costs than changes in the process equipment itself. Hence, the use of contingency factors as large as 100% on the cost of gasifiers, may not be enough to account for likely changes in process parameters. It follows that the comparisons are sensitive to changes in these process parameters.

A further uncertainty is that the technologies are at different stages along the path from conceptual design to commercial reality. Thus, one might expect that the costs of the various processes could increase to different levels by the time they are fully developed. There is no easy way to overcome this difficulty by numerical analysis, though we believe that the data presented in this report are neither optimistic nor pessimistic.

The comparisons made in this report are based on capital costs derived from estimates given by the organisations responsible for the designs. We do not think that their accuracy is better than ±30% and this level of accuracy must be considered in relation to our conclusions.

The results given in this report are therefore tentative; more definite conclusions would require data derived from the actual performance of large plant, and this will take some time to become available.

SNG production

- Large SNG plants cost in the range \$1.3 - 1.8 × 10^9 (in 1979 \$) excluding interest during construction and escalation.

  Using representative coal prices and financial conventions we obtain typical SNG costs as follows:

DCF rate-of-return	SNG costs (\$/GJ) 5%	10%
North American[1]		
Western coal at \$0.5/GJ	3.7 - 5.3	5.3 - 7.9
Bituminous coal at \$1.5/GJ	5.4 - 7.2	7.0 - 9.8
Europe & Japan[2]		
W German lignite at \$0.9/GJ	4.1 - 5.6	5.1 - 7.2
Imported coal at \$2/GJ	5.7 - 7.7	6.7 - 9.6
Imported coal at \$3/GJ	7.3 - 9.6	8.3 - 11.2

Notes:

1 Using 'North American' financial conventions
2 Using 'no-tax' financial conventions

- The above data show that the cost of SNG from Western US coal is comparable with Mexican and Canadian imports of natural gas into the US at about $5/GJ. Similarly SNG from W German lignite is broadly competitive with Algerian ($6/GJ) or Russian gas ($5/GJ) imported into Europe. This assumes that this type of coal can be gasified at about the same cost as western US coal. SNG produced from eastern US coal, or from relatively cheap imported coal into Europe or Japan, is only competitive under the most favourable of conditions, such as very low rates-of-return.

- We cannot see any major cost break-throughs with the processes considered. We do not entirely rule out the possibility that some other process might offer the chance of greater savings, though such a process would be at a comparatively early stage of development.

- The British Gas/Lurgi process has a cost advantage of about 20% compared with dry-ash Lurgi on Eastern US coal. This cost advantage is close to the difference between Eastern and Western (sub-bituminous) coal with dry-ash Lurgi. The Eastern coal is a poor one for dry-ash Lurgi as it has a low ash melting point and is relatively unreactive. We would therefore expect other coals to lie between the Eastern and Western gas costs and to somewhat reduce the potential improvement from the British Gas/Lurgi process. On the other hand, the British Gas/Lurgi process is likely to be more flexible than dry-ash Lurgi in terms of coal type and size distribution. Both the British Gas/Lurgi and dry-ash Lurgi processes appear attractive for **SNG production.**

- The Exxon Catalytic process **appears** to have only marginally superior economics compared with dry-ash Lurgi. While we think that Exxon are conservative in their estimates (though we have eliminated a good deal of this), we do not see any major cost break-through with this process. We stress, however, that our information on this process is limited and that our conclusion is necessarily tentative. This process is at an earlier state of development compared with the others examined in this report.

- The Exxon Catalytic process is sensitive to the level of recovery of the catalyst used. Our analysis suggests that catalyst recoveries in excess of 70% are required. While this level of recovery has been obtained in the pilot plant it will require demonstration on a continuous large-scale basis.

- The Shell Coal process (with HCM combined shift/methanation catalyst) is only marginally superior to the dry-ash Lurgi process for **SNG production**. We do not think that this process is under serious consideration for SNG production. We think that the economics of the process are likely to be relatively insensitive to changes in coal type and size distribution.

- The Texaco process for **SNG production**, even at 65% slurry concentration, has inferior economics in relation to dry-ash Lurgi. We do not think that this process is under serious consideration for SNG production.

- The economics of the Texaco process are profoundly affected by the concentration of the feed coal-slurry. We do not have any information as to whether high (65%) concentrations can be maintained on a continuous basis for all types of coal.

- While our analysis shows both BI-GAS and HYGAS as attractive on Eastern coal, the achieved performance of these processes fails far short of the estimates we have used. Thus, BI-GAS has never operated on the Eastern coal and has inferior economics relative to dry-ash Lurgi on the Western coal, on which it has operated. At the achieved carbon conversion of 80% the economics of the HYGAS process show no improvement over dry-ash Lurgi.

- The broad effect of valuing by-products at oil-related, as opposed to the more conservative coal-related prices used in the data presented above, is to improve the economics of dry-ash Lurgi and British Gas/Lurgi relative to the other processes. The economics of British Gas/Lurgi process are improved by about 16%. This is the maximum change and is not enough to modify our conclusions about the competitiveness of SNG. Moreover, we have not considered any upgrading costs. We doubt whether these higher by-product prices can actually be achieved, in the context of several, large SNG complexes located in many cases well away from potential by-product markets.

- While the precise amount of fines that dry-ash Lurgi gasifiers can handle is uncertain, under most conditions the use of run-of-mine coal is unlikely to significantly affect the economics of this process for SNG, provided any excess fines can be sold for more than half the value of the feed coal with $1/GJ coal or three-quarters with $3/GJ coal.

It should be emphasised that the conclusions above are based on published data available to EAS at the time of writing. However this is a parametric study, and it should be possible (using data given in the Appendices), to modify these results to accommodate newer information published at some later date.

Medium calorific value gas (MCG) production

We assume that highly reliable, and hence multi-stream, stand-alone plant will be required if centrally manufactured MCG is to be substituted for oil or natural gas. We also assume that CO-containing fuel gas can be distributed through local networks. This gas is not suitable for distribution to domestic consumers. Removal of CO for this purpose will give higher gas costs, comparatively close to those quoted for SNG.

- Large MCG plants (3000 MWt – 250 x 10^9 BTU/SD) cost in the range $0.7 - 1.2 \times 10^9$ (in 1979 $). This excludes interest during construction and escalation. Using representative coal prices and financial conventions we obtain typical MCG costs as follows:

DCF rate-of-return	MCG costs ($/GJ) 5%	10%
North America[1]		
Coal[3] at $0.5/GJ	2.1 - 3.4	3.0 - 4.8
Coal[3] at $1.5/GJ	3.5 - 4.9	4.3 - 6.4
Europe & Japan[2]		
Coal[3] at $0.9/GJ	2.6 - 3.7	3.1 - 4.6
Imported coal[3] at $2/GJ	3.9 - 5.4	4.5 - 6.3
Imported coal[3] at $3/GJ	5.2 - 7.0	5.7 - 7.8

Notes:

1 Using 'North American' financial conventions – see Section 2.2
2 Using 'no-tax' financial conventions – see Section 2.2
3 Illinois No.6-type coal

- While the economics are attractive, we think that relatively few 3000 MWt (250 x 10^9 BTU/SD) MCG plants are likely to be built – though obviously both the Ruhr and the US Gulf Coast areas are feasible locations. We consider a 500 MWt (40 x 10^9 BTU/SD) plant as much more likely at this stage of development. Obviously, modest increases or decreases in scale will not invalidate our conclusions. For a 500 MWt (40 x 10^9 BTU/SD) MCG plant investments are $300 x 10^6 for dry-ash Lurgi and about $170 - 230 x 10^6 for British Gas/Lurgi, Shell Coal and Texaco processes (all in 1979 $). On a 'no tax' basis, with coal delivered[1] at $2/GJ, and 10% DCF rate-of-return, gas costs are $8.3/GJ and $5.6 - 6.8/GJ respectively. Corresponding 'North American' with-tax costs are $9.6/GJ and $6.3 - 7.9/GJ. A further consideration is that a 10% DCF rate-of-return may not be acceptable for industrial (as opposed to utility) ventures in all the member countries. The parameter does have a serious impact on gas costs.

- There are no cost savings for a 500 MWt (40 x 10^9 BTU/SD) dry-ash Lurgi MCG plant compared with a 3000 MWt (250 x 10^9 BTU/SD) SNG plant. The advantages of scale with the 3000 MWt SNG plant almost exactly balance the capital cost savings and higher thermal efficiency with the simpler MCG plant. We conclude that dry-ash Lurgi does not look attractive for MCG production in countries with an existing gas distribution network **and** large demands for gas – sufficient to support the size of SNG plant outlined above.

- By contrast, British Gas/Lurgi, Shell Coal and Texaco (65% slurry) look attractive, even at the 500 MWt (40 x 10^9 BTU/SD) scale. The Texaco Process shows gas costs about 20% higher than British Gas/Lurgi or Shell Coal, which both have similar gas costs. All three processes are competitive with gas-oil or No. 2 heating oil at about $7/GJ (end-1981), in Europe, North America or Japan.

1 These plants are less likely to be located at the minemouth and hence delivered coal costs should be considered.

General conclusions

- The effect of decreasing the MCG plant size from 3000 MWt to 500 MWt (250 to 40 x 10^9 BTU/SD) is to increase gas costs by between 30 and 40%, depending on the particular process, for $1/GJ coal at 10% DCF rate-of-return. With $3/GJ coal these increases are about halved, though obviously starting from a higher base-level. This suggests that there are significant benefits of scale where coal is relatively cheap. These benefits are much less significant, however, with high-priced coal. We would expect much the same effect with SNG plants.

- At a 10% DCF rate-of-return capital costs form approximately 40-50% of total gas costs. Coal costs at $1/GJ are about 25-30% of total costs. Clearly, the most suitable coal for gasification is a cheap one. In general terms, reactive coal with low moisture and ash content are preferred. Low sulphur and high oxygen also serve to reduce gas costs. Data on **dry-ash Lurgi** SNG plants (44) suggest that a typical US lignite (38% moisture, 5% ash) is preferable to sub-bituminous coal, which is in turn preferable to bituminous coal.

- There are only small economic penalties for gasifying high sulphur and/or oxygen coal with relatively low calorific value. Since the demand for these types of coal for power generation may well be limited, this could have significant implications for world trade in coal.

Table 1 Comparative process economics – no-tax case

Basis: Eastern U.S. high-sulphur bituminous coal except where indicated.
0.85 load factor. All data rounded. 10% DCF rate-of-return.
'No-tax', depreciation, inflation.
By-products burnt[6]. Electric power self-generated.

Process	Capital cost ($x10^6)[1]	Coal feed (10^6t/a)	Overall thermal efficiency (%)[5,6]	Gas cost ($/GJ) with coal at $1/GJ	$2/GJ	$3/GJ
3000 MWt – 250 x 10^9 BTU/SD SNG plant						
Dry-ash Lurgi:						
Eastern coal	1700	5.4[2]	53(55)	6.6	8.6	10.5
Western coal	1350	6.0[4]	67(70)	5.2	6.7	8.3
British Gas/Lurgi (with HCM)	1300	4.5[2]	63(67)	5.2	6.9	8.5
Exxon Catalytic	1550	4.6[2]	62(62)	6.3	7.9	9.6
Shell Coal (with HCM)	1700	5.1[2]	59(59)	6.9	8.8	10.6
Texaco (65% slurry)	2050	5.3[2]	56(56)	7.3	9.3	11.2
3000 MWt – 250 x 10^9 BTU/SD MCG plant						
Dry-ash Lurgi	1200	4.4[3]	66(68)	4.8	6.3	7.9
British Gas/Lurgi	700	3.6[3]	80(83)	3.2	4.4	5.7
Shell Coal	700	3.6[3]	79(79)	3.2	4.5	7.0
Texaco	1000	3.9[3]	73(73)	4.1	5.6	7.0
500 MWt – 40 x 10^9 BTU/SD MCG plant						
Dry-ash Lurgi	300	0.7[3]	66(68)	6.7	8.3	9.8
British Gas/Lurgi	180	0.6[3]	80(83)	4.5	5.8	7.0
Shell Coal	160	0.6[3]	79(79)	4.2	5.5	6.9
Texaco	230	0.6[3]	73(73)	5.4	6.8	8.2

Notes:

1. Includes contingency, engineering, process royalties, working capital, start-up costs, and initial catalysts and chemicals. Excludes interest during construction. Mid-1979 $.
2. Pittsburgh No. 8 seam coal. As received basis. See Table B1 for coal analysis.
3. Illinois No. 6 coal. As received basis. See Table B1 for coal analysis.
4. Montana sub-bituminous coal. As received basis. See Table B1 for coal analysis.
5. Defined as heat in cold gas/heat in total coal feed. Higher heating values used.
6. Data in brackets relate to export of by-products.

Table 2 Comparative process economics – North American taxes

Basis: Eastern U.S. high-sulphur bituminous coal except where indicated.
0.85 load factor. All data rounded. 10% DCF rate-of-return.
48% tax, 10% investment tax credit, SOYD depreciation. No inflation.
By-products burnt[6]. Electric power self-generated.

Process	Capital cost ($x10^6)[1]	Coal feed (10^6t/a)	Overall thermal efficiency (%)[5,6]	Gas cost ($/GJ) with coal at $0.5/GJ	$1/GJ	$2/GJ
3000 MWt – 250 x 10^9 BTU/SD SNG plant						
Dry-ash Lurgi:						
Eastern coal	1700	5.4[2]	53(55)	6.8	7.8	9.8
Western coal	1350	6.0[4]	67(70)	5.4	6.2	7.8
British Gas/Lurgi (with HCM)	1300	4.5[2]	63(67)	5.3	6.2	7.8
Exxon Catalytic	1550	4.6[2]	62(62)	6.6	7.4	9.1
Shell Coal (with HCM)	1700	5.1[2]	59(59)	7.3	7.6	9.4
Texaco (65% slurry)	2050	5.3[2]	56(56)	6.7	8.8	10.8
3000 MWt – 250 x 10^9 BTU/SD MCG plant						
Dry-ash Lurgi	1200	4.4[3]	66(68)	4.8	5.6	7.2
British Gas/Lurgi	700	3.6[3]	80(83)	3.0	3.6	5.0
Shell Coal	700	3.6[3]	79(79)	3.0	3.7	5.0
Texaco	1000	3.9[3]	73(73)	4.2	4.9	6.3
500 MWt – 40 x 10^9 BTU/SD MCG plant						
Dry-ash Lurgi	300	0.7[3]	66(68)	7.2	8.0	9.6
British Gas/Lurgi	180	0.6[3]	80(83)	4.6	5.2	6.6
Shell Coal	160	0.6[3]	79(79)	4.3	5.0	6.3
Texaco	230	0.6[3]	73(73)	5.1	6.4	7.9

Notes:

1. Includes contingency, engineering, process royalties, working capital, start-up costs, and initial catalysts and chemicals. Excludes interest during construction. Mid-1979 $.
2. Pittsburgh No. 8 seam coal. As received basis. See Table B1 for coal analysis.
3. Illinois No. 6 coal. As received basis. See Table B1 for coal analysis.
4. Montana sub-bituminous coal. As received basis. See Table B1 for coal analysis.
5. Defined as heat in cold gas/heat in total coal feed. Higher heating values used.
6. Data in brackets relate to export of by-products.

1. INTRODUCTION

1.1 PURPOSE AND STRUCTURE OF REPORT

In its programme on the economics of coal conversion technology, the Economic Assessment Service (EAS) has completed a study on economic and technical criteria (1-4) and has issued reports on the economics of power generation (5,6). This report covers a study on the economics of coal gasification.

We have attempted to answer the following basic questions:

- What does gas from coal cost and what affects this cost?
- How do different approaches and processes compare?
- How near to competitive cost-levels is present-day technology?

The first requirement in answering these questions is reasonable process performance and cost data. Performance data for the processes were given in an earlier EAS report (2) and are summarised in Appendix B. Appendix A contains details of the status of each of the processes together with simplified process descriptions. This information is also derived from Reference (2).

However, given that performance and cost data for processes in the development stage are somewhat speculative, it would be unwise to use the results of a single analysis to represent the ultimate performance of a particular process. Consequently, a significant part of this report comprises a sensitivity analysis of the end-results to such parameters as increases in investment and change in load factor.

A considerable part of this report deals with the estimation of capital costs. The methodology used and the capital cost data obtained are presented in Appendix C. Appendix D covers all the other cost items which must be calculated in order to carry out a full economic analysis.

Very few of the reports we have used to estimate capital costs specifically address environmental concerns. Thus, in general, we do not have comprehensive data on plant effluents. We have included non-regenerable flue-gas desulphurisation for the boiler plant, biological oxidation of aqueous effluent and sulphur recovery plant tail-gas treatment. Ash is dewatered before being returned to land-fill. Zero water discharge has been used as the design basis. In a separate report (7), EAS have considered the environmental aspects of liquid effluents from coal gasification plants. EAS are currently examining solid wastes, including those from coal gasification plants.

Section 2 describes the methodology used to calculate costs of gas from the various processes. As several of the processes are at the development stage, estimates of capital costs are subject to considerable uncertainty and the way this is dealt with is also discussed. Finally, the detailed economic conventions used are summarised.

An analysis of the performance and cost data used to derive the product gas cost is presented in Section 3. The evaluation has been carried out for a number of

different coal prices, rates-of-return, and taxation regimes. A complete set of results is given in Appendix E. In Section 3 the sensitivity of the results to by-product values, size of plant, load-factor, capital cost, coal type (rank and sulphur content), and rate-of-return is also investigated. In Section 4 the relative merits of each of the gasification processes are considered. Our conclusions are presented in Section 5.

1.2 GASIFICATION PROCESSES

Serious interest in gasification processes is essentially confined to the following:

(a) Air-blown systems producing a low-calorific value gas (5-7 MJ/Nm^3 or 120-180 BTU/SCF) for:

— Electricity generation in a gas/steam combined-cycle plant
— Local use as a fuel gas

(b) Oxygen-blown systems producing a medium-calorific value gas (10-16 MJ/Nm^3 or 250-400 BTU/SCF) for:

— Electricity generation in a gas/steam combined cycle plant
— Chemical synthesis
— Local use as a fuel gas
— Manufacture of substitute natural gas (SNG)

Systems generating electricity are covered in a separate report (6) while the production and use of synthesis gas forms the subject of future studies by EAS. Air-blown systems providing fuel gas are covered elsewhere (8) and thus this report is confined to oxygen-blown systems producing either a medium-calorific value gas (MCG) for local distribution at pressures above 17 atm or substitute natural gas (SNG) at 70 atm. The essential difference between these two systems is that SNG requires at least partial conversion of CO to H_2, complete (as opposed to partial) CO_2 removal and methanation.

The basis employed for considering a process was as follows:

(a) A process must be technically far enough advanced to have a reasonable chance of becoming commercially available before, say, the end of the century.

(b) Each process chosen should be undergoing development in plants of sufficient size that data are available which adequately describe the process technically, even if commercial-scale experience is inevitably lacking.

(c) Processes chosen must be suitable for large scale applications.

Insufficient data are available at the time of writing this report on the high-temperature Winkler, COGAS (fluidized-bed), and Saarberg-Otto (entrained) processes to permit adequate evaluation.

Representative processes selected for evaluation are shown in the following table:

Table 3 Processes examined

SNG production (3000 MWt – 250 x 10^9 BTU/SD output)	
BCR BI-GAS[1]	(Entrained)
British Gas/Lurgi	(Moving bed – slagging)
Exxon Catalytic	(Fluidized bed)
IGT HYGAS[1]	(Fluidized bed)
Lurgi	(Moving bed – dry ash)
Shell Coal	(Entrained)
Texaco	(Entrained)
MCG production (500 & 3000 MWt – 40 & 250 x 10^9 BTU/SD output)	
British Gas/Lurgi	(Moving bed – slagging)
Lurgi	(Moving bed – dry ash)
Shell Coal	(Entrained)
Texaco	(Entrained)

Note:

1 In view of the current status of these processes they have been excluded from the graphs and tables included in the body of this report. They are discussed in Section 4.6 while full details are included in the appendices.

The basis for selecting the plant sizes was:

(a) 3000 MWt[2] (250 x 10^9 BTU/SD) is the output size commonly used in US evaluations of SNG. This is sufficient to generate about 1000 MWe of power.

(b) 500 MWt[2] (40 x 10^9 BTU/SD) must be considered a substantial output for a MCG plant. This is discussed further in Section 3.1.2.

It should be noted that **metric** tons have been used throughout. We have not considered gas distribution costs in this report.

2 The precise sizes selected were 250 x 10^9 BTU/SD and 500 MWt.

2. METHODOLOGY

In this chapter the approach we have adopted towards gasification is presented. The sources of our data are briefly reviewed, together with the conventions employed.

2.1 DATA SOURCES

In any estimation of product energy costs the following can be regarded as essential steps:

- determination of yield data for the process
- development of plant design data for the process
- estimation of capital costs
- estimation of operating data such as coal and utilities consumption, manpower, etc.
- economic analysis using input variables such as coal and labour costs, rate-of-return on investment, etc.

Our Report on "Economic and Technical Criteria for Coal Utilisation Plant" (1-4) has examined the question of yield data. The detailed plant design is based not only on this yield data but also on other factors, such as the design methods, the desired balance between operating and capital costs, and site-specific considerations (such as coal and water quality and cost and availability of land).

The estimation of capital costs is not an exact science. It is subject to considerable error unless the project is well defined, which almost invariably implies focussing on a specific site and a specific coal. Since the aim of EAS is to compare general energy costs in member countries, such a detailed approach is inappropriate. Moreover, data on such a well defined basis are not generally available for gasification plants.

We make the general assumption that the plant will not be the first of its type or size (Exxon's "pioneer" plant (9)) and that its process design parameters are well established. For MCG we have tried to ensure that the plant is representative of the stand-alone, highly reliable complex that would be required if centrally manufactured MCG replaces oil.

Allen and Page (10) have attempted to quantify the uncertainties arising from the above considerations. They suggest that factored or preliminary estimates of capital costs (see their definitions) could be expected to have an accuracy of about ±20 - 30%. The bulk of the published literature, ie the data available to EAS, falls into these categories and has this level of accuracy (at best). It follows that we can expect (and do find) large differences between estimates even for the same type of plant with the same gasifier design. This is shown in Table D1, for example. Given that differences between the capital costs of gasification projects do not generally exceed this range, the implication is that a direct comparison of different processes using very different sources is unlikely to be particularly fruitful. For this reason a somewhat different approach has been adopted.

For SNG processes the work by Braun (11,12) for the US ERDA/DOE & AGA/GRI represents the most comprehensive and comparable data available. Braun (9,10)

looked at six different gasification processes and two different coals – a Western US (Montana) sub-bituminous coal and an Eastern US (Pittsburgh seam No. 8) high-sulphur bituminous coal. These reports provided much of the basic yield and investment data particularly for the dry-ash Lurgi, BI-GAS and HYGAS processes. These data have been modified substantially, as outlined in Appendix B, and in particular reconciled with that presented by Mobil (with a substantial contribution by Lurgi) to the US DOE (13). The effect of different types of coal on gas costs is discussed in Section 4 of this report.

The work by Fluor (14-17) for EPRI looked at several medium & low-calorific value gasification processes and one type of Eastern US high-sulphur bituminous coal — Illinois No. 6[1]. This set of reports provided the starting basis for the EAS work on MCG gasification processes, in particular the dry–ash Lurgi and Texaco processes.

Yield data on the British Gas/Lurgi process were supplied by British Gas. These data do not include the re–injection through the tuyeres of by–product tars, oils or phenols. The yield data on both the Shell Coal and Texaco processes were obtained using a development of the National Coal Board's ARACHNE equilibrium model (18). This model was validated against the DSM equilibrium model (19) and data from Braun (20), Fluor (15) and Shell (21). We also had some published information on Texaco's own modelling work (22). The above yield data were used to modify the Braun and Fluor data on SNG and MCG respectively. In addition, Shell supplied information on investment and utilities for their process while data presented by Conoco (23) were used to develop the investment cost for British Gas/Lurgi.

The basic data on the Exxon Catalytic gasification process for SNG were obtained from their reports to the US DOE (24,25) and from the work of Braun for GRI (26). Again, we modified this information as far as possible to be in line with the assumptions made in the earlier Braun reports.

Capital cost data of sufficient detail were only found in studies carried out in North America, and our results are largely based on those data. However, we have examined the differences between these and the few European cost estimates both in the course of this study and in another unpublished EAS study. The data support our view that the variations between the various member countries in the cost of constructing large gasification plants are less than the uncertainty of the capital cost estimates in any one country.

Data on the coals used and the assumed performance of the plants are given in Appendix B.

2.2 CONVENTIONS

There is considerable variation in the way in which product energy costs are calculated and which factors are included. The method employed in this work uses a straight-forward discounted cash flow (DCF) analysis, applied to the real resource costs of the plant, to calculate the levelised unit product price which will give an overall net present value of zero at the chosen discount rate. (The 'real resource

1 The particular Illinois No. 6 coal used in the Fluor studies does not differ significantly from the Pittsburgh No. 8 coal – see Table B1.

costs' are those that relate to physical requirements and to such matters as design, as distinct from financial factors such as interest payments or taxes). In financial terms this is equivalent to calculating that product price which would enable the capital borrowed to finance plant construction to be paid back exactly (together with associated interest payments) over the plant life. This procedure is exactly equivalent to calculating interest during construction (IDC) at the specified DCF rate-of-return. This thereby eliminates the need to consider interest during construction as a separate item.

The base case analysis uses real resource costs at constant value and therefore excludes:

- all taxes or other national charges
- all inflation or escalation factors associated either with fuel cost or construction
- all variations associated with financing, for example the debt/equity ratio.

For purposes of comparison we have also studied the effect of using typical North American financial rules including tax and investment tax credits with an accelerated depreciation schedule.

All calculations have been done using a modification of the PRP computer program developed at the Oak Ridge National Laboratory (27). The assumptions made are summarised in Table 4, which is based on our previous work (1) with only a few minor changes. Capital cost data used are given in Appendix C and operating cost data in Appendix D.

One difficulty arises when comparing product energy costs derived from a real resource analysis with those calculated by other methods. For example, how does the DCF analysis relate to the straightforward annualised charge used in many evaluations? This depends on the cash-flow profile over the project life, but an approximate guide is given below:

DCF rate of return (%)	Equivalent annualised capital charge (%)
5	8
10	15
15	25

Another way of examining these product energy costs is to compare them with those derived using the joint US DOE and AGA/GRI Gas Cost Guidelines (9,10) utility financing method and this is presented in Table 5. It can be seen from this table that using the US DOE/GRI guidelines gives first year and constant gas costs which closely approximate our 'North American' case with 10 and 5% DCF rates-of-return respectively. Using the above guidelines, gas costs are within about −6 and +15% of our 10% DCF 'no-tax' case. The reader may wish to try to relate the results of our conventions to those of other methods.

Table 4 Summary of economic conventions

Rate-of-return	•	discounted cash-flow basis
	•	'real' prices and costs based on mid-1979 $
	•	100% equity basis and also 100% equity basis with 48% tax-rate and accelerated depreciation (SOYD) and 10% investment tax credit
Technical considerations	•	plant output: 500 MWt (40×10^9 BTU/SD) (MCG only), 3000 MWt (250×10^9 BTU/SD)
	•	load factor: 0.85
	•	operation during first year: 50% of normal load factor
	•	project expenditure period: 4 years
	•	expenditure during project expenditure period:
		year 1: 10%; year 2: 22.5%; year 3: 47.5%; year 4: 20%
	•	project life (ie working life): 20 years
	•	project contingency allowance: 15%
	•	royalty: 2.5%
Other variables	•	working capital: 30 days' feed and by-products, receivables at 1/12 annual product and by-product revenue. Materials, supplies and spare parts at 1% of total plant investment
	•	start-up costs: 1 months' coal, water, catalyst and chemicals plus one year's labour and overheads
	•	operating labour: 4-shift system at $30,400/shift-operator/year (which includes allowances for sickness, supervision and social security overheads)
	•	maintenance: 4% of investment (divided equally between fixed costs, ie labour, and variable costs, ie materials)
	•	insurance, local taxes and overheads: 3% of investment
Coal costs		$1,2,3/GJ
Cost of water		$0.20/m^3 ($0.76/1000 US gal)
By-product values:		
sulphur		nil
ammonia		burnt (also $145/t)
naphtha		burnt (also $8/GJ)
other hydrocarbons		burnt (also $5/GJ)
excess coal fines		coal cost (see also Section 4.1)
surplus power		$0.040/kWh (also $0.025/kWh)

Table 5 SNG costs using US DOE/GRI gas cost guidelines

Basis: Eastern US high-sulphur coal at $1/GJ
3000 MWt – 250 x 10^9 BTU/SD dry-ash Lurgi gasifier

Method	Reference	DCF Rate	Tax Rate	Gas Cost	Notes
EAS	1	5%	0%	$5.34/GJ	1
		10%	0%	$6.59/GJ	
		5%	48%	$5.68/GJ	1,2
		10%	48%	$7.82/GJ	
US DOE/GRI (Utility Financing)					
First year	9	3	48%	$7.55/GJ	4
Constant	9	3	48%	$6.12/GJ	4

Notes:

1. See Table 4 for assumptions. 100% equity financing. 85% Load factor.
2. 10% investment tax credit and accelerated depreciation.
3. 10.5% return on rate-base.
4. See Reference (9). 75/25 debt/equity ratio.
   90% Load Factor. The data presented are based on the same capital investment data as in our work. We have also made the same assumptions about by-product values and labour costs.

2.3 PROCESS PERFORMANCE AND CAPITAL COST DATA: SOME UNCERTAINTIES

The processes under comparison in this report are all at different points along the path from concept to commercial reality. It is, therefore, misleading to compare them solely on the basis of costs derived from a single set of process yields. Instead, their economic performance should be visualised as a range of gas costs which may apply for any given coal cost. More developed processes can be expected to have a narrow range while newer, more speculative processes will tend to have larger ranges. In graphical terms, the single lines for each process shown in all the Figures are in reality bands of differing widths.

The uncertainty in gasification economics is essentially about process performance, whereas in power generation economics, for example, the process parameters are essentially fixed and the questions are largely confined to the cost of the plant. Thus, an increase of 25% in the gasifier steam consumption for the Exxon Catalytic process, for example, has the same effect on capital and gas costs as a 50% increase in the cost of the gasification section. While an increase in steam consumption of this magnitude is by no means unrealistic, it is hard to justify such a large contingency in the gasifier costs.

It is apparent, therefore, that gas costs are essentially unaffected by modest changes (or contingency factors) in the cost of the equipment. On the other hand, similar changes in process parameters have a pervasive effect and can lead to large changes in gas costs. This phenomenon must be recognised as a characteristic feature of large gasification plants.

Thus a realistic range of economic uncertainty should be derived from examining a range of process parameters reflecting development uncertainty. The difficulty with applying this thorough sensitivity analysis is that it requires, as a minimum, detailed information about heat and mass balances for all sections of the plant. In general, this information is not given adequately in the quoted sources, and to generate it, even approximately, from the information that is given is a long task requiring various assumptions. We observe at this point that it seems highly desirable for the sponsoring organisations to insist that contractors should give this detailed information when they prepare a design, as a matter of course.

In the circumstances, we have not attempted to generate such ranges of economic uncertainty for each process. Instead:-

(a) We invite the reader to visualise the single lines shown for each process as bands and to note that even for relatively developed processes, like dry-ash Lurgi, the width of the band is likely to be about ±10%. Therefore, for a process to be considered economically superior to another the lines have to be separated by at least this margin. Moreover, one has to have good reason to believe that this margin can be maintained over the likely range of performance conditions.

(b) Section 4 has been devoted to a discussion of individual processes and their relative economic merits. In this way suitable individual qualifications can be made.

(c) In some cases detailed sensitivity analysis seems essential. Typical examples are the effect of processing coal fines on the dry-ash Lurgi process and the effect of slurry concentration on the Texaco process. For such cases detailed process analysis has been done and the effects are discussed in Section 4.

We hope therefore, by taking Sections 3 and 4 together, readers will obtain a balanced picture of both overall and comparative process economics, and of some of the uncertainties that need to be resolved during development.

In addition we have made the general assumption that the plant considered will not be first of its type or size, ie we are looking at a 'mature' plant and not a 'pioneer' one. This implies among other things that the costs of research and development will not be reflected in the economics of the plant.

It may be considered that this is an unfair or unrealistic assumption. It gives an obvious advantage to less well-developed processes. These require a much higher level of research and development funding than more developed processes.

However, there are two distinct questions that should be asked:

(a) How economically advantageous is a new process compared with a more developed one, assuming that development has been carried out and that the research and development funding is a 'sunk cost'?

(b) Following on from this, is the advantage enough to justify incurring the projected research and development costs?

Our assumption is made in order to attempt to answer the first question. The answer to the second question depends on the likely cost of the research and development work needed to bring the new process to a suitable state for commercial use – with all that this implies, and on general political considerations.

3. THE COST OF GAS FROM COAL

Gasification costs were calculated using the methodology described in Section 2, capital cost data given in Appendix C and operating cost data contained in Appendix D. In the analysis the sensitivity of costs to variations in a number of parameters was examined, including coal price and rate-of-return. Two different tax regimes were assumed: a no-tax/no-depreciation case, and a typical 'North American' case with 48% tax on profits, 10% investment tax credit and accelerated depreciation (sum-of-the-years-digits) case with 100% equity financing. Variations in load factor, capital investment, by-product values, coal type, and rate-of-return were also examined. Full results are presented in Appendix E.

Base-case results are summarized in Figures 1 – 3 for plants gasifying a high-sulphur coal at a load factor of 0.85. These figures show gas costs in 1979 $ on an ex-plant basis plotted against coal cost for 10% DCF rate-of-return. We present data on SNG and MCG plants at the 3000 MWt (250 x 10^9 BTU/SD) level level and also for a 5000 MWt (40 x 10^9 BTU/SD) MCG plant. An approximate break-down between coal and operating costs and capital charge is shown in Table 6. The importance of coal cost and capital charges is obvious. In general terms the effects of the discount rate on the **comparative** economics of the processes are small, as can be seen later in Figures 13 - 14. Similarly, the differences (in terms of process comparisons) between the 'no-tax' and the 'North American' cases are small, as shown in Table 5. For this reason our presentation in the main body of the report is largely restricted to the no-tax, 10% DCF rate-of-return case.

Throughout this report comparisons have been generally considered in terms of the gas cost savings (or increases) relative to the dry-ash Lurgi process, which must be considered the most highly developed process both for SNG and MCG. As will be seen this treatment gives a relatively narrow spread of results over the range of coal prices considered.

The figures should be interpreted with care. They attempt to show what the cost of gas would be today if coal of a specified price was used in a plant of a given type using an established process. It does not show what the cost of gas would be in the future if coal prices rise to a specified level, because in this case the consequences of this price rise upon other costs (especially capital and labour) need to be investigated. Further, the costs presented here do not represent the economics of the first few 'pioneer' plants, which will be significantly higher.

A sound comparison of processes requires the use of more than one set of process and economic data reflecting the uncertainty in all the processes, even including the relatively fully-developed dry-ash Lurgi process. **Therefore all the figures and tables should be used with caution and reference should be made to the discussion in the following sections.**

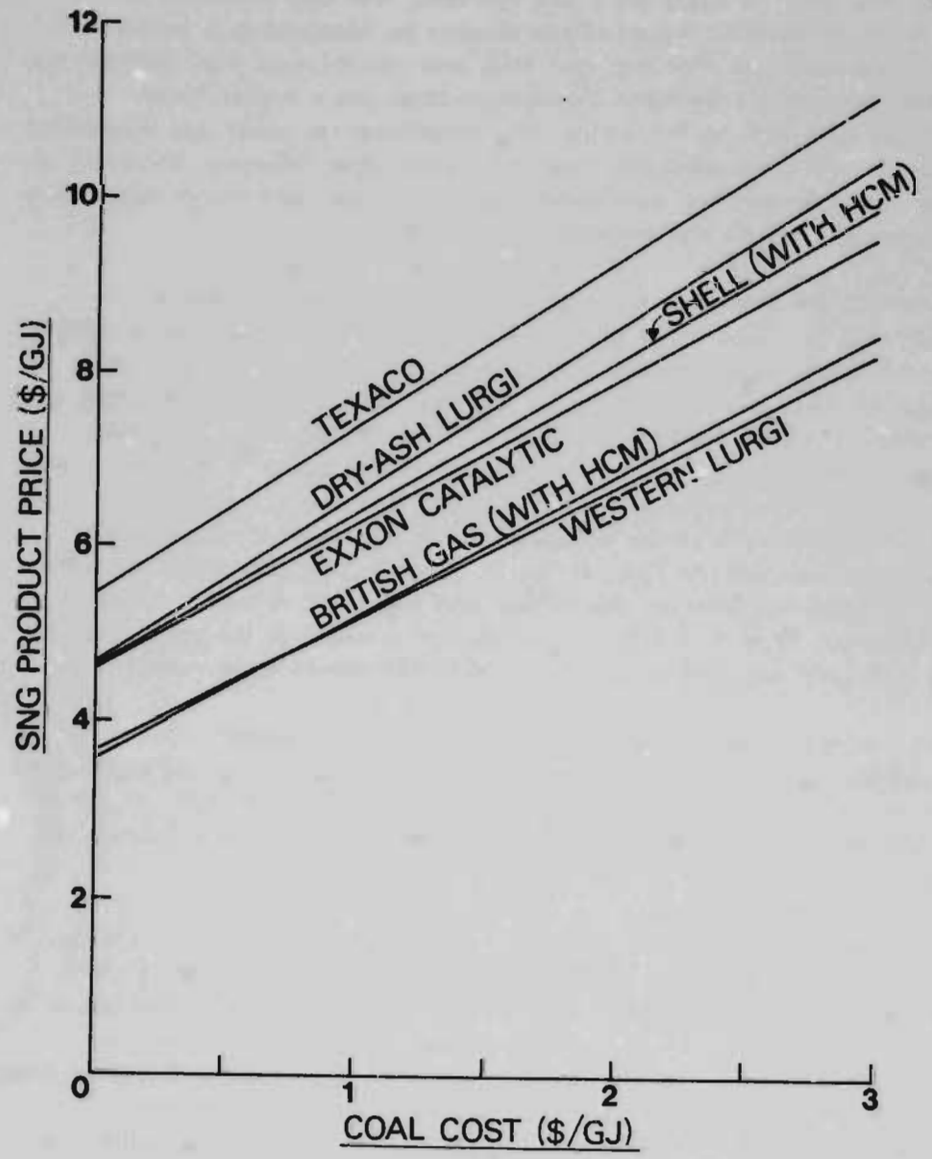

Figure 1 The cost of SNG from coal
(Eastern US coal except Western Lurgi, 'no-tax', 10% DCF, by-products burnt)

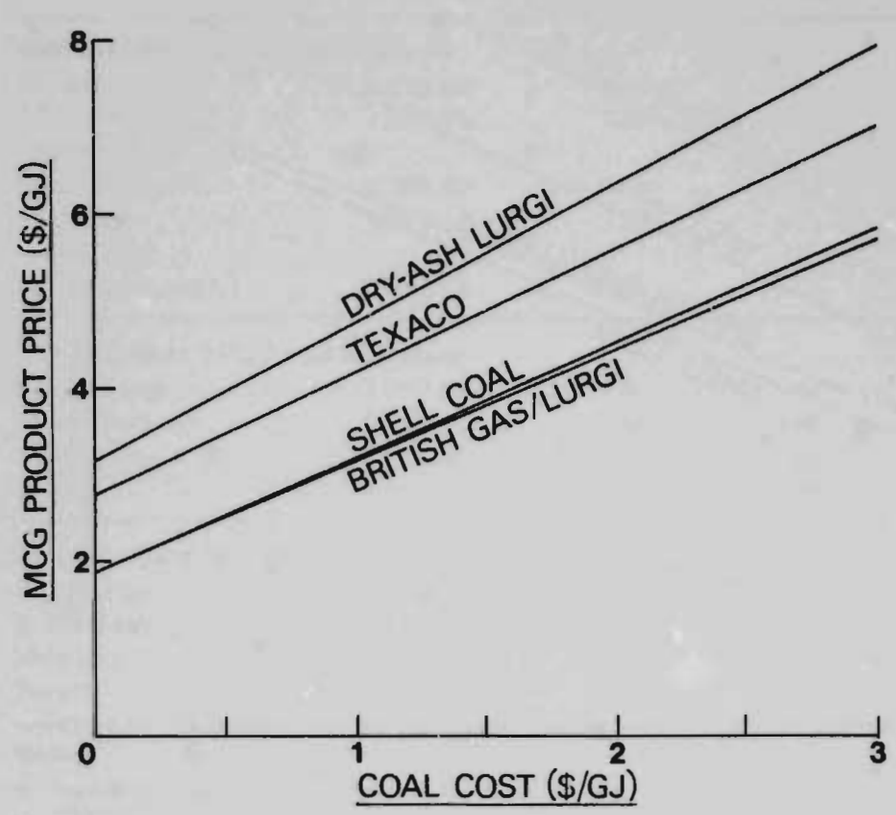

Figure 2 The cost of MCG from coal (3000MWt-250 x 10^9 BTU/SD output)
(Eastern US coal, 'no-tax', 10% DCF, by-products burnt)

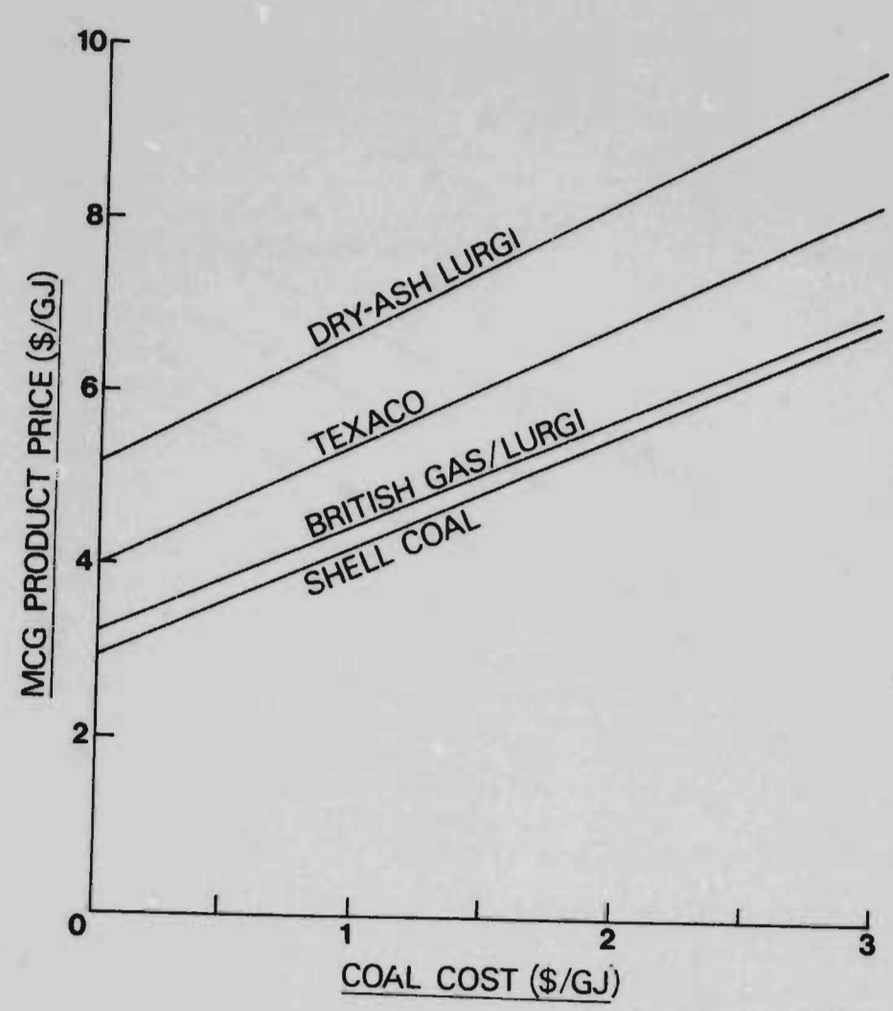

Figure 3 The cost of MCG from coal (500 MWt-40 x 10^9 BTU/SD output)
(Eastern US coal, 'no-tax', 10% DCF, by-products burnt)

In the next section we discuss the general implications of these figures. We then go on to discuss in turn:

- coal type
- DCF rate-of-return
- by-product values
- scale of plant
- load-factor
- capital cost escalation

Table 6 Approximate gas cost breakdown in $/GJ
at 5(10)% DCF rate-of-return for $1/GJ coal[1]

Process	Capital charges[2]	Coal cost[3]	Operating costs[4]	Product price
3000 MWt-250 x 10^9 BTU/SD SNG plant				
Dry-ash Lurgi	1.83(3.09)	1.90	1.60	5.34(6.59)
British Gas/Lurgi (with HCM)	1.38(2.32)	1.58	1.33	4.29(5.23)
Exxon Catalytic	1.70(2.86)	1.62	1.80	5.12(6.28)
Shell Coal (with HCM)	1.88(3.16)	1.72	1.51	5.11(6.39)
Texaco (65% slurry)	2.26(3.79)	1.88	1.68	5.82(7.35)
3000 MWt-250 x 10^9 BTU/SD MCG plant				
Dry-ash Lurgi	1.29(2.16)	1.52	1.09	3.90(4.77)
British Gas/Lurgi	0.74(1.24)	1.24	0.69	2.67(3.17)
Shell Coal	0.76(1.27)	1.27	0.65	2.68(3.19)
Texaco	1.11(1.86)	1.37	0.92	3.40(4.15)
500 MWt-40 x 10^9 BTU/SD MCG plant				
Dry-ash Lurgi	1.99(3.34)	1.52	1.83	5.34(6.69)
British Gas/Lurgi	1.19(1.99)	1.24	1.24	3.67(4.47)
Shell Coal	1.09(1.84)	1.27	1.14	3.50(4.25)
Texaco	1.53(2.57)	1.37	1.47	4.37(5.41)

Notes:

1. Eastern US coal, 'no-tax' by-products burnt, all data rounded. Data shown thus ( ) are for 10% DCF rate-of-return.
2. Includes process royalties, start-up costs and working capital.
   These last two items are a function of coal cost (see Appendix F).
3. Excludes coal component of working capital and start-up costs.
4. Includes credit for by-product power (for Shell Coal and Texaco SNG processes only).

3.1 GENERAL IMPLICATIONS

In this section we discuss some overall implications of the data presented in the previous section on the price of gas. Obviously this depends on several factors including, for example, the quality of the coal and the process used. The reader is referred to later sections of this report for discussions on these topics.

3.1.1 Representative coal prices

Since coal costs vary widely, it is obviously important to consider only those costs which are relevant to the reader. Representative levels of coal prices into power stations in early 1980 (essentially corresponding to the mid-1979 plant cost level) are shown in the following table (5).

Table 7 Representative coal prices 1980

	Early 1980 Price $/GJ
US sub-bituminous Western	0.8
US expensive bituminous	2.0
Canada Western	0.8
Canada expensive bituminous	2.5
W Germany lignite	0.9
W Germany hard coal	3.5
Australia hard coal	0.8
Imported hard coal in Europe or Japan	2 - 3

Though coal prices have increased in real terms subsequently, the effective increases in Europe in dollar terms were more than offset by the changes in currency exchange rates. We will therefore use the levels quoted in Table 7 except for North America. The range of $0.8 - 2.0/GJ for the US refers to delivered costs to power stations and in some cases these may be a long distance from the minemouth. Since gas plants, particularly the 3000 MWt size, will be sited much closer to the mine, if not actually at the minemouth, a more likely cost range would be $0.5 - 1.5/GJ (in early 1980 dollars). Similarly, in Canada the lower end of the range would be $0.5/GJ.

3.1.2 North American SNG costs

Using the above coal costs, typical North American SNG costs (in $/GJ) are as follows:

Table 8 Typical North American SNG costs

DCF rate-of-return	5%	10%
Western coal at $0.5/GJ	3.7 - 5.3	5.3 - 7.9
Bituminous coal at $1.5/GJ	5.4 - 7.2	7.0 - 9.8
Bituminous coal at $2.5/GJ	7.0 - 9.1	8.5 - 11.8

The above data use the 'North American' financial conventions (with tax) outlined in Section 2.2. As can be seen, SNG from coal on a **non-inflated** basis using the cheapest (Western) coal and the least costly process (dry-ash Lurgi) is unlikely to cost less than $5.3/GJ ex-plant using a 10% DCF rate-of-return and mid-1979 prices. Using the US DOE/GRI gas cost guidelines with a 10.5% return on rate-base and a 75/25 debt/equity ratio, corresponding costs are $4.9/GJ for first year, and $4.0/GJ average. Costs using more expensive, bituminous coal would be at least a third higher. These compare with Mexican or Canadian natural gas imports into the US at about $5/GJ (end-1980) and therefore appear to be relatively attractive. They do not, however, allow for any additional infrastructure, which will generally be required in the West. **Moreover, we have assumed 'mature' technology — the first plants to be built will have significantly higher costs** (see for example the methodology presented by Exxon (9). The above figures can be reconciled with the price of gas quoted (28) for the Great Plains project - $7.2GJ in inflated $ at end-1984, after allowing for the smaller scale of plant.

Figures 1 and 4 show that gas costs of the dry-ash Lurgi process on Western sub-bituminous coal are very close to the British Gas/Lurgi process (with HCM), which appears to represent the optimum process on Eastern coal. However, Eastern US coals tend to have a relatively low ash melting-point, which substantially increases the steam consumption with dry-ash Lurgi. While we have not looked at British Gas/Lurgi on Western coal, we think that the cost improvements with this type of coal will be substantially less than on Eastern coal. While some other, newer process **might** alter the position, we do not think that a break-through in gas costs is likely, relative to the above data.

3.1.3 European and Japanese SNG costs

Table 9 Typical European and Japanese SNG costs

DCF rate-of-return	5%	10%
W German lignite at $0.9/GJ	4.1 - 5.6	5.1 - 7.2
Imported hard coal at $2/GJ	5.7 - 7.7	6.7 - 9.6
Imported hard coal at $3/GJ	7.3 - 9.6	8.3 - 11.2
W German hard coal at $3.5/GJ	8.0 - 10.6	9.0 - 12.2

The above data use the 'no-tax' financial conventions outlined in Section 2.2. We have assumed that the gasification of W German lignite gives the same economics as a Western US coal. Compared with Algerian LNG delivered to France at about $6/GJ (29) and Russian gas at about $5/GJ (72), SNG from W German lignite is

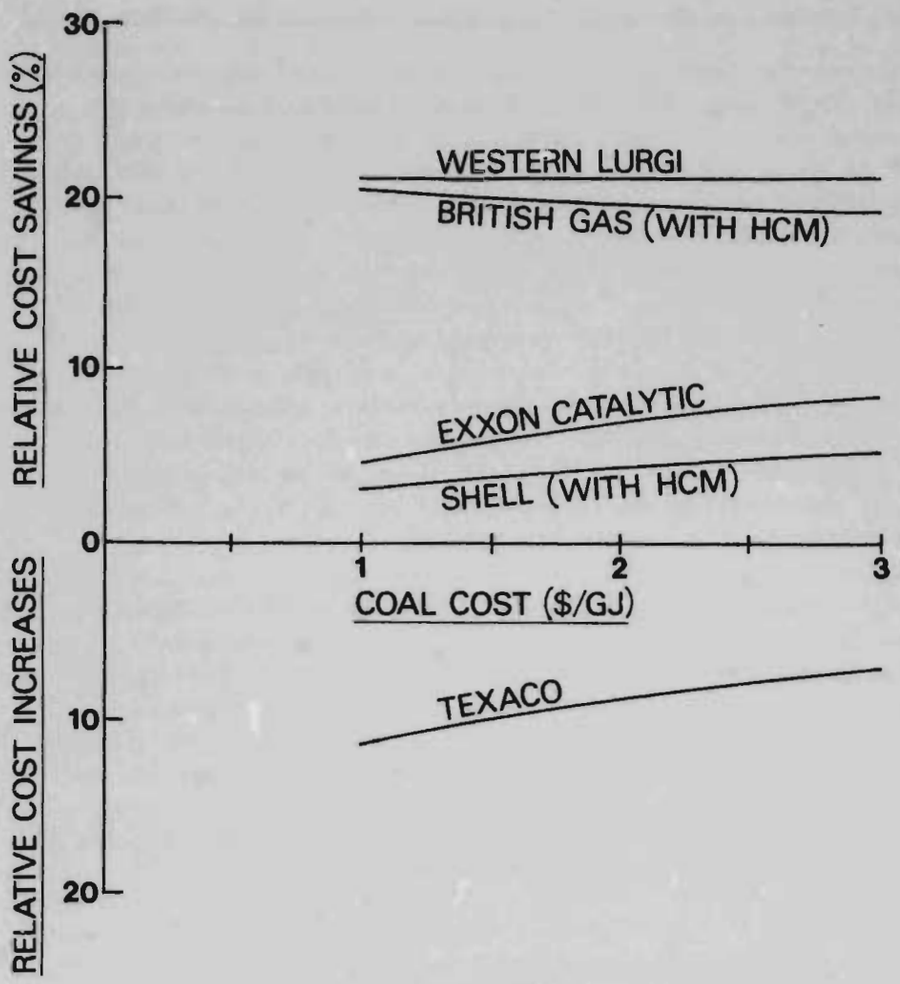

Figure 4 SNG costs relative to the dry-ash Lurgi process
(Eastern US coal except Western Lurgi, 'no-tax', 10% DCF, by-products burnt)

broadly competitive at current prices. Imported LNG into Japan costs about $6/GJ (30). Consequently, hard coal imported into either Europe or Japan at about $2/GJ is only marginally competitive at low rates-of-return. Our gas cost data are in good agreement with that presented by Bonfiglioli and Carella (31) and Bergmann (31).

We have made the assumption that the capital costs of European and US SNG plants will be the same. Some unpublished studies commissioned by EAS suggest that there are no significant variations in capital costs between the countries under consideration – that is, on average and in relation to the ±30% accuracy of most conceptual studies. This conclusion is based on certain specific assumptions, for example, that the time taken to construct the plant is essentially the same in all countries, which may well not hold in reality (32).

3.1.4 MCG costs

We have looked at MCG plants producing a desulphurised fuel gas, suitable for local distribution to industry. This gas contains a significant amount of carbon monoxide and is therefore not suitable for distribution to domestic consumers. If it is necessary to remove the bulk of the carbon monoxide the cost of this MCG will be somewhat higher than the figures quoted in this Section, though still lower than the costs of SNG. We would expect those processes with a relatively high proportion of carbon monoxide – Shell Coal and Texaco, to be more highly penalised compared with dry-ash Lurgi.

The data given in Appendix E suggest that for the 'no-tax' and 'North American' cases with a 10% DCF rate-of-return and low coal costs ($1/GJ) dry-ash Lurgi MCG costs for a 3000 MWt (250 x 10^9 BTU/SD) plant would be about $4.8 and 5.6/GJ respectively, assuming 'mature' technology and 1979 prices. The British Gas/Lurgi, Shell Coal and Texaco processes could reduce costs by 13 – 35% depending on the process.

From Figure 6 it can be seen that dry-ash Lurgi and British Gas/Lurgi MCG costs are typically 60 - 75% of SNG costs for the **same size of plant** and for the same cost of coal and discount rate. MCG costs by the Shell Coal and Texaco processes are 50 – 65% of the comparable SNG costs. However, neither of these two processes is particularly favoured for SNG production, as discussed in Section 4. These cost reductions are a function of the process and especially of the number of gasifiers and parallel processing trains required. Hence they are also affected by the precise scale examined.

In general, however, we must question whether we should be considering the same size of plant. While 3000 MWt (250 x 10^9 BTU/SD) SNG and MCG plants are certainly feasible, we would suggest that 500 MWt (40 x 10^9 BTU/SD) must be regarded as the typical large MCG plant, certainly at this stage of development. Even in the longer term, we believe that 3000 MWt MCG plants are likely to be severely limited by the potential markets available. For the smaller size of plant, the differentials between SNG & MCG costs are lower than mentioned above and range from 2% more to 35% less than that of a large SNG plant for the same cost of coal and discount rate. This is shown in Figure 7. We conclude that the selection of the particular MCG process is critical if MCG is to compete with SNG, in those countries with an existing gas distribution network.

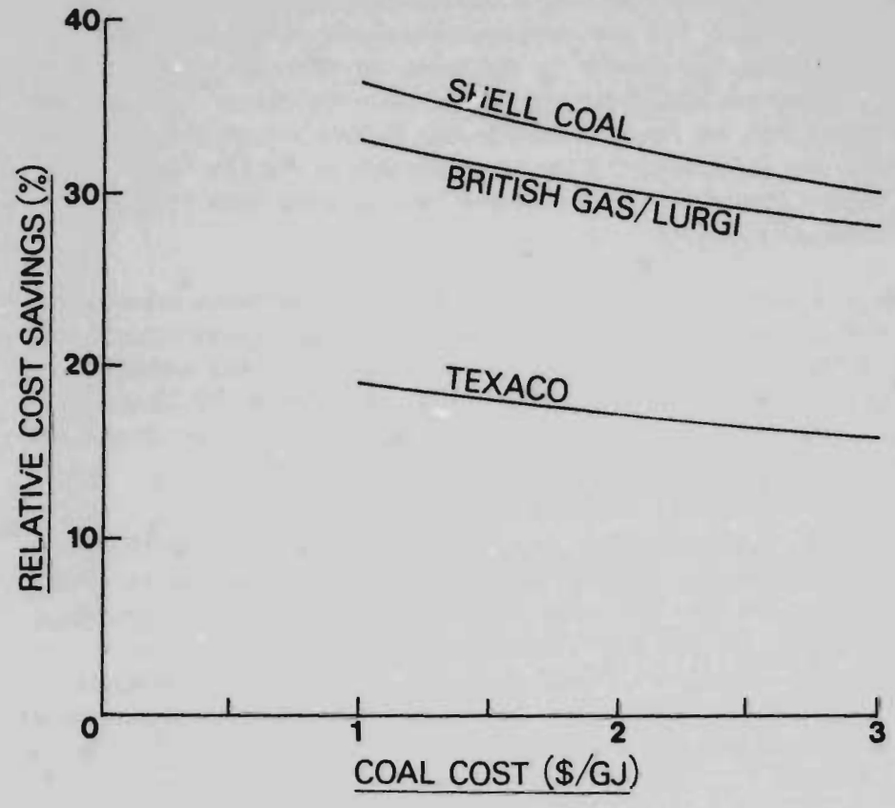

Figure 5 MCG costs relative to the dry-ash Lurgi process (500 MWt—40 x 10^9 BTU/SD output)
(Eastern US coal, 'no-tax', 10% DCF, by-products burnt)

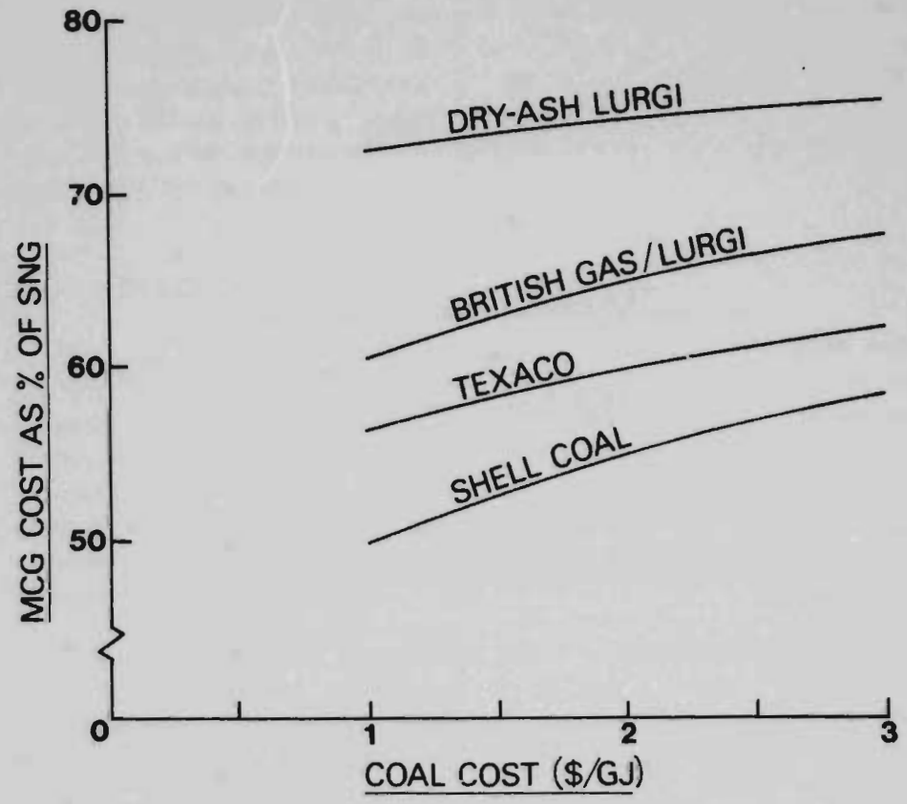

Figure 6 MCG costs as percentage of SNG costs for the same size of plant and the same process
(Plant output: 3000 MWt – 250 x 10^9 BTU/SD)
(Eastern US coal, 'no-tax', 10% DCF, by-products burnt)

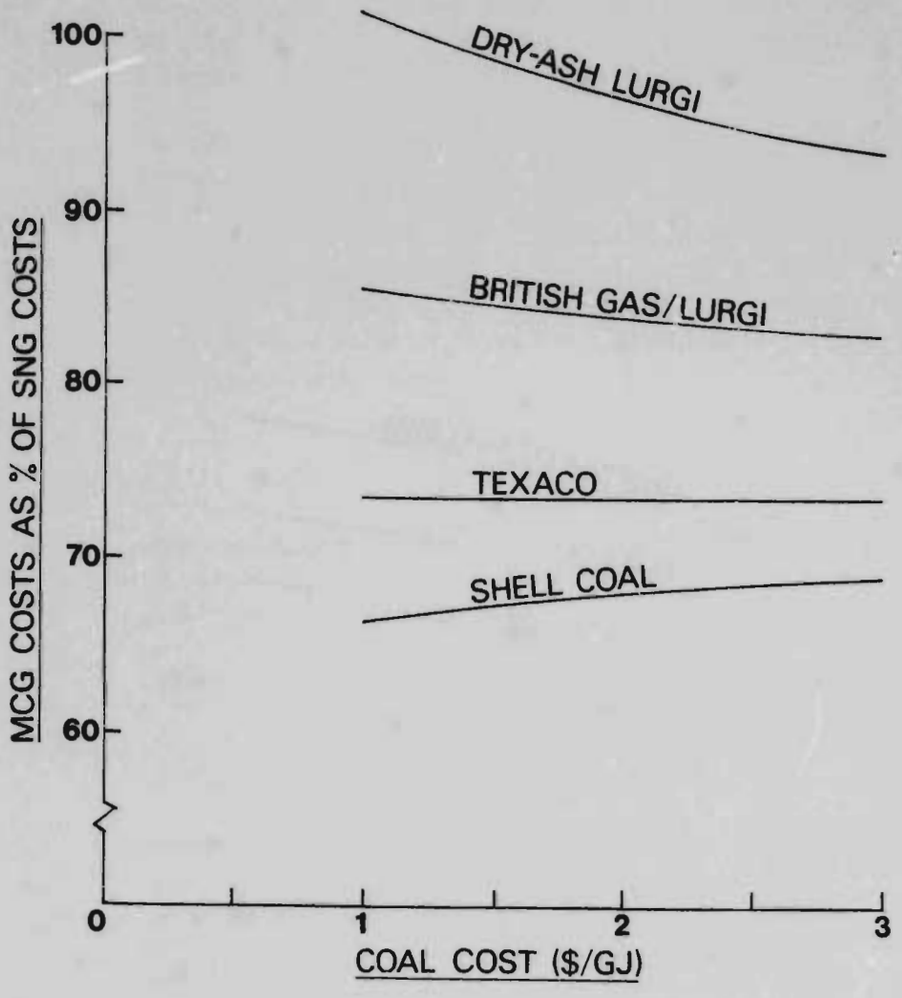

Figure 7 **MCG costs as percentage of SNG costs for the same process**
(SNG plant output: 3000 MWt – 250×10^9 BTU/SD)
(MCG plant output: 500 MWt – 40×10^9 BTU/SD)
(Eastern US coal, 'no-tax', 10% DCF, by-products burnt)

Thus, a 500 MWt (40 x 10^9 BTU/SD) dry-ash Lurgi plant produces MCG typically between 2% more and 7% less than the cost of SNG from a 3000 MWt (250 x 10^9 BTU/SD) plant. The advantages of scale with the 3000 MWt SNG plant almost exactly balance the capital cost savings and higher thermal efficiency with the simpler MCG plant. These MCG costs are clearly unattractive for those countries with an existing gas distribution network and large demands for gas. On the other hand, the British Gas/Lurgi, Shell Coal and Texaco processes give gas cost savings of between 15 and 35% comparing a 500 MWt (40 x 10^9 BTU/SD) MCG plant with the larger SNG plant based on the same process. As might be expected, all these three processes are indeed attractive relative to dry-ash Lurgi for MCG production on a 500 MWt (40 x 10^9 BTU/SD) scale. This can be seen from Figure 5 and is discussed in relation to the processes concerned in Section 4.

We have developed MCG costs at the 500 MWt (40 x 10^9 BTU/SD) scale comparable with the SNG costs quoted above. Our estimates show \$5.6 - 7.9/GJ for the British Gas/Lurgi, Shell Coal and Texaco processes using a 10% DCF rate-of-return, coal delivered[1] at \$2/GJ and 1979 prices. Again, we have assumed 'mature' technology. These figures are close to the current price (end-1981) of competing natural gas imports and rather less than the current price of gas-oil. Again, we caution that the first few 'pioneer' plants can be expected to have significantly higher costs.

3.2 EFFECT OF COAL TYPE

Coal properties vary widely both from country to country and within individual countries. The characteristics most relevant for gasification are sulphur and ash contents, moisture, volatile matter, reactivity and calorific value. Unfortunately, in gasification the influence of coal properties is generally through gasifier yields and this then proceeds to affect the rest of the plant section by section. This is in contrast with power generation, for example, where the properties of the coal affect virtually only the boiler. Further, as we will see from Section 4.6, changes in gasifier yields can have very profound effects.

In Figure 4 and in Table 10 it can be seen that product costs are sensitive to coal type. This is particularly so with the dry-ash Lurgi process. The two coal types we examined were a high-sulphur Eastern US bituminous coal and a low-sulphur Western US sub-bituminous coal. Details on these coals are presented in Appendix B.

1 These plants are less likely to be located at the minemouth and hence delivered coal costs (and ash disposal costs) should be considered.

The cost of gas using low-sulphur sub-bituminous coal with the dry-ash Lurgi process results in SNG costs some 20% lower for a given coal price (expressed as $/GJ) compared with bituminous high-sulphur coal. Some of the difference lies in the sulphur contents, but most lies in the higher reactivity and higher ash melting point of the sub-bituminous coal. This particular sub-bituminous coal has a relatively low moisture and ash content, both of which do have a significant effect on gasifier performance. The differences shown in Table 10 are likely to hold more generally and could well have interesting implications for coal trade. We also conclude that the effect of processing different coals is generally much less than the effect of coal price.

An additional consideration is the question of coal imports. Obviously those countries which have adequate indigenous reserves of coal available at low cost can be expected to consider gasifying this coal. Several member countries are not in this position and might expect to import coal. Under these circumstances gasification processes which are not dependent on a specific coal feed are highly desirable. Slagging processes, such as British Gas/Lurgi, Shell Coal and Texaco are more likely to meet this objective. High ash melting point coal may give problems with these processes, however. Processes using either moving or fluidized beds, such as dry-ash Lurgi, British Gas/Lurgi and Exxon Catalytic, may have excessive fines carry-over with very friable coals.

Table 10 Effect of coal type on dry-ash Lurgi SNG production

Basis: 3000 MWt-250 x 10^9 BTU/SD SNG plant, $1/GJ coal. 'No-tax', 10% DCF rate-of-return, by-products burnt

	Eastern Coal	Western Coal
Coal Analysis:		
Sulphur (wt% dry)	4.42	0.66
Oxygen (wt% dry)	6.50	18.50
Higher heating value (GJ/t as received)	28.83	20.46
Capital Investment[1]	1691	1343
Coal Required[3] (PJ/y)	155	122
Overall thermal efficiency[2] (%)	53	67
SNG cost[3] ($/GJ)	6.59	5.19

Notes:

1. Includes engineering, royalty and contingency, initial catalysts and chemicals, working capital and start-up costs.
2. Excludes sulphur. Higher heating values.
3. At 0.85 load factor.

3.3 BY-PRODUCT VALUES

For the base case, as discussed in the previous section, we adopted a conservative approach to valuing by-products. Our assumptions are shown in Table 11. As can be seen, the by-products have been largely assigned thermal values based on the lowest price of fuel, ie coal, and so we have assumed that they would be consumed within the plants and the coal feed reduced accordingly.

Table 11 By-product values[1]

Product	Base Value	Alternative
sulphur	Nil	Nil
ammonia	coal cost	$145/t
naphtha and benzene	coal cost	$8/GJ
other hydrocarbons	coal cost	$5/GJ

Note:

1 We have also examined change in the value of export coal fines for the dry-ash Lurgi process, and power for the Shell Coal and Texaco SNG processes. These are presented in Section 4 under the relevant processes.

The rationale behind this approach is that the sale of each by-product should be decided on its own economic merits. Sale proceeds should be balanced against the add-on costs of production of each by-product. Further, since by-product values are likely to vary significantly over the life of a plant they should not be allowed to influence the fundamental choice between processes. In general terms, coal gasification plants are likely to be constructed at some distance from the markets they are intended to serve. Thus, it is quite likely that the cost of transporting relatively small quantities of some by-products will be high in relation to their market value. In this case, it may well be uneconomic to market them, though this is obviously site-specific.

Having said this, we recognise that in the face of likely shortages in the supply of petroleum-based liquids, any by-products that are at all comparable, even raw naphtha and tar, will fetch prices that are appreciably higher than that of coal. For this reason we have assigned the alternative by-product values shown in Table 10. While we have assigned fuel-oil value to the tar produced from the dry-ash Lurgi process, we understand that the fines contents of this tar tends to present handling problems for tar refiners, which lower its value.

We have refrained from assigning any value for sulphur, since periods of substantial surpluses and low values are a regular feature of the market for this product. We have not given the crude mixed phenols a value which adequately reflects current market prices for this product since it is generally believed (33-34) that the markets for this material will become rapidly saturated if large numbers of coal gasification plants are constructed.

Some typical results from using these alternative values are plotted in Figure 8, while the complete set of results is presented in Appendix E. The maximum difference in gas costs between the base and alternative cases for the British Gas/Lurgi process is about 16% at 10% DCF rate-of-return with $1/GJ coal. This is not enough to change our conclusions on the competitiveness of SNG from coal. We have not considered any upgrading costs.

As might be expected, the economics of those processes which produce significant quantities of by-products, such as dry-ash Lurgi and British Gas/Lurgi, improve relative to the other processes. Overall, however, the results for this alternative case do support the view that the economics of the coal gasification route as a whole are essentially unaffected by the choice of by-product values, at least under the conditions we have assumed.

3.4 EFFECT OF SCALE

We have not looked at small-scale SNG production since this seems to be of only limited general interest. We have no reason to believe, however, that the effect of scale on SNG production would be any different than for MCG production, which is evaluated here. In Appendix C we present the methodology we have used. Representative data are shown in Figure 9 while the complete set of results are presented in Appendix E. We caution that the methodology and scaling factors used do influence the precise data obtained. In addition, while we have examined the effect of scale at constant average load-factor, there is some evidence that this may not be correct. For example, large power plants have lower availabilities than small ones (35) and olefin plants may be similar (36). We would stress however, that **all** the plants we are examining are large, or very large, by current process industry standards Moreover, we have considered multi-stream plants throughout, which should at least mitigate the effects presented by Walley and Robinson (36).

The effect of decreasing the MCG plant size from 3000 MWt to 500 MWt is to increase gas costs by between 30 and 40% depending on the particular process, for $1/GJ coal at 10% DCF rate-of-return. With $3/GJ coal these increases are about halved, though obviously starting from a higher base-level. The data presented in Figure 9 suggest that there are significant benefits of scale where coal is relatively cheap. These benefits are much less significant, however, when high-priced coal is considered. The differences between the various processes do not influence this conclusion significantly.

3.5 EFFECT OF LOAD-FACTOR

The data in this report assume that the plants will work as designed and will be capable, in effect, of operating for all their operating life at the design load-factor of 0.85, without significant capital expenditure. Figure 10 demonstrates the significance of this assumption. As can be seen a decrease in load-factor from 0.85 to 0.75 over the life of the plant would increase gas costs by between 6 and 9% depending on the particular process (and DCF rate-of-return).

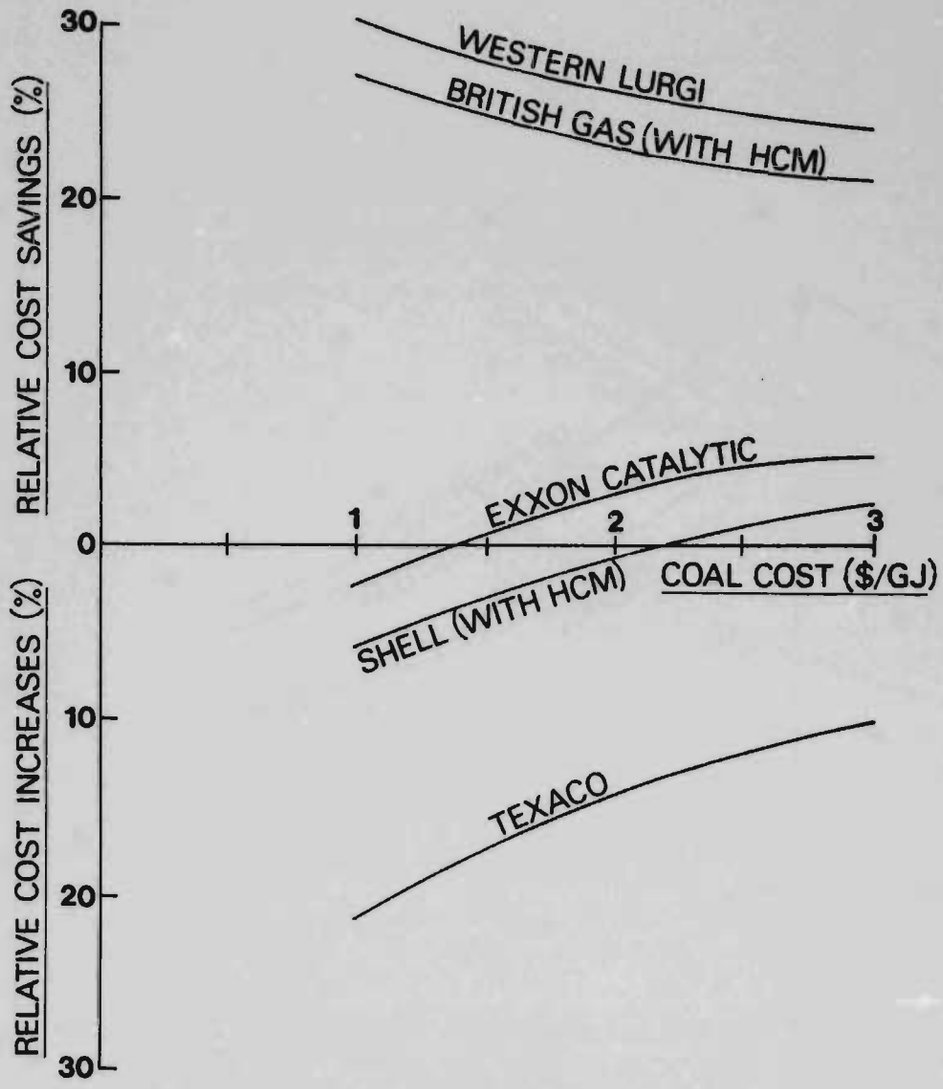

Figure 8 SNG costs relative to the dry-ash Lurgi process – by-products at 1981 oil-related values
(Eastern US coal except Western Lurgi, 'no-tax', 10% DCF)

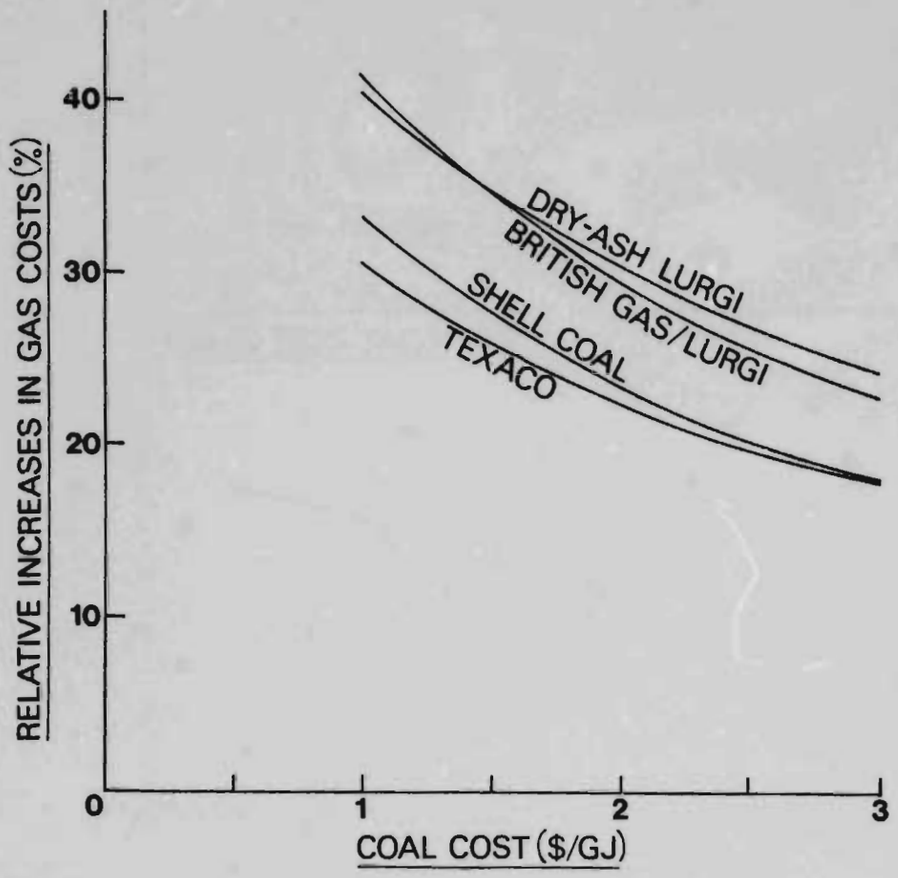

Figure 9 Effect of scale on MCG costs – 500 MWt compared with 3000 MWt
(Eastern US coal, 'no-tax', 10% DCF, by-products burnt)

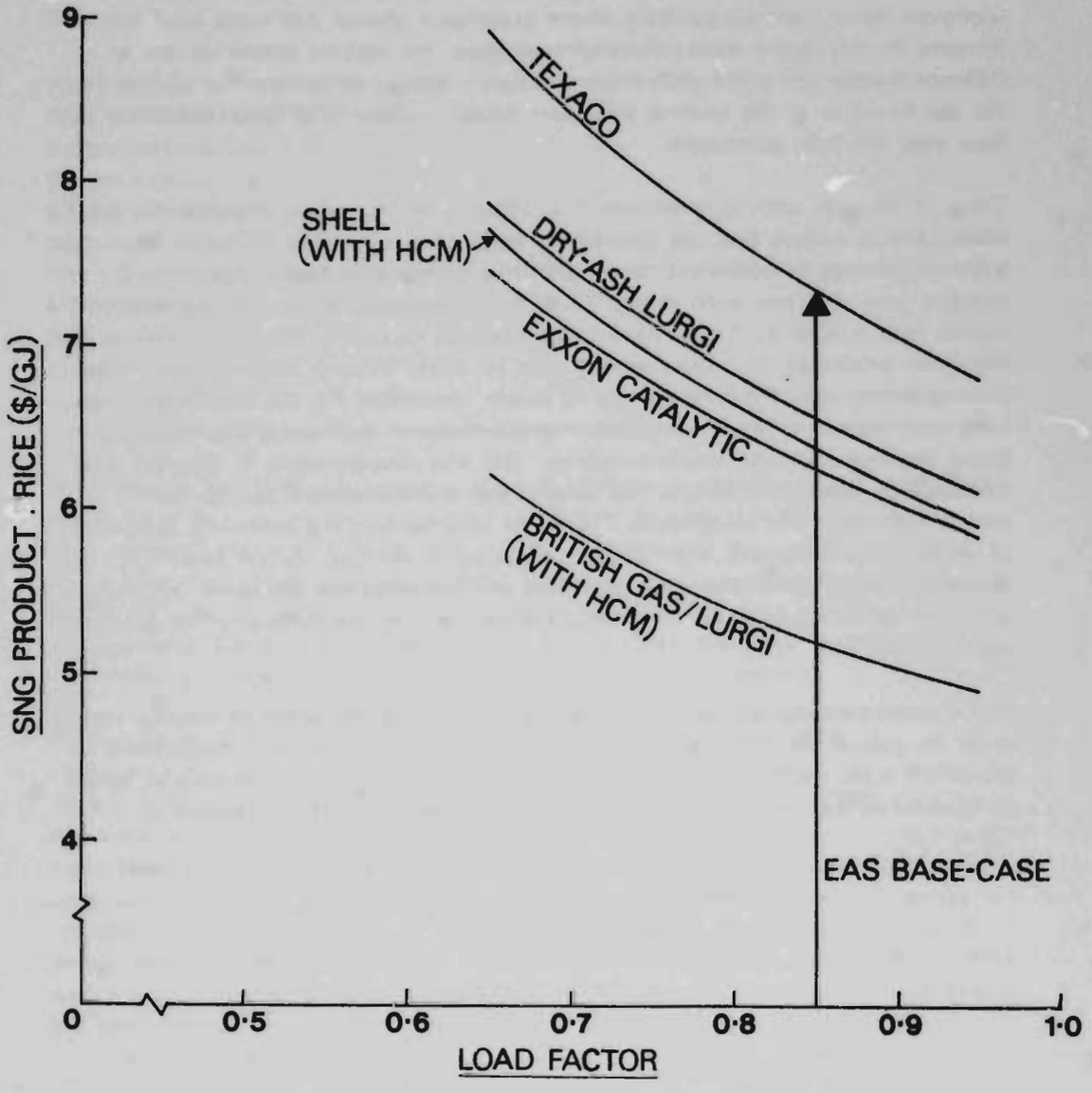

Figure 10 Effect of load-factor on SNG costs
(Eastern US coal, 'no-tax', 10% DCF, $1/GJ coal, by-products burnt)

3.6 CAPITAL COST ESCALATION

The comparisons made in this report are based on plant costs derived from estimates given by the various organisations reponsible for the designs (and are probably accurate to about ±30%). However, some significant costs are for unproven items such as gasifiers where experience shows that costs tend to increase in real terms during development. Also, the various processes are at different stages along the path from conceptual design to commercial reality. Thus, the capital costs of the various processes could increase to different levels by the time they are fully developed.

There is no easy way to overcome this difficulty by numerical analysis. We have taken care to ensure that the investment costs have otherwise (ie, apart from this point of process development) been put on a comparable basis. (Appendix C explains how this has been done). Thus, for example, process contingencies on capital cost quoted by Exxon have been removed to obtain the same basis as for the other processes. It can be argued that by doing this we have chosen to be over-optimistic about the economics of newer processes. On the other hand, we have also chosen to ignore possible improvements in technology (for example, larger gasifiers, hot gas desulphurisation[1] (37) and developments in CO-shift and methanation catalysis[1] (38-42)). We believe that the investment figures are neither optimistic nor pessimistic. The point remains that the economic superiority of all the new processes with respect to dry-ash Lurgi has not yet been demonstrated by extended plant operation and therefore the economic advantages will have to be sizeable (at least 10%) before they can be considered of practical significance.

Some understanding can also be obtained by showing the effect of varying capital costs on gas prices. Figures 11 and 12 do this for SNG and MCG respectively. Based on these figures the capital cost can be derived for each process at which its economics are the same as the dry-ash Lurgi process. This is shown in Table 12.

1 These improvements are generally aimed at existing processes and may well improve the performance of developed processes more than undeveloped ones.

Table 12 Increase in capital costs at which gas costs equal dry-ash Lurgi

Basis: Eastern U.S. coal at $1/GJ, 'no-tax', 10% DCF, by-products burnt
3000 MWt—250 x 10^9 BTU/SD SNG plant
500 MWt— 40 x 10^9 BTU/SD MCG plant

Process	Percentage increase
SNG (3000 MWt – 250 x 10^9 BTU/SD)	
British Gas/Lurgi (with HCM)	45
Exxon Catalytic	4
Shell Coal (with HCM)	2
Texaco (65% slurry)	–16
MCG (500 MWt – 40 x 10^9 BTU/SD)	
British Gas/Lurgi	80
Shell Coal	97
Texaco	35

As examples, for **SNG** the capital cost of the British Gas/Lurgi process (with HCM) would have to undergo an increase of some 45% to eliminate its cost advantage over dry-ash Lurgi with Eastern coal. For **MCG** production the capital costs of British Gas/Lurgi, Shell Coal and Texaco processes would have to increase typically by 30-100% to eliminate their cost advantage over the dry-ash Lurgi process. By any standard this seems to indicate some potential for significant improvements from these processes despite the uncertainty in their development.

Figures 11 & 12 can also be used to give an indication of the effect of improvements in process technology on the cost of gas at constant load factor. Thus a 10% reduction for the dry-ash Lurgi process would reduce SNG costs by 7% from $6.6 to 6.2/GJ. Yet another aspect that can be examined with the aid of these figures is the effect of increases in the real cost of building the plants. The construction of these gas plants involves substantial quantities of steel [typically 110,000 tons for a 3000 MWt SNG plant (40)] which in turn implies a substantial energy input. One might postulate, therefore, that the cost of these gas plants cold well rise at a rate somewhere in between that of energy and inflation in general. Hill and Parker have presented some evidence to substantiate this (43,44).

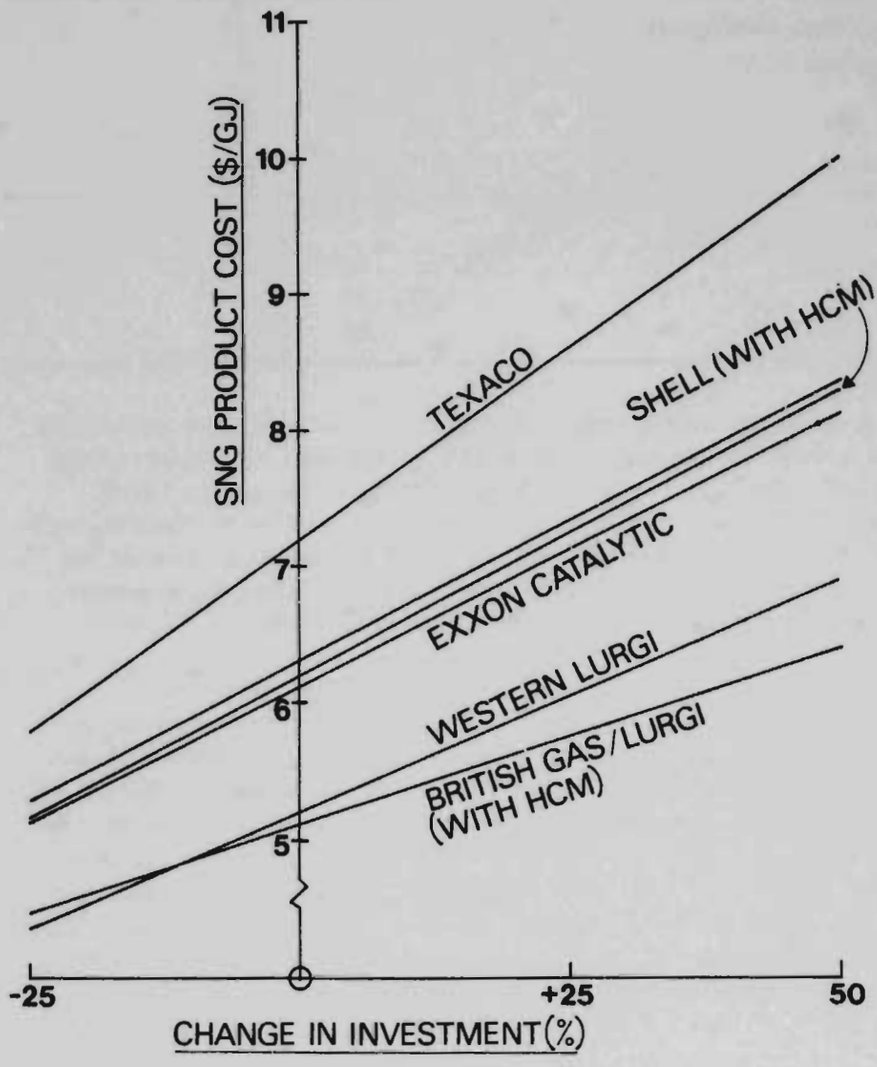

Figure 11 Effect of a real change in capital costs on SNG costs
(Eastern US coal except Western Lurgi, 'no-tax', 10% DCF, $1/GJ coal, by-products burnt)

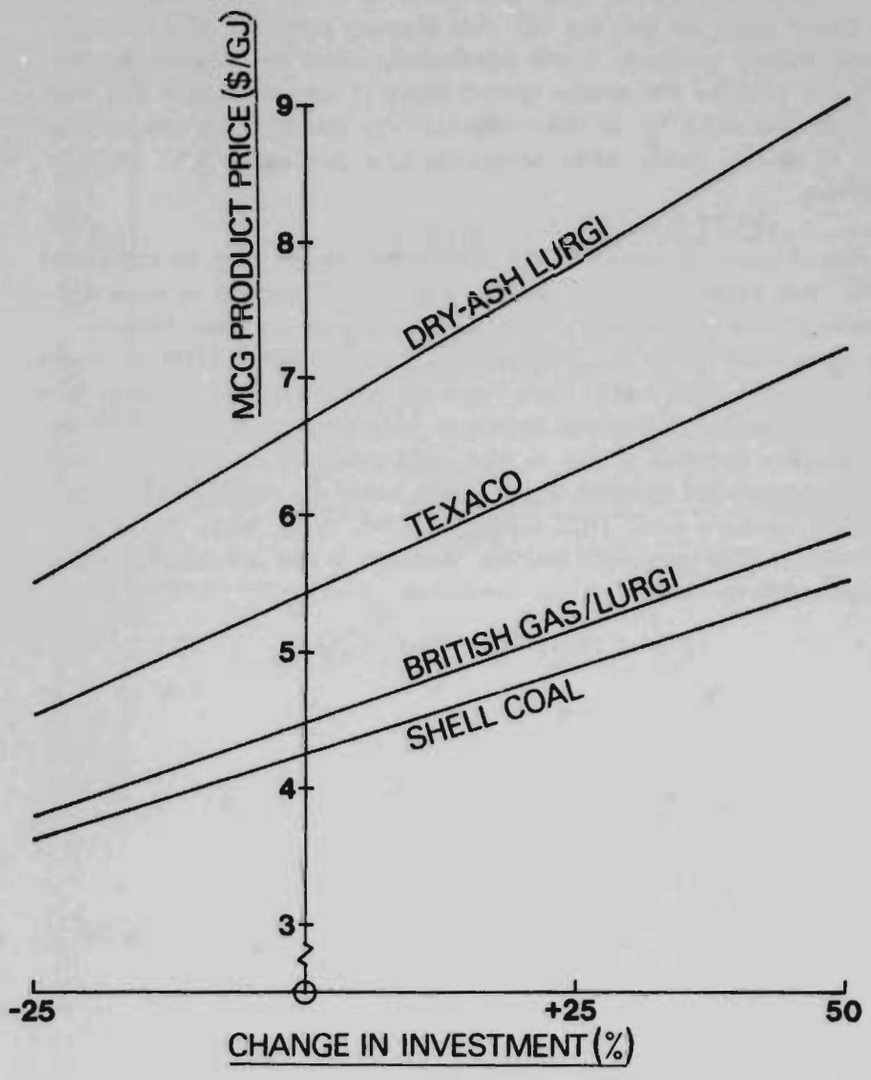

Figure 12 **Effect of a real change in capital costs on MCG costs**
(Plant size: 500 MWt – 40 x 10^9 BTU/SD)
(Eastern US coal, 'no-tax', 10% DCF, $1/GJ coal, by-products burnt)

3.7 EFFECT OF DCF RATE-OF-RETURN

As the required rate-of-return on which technologies are assessed varies widely between member countries, results are presented in Appendix E for real DCF rates-of-return of 3, 5, 10 and 15%. Some of the results are plotted in Figures 13 and 14 for SNG and MCG production respectively. We have plotted the cost savings (or increases) relative to the dry-ash Lurgi process in all cases. The comparative flatness of the curves indicates that the DCF rate-of-return does not affect the choice of process, though obviously it will significantly affect the absolute figures for gas cost. This is because the relative contributions of capital charges and coal costs are essentially the same for all the processes. The choice of an appropriate discount rate is, of course, crucial when comparing coal gasification with other available alternatives.

The 10% DCF rate-of-return presented in the bulk of this report may be compared with the 3 – 8% rates frequently employed for large central projects in several European countries. Similarly, the 10% 'North American' with tax rate-of-return corresponds to those used in the US DOE/GRI Gas Cost Guidelines (11), as shown in Table 5 above. On the other hand, these rates are optimistic when viewed from the aspect of most industriai investment decisions. Real discount rates as high as 15% after tax are quite common in this context, with assumed plant lives as low as 10 years. This corresponds to rates of 20 – 25% using our methodology. We question into which category small MCG plants are likely to fit. While the answer to this question differs from country-to-country, inclusion in the industrial category is certainly unfavourable for MCG.

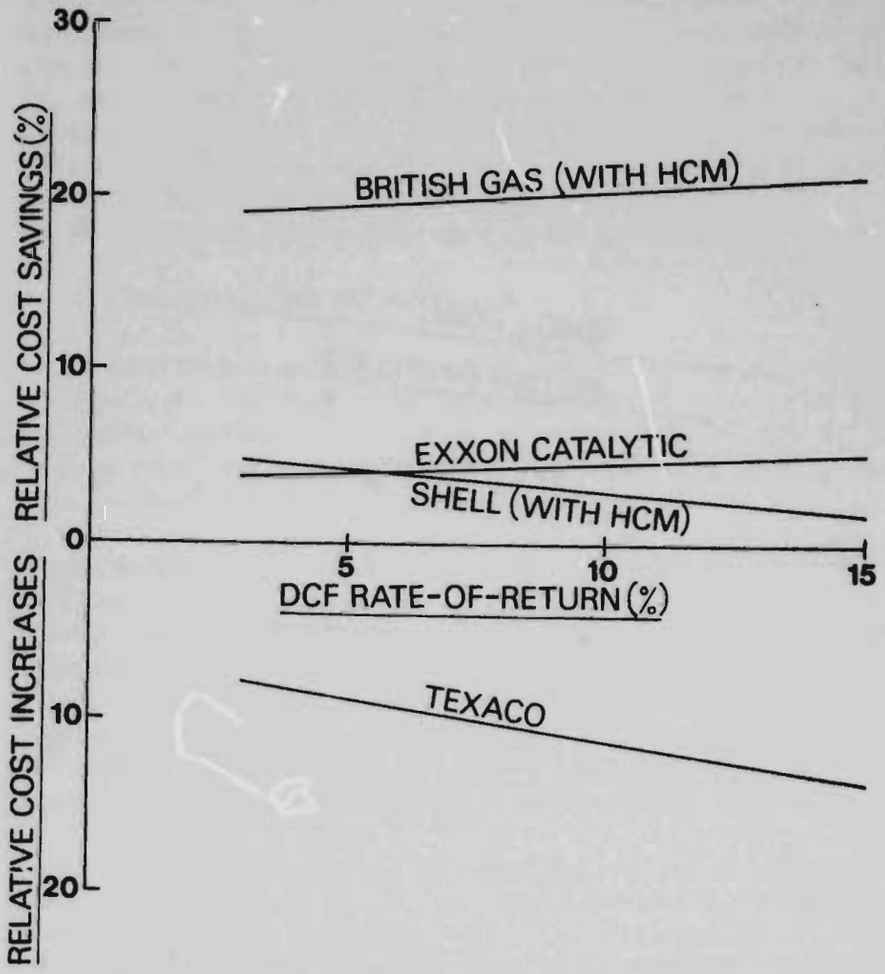

Figure 13 Effect of DCF rate-of-return on SNG cost savings relative to dry-ash Lurgi process
(Eastern US coal, 'no-tax', $1/GJ coal, by-products burnt)

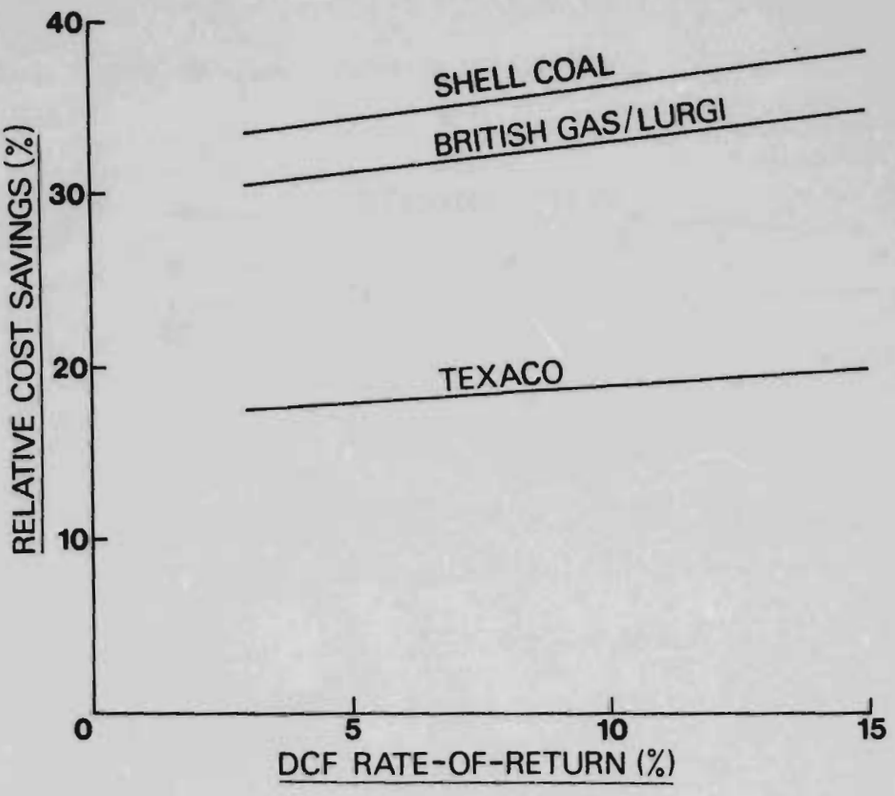

Figure 14 Effect of DCF rate-of-return on MCG cost savings relative to dry-ash Lurgi process

(Plant size: 500 MWt – 40×10^9 BTU/SD)
(Eastern US coal, 'no-tax', $1/GJ coal, by-products burnt)

4. COMPARATIVE PROCESS ECONOMICS

As might be expected, the variety of possible conventions and circumstances mean that the results have to be interpreted with considerable care.

The economics of each process depend greatly on the view taken on operating performance and the evidence selected. While we believe that we have selected the best evidence available, there are points of uncertainty which are sometimes considerable in the case of the newer processes still under development. In fact, even the original dry-ash Lurgi process itself is under the process of development. The only way to reflect these uncertainties adequately is to discuss them and ultimately let the reader make his own judgement how far, for example, the potential savings can be relied on. Therefore this section includes a review of each process. In some instances it has been possible to reflect uncertainty more specifically through process parameters eg the slurry concentration for Texaco.

4.1 DRY-ASH LURGI PROCESS

As indicated elsewhere in this Report, the dry-ash Lurgi process must be considered the most highly developed of all the processes we have examined. For example, the SASOL II complex in South Africa using Lurgi gasifiers consumes approximately twice as much coal as the 3000 MWt (250 x 10^9 BTU/SD) SNG plants contemplated here, so much of the process is already full-scale.

Even with this process, however, development work is likely to lead to some reduction in product gas costs; for example, by using the larger diameter (Mark V) gasifiers now coming into service at SASOL I, or by using higher operating pressures such as in the Ruhr 100 development (87). Further, recycling to extinction the tar and other hydrocarbons produced will tend to raise the overall thermal efficiency of the process (ie, reduce the coal feed for a given output of gas) for very little additional capital investment. We understand that such recycling has been practiced commercially, though we have seen no data for it.

In the absence of firm data on the above improvements we are unable to quantify the effect on gas costs. However, as indicated in Section 3.3 the effect of selling by-products at prices higher than coal cost is significant with this process. Based on these data, we suggest that for a process to be considered economically attractive relative to dry-ash Lurgi it must show gas cost savings of at least 10%. As can be seen from Figure 4, relatively few SNG processes actually achieve this. With MCC the situation is rather different as all the processes examined show gas cost savings well in excess of 10% relative to dry-ash Lurgi (Figure 5).

Hoogendoorn (45) has drawn attention to SASOL's learning curve with the dry-ash Lurgi gasifier. The data used in this report and summarized below have been developed by Fluor and represent a significant improvement on the Westfield trials (46,47). While we believe this improvement is achievable with a 'mature' plant, especially as the Westfield trials were not aimed at optimal performance, this will need demonstration.

Table 13 Dry-ash Lurgi gasifier performance
Basis: Pittsburgh No. 8 coal

Source Reference	Westfield (29), (78)	Braun/Fluor (10)
Steam consumption (t/t maf coal)	3.45 - 3.70	2.80
Oxygen consumption (t/t maf coal)	0.67 - 0.70	0.60

In one respect, however, newer processes may be considered superior to the dry-ash Lurgi process, even if they do not appear to produce cheaper SNG. The dry-ash Lurgi process cannot handle more than a certain amount of fines without adverse effects on throughput. Its economics are, therefore, susceptible both to the quantity and value of any fines that cannot be consumed either in the process or for steam and power generation. The precise level of fines that can be handled without reducing throughput is unclear. Thus a gasifier at SASOL I has been operated (45) at greater than 90% of design throughput on a simulated run-of-mine coal containing 7% below 1 mm in size and 24% below 6.3 mm (1/4"). At the British Gas plant at Westfield, Scotland various US coals were tested (46) and it would appear that satisfactory throughput could be obtained with simulated run-of-mine coal containing about 9 – 10% below 1 mm in size and up to 26% below 6.3 mm (1/4"). It was also reported (46) that a test on a US sub-bituminous coal gave satisfactory results with 9% below 1 mm in size and as much as 45% below 6.3 mm (1/4") after the stirrer arms had been removed. At the STEAG plant at Lünen, West Germany satisfactory throughput was obtained (48) with a screened coal containing approximately 10% below 3 mm in size and with a washed coal containing 20% below 3 mm. These data compare with Lurgi's specified feed-coal of 7% maximum below 5 mm.

The upper limit for fines is a function not only of the size but also of the caking properties of the coal, as mildly caking coal tends to agglomerate the fines. There is also an economic balance between the quantity of fines and the rated output of each gasifier. A further area of uncertainty is the value assigned to the excess fines. While we have given these the same value in $/GJ as the feed coal, Braun (11,12) assumed 75% and Conoco (23) 90% of feed coal value. Conoco have presented the results of a market study on coal fines (49) which indicates, not surprisingly, that this value is a function of the end-use and quality of the fines. A range of between 40 and 98% of the value of the feed-coal was given.

Another possible option, examined by Conoco, is briquetting the excess coal fines. Conoco (50) came to the conclusion, without testing any coals, that the economics of briquetting fines, instead of selling them, were marginally attractive. The ability to make and use briquettes is governed by binder quality and the properties of the coal fines, and any general conclusions are inappropriate.

In this report we have assumed that the coal fines could be sold at the same price as the coal feed. By doing so, we eliminate the economic effects of the coal fines. For this reason, we have not needed to make any assumptions about the ability of the gasifier to handle fines, or about the amount of fines in the feed coal.

Recognising however, that these assumptions will not always be correct, Figure 15 is a nomograph showing the effect on SNG costs of:

- the value of the fines (as % of coal costs)
- the fines in the coal feed (% of thermal energy)
- the allowable fines to the process (% of thermal energy of coal to gasifiers)

We have shown on Figure 15 two typical sets of data (A-F) and (W-Z). Lines A-F are for a coal feed containing 60% fines (point A). The gasifiers are assumed to be capable of handling 10% of their feed as fines without de-rating (point B). The surplus fines will represent 45% of total coal feed (point E). The increase in SNG costs (point F) relative to the base values used elsewhere in this report, is shown for $1/GJ coal (point C) with fines valued at 80% of this (point D). Lines W-Z show the maximum amount of fines (20%, point W) that can be handled assuming no fines to the gasifier (point X), without exporting any coal fines or having any effect on process economics (points Y and Z).

We have assumed that by-product ammonia, phenols, oil and tar are consumed in partially satisfying the boiler fuel requirements, with the balance being made up with coal fines. Obviously, any export of these by-products serves to increase the amount of fines that can be consumed. The percentage of excess fines is also presented in the nomograph. Since the coal fines may have somewhat different calorific value, sulphur content and ash than the feed coal we have defined fines in terms of heat content (rather than as a weight fraction). The difference is likely to be small for practical purposes.

We conclude, from Figure 13, that with a typical run-of-mine coal, significant increases in SNG costs are unlikely as long as the excess coal fines can be sold for more than half the feed coal price (at low coal prices). For example, even with 60% fines in the feed, and allowing 10% fines to the gasifier, SNG costs for the dry-ash Lurgi process do not increase more than 10% compared with the base case, provided the excess coal fines are valued at more than about 55% of feed at a feed coal price of $1/GJ and 75% at $3/GJ.

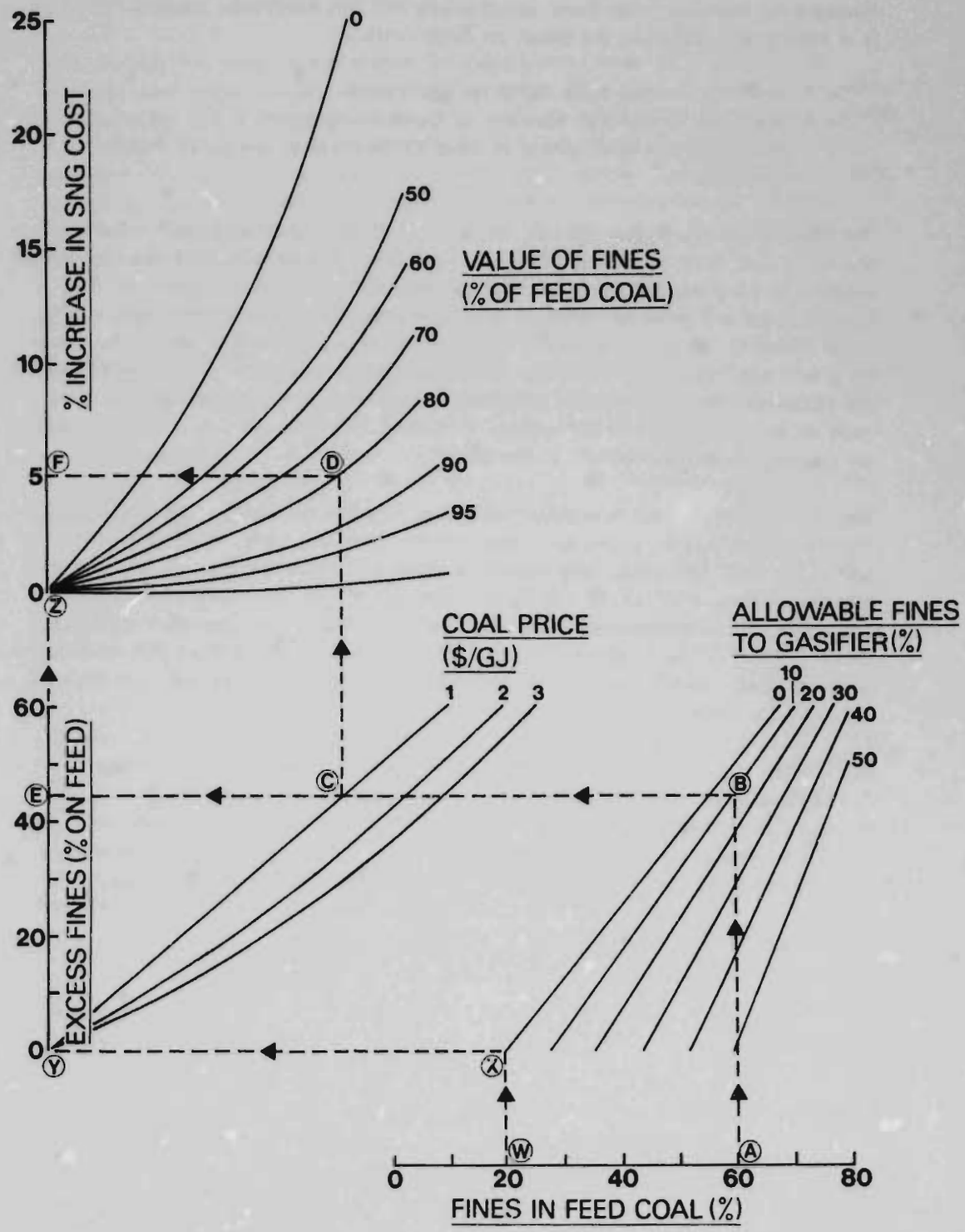

Figure 15 **Effect of coal fines on the economics of the dry-ash Lurgi process for SNG**
(Eastern US coal, 10% DCF, 'no-tax', by-products burnt, excess coal fines exported)

4.2 BRITISH GAS/LURGI PROCESS

This process has been demonstrated on a substantial scale (47,51-58) and is available with the minimum of development work. The ability to recycle tars, other hydrocarbons and phenols to extinction through the tuyeres in the slagging process is significant but does require confirmation over an extended period. The data presented in this report do not include this recycle. British Gas indicate that caking coal containing up to 40% fines has been handled without using the tuyeres for fines injection (which has been demonstrated). We are unsure about the ability of this process to handle high-ash coals or highly refractory ash.

We have evaluated this process for **SNG production** with conventional, sulphur-resistant shift and separate methanation catalysts and also with the British Gas-developed HCM process, which uses a combined shift and methanation catalyst. The conventional two-step process shows only modest gas cost savings (typically 8%) compared with the dry-ash Lurgi process on Eastern US coal. This is not unexpected, as one of the major advantages of the process, low steam consumption, is essentially nullified by the need for additional steam to meet the 2:1 steam to CO ratio required for the shift reaction.

The combined shift-methanation route using the British Gas HCM process looks considerably more attractive. From Figures 4 & 13, it can be seen that the British Gas/Lurgi process and the HCM route shows an advantage over the dry-ash Lurgi process on Eastern US coal of about 20%. If 1981 oil-related by-product values are used (Figure 8) these advantages increase slightly at low coal costs. Capital requirements are 25% lower while coal consumption is 17% lower compared with dry-ash Lurgi.

The HCM process (59) has not yet been tested at the pilot plant stage, and this is an obvious pre-requisite before commercialisation. Some comparative data on the generally similar Conoco Super-meth process (42,60) are presented in Table 14. Other combined shift-methanation catalysts have been developed and can be expected to show generally comparable results (38,40,41).

Table 14 British Gas/Lurgi with combined shift/methanation catalyst

Licensor	**British Gas**		**Conoco**	
Reference	**(40)**		**(82)**	
Route	**Conventional Shift and Methanation**	**HCM**	**Conventional Shift and Methanation**	**Super-Meth**
Relative investment	100	85	100	87
Absolute change in thermal efficiency	—	+7%	—	+2%
Relative off-site steam generation	100	58	100	79
Relative gas cost[1]	100	87	100	91

Note:

1 $1/GJ coal, 'no-tax', 10% DCF

As can be seen, while investment costs and gas costs are in reasonable agreement, there is a substantial difference in the absolute change in thermal efficiency. This appears to stem from differences in steam generation for the two processes.

For **MCG production**, Figures 5 and 14 show that the cost of MCG from the British Gas/Lurgi process is likely to be about 30% lower than that from the dry-ash Lurgi process. This comparison is unaffected by the choice of by-product values (see Appendix E). Capital requirements are typically some 40% lower, with coal consumption down by some 18%. We note, in particular, significant capital cost savings in the gas cooling, process condensate treating and steam systems. This process is clearly highly attractive for producing MCG in a modest sized plant. It should be noted however that the MCG produced contains CO and CO_2; it is not suitable for domestic or process use without further treatment (and significant expense).

As with the dry-ash Lurgi process discussed in Section 4.1 there does appear to be a significant learning curve with this gasifier. Thus, the data we have used (21) give lower steam and oxygen consumption than earlier published information (53,57). This can be seen from the following table.

Table 15 British Gas/Lurgi gasifier performance
Basis: Pittsburgh No. 8 coal

Date **Reference**	**June 1978** **(34)**	**Nov/Dec 1979** **(79)**	**June 1981** **(40)**
Coal gasification rate (t maf/m^2/h)	3.27 - 4.24	3.22 - 4.00	4.24
Steam consumption (t/t maf coal)	0.42 - 0.43	0.39	0.38
Oxygen consumption (t/t maf coal)	0.56	0.59 - 0.60	0.52

Our comparisons have been based on Pittsburgh No. 8 and Illinois No. 6 coals. These are typical Eastern US coals with comparatively low ash melting points. While this results in a heavy steam requirement with the dry-ash Lurgi process, it enhances the relative economics of the British Gas/Lurgi slagging gasifier. We would expect to see a substantial narrowing of the differentials when a more normal ash melting point coal is processed.

4.3 EXXON CATALYTIC PROCESS

Because of the high methane production in the gasifier, this process has only been considered for SNG production.

This process has so far been demonstrated in small pilot plants with capacities of up to 40 kg/h. It is at a relatively early stage of development compared with the other processes in this report.

The information presented by Braun (26) was based upon pilot plant tests on Illinois No.6 coal with modifications suggested by Exxon. This adjustment of the

data to Pittsburgh seam coal can only be approximate in the absence of information from the pilot plants, particularly on the long-term activity of the catalyst and its recovery. The lower conversion and additional capital costs (61) necessitated by the need to pre-oxidise caking coals is not included. Exxon's current thinking on catalyst recovery is similarly not included, nor have we been able to reflect the lower-than-expected methane yield (62). On the other hand, there is some evidence that Exxon's design basis is conservative relative to some of the other designs we have used, particularly with respect to on- and off-site integration. We do not have enough information, especially about the process energy balances, to be certain on this point. Thus, our conclusions with respect to the Exxon Catalytic process are necessarily tentative and subject to confirmation when data become available from the planned 4 t/h plant at Rotterdam, Netherlands. The data we have used are summarised in Appendices B, C and D.

It could be seen from Figures 4 and 13 that the Exxon Catalytic process appears to have an advantage of between 3 and 9% relative to dry-ash Lurgi depending on the cost of coal, the value of by-products and the required DCF rate-of-return. Arising from the relatively high thermal efficiency of the process (62% compared with 53 – 55% for dry-ash Lurgi on Eastern coal) the relative economics will improve with increasing coal cost.

One additional factor to be considered with this process is the use and recovery of the catalyst. In the Exxon reports (24,25) a potassium hydroxide (caustic potash) solution was assumed together with calcium hydroxide (slaked lime) digestion and multi-stage counter-current water washing to recover 87% of the catalyst. Some data were also presented without calcium hydroxide digestion, giving a lower catalyst recovery of 70% with lower capital costs. We have estimated economics for both 50 and 70% catalyst recoveries and some typical data are presented in Table 16.

Table 16 Exxon Catalytic process – catalyst recovery
Basis: 3000 MWt-250 x 10^9 BTU/SD SNG plant, Eastern US coal
10% DCF, 'no-tax', by-products burnt

Catalyst Recovery (%)	Catalyst Recovery Method	SNG costs in $/GJ with coal at		
		$1/GJ	$2/GJ	$3/GJ
87	Digestion+washing	6.28 (4.8)	7.94 (7.0)	9.61(8.5)
70	Water washing only	6.51 (1.2)	8.18 (4.3)	8.85(6.2)
50	Water washing only	6.94(−5.3)	8.61(−0.7)	10.27(2.2)

Note: Figures in brackets ( ) are percentage cost savings relative to the dry-ash Lurgi process. A negative sign implies cost **increases**.

As can be seen from the above table, the more complex catalyst recovery scheme does show some economic advantages, which is in agreement with Exxon's conclusions. As expected, there are significant penalties at lower catalyst recoveries, which suggest that a comparatively high recovery is a fundamental requirement. We do not doubt that this can be achieved, however it does raise the question of the flexibility of the process to handle different coals. It is likely that the quality and

composition of the ash (particularly silica content) will have an effect on catalyst recovery. We have not seen any information addressing this particular subject.

Table 17 shows some typical data on catalyst costs. As can be seen, varying the cost of potassium hydroxide by ±50% changes the cost of SNG by 13 - 14¢/GJ. We conclude that the economics of this process are fairly insensitive to likely changes in the cost of the catalyst provided that the process operates with high catalyst recovery (70% or more).

Table 17 Exxon Catalytic process – catalyst costs
Basis: 3000 MWt—250 x 10^9 BTU/SD SNG plant, Eastern US coal at $1/GJ, 10% DCF, 'no-tax', by-products burnt

Cost of potassium hydroxide[1] ($/t)	SNG cost ($/GJ)	Cost savings relative to dry-ash Lurgi (%)
200	6.14	6.9
400[2]	6.28	4.8
600	6.41	2.7

Notes:
1 100% basis.
2 $400/t was used for the base-case.

4.4 SHELL COAL PROCESS

For SNG production the Shell Coal process shows almost the same economics as the dry-ash Lurgi process on Eastern coal (Figures 4 & 13). The Shell Coal process has a cost advantage of between 2 and 6% depending on the cost of coal, the value of by-products and the required DCF rate-of-return.

The Shell Coal process gives a raw gas with a high $CO:H_2$ ratio and virtually no methane (see Table B4). This requires large shift and methanation facilities for SNG production. The Shell Coal gasifier has a very low steam consumption and hence produces a virtually water-free raw gas. Consequently a combined shift/methanation process, such as the British Gas HCM process, does have significant advantages. However, in both cases, the production of substantial quantities of CO_2 largely eliminates the benefits of the very low gasifier CO_2 production. This can be seen from Table 18 where an HCM-based route is compared with conventional sulphur-resistant shift-based route.

Table 18 Shell Coal process with combined shift/methanation catalyst
Basis: 3000 MWt—250 x 10^9 BTU/SD SNG plant, Eastern US coal 10% DCF, 'no-tax', by-products burnt

	Conventional Shift	HCM
Relative investment	100	92
Overall thermal efficiency (%)	55.8	59.1
Relative gas cost	100	92

The information supplied by Shell does not reflect the optimum process arrangement for SNG production. Moreover, there may be unnecessary duplication of equipment. The data given to us by Shell are based on each gasifier requiring its own coal pressurising and feeding train, waste heat boiler, solids removal and recycle gas compressor.

One significant advantage of this process, which it shares with Texaco, is that its economics are likely to be relatively insensitive to changes in coal type and size distribution. We would expect this process to handle a wide range of coals with little or no effect on the process economics (for a given $/GJ coal price). Obviously, this would need to be considered prior to the detailed design stage.

According to our data, some 18 MWe of power could be exported. In our base-case economics, discussed above, we assumed a price of 4¢/kWh. We also looked at 2.5¢/kWh, which typically increases gas costs by 3¢/GJ (0.5%), which is clearly not significant.

For **MCG production** the Shell Coal process shows gas costs typically about 30 - 36% less than dry-ash Lurgi, depending on the cost of coal and the required DCF rate-of-return (higher at low coal costs and high DCF rates-of-return). Using 1981 oil-related by-product values the cost advantages are reduced to about 23%. These cost savings result from lower coal consumption (some 16%) and significantly lower capital costs (some 46% for 500 MWt - 40 x 10^9 BTU/SD output).

As discussed above in relation to SNG production, we have assumed that each gasifier will require its own coal pressurising and feeding train, waste heat boiler, solids removal and recycle gas compressor. We think that some further capital cost savings are feasible by combining, for example, the recycle gas compression equipment for all the trains. We do not have information at present to examine this.

4.5 TEXACO PROCESS

For **SNG production** the Texaco process, with a 65% slurry feed concentration, has inferior economics relative to the dry-ash Lurgi process. This disadvantage ranges from 7 to 14% depending on the cost of coal, the value of by-products and the required DCF rate-of-return (Figures 4 and 13). The Texaco process gives a raw gas with a high $CO:H_2$ ratio and virtually no methane. This requires large shift and methanation facilities for SNG production. For this reason we do not think that Texaco is a serious prospect for SNG.

While operation at 65% slurry concentration is the design basis for the Ruhrchemie/Ruhrkohle Oberhausen-Holten pilot plant (63), it has been reported (64,65) that this plant has operated satisfactorily at 70% slurry feed concentration. Some doubts remain, for example, the recent tests on Illinois No. 6 coal at Oberhausen-Holten were performed at slurry concentration of 57-59% (66). Table 19 shows the effect of operating at only 50% slurry feed concentration. SNG costs increase typically by 16%. The effect of a relatively small change in design parameters is noteworthy. In our earlier work (2) we showed that entrained processes, such as Saarberg-Otto, Shell Coal and Texaco were sensitive to the degree of high-level heat recovery, and feed concentration and temperature. There is an obvious need to demonstrate all these features.

Table 19 Texaco process for SNG – slurry concentration
Basis: 300 MWt (250 x 10^9 BTU/SD) SNG plant, Eastern US coal
10% DCF, 'no-tax', by-products burnt

	Slurry concentration[1]	
	65%	50%
Relative investment	100	118
Overall thermal efficiency (%)	55.6	49.9
Relative gas cost	100	116

Note:

1 Defined as moisture-free coal per unit of total feed.

In the above data the calculated 52 MWe of export power (at 65% slurry concentration) was valued at 4.0 ¢/kWh. We also looked at 2.5 ¢/kWh, which typically increases gas costs by 9 ¢/GJ (1.3%), which is clearly not significant.

One significant advantage of entrained processes is that their economics are likely to be relatively insensitive to changes in coal type and size distribution. We expect this type of process could be designed to handle a wide range of coals with little or no effect on the process economics (for a given $/GJ coal price). Further, it is conceivable to switch from a residual oil feed to coal at some stage in the plant's life. This may ease the introduction of this process.

For **MCG production** cost savings for Texaco (with a 65% slurry feed) relative to dry-ash Lurgi range from 16 to 19%. These gas cost savings are a result of both lower coal consumption (some 10%) and 24% lower capital costs for 500 MWt (40 x 10^9 BTU/SD) output.

The capital costs we have used for the Texaco gasifiers are based on information supplied by Texaco and presented by Braun (20). While these costs can be reconciled with those presented by Parsons (67), they are appreciably higher than the estimate by Fluor (15).

The capital costs presented for both SNG & MCG include a substantial investment in an off-site boiler which would be required only to start-up the process (or an additional train). Optimisation of the steam system, ie obtaining a better balance between waste heat generation and start-up requirements, could marginally improve these economics.

Generation of superheated steam, as with Shell Coal, would also contribute. On the other hand, the nature of the Texaco process, with much more integration between the gasifier and the plant steam system, is likely to lead to more sophisticated control systems, which are not reflected in the costs presented here. Nevertheless, the Texaco process is clearly attractive for producing MCG in a relatively modest-sized plant. It is likely to be even more attractive where steam for start-up is already available, or where excess steam during normal operation can be readily consumed.

4.6 BCR BI-GAS AND IGT HYGAS PROCESSES

Both of these processes have high methane production from the gasifier and are only suitable for SNG production.

At first sight, BI-GAS and HYGAS appear attractive on Eastern coal, with about 21 and 15% gas cost improvement over dry-ash Lurgi, respectively. On Western coal only HYGAS is attractive with cost savings of about 11%.

However, we note that the steam/oxygen and oxygen/coal ratios used for the Braun Eastern design (12) for BI-Gas are substantially lower than for the pilot plant design (68) on a similar coal. Moreover, the pilot plant has never operated on this coal. The only coal the pilot plant has processed is a Western coal, on which the economics look unfavourable. Moreover, the pilot plant has achieved a methane yield of about 10% (69) compared with 14.5% used in the Braun Western design. Arising from this lack of demonstration comes the conclusion that the development risk with BI-GAS is somewhat higher than most of the others considered here. Further, the apparent cost advantages outlined above are likely to be reduced in the course of demonstration.

For HYGAS, we have used data derived from IGT's computer model and supplied by them to Braun (11,12). These show a 97% carbon conversion.

Doubts have been raised about the IGT model (70), while an examination of the HYGAS pilot plant data (71) suggests that in steady-state operation the carbon conversion is significantly lower than IGT predictions, with a substantially higher steam consumption. For this reason, we have assumed a 30% higher steam consumption in our work. Table 20 shows the effect of lowering the carbon conversion towards the pilot plant level using the western coal and assuming that the resulting char can be burnt (which has not been demonstrated). As can be seen, at a carbon conversion of 80%, the process offers no advantages over the dry-ash Lurgi process. Carbon conversions greater than 80% have not been demonstrated on a steady-state basis and this must be regarded as an **essential** pre-requisite for the commercialisation of this process.

Table 20 HYGAS process – lower carbon conversion

Basis: 3000 MWt—250 x 10^9 BTU/SD plant, Western US sub-bituminous coal, 10% DCF, 'no-tax', $1/GJ coal, by-products burnt.

Carbon conversion (%)	97[1]	90	80	70
Overall thermal efficiency (%)[3]	74	71	65	62
Total capital investment[2] (mid-79 $ x 10^6)	1195	1256	1335	1393
Coal required (TJ/d)	358	372	406	427
Gas cost ($/GJ)	4.63	4.85	5.18	5.42
Savings relative to dry-ash Lurgi on Western coal (%)	11	7	0	−4

Notes:

1. Based on IGT process assumptions (9) with 30% higher steam consumption.
2. Includes contingency, engineering, royalty, initial catalyst and chemicals, working capital and start-up costs.
3. Excludes sulphur and ammonia. Based on nigher heating values.

5. CONCLUSIONS

The conclusions of this study apply to the base-load operation of substantial gasification plants (500 MWt (40 x 10^9 BTU/SD) or 3000 MWt (250 x 10^9 BTU/SD) and load factor of 0.85). It should be borne in mind that the differences between the various processes are relatively small and that the comparisons are sensitive to quite small changes in process parameters (such as carbon conversion or slurry concentration) and capital costs. Also, gas costs have been calculated on the assumption of a mature technology and will be significantly higher for 'pioneer' plants. These results are therefore indicative; more definite conclusions would require data derived from the actual performance of large plants, which is not available. We have not included any gas distribution costs.

5.1 SNG PRODUCTION

(1) Large SNG plants (3000 MWt - 250 x 10^9 BTU/SD) cost in the range \$1.3 - 1.8 x 10^9 (in 1979 \$). This excludes interest during construction and escalation. Using representative coal prices and financial conventions we obtain typical SNG costs as follows:

Table 21 Typical SNG costs

DCF rate-of-return	SNG costs (\$/GJ) 5%	10%
North America[1]		
Western coal at \$0.5/GJ	3.7 - 5.3	5.3 - 7.9
Bituminous coal at \$1.5/GJ	5.4 - 7.2	7.0 - 9.8
Europe & Japan[2]		
W German lignite at \$0.9/GJ	4.1 - 5.6	5.1 - 7.2
Imported coal at \$2/GJ	5.7 - 7.7	6.7 - 9.6
Imported coal at \$3/GJ	7.3 - 9.6	8.3 - 11.2

Notes:

[1]Using 'North American' financial conventions – see Section 2.2
[2]Using 'no-tax' financial conventions – see Section 2.2

The above data show that the cost of SNG from Western US coal is comparable with Mexican and Canadian imports of natural gas into the US at about \$5/GJ. Similarly, assuming that W German lignite can be gasified with the same economics as Western US coal, SNG so produced is broadly competitive with Algerian (\$6/GJ) or Russian gas (\$5/GJ) imported into Europe. SNG produced from Eastern US coal, or from relatively cheap imported coal into Europe or Japan is only competitive under the most favourable of conditions, such as very low rates-of-return.

(2) We cannot see any major cost break-throughs with the processes considered. We do not entirely rule out the possibility that some other process might offer the chance of greater savings, though such a process would be at a comparatively early stage of development.

(3) The British Gas/Lurgi process (with HCM combined shift/methanation catalyst) has a cost advantage of about 20% compared with dry-ash Lurgi on Eastern US coal. This cost advantage is close to the difference between Eastern and Western (sub-bituminous) coal with dry-ash Lurgi. The Eastern coal is a poor one for dry-ash Lurgi as it has a low ash melting point and is relatively unreactive. We would therefore expect other coals to lie between the Eastern and Western gas costs and to somewhat reduce the potential improvement from the British Gas/Lurgi process. In addition, the HCM stage with the British Gas/Lurgi process requires demonstration. Both the British Gas/Lurgi and dry-ash Lurgi processes appear attractive for **SNG production**. With both processes we note some differences between published and assumed performance. While we are confident that the assumed performance can be eventually achieved, this may well not happen in 'pioneer' plants. The British Gas/Lurgi process is likely to be more flexible than dry-ash Lurgi in terms of coal type and size distribution. This may be attractive to those countries dependent on importing coal from a wide variety of sources.

(4) The Exxon Catalytic process **appears** to have only marginally superior economics compared with dry-ash Lurgi, with cost savings of about 3 – 9%. While we think that Exxon are conservative in their estimates (though we have eliminated a good deal of this), we do not see any major cost break-throughs with this process. We stress, however, that our information on this process is limited and that our conclusion is necessarily tentative. This process is at an earlier state of development compared with the others examined in this report.

(5) The Exxon Catalytic process is sensitive to the level of recovery of the catalyst used. Our analysis suggests that catalyst recoveries in excess of 70% are required. While this level of recovery has been obtained in the pilot plant it will require demonstration on a large-scale continuous basis. We have no information on the likely sensitivity of catalyst use and recovery to different types of coal.

(6) The Shell Coal process (with HCM combined shift/methanation catalyst) is only marginally superior to the dry-ash Lurgi process (2 – 6%). We do not think that this process is under serious consideration for **SNG production**. We think that the economics of the process are likely to be relatively insensitive to changes in coal type and size distribution. This may be attractive to those countries dependent on importing coal from a wide variety of sources.

(7) The Texaco process for **SNG production**, even at 65% slurry concentration, has inferior economics relative to dry-ash Lurgi. We do not think that this process is under serious consideration for SNG production. Like the Shell Coal process, we think that the economics of the process are likely to be relatively insensitive to changes in coal type and size distribution. This may be attractive to those countries dependent on importing coal from a wide variety of sources.

(8) The economics of the Texaco process are profoundly affected by the concentration of the feed coal-slurry. We do not have any information as to whether high (65%) concentrations can be maintained on a continuous basis for all types of coal. One advantage of the Texaco process may be the ability to change a plant from being oil-based to being coal-based at some stage.

(9) While at first sight, both BI-GAS and HYGAS appear attractive on Eastern coal, the achieved performance of these processes falls far short of the estimates we have used. Thus, BI-GAS has never operated on the Eastern coal and has inferior economics relative to dry-ash Lurgi on the Western coal, on which it has operated. At the achieved carbon conversion of 80% the economics of the HYGAS process show no improvement over dry-ash Lurgi.

(10) The effect of valuing by-products at oil-related, as opposed to the more conservative coal-related prices used in the body of this Report (see Section 3.3), is to improve the economics of dry-ash Lurgi and British Gas/Lurgi relative to the other processes. The economics of the British Gas/Lurgi are improved by about 16%. This is not enough to modify our conclusions about the competitiveness of SNG. Moreover, we have not considered any upgrading costs. We doubt whether these higher by-product prices can actually be achieved, in the context of several, large SNG complexes located in many cases well away from potential by-product markets.

(11) While the precise amount of fines that dry-ash Lurgi gasifiers can handle is uncertain, under most conditions the use of run-of-mine coal is unlikely to significantly affect the economics of this process for SNG. For example, even with 60% fines in the feed and allowing 10% to the gasifier, while consuming all the tar and naphtha in the off-site boilers, SNG costs do not increase by more than 10% unless the excess fines are valued at less than 55% of feed with \$1/GJ coal or 75% of feed with \$3/GJ coal.

5.2 MCG PRODUCTION

(1) We assume that highly reliable, and hence multi-stream, stand-alone plants will be required if centrally manufactured MCG is to be substituted for oil or natural gas. We also assume that CO-containing fuel gas can be distributed through local networks. This gas is not suitable for distribution to domestic consumers. Removal of CO for this purpose will give higher gas costs, comparatively close to those quoted for SNG.

(2) Large MCG plants (3000 MWt – 250 x 10^9 BTU/SD) cost in the range \$0.7 – 1.2 x 10^9 (in 1979 \$). This excludes interest during construction and escalation. Using representative coal prices and financial conventions we obtain typical MCG costs as follows:

Table 22 Typical MCG costs (3000 MWt – 250 x 10^9 BTU/SD)

DCF rate-of-return	MCG costs ($/GJ) 5%	10%
North America[1]		
Coal[3] at $0.5/GJ	2.1 - 3.4	3.0 - 4.8
Coal[3] at $1.5/GJ	3.5 - 4.9	4.3 - 6.4
Europe & Japan[2]		
Coal[3] at $0.9/GJ	2.6 - 3.7	3.1 - 4.6
Imported coal[3] at $2/GJ	3.9 - 5.4	4.5 - 6.3
Imported coal[3] at $3/GJ	5.2 - 7.0	5.7 - 7.9

Notes:

1 Using 'North American' financial conventions – see Section 2.2
2 Using 'no-tax' financial conventions – see Section 2.2
3 Illinois No.6-type coal

These costs are 50 -- 75% of the corresponding SNG cost (see Figure 6). They are a function of the process and especially of the number of gasifiers and parallel processing trains required. Hence they are also affected by the precise scale examined.

(3) While the economics are attractive, we think that relatively few MCG plants of this scale are likely to be built – though obviously both the Ruhr and the US Gulf Coast are feasible locations. We consider a 500 MWt (40 x 10^9 BTU/SD) plant as much more likely at this stage of development. Obviously, modest increases or decreases in scale will not invalidate our conclusions. A plant of this size is rather less likely to be located at the minemouth.

For a 500 MWt (40 x 10^9 BTU/SD) MCG plant, investments are (in 1979 $) $300 x 10^6 for dry-ash Lurgi and about $170 – 230 x 10^6 for British Gas/Lurgi, Shell Coal and Texaco processes. On a 'no-tax' basis with coal delivered at $2/GJ and 10% DCF rate-of-return this gives gas costs of $8.3/GJ and $5.6 – 6.8/GJ respectively. This is shown in Figure 3. Corresponding 'North American' with-tax costs are $9.6/GJ and $6.3 - 7.9/GJ. A 10% DCF rate-of-return may not be acceptable for industrial (as opposed to utility) ventures in all the member countries. The rate-of-return has a serious impact on gas costs, as can be seen from the data in Appendix E.

(4) There are no cost savings for a 500 MWt (40 x 10^9 BTU/SD) dry-ash Lurgi MCG plant compared with a 3000 MWt (250 x 10^9 BTU/SD) SNG plant. The advantages of scale with the 3000 MWt SNG plant almost exactly balance the capital cost savings and higher thermal efficiency with the simpler MCG plant. We conclude that dry-ash Lurgi does not look attractive for MCG production in countries with an existing gas distribution network and large demands for gas – sufficient to support the size of SNG plant outlined above.

(5) By contrast, British Gas/Lurgi, Shell Coal and Texaco (65% slurry) look attractive, even at the 500 MWt (40 x 10^9 BTU/SD) level. The Texaco process shows gas costs about 20% higher than British Gas/Lurgi or Shell Coal which both have similar gas costs. This is based on capital cost data supplied by Texaco and presented by Braun (20) and is entirely consistent with other

estimates by Fluor (15). All these processes are competitive with gas-oil or No. 2 heating oil at about $7/GJ (end-1981) in Europe, North America or Japan.

5.3 GENERAL CONCLUSIONS

(1) There is a close relationship between gasifier process parameters, such as carbon conversion, oxygen and steam consumption, and the cost of the plant. Changes in these parameters will generally have a much greater effect on total plant costs than changes in the process equipment itself. Hence, the use of contingency factors as large as 50% on the cost of gasifiers may not be enough to account for likely changes in process parameters.

(2) A further degree of uncertainty is that the processes are all at different stages along the path from conceptual design to commercial reality. Thus, one might expect that the costs of the various processes could increase to different levels by the time they are fully developed. There is no easy way to overcome this difficulty by numerical analysis, though we believe that the data presented in this report are neither optimistic nor pessimistic.

(3) The comparisons made in this report are based on capital costs derived from estimates given by the organisations responsible for the designs. We do not think that their accuracy is better than ±30% and this level of accuracy must be considered in relation to our conclusions.

(4) For a given type of gas – SNG or MCG – the choice of process in general (but **not** the absolute level of gas costs) is unaffected by most **economic** parameters, such as, DCF rate-of-return, debt/equity ratio, taxation, load-factor and price of coal. This conclusion also holds for a given set of by-product values. These conclusions will not hold, of course, if the make-up of gas costs is very different, as for example, with in-situ gasification. Obviously, as discussed above, the type of coal available does have a significant impact on the choice of process. Our unpublished work suggests that the differences in the costs of constructing large SNG plants on a normal site in the member countries are generally less than the uncertainty in the capital cost in any one country. Hence, we conclude that, in general, the choice of gasification process is very largely independent of the country under consideration. International co-operation in this field is, therefore, likely to be of mutual benefit to all the countries concerned.

(5) The most suitable coal for gasification is a cheap one! In general terms, reactive coal with low moisture and ash are preferred. Low sulphur and high oxygen also serve to reduce gas costs. Data on **dry-ash Lurgi** SNG plants (11,12,72) suggest that a typical US lignite (38% moisture, 5% ash) is preferable to sub-bituminous coal, which is in turn preferable to bituminous coal.

There are only small economic penalties for gasifying high sulphur and/or oxygen coal with relatively low calorific value. This particular conclusion should hold with most of the other processes. Since the demand for these types of coal for power generation may well be limited, this could have significant implications for world trade in coal.

(6) The effect of decreasing MCG plant size from 3000 MWt to 500 MWt (250 to 40 x 10^9 BTU/SD) is to increase gas costs by 30 to 40% depending on the particular process, for $1/GJ coal at 10% DCF rate-of-return. With $3/GJ coal these increases are about halved, though obviously starting from a higher base-level. Our data suggest that while there are significant benefits of scale where coal is relatively cheap, these benefits are much less significant with high-priced coal. We would expect to see the same effect with SNG plants.

(7) We have confirmed that both the National Coal Board's ARACHNE (67) and DSM (19) process models can be used to describe the Shell Coal and Texaco processes adequately. The models are both essentially single-stage equilibrium models. Such a model should, therefore, be able to predict the behaviour of other high-temperature processes as well, such as Saarberg-Otto.

6. APPENDICES

APPENDIX A PROCESS DESCRIPTIONS AND STATUS

The information given in this appendix is in large part a summary of the results of a previous EAS report (2). Developments since this report have been incorporated as far as possible.

A.1 PROCESS DESCRIPTIONS

SNG production

Each process considered differs in the type of gasification reactor and, hence, in the pressure, temperature and composition of the product gas. This of course affects the size and operation of the downstream processing steps. However, in general, the process schemes are as illustrated in Figures A1 – A3 and as described below.

First, the coal undergoes some pre-treatment depending on the particular gasification process. This may simply be drying and pulverizing or may involve more complex steps such as pre-oxidation or slurrying with water. The details of the pre-treatment, coal feeding and size requirements for each process are given in Table A1.

In the gasifiers several reactions take place. In the absence of any recycle or catalyst the predominant reaction is the highly endothermic (heat absorbing) formation of carbon monoxide and hydrogen from carbon and steam. The heat for this reaction is provided by burning coal with oxygen, producing carbon dioxide. In the lower temperature gasifiers, such as dry-ash Lurgi or British Gas/Lurgi methane is also produced in the gasifier. In the Exxon Catalytic process a potassium-based catalyst enhances the reaction of carbon and steam and enables the highly exothermic (heat releasing) methanation reaction to take place – methane formation from carbon monoxide and hydrogen. This eliminates the need to burn coal in the reactor, and hence the oxygen plant, but does require the recycle and preheating of carbon monoxide and hydrogen.

After cleaning and cooling, the composition of the raw gas is adjusted. With the dry-ash Lurgi, BI-GAS, HYGAS and Texaco processes (Figure A1) part of the raw gas undergoes shift conversion; carbon monoxide reacting with the excess steam to produce the required hydrogen for methanation. Insufficient steam is present in the British Gas/Lurgi and Shell Coal processes and may either be added and a conventional shift catalyst used, as above, or a combined shift-methanation catalyst used, eg the HCM process (Figure A2). This catalyst is not sulphur resistant and consequently sulphur compounds, primarily hydrogen sulphide, must first be removed. No shift conversion is required with the Exxon Catalytic process (Figure A3).

With all the processes, acid gas, mainly carbon dioxide and hydrogen sulphide (if still present), is then removed. Except when a combined shift-methanation catalyst is used, or in the Exxon Catalytic process, carbon monoxide and hydrogen are catalytically reacted to produce methane. In the Exxon Catalytic process the methane

Table A1 Description of gasification processes[1]

Process Name	Dry-ash Lurgi	British Gas/Lurgi	BI-GAS	Exxon Catalytic	HYGAS	Shell Coal	Texaco
Type	Moving bed	Moving bed	Entrained	Fluidized bed	Fluidized bed	Entrained	Entrained
Gasifier description	Single stage, non-slagging. Counter-current flow of coal and gas	Modified Lurgi – slag tap, tuyeres to inject steam and oxygen	Coal fed to upper stage. Residual char entrained in gas and returned to lower stage where gasified with steam and oxygen	Single stage. Coal impregnated with catalyst and H_2/CO mixture recycled. Oxygen plant not required	Three-stage hydro-gasification. Direct hydrogenation in two reactor stages. H_2 produced by steam-oxygen char gasification	Refractory-lined vessel with opposed firing and liquid slag removal from the bottom	Refractory-lined vessel downwards firing into radiant boiler. Slag collects in water bath at bottom
Operating temperature	Gas outlet: 300-650°C Bottom: 1200°C	Gas outlet: 300-550°C Bottom: 1500°C	(1) 900°C (2) 1500°C	700°C	(1)650-750°C (2)900°C (3)1000°C	Gas outlet: 1500°C	Gas outlet: 1500°C
Operating pressure	20-30 atm	As Lurgi	52 atm	34 atm	68 atm	30 atm	40 atm
Coal requirements	Preferred properties: weakly caking, high reactivity. Low ash melting point undesirable	High ash melting point undesirable.	Any – high ash melting point undesirable.	Caking coals require pre-treatment	Caking coals require pre-treatment	Any – high ash melting point undesirable. Low moisture and ash preferred	Any – high ash melting point undesirable. Low inherent moisture desirable.
Coal pre-treatment	Preheated with exit product gas within gasifier	As Lurgi	Dried to 3% moisture and pulverised	Dried to 4% moisture and pulverised. Impregnated with potassium hydroxide	Dried to 10% moisture. Surface oxidation of caking coals. Preheated with exit product gas within gasifier	Dried to 2-8% moisture and pulverised	Pulverised
Coal feed method	Lock-hopper and distributor	As Lurgi	Water slurry to spray drier	Pneumatic	Slurried with light aromatic oil or water	Pneumatic	Water slurry
Coal size	3 - 50 mm 7% fines max.	4 - 50 mm 15% fines max. Possibility of injecting fines through tuyeres	70% below 0.07mm	2 mm max.	1.2 mm max.	0.10 mm max.	0.20 mm max.
Ash removal	Revolving grate, lock-hoppers	Slag tap, quench chamber	Slag tap, quench chamber	Slurried with water prior to catalyst recovery	Slurried with water	Slag tap, quench chamber	Liquid slag quenched in water

Note:

1 Based on the current status of each process. See, however, discussion on individual process

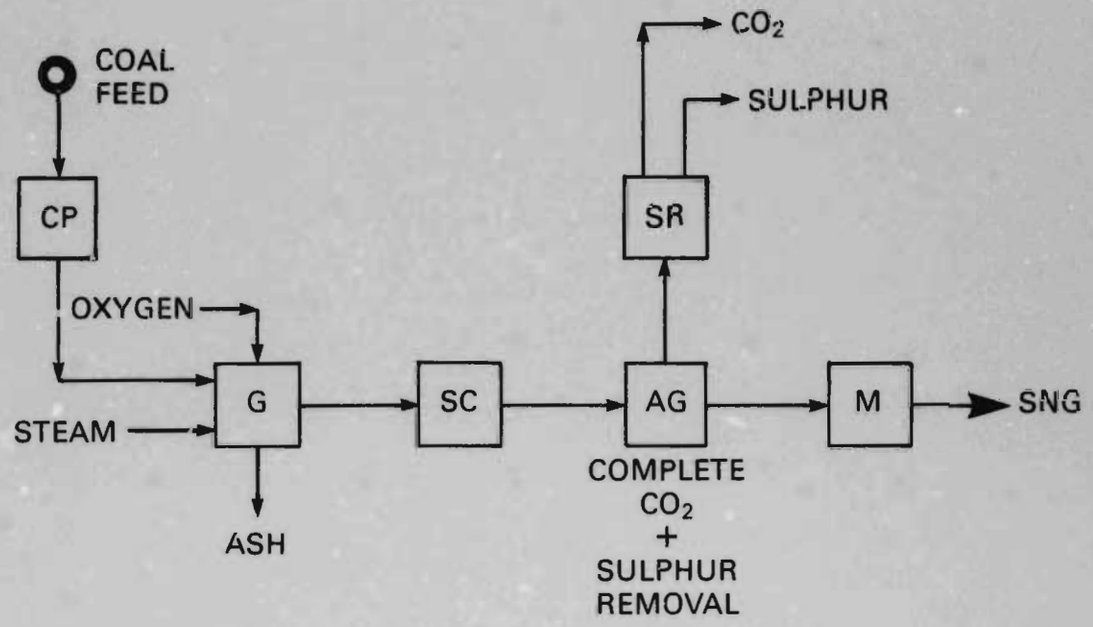

KEY: SEE BELOW

FIGURE A1 SULPHUR-RESISTANT CO-SHIFT CATALYST

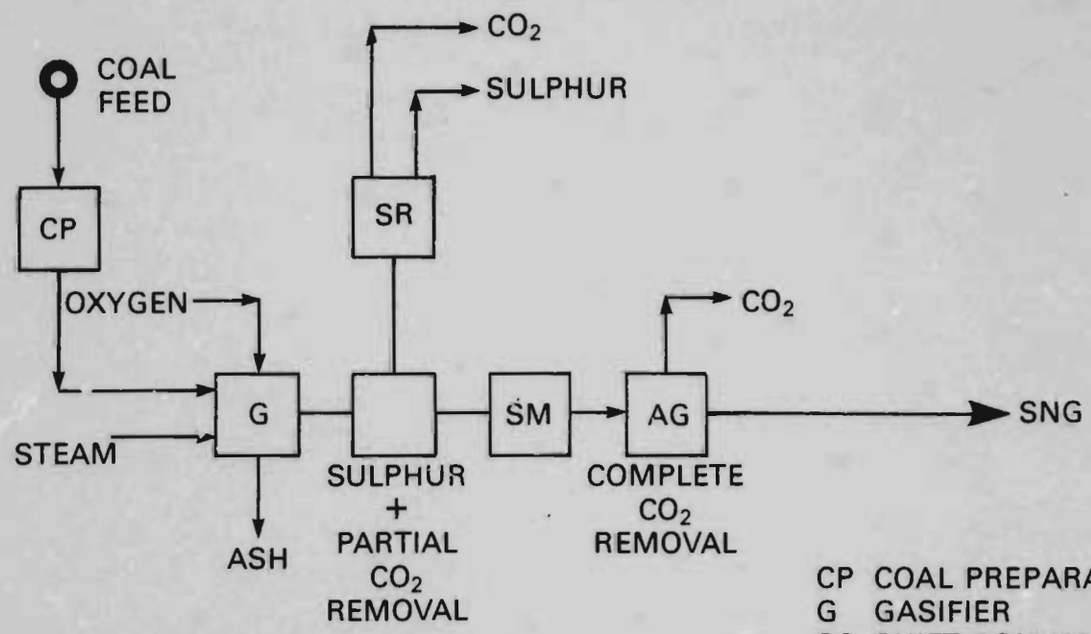

FIGURE A2 COMBINED SHIFT-METHANATION CATALYST

CP COAL PREPARATION
G GASIFIER
SC SHIFT CONVERSION
AG ACID GAS REMOVAL
SR SULPHUR RECOVERY
M METHANATION
SM COMBINED
SHIFT-METHANATION

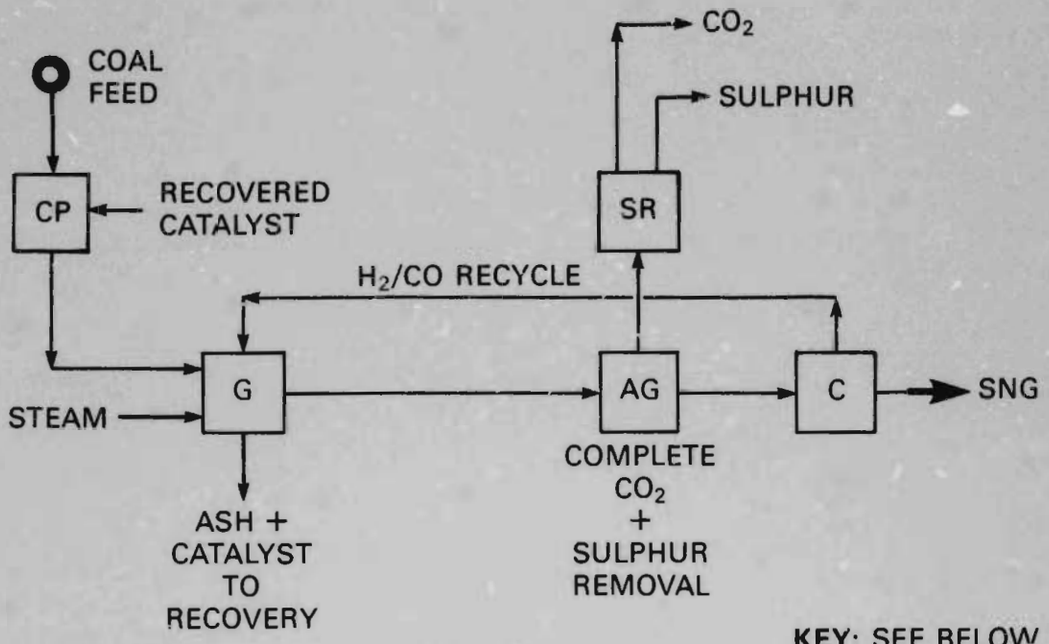

FIGURE A3 EXXON CATALYTIC PROCESS

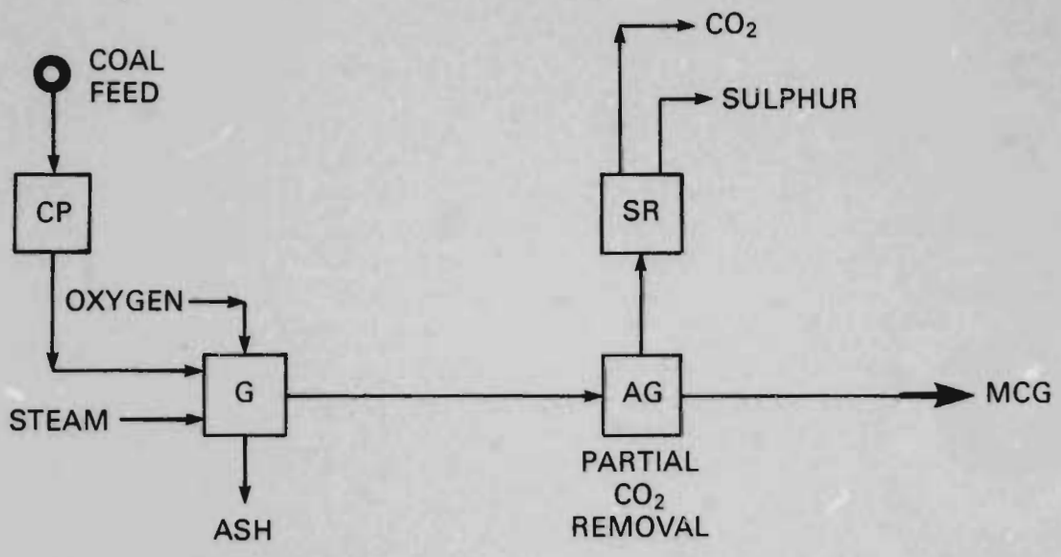

CP COAL PREPARATION
G GASIFIER
AG ACID GAS REMOVAL
SR SULPHUR RECOVERY
C CRYOGENIC SEPARATION

FIGURE A4 MCG PRODUCTION

is separated cryogenically and the carbon monoxide and hydrogen recycled. With the dry-ash Lurgi, British Gas/Lurgi and Exxon Catalytic processes the gas is compressed to 70 atm delivery pressure.

MCG production

As can be seen from Figure A4, this is essentially similar to the production of SNG, except that we have assumed that shift conversion and methanation are not required. This naturally affects the design and costs of the gas cooling section. Only part of the CO_2 is removed. As discussed in the text, this gas is unlikely to be acceptable for domestic use, or directly for synthesis purposes.

We have assumed that the product gas is required at a plant battery-limits pressure of about 17 atm. This would permit gas-consumers to be at some distance from the gasification plant.

A.2 PROCESS STATUS

In this Section a brief report on the state of development of the processes is given. This covers the operating experience in existing plants and outlines the critical problems that still require investigation or need further substantial research and development effort. The material in this Section was obtained from published sources and in discussions with the process developers.

A.2.1 Dry-ash Lurgi

Existing plants

The Lurgi process has been under development since the 1930's and there have been many commercial applications. The largest in use today is the SASOL II plant operated by the South African Coal, Oil and Gas Corporation (SASOL) at Secunda, South Africa. This plant has 36 gasifiers each with an internal diameter of 3.85m (13 ft.) treating approximately 1000 t/d coal and producing about 55,000 Nm^3/h (50 x 10^6 SCF/d) synthesis gas. Five metre (16.4 ft) internal diameter gasifiers have also been installed at SASOL I which can produce in excess of 70,000 Nm^3/h (63 x 10^6 SCF/d) each.

A modified Lurgi gasifier is being tested at Dorsten, West Germany which will be able to gasify up to 10 t/h coal at pressures of up to 100 atm.

All the above plants are oxygen-blown. In addition, five air-blown Lurgi gasifiers were installed at Lünen, West Germany operated by STEAG AG. These operated at 20 atm as part of an integrated 170 MWe combined cycle power plant. Each gasifier was 3.5m (11.5 ft.) in diameter with a design coal throughput of 15 t/h.

Operating experience

As is clear from the above, there is extensive operational experience with the Lurgi system on a large, commercial scale. At SASOL I, gasifier availability in 1974 was 83%.

The Westfield, Scotland town-gas plant operated for fourteen years with a very high availability though this was achieved with extensive in-built duplication of major plant items. The stirrer and distributor of one of the Westfield gasifiers were modified to enable US coals to be tested in 1973. The coal throughput ranged from 5 t/h for highly caking Pittsburgh coal to 9 t/h for non-caking Montana coal with corresponding production of 8 - 11,000 Nm^3/h (7-10 x 10^6 SCF/d) raw gas (46). This is a reduced throughput from that obtained with the local, design coal. On the whole, these trials were reasonably successful and demonstrated that the Lurgi system could be used to gasify American coals. Major problems were encountered with the feed distributor stalling on Pittsburgh-steam coal due to the high swelling of this coal. Subsequent modifications have eliminated this problem.

The Lünen gasifiers rarely reached design load because of the difficulty in handling fine material. STEAG developed a compacting technique which allows fines to be fed to the gasifier as pellets. However, this material has a different ash melting point which affects the operation of the gasifier. There have been a large number of modifications to the gasifier but there were still significant mechanical failures.

Critical problems

The difficulties with the Lurgi system are well-known — the limitations in range of coal types that can be utilized, the problems with fine material, and the large production of tars, oils and phenols.

References: 11 - 14, 17, 73 - 85

A.2.2 British Gas Corporation/Lurgi:

Existing Plants

After completion of the US coal trials in the dry-ash Lurgi gasifiers at Westfield, Scotland (46), the internal diameter of one of the gasifiers was reduced and converted to slagging operation. This gasifier has a coal throughput of about 15 t/h at an operating pressure of about 25 atm.

Operating experience

The first run of the slagging gasifier took place in April 1975. The plant has operated for over 50000 hours by March 1981, with the longest continuous run lasting 22 days. The plant has operated in Illinois No. 6, Pittsburgh No. 7, Ohio No. 9 and seven different UK coals. Up to 40% fines (below 6.3mm or ¼") have been handled with the highly-caking US coals. British Gas have experimented with reinjecting tars and fines through the tuyeres at the base of the gasifier.

The problems encountered with handling fines, and recycling tar and phenols are considered in Sections 4.1 and 3.3 respectively.

Critical Problems

Refractory life in the slagging zone appears critical. The use of the tuyeres to inject tars and fines is a significant development. The ability to accept additional quantities of fines in this manner enhances the applicability of the process. The elimination of net tar production, and possibly phenols as well, offer significant advantages.

References: 15, 17, 23, 47, 52 - 59

A.2.3 Exxon Catalytic

Existing plants

A modified pilot plant was re-commissioned at Baytown, Texas in December 1976 and has a throughput of 11 kg/h of coal. A 40 kg/h plant was commissioned at Baytown, Texas in July 1979.

Operating experience

The Exxon Catalytic process uses alkali metal salts which promote the rate of steam gasification and accelerate the methanation reaction. Consequently gasification occurs at relatively low gasification temperatures. While the catalyst reduces agglomeration of caking coals, pre-oxidation is required.

The 40 kg/y pilot plant has operated for over 4000 hours up to June 1981, with a longest continuous run of over 33 days on Illinois No. 6 coal. Methane production has been lower than originally predicted, with slightly lower steam and carbon conversion.

Critical problems

A larger-scale unit is to be constructed at Rotterdam, Netherlands with a capacity of 4 t/h. Successful testing at this scale is an essential pre-requisite for commercialisation.

Typically, the catalyst is potassium hydroxide and is added at a rate of 15% potassium carbonate equivalent on dry coal. Catalyst recovery from the ash and recycle is an obvious necessity and requires large-scale demonstration over an extended period. The ability of the process to operate on coals other than Illinois No. 6 and maintain adequate catalyst recovery also requires demonstration. This is particularly relevant for those countries which are likely to import coal and might wish to use this process.

References: 24 - 26, 61, 62, 86, 87

A.2.4 Shell Coal

Existing plants

The Shell Coal gasification process is a development of the Koppers-Totzek process, operating at a pressure of 20-40 atm. A 0.25 t/h plant has been operating at

the Shell research laboratories in Amsterdam since January 1977. A 6 t/h plant was commissioned at Harburg, West Germany in late 1978.

Operating experience

The Shell Coal process is being developed for use in both air-blown combined cycle applications and oxygen-blown synthesis gas production. Both modes have been tested at the Amsterdam plant. The longest continuous run at the Amsterdam plant has been 8 days. By the end of 1980 the Harburg plant had accumulated over 1000 hours of operation, the longest continuous run being 10 days.

Critical problems

Refractory life and fouling of the waste heat boiler appear to be critical items. General operability on a variety of coals has scarcely been proven at any significant scale.

References: 88-90

A.2.5 Texaco

Existing plants

A 0.6 t/h plant has been operating at Montebello, Cal. since 1973. A 6 t/h plant was commissioned at Oberhausen-Holten, West Germany in 1978 and a 7 t/h plant is being commissioned at Muscle Shoals, Ala. as a major modification to an existing ammonia plant.

Operating experience

The Montebello plant has operated for several thousand hours with the largest run being in excess of 4 days. The Oberhausen-Holten plant has operated for 6500 hours by May 1981 with the longest run being 33 days. At the Oberhausen-Holten plant slurry concentrations of up to 70% have been demonstrated. This plant has operated on eleven different coals including Illinois No.6, Pittsburgh No. 8, Utah and five German coals.

Critical problems

Refractory and temperature-measuring element life appear critical. We have no information on waste heat boiler fouling except that it appeared to be an initial problem at Oberhausen-Holten. The maintenance of high slurry concentrations (65%+) is essential for the commercial viability of the process.

References: 15, 16, 20, 63-7, 91-4

A.2.6 BCR BI-GAS and IGT HYGAS

Existing plants

The BI-GAS pilot plant was completed at Homer City, Pennsylvania in September 1976. It has a design coal throughput of 5 t/h at 80 atm. The HYGAS process is being developed by the Institute of Gas Technology, Chicago, Illinois. A pilot plant was completed in 1972 and has a design coal throughput of 3 t/h. Both pilot plants include all the facilities to produce SNG.

Operating experience

The BI-GAS process, developed by Bituminous Coal Research, is a two-stage slagging gasifier with char recycle. The upper stage has been studied on a bench scale but the lower stage is essentially unproven. Early runs had problems with temperature control in the bottom stage of the gasifier, and with recycle line plugging. There were also difficulties with the cyclones or separating char from the gas stream, probably due to excessive fines. Subsequent problems include thermocouple failures, difficulties with slag tapping on a continuous basis, char-flow problems and severe and dangerous burner overheating (69). Several hundred hours of operation on a Western coal were reported in 1981. This process remains unproven on an Eastern coal.

The HYGAS pilot plant, incorporating a steam-oxygen gasification stage (one of three methods for producing hydrogen for the upper hydrogasification stages), was first run on a self-sustained basis in April 1975. In general, runs are scheduled for 10 days, with the longest run to date (on lignite) lasting 27 days. Successful runs on Illinois No. 6 coal have been reported.

During operation, considerable amounts of fines are elutriated from the bed which have not been recycled (with consequent low carbon conversion efficiencies). Tar formation during pre-treatment of caking coal is a serious problem. Further difficulties have been experienced with agglomeration (clinkering) in the bottom of the reactor causing problems with the discharge of ash. The pilot plant has only operated at significantly higher steam flow-rates than used in the Braun designs (11,12). Carbon conversion has been in the 60 - 80% range compared with the Braun design of 97%.

Critical problems

The main difficulty with multi-stage processes such as BI-GAS and HYGAS is ensuring steady-state operability. In fact, it is an open question whether HYGAS have ever operated in true steady-state. There are complex control problems with the multiple fluidized beds in this process. Without adequate temperature and recycle char flow measurement, we have serious doubts about the ability of BI-GAS to maintain steady-state conditions. A thermocouple which can withstand the environment in the lower stage of the BI-GAS gasifier has not yet been found, nor is there a reliable method for measuring the recycle char flow. The problems of dealing with hot flowing solids at high pressure are compounded by these instrumentation difficulties. The mechanical problems of slag tapping and overheated burners appear to have been resolved in other pilot plants, for example British Gas/Lurgi and Shell Coal.

Recyle or elutriated fines with HYGAS needs investigation if high carbon conversion figures are actually to be achieved. The different residence times required with different coal types suggest difficulties in maintaining design throughput when handling a wide variety of coal types.

References: 11, 12, 68-71, 95-97

APPENDIX B TECHNICAL DATA ON PROCESSES

In this appendix, the performance data we have assumed for the gasification processes are given. There is considerable uncertainty in the projected performance of the processes examined, so that the data presented here are by no means definitive. As such, they constitute one representative view of process performance, serving to define important parameters for the economic analysis. The data summarise the results of the previous EAS report (2) as modified in the light of subsequent information.

The problem with comparing performance data for the different systems is that they represent processes at various stages of development. In the case of gasification processes in particular, performance of the gasifier – in terms of raw material requirements and gas production and composition, significantly affects the rest of the plant. Thus, as we discussed in Section 2.3, any uncertainty in the gasifier performance has a subtle effect on the overall economics by influencing each section of the plant.

Table B1 shows the assumed properties of the coal feeds while Tables B2 – B3 show the technical data we have assumed for the various processes.

It should be noted that in all the following tables we have disregarded coal fines. Further, except where indicated, by-products (other than sulphur) are consumed in the off-site boilers or superheaters. Sufficient data are presented, however, to make other assumptions about these by-products.

Table B1 Coal feed properties

	Montana sub-bituminous	Pittsburgh seam bituminous	Illinois No.6 bituminous
Proximate analysis (wt% as received)			
Moisture	22.0	6.0	4.2
Volatile Matter	29.4	31.9	34.2
Fixed Carbon	42.6	51.5	52.0
Ash	6.0	10.6	9.6
	100.0	100.0	100.0
Ultimate analysis (wt % dry)			
Carbon	67.70	71.50	69.52
Hydrogen	4.61	5.02	5.33
Nitrogen	0.85	1.23	1.25
Oxygen	18.46	6.53	10.02
Sulphur	0.66	4.42	3.86
Ash	7.72	11.30	10.02
	100.0	100.0	100.0
Higher heating values (as received)			
GJ/tonne	20.46	28.83	28.45
BTU/lb	8800	12400	12235
Ash softening point (°C) (Reducing atmosphere)	1227	1171	1043[1]

Note:

[1]Estimated

Table B2 Coal requirements[1]

Process	Coal	Coal preparation		Coal to gasification[4]		Coal to off-site boilers	
		t/h	TJ/d	t/h	TJ/d	t/h	TJ/d
SNG (3000 MWt – 250 x 10^9 BTU/SD)							
Dry-ash Lurgi[2]	Eastern	724	500.67	581	401.88	143	98.78
	Western	804	394.75	747	366.60	57	28.16
BI-GAS	Eastern	574	397.10	491	339.53	83	57.57
	Western	868	426.10	672	330.07	196	96.03
British Gas/Lurgi[2]:							
(with Shift)	Eastern	675	467.22	608	420.95	67	46.27
(with HCM)	Eastern	601	416.14	591	408.71	11	7.43
Exxon Catalytic	Eastern	617	426.94	470	324.96	147	101.97
HYGAS (97% conv.)	Eastern	618	427.93	544	376.30	75	51.63
(97% conv.)	Western	729	357.99	661	324.33	69	33.65
(80% conv.)	Western	826	405.70	778	382.04	48	23.72
Shell Coal:							
(with Shift)	Eastern	683	472.76	626	433.09	57	39.68
(with HCM)	Eastern	655	453.07	630	435.57	25	17.50
Texaco:							
(50% slurry)	Eastern	803	555.57	729	504.38	74	51.18
(65% slurry)	Eastern	717	496.06	646	446.89	71	49.17
MCG (3000 MWt – 250 x 10^9 BTU/SD)							
Dry-ash Lurgi[2]	Eastern[3]	586[3]	400.17	492[3]	335.87	94[3]	64.31
British Gas/Lurgi[2]	Eastern[3]	480[3]	327.92	477[3]	325.90	3[3]	2.01
Shell Coal	Eastern[3]	490[3]	334.21	484[3]	330.21	6[3]	4.00
Texaco	Eastern[3]	530[3]	361.88	508[3]	346.96	22[3]	14.92
MCG (500 MWt – 40 x 10^9 BTU/SD)							
Dry-ash Lurgi[2]	Eastern[3]	96[3]	65.55	81[3]	55.02	15[3]	10.53
British Gas/Lurgi[2]	Eastern[3]	79[3]	53.73	78[3]	53.39	0.5[3]	0.34
Shell Coal	Eastern[3]	80[3]	54.73	79[3]	54.09	0.9[3]	0.65
Texaco	Eastern[3]	87[3]	59.29	83[3]	56.84	4[3]	2.44

Notes:

1. By-products (except sulphur) consumed in boilers. All data rounded and based on higher heating values. Coal flows in t/h are on an as-received basis.
2. Excess coal fines excluded.
3. Illinois No. 6 coal.
4. Coal required for pre-drying included where relevant.

Table B3 Gasifier feeds and products[1]

Process	Coal	Feeds t/h			Raw gas (wet basis)				Cold gas efficiency[7] (%)
		Coal	Oxygen[3]	Steam	$Nm^3/h \times 10^6$	$SCF/d \times 10^6$	TJ/d	$BTU \times 10^9/h$	
SNG (3000 MWt – 250 x 10^9 BTU/SD)									
Dry-ash Lurgi[4]	Eastern	581	289	1356	[9]	[9]	[9]	[9]	[9]
	Western	747	184	838	[9]	[9]	[9]	[9]	[9]
BI-GAS	Eastern	491	206	395	1.80	1613	302	11.93	89
	Western	672	222	552	2.49	2228	301	11.89	91
British Gas/Lurgi[4]:									
(with Shift)	Eastern	608	266	194	1.31	1170	361[6]	14.26[6]	85
(with HCM)	Eastern	591	258	189	1.27[11]	1136[11]	351[6]	13.85[6]	85[11]
Exxon Catalytic	Eastern	470[8]	—	626[10]					
HYGAS (97% conv.)	Eastern	544	111	696	1.27[6]	1135[6]	279[6]	11.02[6]	74[6]
(97% conv.)	Western	661	112	645	2.00[6]	1795[6]	302[6]	11.94[6]	93[6]
(80% conv.)	Western	778	114	763	2.36[6]	2113[6]	307[6]	12.12[6]	80[6]
Shell Coal:									
(with Shift)	Eastern	626[8]	490	11	1.10	986	347	13.71	84
(with HCM)	Eastern	630[8]	493	11	1.11	992	349	13.79	84
Texaco:									
(50% slurry)	Eastern	729	718	—	2.16	1933	355	14.02	76
(65% slurry)	Eastern	646	543	—	1.53	1368	352	13.92	79
MCG (3000 MWt – 250 x 10^9 BTU/SD)									
Dry-ash Lurgi[4]	Eastern[5]	492[5]	230	1093	2.00[6]	1788[6]	269[6]	10.63[6]	80
British Gas/Lurgi[4]	Eastern[5]	477[5]	200	158	1.00[6]	898[6]	271[6]	10.72[6]	85
Shell Coal	Eastern[5]	484[5]	377	8	0.92	826	264	10.42	80
Texaco	Eastern[5]	508[5]	428	—	1.31	1172	272	10.75	78
MCG (500 MWt – 40 x 10^9 BTU/SD)									
Dry-ash Lurgi[4]	Eastern[5]	81[5]	33	180	0.33[6]	294[6]	44[6]	1.74[6]	80
British Gas/Lurgi[4]	Eastern[5]	78[5]	33	26	0.16[6]	147[6]	44[6]	1.76[6]	85
Shell Coal	Eastern[5]	79[5]	62	1.3	0.15	135	43	1.71	80
Texaco	Eastern[5]	83[5]	70	—	0.21	192	45	1.76	78

Notes:

1. All data rounded and based on higher heating values
2. As received basis
3. As 100% oxygen
4. Excess coal fines excluded
5. Illinois No. 6 coal
6. Tar, oil and phenol free
7. Sulphur, ammonia and C_3+ free
8. Dried before feeding to gasifier
9. Data not available
10. To preheat furnace. Estimated.
11. Because of the recycle gas flow these data are not comparable

Table B4 Gasifier product gas[1]

Not all of this data corresponds to the information in the previous tables – see below

Process	Coal	Raw gas analysis (dry basis, vol%)								Higher Calorific Value (dry, ammonia, sulphur & C_3+ free)	
		Hydrogen	Carbon monoxide	Carbon dioxide	Methane	Nitrogen & Argon	Ammonia	Sulphur compounds	Others	MJ/Nm^3	BTU/SCF
SNG											
Dry-ash Lurgi[6]	Eastern[5]	39.4	16.9	31.5	9.0	1.5	0.1	0.8	0.8[6]	11.6	294
	Western[5]	41.1	15.1	30.4	11.2	1.2	—	0.5	0.5[6]	12.1	308
BI-GAS	Eastern	30.3	29.7	21.6	15.9	0.3	0.6	1.6	—	14.3	363
	Western	32.3	23.9	28.4	14.5	0.2	0.5	0.2	—	13.0	331
British Gas/Lurgi[6]	Eastern	28.0	55.5	4.6	8.0	1.2	0.3	1.7	0.7[6]	14.5	370
Exxon Catalytic	Eastern[2,3]	32.1[7]	9.0[7]	21.1[7]	32.7[7]	3.1[7]	1.1[7]	0.9[7]	—[7]	18.7[7]	474[7]
HYGAS (97% conv.)	Eastern	21.5	18.1	20.5	16.5	—	0.5	1.0	21.9	15.5	395
(97% conv.)	Western	29.4	25.1	25.3	17.8	—	0.6	0.3	1.5	15.1	384
Shell Coal[4]	Eastern	26.8	68.5	0.5	1.8	0.7	—	1.7	—	13.0	331
Texaco[4]:											
(50% slurry)	Eastern	34.8	42.9	20.2	—	0.6	—	1.5	—	10.0	255
(65% slurry)	Eastern	34.6	52.9	10.3	0.1	0.6	—	1.5	—	11.3	288
MCG											
Dry-ash Lurgi[6]	Eastern[2]	42.3	15.1	30.9	8.6	0.4	0.8	1.2	0.7[6]	11.6	294
British Gas/Lurgi[6]	Eastern	28.0	55.5	4.6	8.0	1.2	0.3	1.7	0.7[6]	14.5	370
Shell Coal[4]	Eastern[2]	30.6	64.1	1.3	—	2.6	—	1.4	—	12.2	310
Texaco[4]	Eastern[2]	35.1	51.6	10.7	0.1	1.0	0.2	1.3	—	11.2	286

Notes:

1. All data rounded
2. Illinois No. 6 coal
3. Pittsburgh seam data not available
4. Data from NCB model
5. From Reference 29. Data on Brayton design not available
6. Tar and oil free
7. Includes recycle gas

Table B5 Gas processing data[1]

Process	Coal	Raw gas (wet basis) Nm³/h x 10⁶	Raw gas (wet basis) SCF/d x 10⁶	Shift feed %	Acid gas removal feed (dry basis) Nm³/h x 10⁶	Acid gas removal feed (dry basis) SCF/d x 10⁶	Methanation feed (dry basis) Nm³/h x 10⁶	Methanation feed (dry basis) SCF/d x 10⁶	Product Gas (dry basis) Nm³/h x 10⁶	Product Gas (dry basis) SCF/d x 10⁶	Thermal loss in gas processing[7] (%)
SNG (3000 MWt – 250 x 10⁹ BTU/SD)											
Dry-ash Lurgi	Eastern	[3]	[3]	46	[3]	[3]	0.77	687	0.31	277	[3]
	Western	[3]	[3]	[3]	1.09[2]	980[2]	0.75	672	0.32	282	[3]
BI-GAS	Eastern	1.80	1613	78	1.03	920	0.69	615	0.32	282	12
	Western	2.49	2228	63	1.06	945	0.69	621	0.31	276	12
British Gas/Lurgi:											
(with Shift)	Eastern	1.31[4]	1171[4]	99[6]	1.39[4]	1246[4]	0.97[8]	873[8]	0.33	292	20
(with HCM)	Eastern	1.24[4]	1137[4]	—	[8]	[8]			0.29	262	20[8]
Exxon Catalytic	Eastern	[8]	[8]	—	1.09	977	—	—	0.28	247	
HYGAS (97% conv.)	Eastern	1.27[4]	1135[4]	74	0.82[4]	732[4]	0.58	519	0.30	269	13
(97% conv.)	Western	2.00[4]	1795[4]	66	0.93[4]	836[4]	0.62	556	0.31	278	13
(80% conv.)	Western	2.36[4]	2113[4]	42	0.99[4]	885[4]	0.69	616	0.32	285	13
Shell Coal:											
(with Shift)	Eastern	1.10	986	96[6]	1.56[8]	1396[8]	1.05[8]	944[8]	0.30	270	22
(with HCM)	Eastern	1.11	998	—					0.29	262	22
Texaco:											
(50% slurry)	Eastern	2.16	1933	82	1.98	1777	1.12	1001	0.30	273	23
(65% slurry)	Eastern	1.53	1368	87	1.65	1473	1.11	993	0.31	273	23
MCG (3000 MWt – 250 x 10⁹ BTU/SD)											
Dry-ash Lurgi	Eastern[5]	2.00[4]	1788[4]	—	1.61[4]	1445[4]	—	—	0.66	587	2
British Gas/Lurgi	Eastern[5]	1.03[4]	922[4]	—	0.78[4]	695[4]	—	—	0.74	663	1
Shell Coal	Eastern[5]	0.92	826	—	0.92	825	—	—	0.90	802	1
Texaco	Eastern[5]	1.33	1195	—	1.01	906	—	—	0.97	873	2
MCG (500 MWt – 40 x 10⁹ BTU/SD)											
Dry-ash Lurgi	Eastern[5]	0.33[4]	294[4]	—	0.26[4]	237[4]	—	—	0.11	96	2
British Gas/Lurgi	Eastern[5]	0.17[4]	151[4]	—	0.13[4]	114[4]	—	—	0.12	109	1
Shell Coal	Eastern[5]	0.15	135	—	0.15	135	—	—	0.15	131	1
Texaco	Eastern[5]	0.22	196	—	0.17	148	—	—	0.16	143	2

Notes.

1. All data rounded and based on higher heating values
2. Wet Basis
3. Data not available
4. Tar and oil free
5. Illinois No. 6 coal
6. Shift designed for 100% raw gas feed
7. Sulphur, ammonia and C_3+ free
8. Because of the nature of the process these data are not comparable

Table B6 Steam and power plant data [1]

Process	Coal	Steam flows (t/h)				Power required (MWe)	Fuel to off-site boilers & superheaters (TJ/d)				
		Gasifier steam[2]	Process generation[3]	Process & off-site requirements[4]	Off-site boiler generation		Total	Ammonia	Phenols	Oil & fuel gas	Coal & char
SNG (3000 MWt – 250 x 10^9 BTU/SD)											
Dry-ash Lurgi	Eastern	1356	1584	1916	1688	68	130.14	2.51	1.21	27.64	98.78
	Western	838	954	1263	1147	53	83.08	2.86	4.55	47.51	28.16
BI-GAS	Eastern	525	1153	1226	600	67	59.82	2.25	—	—	57.57
	Western	671	1239	1938	1370	72	97.91	1.88	—	—	96.03
British Gas/Lurgi:											
(with Shift)	Eastern	194	1496	2628	1326	68	96.21	1.07	1.72	47.15	46.27
(with HCM)	Eastern	189	1550	1747	386	68	55.92	1.04	1.67	45.78	7.43
Exxon Catalytic[8]	Eastern	626	559	1181	1248	128	106.53	4.56	—	—	101.97
HYGAS (97% conv.)	Eastern	696	1085	1055	666	40	69.43	1.88	—	15.92	51.63
(97% conv.)	Western	647	749	874	772	38	53.23	1.81	—	20.77	33.65
(80% conv.)	Western	762	698	856	920	38	69.88	2.13	—	18.16	49.59
Shell Coal:											
(with Shift)	Eastern	10	2739	2824	95	67	39.68	—	—	—	39.68
(with HCM)	Eastern	11	1969	1958	—	67[7]	17.50	—	—	—	17.50
Texaco:											
(50% slurry)	Eastern	—	2985	2985	—	67[7]	51.18	—	—	—	51.18
(65% slurry)	Eastern	—	2626	2626	—	67[7]	49.17	—	—	—	49.17
MCG (3000 MWt – 250 x 10^9 BTU/SD)											
Dry-ash Lurgi[4]	Eastern[5]	1092	591	673	1174	27	100.26	2.86	3.71	29.36	64.31
British Gas/Lurgi	Eastern[5]	157	239	556	474	18	42.17	0.77	1.32	38.08	2.00
Shell Coal	Eastern[5]	8	765	822	65	24	5.52	—	—	1.52	4.00
Texaco	Eastern[5]	—	1027	1027	—	27	16.40	—	—	1.48	14.92
MCG (500 MWt – 40 x 10^9 BTU/SD)											
Dry-ash Lurgi	Eastern[5]	179	97	110	192	4.5	16.42	0.47	0.61	4.81	10.53
British Gas/Lurgi	Eastern[5]	26	39	91	78	3.0	6.93	0.13	0.22	6.24	0.34
Shell Coal	Eastern[5]	1	125	135	11	4.0	0.90	—	—	0.25	0.65
Texaco	Eastern[5]	—	168	168	—	4.4	2.68	—	—	0.24	2.44

Notes:

1. All data rounded and based on higher heating values
2. Gross requirements
3. Includes sulphur and methanation plant generation, etc.
4. Excludes gasifier steam. Net total.
5. Illinois No. 6 coal
6. Includes char from gasifier
7. Excludes export power
8. Some fuel gas is also used in process heaters

Table B7 Parallel processing streams

Process	Coal preparation	Coal Feed quench, shift, acid gas removal, methanation	Gasifiers (spares included)	Oxygen Plants
SNG (3000 MWt – 250 x 10^9 BTU/SD)				
Dry-ash Lurgi	1	[4]	28[5](4)	3[1]
BI-GAS	1	2	3(1)	2[3]
British Gas/Lurgi	1	3	18(3)	3
Exxon Catalytic	1	4[2]	5(1)	—
HYGAS	1	2	3(1)	2
Shell Coal	1	3	8(2)	5
Texaco:				
50% slurry	1	4	8(2)	8
65% slurry	1	3	8(2)	6
MCG (3000 MWt – 250 x 10^9 BTU/SD)				
Dry-ash Lurgi	1	4	25(4)	3
British Gas/Lurgi	1	3	15(3)	3
Shell Coal	1	3	8(2)	4
Texaco	1	3	8(2)	4
MCG (500 MWt – 40 x 10^9 BTU/SD)				
Dry-ash Lurgi	1	2	5(1)	2
British Gas/Lurgi	1	2	3(1)	2
Shell Coal	1	2	3(1)	2
Texaco	1	2	3(1)	2

Notes:

1. Two streams for Western coal.
2. Two streams for acid gas removal and downstream sections.
3. Three streams for Western coal.
4. Data not available.
5. Western coal.

Table B8 Overall plant performance[1]

Process	Coal	Coal Requirements (TJ/d)	Product Gas (TJ/d)	Export Power (MWe)	Overall Thermal Efficiency[2] (%)	Raw Water Requirements (t/d)
SNG (3000 MWt – 250 x 10^9 BTU/SD)						
Dry-ash Lurgi[3]	Eastern	500.67	263.65	—	52.7(55.4)	61100
	Western	394.75	263.65	—	66.8(70.4)	10000
BI-GAS	Eastern	397.10	263.65	—	66.4(66.6)	40300
	Western	426.10	263.65	—	61.9(62.0)	13800
British Gas/Lurgi[3]:						
(with Shift)	Eastern	467.22	263.65	—	56.4(60.6)	65500
(with HCM)	Eastern	416.14	263.65	—	63.4(67.3)	58300
Exxon Catalytic	Eastern	426.94	263.65	—	61.8(62.2)	46000
HYGAS (97% conv.)	Eastern	427.93	263.65	—	61.6(63.1)	45800
(97% conv.)	Western	357.99	263.65	—	73.6(75.0)	11200
(80% conv.)	Western	405.76	263.65	—	65.0(66.6)	10300
Shell Coal:						
(with Shift)	Eastern	472.76	263.65	—	55.8(55.8)	51800
(with HCM)	Eastern	453.07	263.65	18	59.1(59.1)	52900
Texaco:						
(50% slurry)	Eastern	556.57	263.65	58	49.9(49.9)	73900
(65% slurry)	Eastern	496.06	263.65	52	55.6(55.6)	61600
MCG (3000 MWt – 250 x 10^9 BTU/SD)						
Dry-ash Lurgi[3]	Eastern[4]	400.17	263.65	—	65.9(66.5)	38300
British Gas/Lurgi[3]	Eastern[4]	327.92	263.65	—	80.4(82.5)	18800
Shell Coal	Eastern[4]	334.21	263.65	—	78.9(78.9)	26000
Texaco	Eastern[4]	361.88	263.65	—	72.9(72.9)	34900
MCG (500 MWt – 40 x 10^9 BTU/SD)						
Dry-ash Lurgi[3]	Eastern[4]	65.55	43.19	—	65.9(68.5)	6300
British Gas/Lurgi[3]	Eastern[4]	53.73	43.19	—	80.4(82.5)	3100
Shell Coal	Eastern[4]	54.73	43.19	—	78.9(78.9)	4200
Texaco	Eastern[4]	59.29	43.19	—	72.9(72.9)	5700

Notes:

1. All data rounded and based on higher heating values.
2. Defined as heat in cold gas/heat in total coal feed with by-products burnt. Figures in brackets assume export of by-products.
3. Excess coal fines excluded.
4. Illinois No. 6 coal.

APPENDIX C CAPITAL COST DATA

In examining plant costs it is important to recognise that, in general, all large plants, including coal-based gasification plants, have the following characteristics:

(i) The plants take several years to design, order and construct. This implies that the variation of labour and equipment costs over this period must be considered.

(ii) The equipment in plants is not generally available "off-the-shelf", i.e., it is manufactured singly or in small numbers specifically for the project in question. This characteristic holds even for the relatively small, 500MWt (40×10^9 BTU/SD) MCG plants considered in this report. Only rarely is a list price available; usually, costs of equipment are determined as a result of commercial negotiations.

(iii) The workload in both the process plant fabrication and contracting industries has always been highly cyclical in nature and wide variations in profitability and hence price of the plant can be expected.

(iv) In general, plants are located some distance from the source of manufacture of the equipment, and transport costs are inevitably incurred. There may be restrictions on the maximum size of equipment that can be transported to a particular site – this has obvious cost implications.

(v) Only very rarely are plants constructed with a pre-existing labour force (pipe-fitters, welders, electricians, etc.). Almost invariably the bulk of the construction labour force is mobilised specifically for a particular project. In the member countries this implies the use of locally available labour whose quality (productivity) and cost can be expected to vary from area to area.

Thus, major assumptions are built into all estimates of plant costs however well defined the plant design might be and these continue to apply, to a greater or lesser extent, until the plant is actually built and operating. Obviously, between the very first estimates for a given plant and the final estimates the scope for error decreases and the accuracy correspondingly increases. The use of a contingency factor (1) is a reflection of this uncertainty. The approach taken by EAS to the problems outlined above is discussed in the next section.

C.1 METHODOLOGY

Capital cost estimates can be considered in two parts – physical costs, which represent the actual purchase and installation of the plant itself, and those additional factors which are essentially judgmental in nature, such as process contingency allowances. The relative importance of the two categories is illustrated by the following figures, taken directly from a cost estimate for a large SNG plant based on the dry-ash Lurgi process, prepared by Braun for US DOE and GRI (12) and escalated forward to mid-1979 dollars. Other processes shown in this particular report have a generally similar capital analysis.

	$\$x10^6$	%
Installed plant costs (except general facilities)	825	48
General Facilities	92	5
Contractors fees	102	6
Contingency	151	9
Escalation	313	18
Interest during construction	250	14
	1733	100

Only the first two cost categories represent the purchase and installation of the plant itself. Indeed, in this particular example, even the cost of the general facilities was estimated simply as percentage of the first category. In conceptual estimates, of which this example is typical, the last four items, representing nearly half the total cost, are all add-on factors. Of these, the contractor's fee would be a function of the design and management effort, while the other three are all essentially judgemental additions. Because of the factorial nature of these items and their magnitude, it is obviously important to ensure that the basic installed plant costs are adequately defined and complete, and that all the add-on factors are treated comparably.

Because of the importance of capital cost data in the calculation of product prices, an attempt has been made to obtain comparable data for each of the processes. We have attempted to disentangle physical costs and additional costs using the basic capital costs estimates taken from published sources. Turning to Table B2, it can be seen that even for a given, well-defined process (dry-ash Lurgi for SNG) there are very large variations in the published data, even after excluding all the non-physical, judgemental costs as far as possible. It is clear from this table that, as we outlined in Section 2.1, a different approach is necessary if we are to obtain a realistic estimate of the relatively small differences between processess. It is necessary to obtain a single, consistent set of cost estimates and use these as a basis for estimating the cost of each plant section for each process. Having done this, we can then present a set of self-consistent estimates of the purchase and installation costs for each of the processes. In turn, these were checked against published data from other sources. These estimates are given in Section C.2 for SNG and Section C.3 for MCG.

This approach has only been possible for data on North American coals. No data of comparable detail based on other coals have been found. Our unpublished work on the subject of international cost comparisons concluded that there are indeed substantial differences between capital costs in different EAS member-countries. However, these differences are generally much less than the uncertainty in any one individual estimate and, moreover, are frequently of a subjective nature. For international projects, subjective judgements need to be made on:

- the appropriate currency exchange rate
- the likely inflation rate in each country during the design and construction phase
- the assumed source of major items of equipment
- obstacles to free movement of these items.

By far the most significant assumption that has to be made concerns labour productivity in different locations. Labour productivity can vary dramatically even within a single country (98), and obviously, past performance is no more than a guide to future experience – a relevant consideration when the construction period extends over several years.

However, the purpose of this report is **technology comparison**, and there is no reason to believe that the make-up of the costs is significantly different between the processes under consideration. Hence, the results should be valid for all the member countries.

C.1.1 Capital cost escalation

One significant component in comparing cost data is the need to put the data on a comparable time basis. Two distinct elements must be recognised: First, estimates performed in different years include some implicit recognition of inflation over the years. Second, in general, estimators make some explicit recognition of the escalation in plant costs likely to occur between the start of a project and its completion. With respect to this escalation during construction we have made the assumption that this will not occur, ie, we use mid-1797 US dollars. With respect to general inflation, we have extrapolated cost estimates prepared in previous years using the Chemical Engineering Plant Cost Index (99-100). This Index was established in 1963 and gives a measure of the escalation of materials, equipment and labour costs since 1947. The annual averages for the period 1974 - 79 are given below.

Table C1 CE Plant Cost Index – Annual Averages

Year	Index
1974	165.4
1975	182.4
1976	192.1
1977	204.1
1978	218.8
1979	238.7

As with most cost indices, the CE Plant Cost Index is based on a mix of materials and labour costs considered by its authors to be representative of oil and chemical plant design and construction costs. Several other indices are published, but certainly this US-based index commands as wide a support as any other within the oil and chemical industries. It is generally accepted that over relatively small time-periods (say, three or four years), and excluding periods of very rapid escalation of plant costs, eg the aftermath of the 1973 – 74 surge in oil prices, virtually any index can be used without serious error.

Over long periods, or in some exceptional cases, serious deviations can occur between actual plant costs and those predicted using these indices. This is particularly true for very specialised equipment – most gasifiers probably fall into this category. Apart from this type of equipment, there is little reason to suppose that a specific cost index for a coal conversion plant would differ markedly from those already used in the oil and chemical industries. However, no index can account for changes in the design caused by revisions to design requirements, for example, to meet more severe environmental regulations.

C.1.2 Effect of scale on capital costs

One other area of difficulty meriting specific attention is the effect on capital costs of different plant sizes. There are capital cost benefits of scale which extend to the size of plant under consideration (101). It is necessary to relate the estimates of different sizes of plant back to some common denominator.

Williams (102) was perhaps the first to draw attention to what is now known as the 'six-tenths factor', which in its simplest form can be expressed as:

$$I = kC^{0.6}$$

where I is the fixed capital investment
k is a constant
and C is the capacity of the plant or plant section

Williams work was extended by Chilton (103) to cover a wider selection of processes and plant sizes. In reviewing the work of both Chilton and others, Cran (104) showed the wide variations in this power factor - from as low as 0.33 to as high as 0.91. The work by Taylor et al (105) of ICI suggests that some of this spread may arise because the power factor is itself a function of capacity; that is, the cost/capacity relationship is not a straight line when plotted on log-log graph paper. This conclusion was reached on the basis of an analysis of actual plant cost data and has been confirmed, at least in outline, by Burgert (106) of BASF and by DSM (21).

Accepting Taylor's premise and extrapolating his curve to the gasification capacities that we are considering (500 – 3000 MWt) gives a power factor of about 0.81. The same curve gives a power factor of about 0.66 in the range of 300 – 600 MWt. The degree of extrapolation is substantial, however. Unreported studies which EAS have commissioned give factors of 0.77 (Humphreys & Glasgow) and 0.80 (Fluor) while Lummus in their work for Saskatchewan Power (73) give a range of 0.80 to 0.85 and suggest that below 1000 MWt a factor in the range 0.60 – 0.65 is more representative.

Thus, we can see substantial agreement between both plant operators and contractors covering a wide range of plant sizes. We have adopted power-factors of 0.75 and 0.80 for individual plant sections and adjusted them for the number of parallel processing streams. We have used the 0.80 power factor for those parts of the plant, such as coal preparation, feeding, and gasification which can be expected to have a higher power-factor.

C.1.3 Project contingency allowance

A project contingency is added to reflect uncertainties in the estimation of the capital cost of a plant. These may arise in two ways. First, it is impossible to eliminate, even with a detailed estimate, all uncertainty concerning details of quantities and prices of small items, let alone labour productivity during installation. This applies to a greater or lesser extent to all items and all plants, though the less well-defined the plant (or the less mature the technology), the greater the uncertainty. Second, during the design and construction phase of even well-defined

(but complex) plants, such as conventional coal-fired power stations, small design changes may be required, small errors will be corrected, and other unavoidable extra costs may be incurred. In general, a percentage factor is added to the capital costs to cover these contingencies. In this report, a straightforward 15% project contingency allowance has been used. Inherent in this figure is the assumption that each plant will not be the first of its type.

C.1.4 Other capital cost items

Contractors fees

This item relates to the fees paid to the contractors responsible for the design and construction. In reality, these fees would be a complicated function of the materials, equipment, labour and supervision supplied by the contractors. To this should be added the costs of contractor's items such as soil and environmental consultants. A complex approach is unwarranted; a cost representing 10% of the total capital cost has been used. Obviously, this has not been done where the cost data is already quoted on an inclusive basis.

Licensors fees

This item relates to the cost of obtaining a licence to use specific processes and the costs incurred by the licensor in providing the basic data for the design of the plant. All the processes involve one or more licensed sections – typically the gasifiers, acid gas removal, and sulphur recovery. While licence fees are obviously negotiable, a typical figure would be 6% of the capital cost of the licensed plant section. Large parts of the plant are clearly not licensed processes, and we have, therefore, used a factor of 2.5% of total capital cost, which is the same as for the EPRI reports prepared by Fluor (14-17). To simplify the treatment, the royalty has been treated as a lump-sum payment during the final year of construction of the plant. In reality, payments would be staggered throughout the design and construction phase, and an annual running royalty may be payable in addition.

Initial catalyst and chemicals

We assume that all the inventory of catalyst and chemicals would be consumed at the end of the plant's working life. This is exactly equivalent to treating this item as part of the working capital.

C.2 SNG PLANT COSTS

As indicated above, the end-product of the data presented in this section is comparability rather than absolute accuracy. All the data are based ultimately on conceptual studies and none of it represents actual costs.

We have assumed the use of the Selexol process for the removal of acid gas – mainly carbon dioxide and hydrogen sulphide. This process has not been demonstrated for coal gasification, though it is included in the Texaco demonstration plant at Muscle Shoals, Alabama (94). Its ability to handle traces of tar and naphtha is unclear. The selection of a particular acid gas removal process is related to the precise composition of the gas being treated (107-109) and also to the cost of the energy required to remove the acid gas. The acid gas removal

step has a measurable effect on the economics of SNG production both directly in terms of capital investment and indirectly in terms of steam and power consumption.

Where start-up or other operational considerations are relevant, and this applies especially to processes with a high degree of heat recovery, such as Shell Coal and Texaco, we have tried to ensure that all the equipment is adequately sized (especially the boiler plant). As far as possible, equipment redundancy, particularly spare gasifiers and the number of process trains, have been made consistent throughout.

Table C4 shows the comparative data we have derived, while the following sections indicate the sources of our data, etc.

C.2.1 Dry-ash Lurgi process

Dry-ash Lurgi process capital costs have been examined from a variety of sources (11-13,17,21,73-77). Results are given in Table C2, where the costs allocated among the various plant sections are presented for a standard-size plant. The spread of the data for total capital cost is noteworthy and this extends down to the various plant sections. Moreover, the later estimates tend to show higher costs (43). The effects of plant location and coal properties are also clearly significant. We believe that the differences between the two Braun estimates (about 10%) arise almost entirely from the change in coal feed.

As indicated in Section 2.1, the work by Braun (11,12) represents the most comprehensive and comparable data available. We have used these data, with some modifications. Thus, we have included a 5% process contingency for the oxygen plants. This is in line with Conoco (23). For the oxygen plants we have used Union Carbide cost and energy data (110) since this is the most consistent data we have seen. We have used a conventional Claus plant, with tail-gas cleaning, for sulphur recovery and non-regenerable flue gas desulphurisation rather than the integrated, but unproven, IFP Clauspol 150 process. This reflects the later Braun work (107-108) and represents a more nearly optimal process selection for these steps when compared with the original data. We have pro-rated TVA data (20) for the sulphur plant and tail-gas clean-up. For the boiler plant, with flue gas desulphurisation we have used the Mobil/Lurgi data (13) which assumed the incineration of the sulphur recovery off-gas in the boiler itself.

Such data as we have available suggests that typical figures for the cooling water system and balance-of-plant are 2 and 14% of total capital investment, respectively (in both cases, capital cost before including these items). We have used these factors so as to represent more effectively the changes in total plant costs. One further revision has been to adjust the coal preparation plant investment to reflect the consumption of by-products in the steam plant.

Table C2 Dry-Ash Lurgi SNG plant installation costs[1]

Client	BC Hydro	DOE/AGA	DOE/GRI	PG & E	—	Wesco	Sask. Power	Great Plains
Contractor	Lummus	Braun/Fluor	Braun/Fluor	Fluor	Lurgi	Fluor	Lummus	Lummus
Location	B. Columbia	Western	Eastern	Wyoming	U.S.	New Mexico	Saskatchewan	Wyoming
Study date	Sep 75	Jan 76	Jan 76	1st Quart 76	1976	Jan 77	Jul 77	1978
Plant size (10^9 BTU/SD)	242.5	250.0	250.0	270.1	262.8	269.5	30.3[3]	134.6
(MWt)	2960	3052	3052	3297	3209	3290	370[3]	1643
				Mid-79 Escalated cost for 3052 MWt plant ($ x 10^6)[2]				
Coal preparation & handling	58	57[5]	24[5]	37	93	11[5]	106	110
Casification & quench	125	269[12]	360[12]	163[6]	233	168	115	178
Oxygen	84	92	129	114	129	112	122	113
Ash handling	15	4	4	34[8]	-[9]	38	31	153[14]
CO shift & gas cooling	33	-[9]	-[9]	22[7]	35	62	48	228[15]
Acid gas removal	89	164	141	144	115	177	130	-[9]
Sulphur recovery	19	76	115	60	35	37	31	-[9]
Methanation	47	83[13]	66[13]	49	70[13]	70	60	59
Gas compression & drying	13	-[9]	-[9]	14	-[9]	11	24	-[9]
Gas liquor separation	15	-[9]	-[9]	23	81[14]	29	22	-[9]
Phenolsolvan	47	-[9]	-[9]	31	-[9]	36	56	-[9]
Process condensate treatment	7	27	31	-[9]	[9]	20	15	-[9]
Steam and power plant	12[10]	251	222	112[11]	210	187[11]	84[11]	126[11]
Balance-of-plant	61	148	200	157	162[16]	118	117	358
Correction for power, steam imports	226	-	-	99	-	72	197	139
Total (excluding contingency, interest during construction, start-up costs, working capital, initial catalysts and chemicals, royalties)	851[17]	1171	1292	1059[18]	1163[17]	1148[17]	1048[17]	1464[17]
Reference	(56)	(9)	(10)	(40)	(57)	(40)(58)	(55)	(59)

Notes:

1. All data rounded and in mid-79 $ x 10^6. Higher heating values used.
2. 0.80 capacity exponent used except where shown.
3. 0.75 capacity exponent used.
4. Excludes coal preparation.
5. Excludes some coal handling – included under gasification.
6. Includes gas cooling.
7. Excludes gas cooling.
8. Includes effluent water treatment.
9. Included elsewhere.
10. Steam and power imported.
11. Power imported
12. Includes CO shift, gas liquor separation, Phenolsolvan.
13. Includes gas compression.
14. Includes process condensate treating, Phenolsolvan.
15. Includes acid gas removal & sulphur recovery.
16. Includes ash handling.
17. No information on initial catalysts and chemicals or royalties.
18. Includes intial catalysts and chemicals.

C.2.2 British Gas/Lurgi process

We have used the Conoco data (23) for the gasification, gas liquor seperation, Phenolsolvan and ammonia recovery sections and Mobil/Lurgi (13) for conventional CO-shift section. For the HCM combined shift-methanation route we have used Mobil/Lurgi for gas cooling and Braun (11) for the HCM section. We have assumed that HCM catalyst behaves in the same way as a conventional methanation catalyst but costs twice as much. For the rest of the process and offsite units we have used the same basis as dry-ash Lurgi adjusted for the different flows and compositions.

C.2.3 Exxon Catalytic process

Virtually all the pilot plant work by Exxon (24,25,61,62) has used Illinois No. 6 coal. Braun (26) have presented information based on the same coal but with adjustments suggested by Exxon to reflect the use of Pittsburgh seam coal. In the absence of pilot plant experience, these can only be approximate.

We have had to largely infer the plant steam balance from data supplied to us by Exxon (21) and from the published reports by Exxon (24,25,61,62) and Braun (26).

The effect of these approximations is to add an additional element of uncertainty, which is not present for the other processes.

C.2.4 Shell Coal process

The yield data for this process were obtained using a development of the National Coal Board's ARACHNE equilibrium model (18). This model was validated against the DSM equilibrium model (19) and data from Braun (20), Fluor (15) and Shell (21). We assumed that the ash would contain 2% carbon and that the feed coal would be dried to 2% moisture.

The composition of the quenched and cooled raw gas implies that 96% of this gas would require conversion over a conventional sulphur-resistant CO-shift catalyst to provide the desired methanation feed gas composition. We have assumed that the CO shift facilities would be sized to take 100% of the gas. Additional steam would be required to provide a 2:1 steam to CO ratio. For the HCM combined shift-methanation route we have made the same assumptions as we did with British Gas/Lurgi.

The nature of the data supplied by Shell has necessitated some significant process assumptions. We assumed that eight parallel gasification, waste heat boiler, solids removal and recycle gas compressor trains each with its own coal pressurising and feeding system would be required. Two complete spare trains have been included. Separate cooling of the recycle gas coupled with a reduction in size, or even elimination, of the waste heat boiler could reduce capital costs when using the conventional CO-shift catalyst. We have assumed that heat cannot be economically recovered from the raw gas below 90°C (184°F). This assumption is similar to the assumptions made by Braun (11,12), Fluor (14-17) and Conoco (23), but differs from Shell's assumption of 25°C (21).

We have estimated that the start-up of a single gasification train would require an additional 640 t/h of high pressure steam from an off-site boiler, which we included in our estimates. The normal steam requirement for this boiler is very low (100 t/h with the conventional shift and nil with the HCM route) and this implies some non-optimisation in the steam system. We do not think, however, that substantial improvements in capital and/or operating costs can be made.

We assumed that the cost data supplied to us by Shell includes engineering costs and fees but not process royalties. We also assumed 8% escalation from the middle of 1979 to the Shell base-date of mid-1980.

C.2.5 Texaco process

As for Shell Coal, we have used a development of the National Coal Board's ARACHNE equilibrium model as our source of data. We assumed that the ash would contain 2% carbon. For the capital cost of the gasification and quench sections we used the data presented by Braun to TVA (68). As for Shell Coal, the composition of the quenched and cooled raw gas implies that virtually all this gas requires shifting to provide the desired methanation feed-gas composition.

We assumed that eight gasifiers and waste heat boilers would be required (including two spare units). We also assumed four coal grinding and slurrying trains.

The estimated start-up steam requirements are 780 and 960 t/h for the 50 and 65% slurry cases, respectively. In both cases the process generates surplus power under normal running conditions. Substantial start-up boilers are therefore required. As with Shell Coal this is non-optimal, though we do not think that substantial improvements in capital and/or operating costs can be made.

C.2.6 BCR BI-GAS & IGT HYGAS Processes

The reports by Braun (11,12) contain virtually the only comprehensive data on these processes There are some comparatively minor discrepancies in the cost data, which we have tried to eliminate. In addition, we have included spare coal feeding equipment, where appropriate, since we do not feel that an entire plant should be put in jeopardy by a single conveyor, for example. We have also included a single spare gasifier: we feel that this is an absolute minimum.

As discussed in Section 4.6 the data provided by IGT to Braun for the HYGAS process assumes a very high carbon conversion (97%) and a low steam consumption. Based on pilot plant results (71), we have increased the reactor steam consumption by 30% and made the assumption that this will appear as excess steam to be condensed. Since we are unable to revise the material balance to maintain heat balance, we may have treated this change optimistically.

We examined the effect on the HYGAS process of changing the carbon conversion with a Western US sub-bituminous coal. The assumptions we made and the results obtained are summarised in Table C3. Apart from throughput effects, we assumed that the cost of handling the ash or char leaving the gasifier does not change as its composition goes from 19 to 72% carbon. We also assumed that the

Table C3 Effect of carbon conversion on IGT HYGAS process[1]

Carbon conversion	97%	90%	80%	70%
Coal to process (%)	100	106	118	127
Net boiler heat duty[2] (%)	100	114	147	173
Carbon in ash (%)	19	47	64	72
Assumed carbon recovery in boilers (%)	NIL	80	80	80
Coal to boilers[3] (%)	100	79	70	49
Total coal to plant (%)	100	104	113	119
		Mid-1979 $ x 10^6		
Coal preparation & handling	80	83	88	93
Gasification CO-shift & gas cooling	175	181	186	191
Oxygen plant	60	61	61	59
Acid gas removal & sulphur recovery	166	166	167	169
Methanation & drying	42	42	42	42
Ash & char handling	13	26	34	42
Process condensate treatment	101	110	124	134
Steam & power	177	187	208	221
Cooling water system	16	17	18	19
Balance-of-plant	114	120	128	133
Total (excuding contingency, interest during construction, start-up costs, working capital)	944	993	1056	1103
Contingency (15%)	142	149	158	165
Process royalties (2.5%)	27	29	30	32

Notes

1. All data rounded. Western US coal
2. After consumption of by-products. Includes superheater duty
3. After consumption of ash/char. Includes superheater duty

Table C4 Comparable SNG plant installation costs – 3000 MWt (250 x 10^9 BTU/SD) Plant

Process	Dry-ash Lurgi		BI-GAS		British Gas/Lurgi		Exxon Catalytic	HYGAS			Shell Coal		Texaco	
Coal	Eastern	Western	Eastern	Western	Eastern (Shift)	Eastern (HCM)	Eastern	Eastern (97% conv)	Western	Western (80% conv)	Eastern (Shift)	Eastern (HCM)	Eastern (50% slurry)	Eastern (65% slurry)
Coal prepn. & handling	27[4]	29[4]	97	96	28[4]	28[4]	77[4]	83	80	88	76[4]	77[4]	129[4]	118[4]
Coal pre-treatment	—	—	—	—	—	—	—	72	—	—	—	—	—	—
Gasification, CO-shift and gas cooling	359[2]	269[2]	205	210	242[2]	138[2]	247	235	175	186	394[2]	286[2]	434[4]	425[4]
Oxygen plant	117	75	98	113	110	107	—	60	60	61	236	238	352	266
Acid gas removal and sulphur recovery	194	179	206	180	217	233	147	191	166	167	295	329	440	308
Methanation or HCM, compression, drying	66	73	41	42	77	166	141[5]	38	42	42	75	105	80	79
Ash & sludge handling	14	11	17	13	15	14	18	14	13	34[8]	20	20	24	21
Process condensate treatment	24[7]	27[7]	41	52	42[7]	10[7]	33	91	101	124	51	2	43	43
Steam and power	345	250	182	275	276	163	310	198	177	208	142	124	164	156
Cooling water system	23	18	18	20	20	17	21	20	16	18	26	24	33	28
Balance-of-plant	161	128	124	137	141	120	239[6]	137	114	128	179	165	234	199
Total (excluding contingency, interest during construction, start-up costs, working capital)	1330	1059	1029	1138	1168	996	1233	1139	944	1056	1484	1370	1933	1643
Contingency (15%)	200	159	154	171	175	150	185	171	142	158	223	205	290	246
Process royalties (2.5%)	38	30	38	33	34	29	35	33	27	30	43	39	56	47

Notes:

1. All data rounded and in mid-79 $ x 10^6
2. Includes gas liquor separation & Phenolsolvan
3. Included elsewhere
4. Some of the coal feeding costs are included in the gasification section
5. Cryogenic unit
6. Includes catalyst recovery ($74 x 10^6) and chemicals handling ($16 x 10^6)
7. Excludes gas liquor separation and Phenolsolvan
8. Includes char handling

char could be burnt in the offsite boilers when its carbon content exceeded 47%, without any cost penalties (other than throughput effects). While we are confident that this could be done in a fluidised bed, no work has been done on this and hence any estimate of combustion efficiency and capital cost must be regarded as speculative.

C.3 MCG PLANT COSTS

As with the SNG costs given in the previous section, we have aimed at comparability rather than absolute accuracy. In particular, equipment redundancy, especially spare gasifiers and the number of process trains, has been made consistent throughout. We have assumed that CO and complete CO_2 removal will not be required for this type of industrial fuel gas. This gas would be unsuitable for either synthesis or domestic purposes without substantial additional processing costs. We have again used Selexol to remove the acid gases – in a single-stage process. The selection of a suitable acid gas removal process significantly influences the economics of MCG production. Table C6 summarises the comparative data we have developed, while the following sections indicate the sources of our data, etc.

C.3.1 Dry-ash Lurgi process

We do not have as extensive data on the capital costs of dry-ash Lurgi MCG production as we do on SNG. Such data as we do have are presented in Table C5 and are clearly conflicting even after allowing for different coals and processing schemes. For the purposes of comparability we have taken the Fluor data as representative, though we have modified them extensively by bringing them into line with the process and capital cost assumptions made for SNG. Thus, for example, Braun data have been used for the coal handling and preparation equipment, and we have used the Selexol process for acid gas removal. We have assumed proportionately the same numbers of spare gasifiers and associated equipment (see Table B7). We assumed that the product gas will be required at a battery-limit pressure of at least 17 atm. This implies deletion of the gas expanders (and hence surplus power production) and requires consumption of the low-pressure acid gas removal flash gas in the off-site boilers. We have also assumed that these off-site boilers consume coal, with flue-gas desulphurisation, rather than using a portion of the product gas.

C.3.2 British Gas/Lurgi process

We have used the Conoco data (23) for the gasification, gas liquor separation, Phenolsolvan and ammonia recovery sections. We have made the same modifications as we made for the dry-ash Lurgi process, outlined in the previous section. The most significant changes are the change in raw gas composition to reflect the data supplied to us by British Gas (21), the deletion of the gas expanders and the consumption of coal in the off-site boilers (with flue-gas desulphurisation).

Table C5 Dry-ash Lurgi MCG plant installation costs[1]

Client	—	BC Hydro	EPRI	Shell	Sask. Power
Contractor	Lurgi	Lummus	Fluor	SNC-Tottrup	Lummus
Location	—	B. Columbia	Illinois	Alberta	Saskatchewan
Study date	1974	Sept 75	Mid-76	1977	Jul 77
Plant output					
(10^9 BTU/SD)	75.4	229.5[3]	131.9	150.0	30.3
(MWt)	920	2802[3]	1610	1831	370
Gas heating value					
(BTU/SCF)	423-444	300	302	424	307
(MJ/Nm^3)	16.7-17.5	11.8	11.9	16.7	12.1
Mid-79 escalated cost for 500 MW plant ($ x 10^6)[2]					
Coal preparation & handling		11	8		23
Gasification & quench		22	35[4]		28
Oxygen plant		13	35		26
Ash handling		1	-[5]		7
Gas cooling		2	29		3
Acid gas removal		–	17[7]		–
Sulphur recovery	[6]	4[3]	-[5]	[6]	8[3]
Gas liquor separation		2	-[5]		5
Phenolsolvan		9	-[5]		13
Process condensate treatment		1	44[8]		3
Steam and power plant		3	49[9]		33
Balance-of-plant		8	-[5]		26
Correction for power, steam imports		67[10]	8[11]		27[11]
Total (excluding contingency, interest during construction start-up costs, working capital, initial catalysts and chemicals, royalties)	52	143	225	246[12]	204
Reference	(62)	(56)	(14)	(63)	(55)

Notes:

1. All data rounded. Higher heating values used.
2. 0.80 capacity exponent used.
3. Stretford process assumed.
4. Includes ash handling.
5. Included elsewhere.
6. No cost breakdown presented.
7. Includes sulphur recovery.
8. Includes gas liquor separation, Phenolsolvan.
9. Includes balance-of-plant.
10. Steam and power imported.
11. Power imported.
12. Includes gas storage, mine, start-up costs, initial catalysts and chemical royalties.

C.3.3 Shell Coal process

The National Coal Board's ARACHNE equilibrium model was used to obtain the basic process data. We used 98% oxygen as assumed by Fluor. Use of 90% oxygen, as assumed by Shell, is obviously applicable to all the MCG processes. This would reduce the oxygen plant costs with only minor increases elsewhere. The overall economic effect is likely to be small, however (111).

As with the SNG plant data, described in Section C.2.4, we have made some significant process assumptions. Thus, for the 500 MWt plant we have assumed that three parallel coal pressurising and feeding systems, gasifiers, waste heat boilers and solids removal trains would be required. This includes one complete spare train. Common equipment, for example, recycle gas compressors - could reduce costs. We do not have enough information to make the appropriate adjustments. 50 t/h of additional steam is required to start-up one train of the 500 MWt plant. We have assumed an off-site boiler sized to provide this additional quantity (ie above the normal demand). As noted previously, this is not an optimal situation.

We assumed that an acid gas removal feed temperature of 38°C (100°F) is required and that heat cannot be economically recovered from the raw gas below 60°C (140°F). This is similar to Fluor (14-17), but differs from Shell's assumption (21) of 25°C (77°F).

We assumed that the cost data supplied to us by Shell included engineering costs and fees but not process royalties. We also assumed 8% escalation from the middle of 1979 to the Shell base-date of mid-1980.

C.3.4 Texaco process

The National Coal Board's ARACHNE model was used to obtain the basic process data. We have used data supplied by Texaco and presented by Braun (20) for the capital cost of the gasifiers. These costs can be reconciled with those given by Parsons (67) but are appreciably higher than Fluor (15). We have added spare coal grinding trains and revised the process condensate treatment to be in line with the Braun BI-GAS flow-scheme. We have also deleted the power recovery system. The off-site steam superheater has been revised to consume coal (with flue-gas desulphurisation). A coal-fired boiler for start-up is required and, as noted above, this is not optimal.

Table C6 Comparable MCG plant installation costs[1]

Plant Capacity	3000 MWt—250 x 10^9 BTU/SD				500 MWt—40 x 10^9 BTU/SD			
Process	**Dry-ash Lurgi**	**British Gas/ Lurgi**	**Shell Coal**	**Texaco**	**Dry-ash Lurgi**	**British Gas/ Lurgi**	**Shell Coal**	**Texaco**
Coal prepn. & handling[2]	24	24	39	41	11	11	15	15
Gasification[2], ash handling and gas cooling	208	88	174	373	46	24	39	78
Oxygen plant	97	87	153	170	21	19	31	35
Acid gas removal and sulphur recovery	56	47	29	43	11	10	6	10
Process condensate treatment	135	40	2	5	35	10	1	1
Steam and power generation	284	165	69	56	79	45	19	16
Cooling water system	16	9	9	14	4	3	2	3
Balance-of-plant	112	63	65	96	29	17	15	22
Total (excluding contingency, interest during construction, start-up costs, working capital)	932	523	540	798	236	139	128	180
Contingency (15%)	140	78	81	120	35	21	19	27
Process royalties (2.5%)	27	15	16	23	7	4	4	5

Notes:

1. All data rounded and in mid-79 $ x 10^6
2. Some of the coal feeding costs are included in the gasification section

APPENDIX D OPERATING COST DATA

This appendix deals with all items, other than capital costs, that must be estimated in order to calculate gas costs. These comprise material inputs (coal and water), labour, working capital, start-up costs, maintenance, insurance, tax and overheads. These costs may be off-set by revenue from sales of by-products. We have assumed $4/t (dry basis) ash disposal cos's for the 500 MWt (40 x 10^9 BTU/SD) plant in addition to the cost of the ash handling plant. For the 3000 MWt (250 x 10^9 BTU/SD) plants we have not included any waste disposal costs, apart from the cost of the ash handling plant. This implies on-site disposal.

D.1 COAL CONSUMPTION AND COSTS

Coal is clearly the most significant component of operating costs. Gas costs have been calculated for three different coal costs – $1, 2 and 3/GJ. The coal input to all the processes considered are given in Table D3 while the costs are shown in Table D5.

We stress that estimates of coal consumption vary about as much as the capital cost estimates discussed previously. This can be seen from Table D1 which shows the thermal efficiency data corresponding to the dry-ash Lurgi plant investment data in Table C2. Some of this variability can be attributed to differences in the coal processed and some to different assumptions regarding the source of power and steam for the plants. Different process assumptions are also involved, and, as discussed previously, these differences are inherently difficult to estimate.

Our aim has been to use comparable and representative data throughout and this implies that not all the designs are optimal. We have looked carefully at plant steam balances since, in general, they contribute significantly to total coal feed requirements. Non-regenerable flue-gas desulphurisation has been included in all the designs.

We do have reservations with respect to the Exxon Catalytic process, as outlined in Section C.2.4 – we do not have enough information to ensure total comparability.

In revising the Fluor data on MCG processes, we have assumed that the product gas is required at a battery-limits pressure of at least 17 atm. This would permit delivery of the gas over distances of several miles. For the base-case we have made the assumption that all by-products (except sulphur) would be consumed in the off-site boilers and super-heaters and the quantity of feed coal reduced accordingly. Table D3, D4 and D5 are particularly affected by this assumption. However, the information in Table D6 can be used to make appropriate corrections if required. We have not included excess coal fines in these tables.

D.2 WATER CONSUMPTION AND COSTS

All coal gasification plants consume considerable quantities of water. This is obviously a serious consideration in areas where the availability of water is limited. However, viewed solely in terms of economics, the cost of water is generally only a small fraction of the total cost of gas and is unlikely to affect the choice of process – coal consumption and the cost of the plant usually dominate.

The water consumption of coal gasification plants tends to vary considerably. This is shown in Table D2, which shows dry-ash Lurgi SNG plant data and corresponds to Tables C2 and D1. Relatively small changes in the quality of the coal – especially chloride content – can have dramatic effects on water consumption by restricting the degree of re-use of process water. None of the designs represents an attempt to specifically minimise water consumption, though the Braun Western design attempts to maximise water re-use.

Water consumption in general is a function of:

- the type of gasifier
- the processing scheme (the CO-shift reactor requires a certain minimum water/steam concentration, for example)
- the method of process cooling (air or water; evaporative or dry cooling towers)
- the quality and cost of the raw water (high solids concentrations requires heavy blow-down and hence higher make-up requirements). This also affects, and is affected by, the method of process cooling.
- the quality of the coal (chloride content is particularly important)

The cost of water also varies considerably (1) and this is also shown in Table D2. We have not escalated these cost figures to a common date. In this report we have used \$0.20/m^3 (\$0.76/1000 US gal) for the cost of raw water. Water consumption and costs for all the processes considered are shown in Tables D3 and D5 respectively. We emphasise that we have aimed at comparability of data. We note that the Braun data on Western coal assumes a high-degree of water re-use, which would not be feasible with a coal containing more than a very few ppm of chlorides.

D.3 CATALYSTS AND CHEMICALS

The initial charge of catalysts and chemicals is usually treated as a capital item. We have assumed that the inventory of catalysts and chemicals will be consumed at the end of the plant's operating life. This is exactly equivalent to treating the initial charge as working capital. As the initial charge is replenished an annual operating cost is incurred, and this is tabulated in Table D5. The data presented have been adjusted in accordance with the other changes we have made and have also been adjusted to a mid-1979 base-date using the US Department of Labor Wholesale Price Index for chemicals and allied products. This index does not properly reflect the escalation in cost of the metals used in many catalysts (cobalt, molybdenum, nickel).

D.4 OPERATING LABOUR

In general, manpower estimates have been based on data from the original sources. These have been adjusted to reflect variations in plant complexity, for example, the number of gasifiers. The numbers and costs of personnel required for each system (based on three operating shifts per day and a four-shift system) are given in Tables D3 and D5, respectively. These have been calculated assuming a cost of \$30,400 per man per year, which includes an allowance for sickness, supervision and a social cost burden.

Table D1 Dry-ash Lurgi SNG plant performance[1]

Client	BC Hydro	DOE/AGA	DOE/GRI	PG & E	—	Wesco	Sask. Power	Great Plains	—
Contractor	Lummus	Braun/Fluor	Braun/Fluor	Fluor	Lurgi	Fluor	Lummus	Lummus	Lurgi
Location	B. Columbia	Western	Eastern	Wyoming	US	New Mexico	Saskatchewan	Wyoming	W Germany
Study date	Sep 75	Jan 76	Jan 76	1st Quart 76	1976	Jan 77	Jul 77	1978	1980
Plant size (10^9 BTU/SD)	242.5	250.0	250.0	270.1	262.8	269.5	30.3	134.6	—
(MWt output)	2960	3052	3052	3297	3290	3290	370	1643	—
Energy Input(%)									
Coal to process	81.9	80.5	84.0	81.4	-[2]	79.8	88.6	91.8	100.0
Coal to steam plant	-	19.5	16.0	11.9	-[2]	18.7	-	-	-
Power[3]	3.0	-	-	4.6	-	1.5	11.4	8.2	-
Steam[4]	15.1	-	-	-	-	-	-	-	-
Fuel oil[5]	-	-	-	2.1	-	-	-	-	-
Total input	100.0	100.0	100.0	100.0	100.0	100.0	100.0	100.0	100.0
Energy Distribution(%)									
Product gas	55.7	59.7	55.1	52.4	-[2]	55.4	61.1	66.7	-[2]
By-products									
Ammonia	0.9	0.6	0.5	0.8	-[2]	0.8	0.3	1.0	-[2]
Hydrocarbons	10.7	11.9	1.8[6]	16.5	-[2]	10.8	-[6]	-[6]	-[2]
Phenols	0.8	1.0	0.2	0.6	-[2]	0.7	1.0	-[6]	-[2]
Total products	68.1	73.2	57.6	70.3	68.0	67.7	62.4	66.7	63.6
Losses (and sulphur)	32.9	26.8	42.4	29.7	32.0	32.3	37.6	33.3	36.4
Cold gas efficiency(%)	55.7	59.7	55.1	52.4	-[2]	55.4	61.1	66.7	-[2]
Overall thermal efficiency(%)	68.1	73.4	57.6	70.3	68.0	67.7	62.4	66.7	63.6
Reference	(56)	(9)	(10)	(40)	(57)(62)	(40)(64)	(55)	(59)	(40)

Notes:

1. All data rounded. Higher heating values assumed.
2. Data not available
3. Imported. Converted at 10000 BTU/kWh
4. Imported. 90% thermal efficiency assumed
5. Imported.
6. Consumed as fuel internally in all or part.

Table D2 Dry-ash Lurgi SNG plant water consumption[1]

Client	Contractor	Location	Study date	US gallons/ 10^6 BTU SNG	m^3/MJ SNG	Water cost[4] (¢/m^3)	Reference
BC Hydro	Lummus	B. Columbia	Sept 75	20.7[2]	74[2]	5.7	(56)
DOE/AGA	Braun	Western	Jan 76	14.0	50	10.6	(9)
DOE/GRI	Braun	Eastern	Jan 76	63.8	229	10.6	(10)
PG & E	Fluor	Wyoming	1st Quart 76	29.3[3]	105[3]	5.0	(40)
Wesco	Fluor	N. Mexico	Jan 77	28.4[3]	102[3]	-	(58)
Sask. Power	Lummus	Saskatchewan	Jul 77	38.5[3]	138[3]	19.0	(55)
Great Plains	Lummus	Wyoming	1978	31.5[3]	113[3]	-	(59)

Notes:

1. All data rounded. Higher heating values assumed.
2. Imported steam and power
3. Imported power
4. At date of study shown.

Table D3 Coal and water consumption[1]

Process	Coal	Coal consumption (10^6 t/y)[1,2]	Coal consumption (TJ/d)[3]	Water consumption (10^6 t/y)[1]	No. of operators
SNG (3000 MWt – 250 x 10^9 BTU/SD)					
Dry-ash Lurgi[4]	Eastern	5.39	500.67	18.95	240
	Western	5.98	394.75	3.12	240
BI-GAS	Eastern	4.27	397.10	12.50	200
	Western	6.46	426.10	4.27	200
British Gas/Lurgi[4]:					
(with Shift)	Eastern	5.03	467.22	20.33	220
(with HCM)	Eastern	4.48	416.14	18.09	220
Exxon Catalytic	Eastern	4.59	426.94	14.25	200
HYGAS (97% conv.)	Eastern	4.60	427.93	14.20	200
(97% conv.)	Western	5.43	357.94	3.47	200
(80% conv.)	Western	6.15	405.76	3.18	200
Shell Coal:					
(with Shift)	Eastern	5.09	472.76	16.06	200
(with HCM)	Eastern	4.87	433.07	16.42	200
Texaco:					
(50% slurry)	Eastern	5.98	555.57	22.94	200
(65% slurry)	Eastern	5.34	496.06	19.11	200
MCG (3000 MWt – 250 x 10^9 BTU/SD)					
Dry-ash Lurgi[4]	Eastern[5]	4.36[5]	400.17[5]	11.89	180
British Gas/Lurgi[4]	Eastern[5]	3.58[5]	327.92[5]	5.85	180
Shell Coal	Eastern[5]	3.64[5]	334.21[5]	8.06	140
Texaco	Eastern[5]	3.95[5]	361.88[5]	10.83	140
MCG (500 MWt – 40 x 10^9 BTU/SD)					
Dry-ash Lurgi[4]	Eastern[5]	0.715[5]	66.55[5]	1.96	120
British Gas/Lurgi[4]	Eastern[5]	0.586[5]	53.73[5]	0.96	120
Shell Coal	Eastern[5]	0.597[5]	54.73[5]	1.32	120
Texaco	Eastern[5]	0.646[5]	59.29[5]	1.77	120

Notes:

1. All data rounded and annual data presented at 0.85 load-factor.
2. As-received basis. Higher heating values. See Table A2 for coal analysis.
3. Stream-day basis.
4. Excess coal fines excluded.
5. Illinois No. 6 coal.

D.5 WORKING CAPITAL & START-UP COSTS

The conventions derived in previous EAS work (1) and summarised in Section 2.2 have been used to calculate working capital and start-up costs.

Working capital was calculated as the sum of the cost of 30 days actual feed (coal and water)[1], receivables at 1/12th of annual product and by-product revenue, and maintenance materials and spare parts charged at 1% of total plant investment. Working capital consequently becomes a function of rate-of-return on investment. Working capital for the base investment level and three coal costs are given in Table D4.

Start-up costs are calculated as the cost of supplies for 30 days operation plus labour costs for a year. This is also given in Table D4 for three different coal costs.

D.6 MAINTENANCE, INSURANCE, LOCAL TAXES AND OVERHEADS

Using the conventions set out in previous EAS work (1) and shown in Table 3, annual maintenance costs are taken to be 4% of plant investment; annual charges for insurance, local taxes and overheads are taken as 3% of plant investment. Maintenance costs are assumed to be equally divided between fixed costs (ie labour) and variable costs (ie materials and spare parts), the latter being proportional to throughput. Costs of maintenance, insurance, etc. are summarised in Table D5. The treatment we have used assumes that maintenance costs are linear throughout the operating life of the plants. This is not usually the case as costs generally follow a 'bath-tub' shaped curve with higher costs both early and late in a plant's life.

D.7 BY-PRODUCTS

In Table 3 we show the values we have assumed for the by-products from the various gasification processes. This topic is discussed in Section 3.2. In the base case, where we have assigned only coal values to most by-products, we have assumed that the by-products would be consumed in the off-site boilers. This reduces coal requirements and minimises working capital. Data on by-products quantities and values are presented in Table D6 to allow costs to be developed using alternative assumptions.

---

1 Also potassium hydroxide and lime for the Exxon Catalytic Process.

Table D4 Working capital and start-up costs[1]

Process	Coal	Initial Catalysts & Chemicals[4]	Working capital ($x10^6) 5% DCF rate-of-return			10% DCF rate-of-return			Start-up costs ($x10^6) 5 & 10% DCF rate-of-return		
			$1/GJ	$2/GJ	$3/GJ	$1/GJ	$2/GJ	$3/GJ	$1/GJ	$2/GJ	$3/GJ
SNG (3000 MWt – 250 x 10^9 BTU/SD)											
Dry-ash Lurgi[2]	Eastern	11.5	79.8	108.0	136.2	88.3	116.7	145.0	23.9	38.9	54.0
	Western	7.4	60.8	83.0	105.3	67.6	90.0	112.3	20.0	31.8	43.7
BI-GAS	Eastern	4.5	58.7	81.0	103.4	65.3	87.7	110.2	19.7	31.6	43.5
	Western	6.1	64.1	88.1	112.1	71.4	95.6	119.7	20.1	32.9	45.7
British Gas/Lurgi[2]:											
(with Shift)	Eastern	17.2	80.4	106.7	133.0	87.9	114.4	140.8	23.0	37.0	51.0
(with HCM)	Eastern	10.7	66.0	89.4	112.9	72.5	96.0	119.6	21.3	33.8	46.3
Exxon Catalytic	Eastern	6.5[5]	69.3	93.3	117.4	77.2	101.3	125.5	22.9	35.7	48.5
HYGAS (97% conv.)	Eastern	5.5	63.2	87.2	111.4	70.5	94.7	118.9	19.9	32.7	45.6
(97% conv.)	Western	5.4	53.2	73.3	93.5	59.2	79.5	99.8	17.5	28.2	38.9
(80% conv)	Western	5.2	58.8	81.6	104.4	65.5	88.5	111.5	18.9	31.1	43.3
Shell Coal:											
(with Shift)	Eastern	10.4	80.7	107.4	134.0	90.2	117.0	143.7	21.6	35.8	50.0
(with HCM)	Eastern	5.9	71.7	97.2	122.7	80.4	106.1	131.8	20.9	34.5	48.1
Texaco:											
(50% slurry)	Eastern	9.1	96.6	127.9	159.2	108.9	140.4	171.8	24.2	40.9	57.5
(65% slurry)	Eastern	9.1	85.2	113.2	141.1	95.7	123.8	151.9	22.3	37.2	52.1
MCG (3000 MWt – 250 x 10^9 BTU/SD)											
Dry-ash Lurgi[2]	Eastern[3]	3.3	53.5	75.9	98.5	59.4	82.1	104.7	18.3	30.3	42.3
British Gas/Lurgi[2]	Eastern[3]	2.7	37.6	56.0	74.5	41.0	59.5	78.1	16.1	26.0	35.8
Shell Coal	Eastern[3]	2.6	37.7	56.4	75.2	41.2	60.0	79.0	14.8	24.9	34.9
Texaco	Eastern[3]	2.9	46.3	67.1	87.4	51.8	72.3	92.8	16.0	26.7	37.5
MCG (500 MWt – 40 x 10^9 BTU/SD)											
Dry-ash Lurgi[2]	Eastern[3]	0.6	11.3	15.0	18.7	12.8	16.6	20.3	5.8	7.8	9.7
British Gas/Lurgi[2]	Eastern[3]	0.5	7.6	10.9	13.9	8.8	11.8	14.9	5.4	7.0	8.6
Shell Coal	Eastern[3]	0.4	7.5	10.6	13.7	8.4	11.5	14.6	5.4	7.1	8.7
Texaco	Eastern[3]	0.5	9.3	12.6	16.0	10.5	13.8	17.2	5.6	7.3	9.1

Notes:

1. All data rounded, in mid-1979 $x10^6 and at a load-factor of 0.85
2. Excess coal fines excluded.
3. Illinois No. 6 coal.
4. Included in working capital
5. Includes potassium hydroxide and lime

Table D5 Summary of annual operating costs[1]

Process	Coal	Coal cost $1/GJ	Coal cost $2/GJ	Coal cost $3/GJ	Water[2]	Catalyst & chemicals	Ash Removal[9]	Operating labour	Maintenance[4]	Insurance, local taxes	Total non-fuel costs
SNG (3000 MWt – 250 x 10^9 BTU/SD)											
Dry-ash Lurgi[5]	Eastern	155.33	310.66	466.00	3.81	12.74	—	7.30	56.61	45.90	126.36
	Western	122.47	244.94	367.42	0.63	7.96	—	7.30	45.07	36.54	97.53
BI-GAS	Eastern	123.20	246.40	369.60	2.51	14.65	—	6.08	43.79	35.50	102.53
	Western	132.20	264.40	396.60	0.86	12.10	—	6.08	48.41	39.25	106.70
British Gas/Lurgi[5]:											
(with Shift)	Eastern	144.95	289.91	434.86	4.09	19.23	—	6.69	49.66	40.27	119.94
(with HCM)	Eastern	129.11	258.21	387.32	3.64	18.23	—	6.69	42.36	34.34	105.26
Exxon Catalytic	Eastern	132.46	264.92	397.37	2.87	38.64[8]	—	6.08	52.47	42.55	142.61
HYGAS (97% conv.)	Eastern	132.77	265.53	398.30	2.66	7.30	—	6.08	48.47	39.30	104.01
(97% conv.)	Western	111.07	222.13	333.20	0.70	5.87	—	6.08	40.17	32.57	85.39
(80% conv.)	Western	125.89	251.78	377.66	0.64	6.15	—	6.08	44.94	36.44	94.25
Shell Coal:											
(with Shift)	Eastern	146.67	293.35	440.02	3.23	10.45	—	6.08	63.15	51.20	134.11
(with HCM)	Eastern	140.56	281.13	421.69	3.30	9.14	—	6.08	58.26	47.24	124.02[7]
Texaco:											
(50% slurry)	Eastern	172.35	344.73	517.09	4.61	10.49	—	6.08	82.23	66.67	170.08[7]
(65% slurry)	Eastern	153.90	307.81	461.71	3.84	10.49	—	6.08	69.92	56.69	147.02[7]
MCG (3000 MWt – 250 x 10^9 BTU/SD)											
Dry-ash Lurgi[5]	Eastern[6]	124.15	248.31	372.46	2.39	6.25	—	5.47	39.65	32.15	85.91
British Gas/Lurgi[5]	Eastern[6]	101.74	203.47	305.21	1.18	7.33	—	5.47	22.27	18.05	54.30
Shell Coal	Eastern[6]	103.69	207.38	311.07	1.62	4.10	—	4.26	22.98	18.63	51.59
Texaco	Eastern[6]	112.27	224.55	336.82	2.18	4.84	—	4.26	33.95	27.53	72.76
MCG (500 MWt – 40 x 10^9 BTU/SD)											
Dry-ash Lurgi[5]	Eastern[6]	20.34	40.67	61.01	0.39	1.02	0.32	3.65	10.06	8.16	23.65
British Gas/Lurgi[5]	Eastern[6]	16.67	33.34	50.01	0.19	1.20	0.25	3.65	5.91	4.79	15.99
Shell Coal	Eastern[6]	16.98	33.96	50.94	0.26	0.67	0.26	3.65	5.44	4.41	14.69
Texaco	Eastern[6]	18.39	36.79	55.18	0.36	0.79	0.28	3.65	7.67	6.22	18.97

Notes:
1. All data rounded in mid-1979 $\$ \times 10^6$ and based on 0.85 load factor.
2. At \$0.20/m^3 (\$0.76/1000 US gallons)
3. At \$30400/man-year including social burden
4. At a load factor of 1.00 maintenance cost is assumed to consist of equal contributions from materials and labour (each being 2% of capital investment). At a load factor of 0.85 the contribution arising from maintenance materials is assumed to be reduced proportionally.
5. Excess coal fines excluded
6. Illinois No. 6 coal
7. Excludes export power sales revenue (see Table D6)
8. Includes 54900 t/y potassium hydroxide at \$400/t and 264,000 t/y lime at \$37.3/t.
9. \$4/t of dry ash assumed for 500 MWt plants only.

Table D6 By-product quantities and revenue[1]
Note: With the exception of export power all data in this table relate to the alternative, high-value by-products case

Process	Coal	Base-Case		High-value By-products Case								Total by-product revenue ($x10^6/y)[6]	Additional coal requirement (TJ/y)[6]
		Export Power (MW)	($x10^6/y)[5]	Ammonia (t/d)	($x10^6/y)[2]	Phenols (t/d)	($x10^6/y)[3]	Naphtha & benzene (t/d)	($x10^6/y)[4]	Tar and tar oils (t/d)	($x10^6/y)[3]		
SNG (3000 MWt – 250 x 10^9 BTU/SD)													
Dry-ash Lurgi[7]	Eastern	—	—	112	5.02	40	1.87	126	13.09	583	34.70	54.68	9700
	Western	—	—	127	4.87	152	7.05	332	34.49	876	52.15	98.56	17900
BI-GAS	Eastern	—	—	100	4.50	—	—	—	—	—	—	4.50	700
	Western	—	—	84	3.77	—	—	—	—	—	—	3.77	600
British Gas/Lurgi[7]:													
(with Shift)	Eastern	—	—	48	2.15	58	2.66	190	19.71	1022	60.83	85.35	15500
(with HCM)	Eastern	—	—	46	2.08	56	2.59	184	19.14	992	59.05	82.86	15000
Exxon Catalytic[8]	Eastern	—	—	203	9.14	—	—	—	—	—	—	9.14	1400
HYGAS (97% conv.)	Eastern	—	—	84	3.77	—	—	377	39.51	—	—	43.28	5500
(97% conv.)	Western	—	—	81	3.62	—	—	488	51.55	—	—	55.40	7000
(80% conv.)	Western	—	—	95	4.27	—	—	426	45.08	—	—	49.35	6300
Shell Coal:													
(with Shift)	Eastern	—	—	—	—	—	—	—	—	—	—	—	—
(with HCM)	Eastern	18	5.34	—	—	—	—	—	—	—	—	5.34	—
Texaco:													
(50% slurry)	Eastern	58	17.39	—	—	—	—	—	—	—	—	17.39	—
(65% slurry)	Eastern	52	15.37	—	—	—	—	—	—	—	—	15.37	—
MCG (3000 MWt – 250 x 10^9 BTU/SD)													
Dry-ash Lurgi[7]	Eastern[8]	—	—	127	5.72	124	5.76	122	12.70	571	33.96	58.14	10400
British Gas/Lurgi[7]	Eastern[8]	—	—	34	1.54	44	2.05	147	15.32	793	47.22	66.13	12000
Shell Coal	Eastern[8]	—	—	—	—	—	—	—	—	—	—	—	—
Texaco	Eastern[8]	—	—	—	—	—	—	—	—	—	—	—	—
MCG (500 MWt – 40 x 10^9 BTU/SD)													
Dry-ash Lurgi[7]	Eastern[8]	—	—	21	0.94	20	0.94	20	2.08	93	5.56	9.52	1700
British Gas/Lurgi[7]	Eastern[8]	—	—	6	0.25	7	0.34	24	2.51	130	7.74	10.84	2000
Shell Coal	Eastern[8]	—	—	—	—	—	—	—	—	—	—	—	—
Texaco	Eastern[8]	—	—	—	—	—	—	—	—	—	—	—	—

Notes:

1. All data rounded and all annual data based on a load factor of 0.85
2. At $145/t
3. At $5/GJ
4. At $8/GJ
5. At $0.040/kWh. Data in this column represents **total** base-case by-product revenue
6. Data in this column represents alternative, high-value by-products case
7. Excess coal fines excluded
8. Illinois No. 6 coal

APPENDIX E TABULATION OF RESULTS

In this appendix gas costs are presented as a function of DCF rate-of-return and coal cost for the following cases:

Table E1 Base case, no-tax
Table E2 Base case, 'North American' taxes
Table E3 High value by-products, no-tax
Table E4 Base case, no-tax, 150% base investment
Table E5 Base case, no-tax, lower load factor – 75%

Table E1 Gas costs ($/GJ) – base case, 'no-tax'

DCF rate-of-return		3%			5%			10%			15%		
Coal cost ($/GJ)		1	2	3	1	2	3	1	2	3	1	2	3
SNG (3000 MWt – 250 x 10^9 BTU/SD)													
Dry-ash Lurgi	Eastern	4.95	6.87	8.79	5.34	7.27	9.20	6.59	8.55	10.50	8.27	10.25	12.23
	Western	3.89	5.40	6.92	4.20	5.72	7.25	5.20	6.74	8.28	6.53	8.09	9.66
BI-GAS	Eastern	3.92	5.45	6.97	4.23	5.76	7.29	5.19	6.74	8.30	6.49	8.06	9.63
	Western	4.21	5.84	7.48	4.54	6.18	7.83	5.61	7.27	8.94	7.04	8.73	10.41
British Gas/Lurgi:													
(with Shift)	Eastern	4.56	6.36	8.15	4.91	6.71	8.52	6.02	7.84	9.67	7.50	9.35	11.20
(with HCM)	Eastern	4.00	5.60	7.19	4.29	5.90	7.50	5.23	6.86	8.49	6.50	8.14	9.79
Exxon Catalytic	Eastern	4.76	6.40	8.03	5.12	6.77	8.41	6.28	7.94	9.61	7.83	9.52	11.21
HYGAS (97% conv.)	Eastern	4.18	5.82	7.47	4.51	6.17	7.82	5.58	7.25	8.93	7.01	8.71	10.40
(97% conv.)	Western	3.47	4.84	6.22	3.75	5.13	6.51	4.63	6.03	7.43	5.82	7.24	8.66
(80% conv.)	Western	3.88	5.44	7.00	4.19	5.76	7.32	5.18	6.77	8.36	6.51	8.12	9.73
Shell Coal:													
(with Shift)	Eastern	5.10	6.92	8.73	5.54	7.36	9.19	6.93	8.77	10.62	8.79	10.66	12.53
(with HCM)	Eastern	4.71	6.45	8.19	5 11	6.86	8.61	6.39	8.16	9.93	8.11	9.90	11.70
Texaco:													
(50% slurry)	Eastern	6.14	8.28	10.41	6.70	8.85	10.99	8.50	10.68	12.85	10.92	13.12	15.32
(65% slurry)	Eastern	5.34	7.24	9.15	5.82	7.73	9.64	7.35	9.29	11.23	9.41	11.37	13.34
MCG (3000 MWt – 250 x 10^9 BTU/SD)													
Dry-ash Lurgi	Eastern	3.62	5.16	6.70	3.90	5.44	6.98	4.77	6.34	7.90	5.95	7.53	9.12
British Gas/Lurgi	Eastern	2.51	3.77	5.03	2.67	3.93	5.20	3.17	4.45	5.73	3.83	5.13	6.43
Shell Coal	Eastern	2.52	3.80	5.08	2.68	3.97	5.26	3.19	4.50	5.80	3.88	5.20	6.53
Texaco	Eastern	3.17	4.56	5.94	3.40	4.80	6.19	4.15	5.56	6.98	5.16	6.59	8.02
MCG (500 MWt – 40 x 10^9 BTU/SD)													
Dry-ash Lurgi	Eastern	4.92	6.45	7.99	5.34	6.88	8.43	6.69	8.26	9.82	8.51	10.09	11.67
British Gas/Lurgi	Eastern	3.42	4.67	5.93	3.67	4.93	6.20	4.47	5.76	7.04	5.55	6.85	8.15
Shell Coal	Eastern	3.27	4.55	5.83	3.50	4.79	6.08	4.25	5.55	6.86	5.24	6.56	7.89
Texaco	Eastern	4.05	5.44	6.83	4.37	5.77	7.16	5.41	6.82	8.24	6.80	8.23	9.67

Mid-1979 $
All data rounded

Table E2 **Gas costs ($/GJ) – base case, with 'North American' taxes**
Tax rate 48% – SOYD depreciation method, 10% investment tax credit

DCF rate-of-return		3%			5%			10%			15%		
Coal cost ($/GJ)		1	2	3	1	2	3	1	2	3	1	2	3
SNG (3000 MWt – 250 x 10^9 BTU/SD)													
Dry-ash Lurgi	Eastern	5.04	6.37	8.90	5.68	7.63	9.58	7.82	9.81	11.80	10.80	12.83	14.87
	Western	3.96	5.48	7.01	4.47	6.01	7.54	6.17	7.74	9.31	8.54	10.15	11.75
BI-GAS	Eastern	3.99	5.53	7.06	4.49	6.03	7.58	6.14	7.72	9.30	8.44	10.06	11.67
	Western	4.28	5.93	7.57	4.83	6.49	8.15	6.65	8.34	10.04	9.20	10.93	12.66
British Gas/Lurgi:													
(with Shift)	Eastern	4.65	6.45	8.25	5.22	7.04	8.85	7.10	8.96	10.82	9.74	11.64	13.54
(with HCM)	Eastern	4.07	5.67	7.28	4.55	6.17	7.79	6.16	7.81	9.47	8.40	10.10	11.79
Exxon Catalytic	Eastern	4.84	6.49	8.13	5.43	7.09	8.76	7.41	9.10	10.80	10.17	11.90	13.64
HYGAS (97% conv.)	Eastern	4.26	5.91	7.56	4.80	6.47	8.13	6.63	8.33	10.03	9.17	10.91	12.65
(97% conv.)	Western	3.53	4.91	6.30	3.99	5.38	6.77	5.50	6.92	8.34	7.61	9.07	10.52
(80% conv.)	Western	3.96	5.52	7.09	4.46	6.04	7.62	6.15	7.77	9.38	8.51	10.16	11.81
Shell Coal:													
(with Shift)	Eastern	5.20	7.03	8.85	5.91	7.75	9.59	8.28	10.16	12.04	11.60	13.52	15.44
(with HCM)	Eastern	4.60	6.55	8.30	5.46	7.22	8.98	7.64	9.44	11.24	10.69	12.54	14.38
Texaco:													
(50% slurry)	Eastern	6.27	8.41	10.56	7.19	9.35	11.51	10.26	12.47	14.68	14.57	16.82	19.08
(65% slurry)	Eastern	5.45	7.36	9.28	6.23	8.16	10.09	8.85	10.82	12.79	12.51	14.53	16.55
MCG (3000 MWt – 250 x 10^9 BTU/SD)													
Dry-ash Lurgi	Eastern	3.69	5.23	6.77	4.13	5.69	7.25	5.63	7.22	8.81	7.72	9.34	10.97
British Gas/Lurgi	Eastern	2.55	3.81	5.08	2.80	4.08	5.36	3.65	4.90	6.16	4.84	6.17	7.51
Shell Coal	Eastern	2.56	3.84	5.13	2.82	4.12	5.42	3.70	5.02	6.33	4.92	6.28	7.63
Texaco	Eastern	3.22	4.62	6.01	3.60	5.01	6.42	4.88	6.32	7.76	6.67	8.15	9.62
MCG (500 MWt – 40 x 10^9 BTU/SD)													
Dry-ash Lurgi	Eastern	5.01	6.55	8.10	5.70	7.26	8.81	8.00	9.59	11.18	11.22	12.85	14.47
British Gas/Lurgi	Eastern	3.47	4.74	6.00	3.88	5.16	6.44	5.25	6.56	7.86	7.16	8.49	9.83
Shell Coal	Eastern	3.32	4.61	5.90	3.70	5.00	6.30	4.96	6.29	7.62	6.73	8.08	9.44
Texaco	Eastern	4.12	5.52	6.91	4.65	6.06	7.47	6.41	7.85	9.29	8.88	10.35	11.82

Mid-1979 $
All data rounded

Table E3 Gas costs ($/GJ) – high value by-products case, 'no-tax'

DCF rate-of-return		3%			5%			10%			15%		
Coal cost ($/GJ)		1	2	3	1	2	3	1	2	3	1	2	3
SNG (3000 MWt – 250 x 10^9 BTU/SD)													
Dry-ash Lurgi	Eastern	4.40	6.44	8.48	4.75	6.84	8.90	6.04	8.12	10.20	7.72	9.83	11.94
	Western	2.89	4.63	6.37	3.21	4.95	6.70	4.20	5.97	7.74	5.54	7.33	9.12
BI-GAS	Eastern	3.88	5.41	6.94	4.18	5.72	7.26	5.15	6.71	8.27	6.44	8.02	9.61
	Western	4.17	5.81	7.45	4.50	6.15	7.80	5.57	7.24	8.91	7.00	8.70	10.39
British Gas/Lurgi													
(with Shift)	Eastern	3.71	5.70	7.68	4.06	6.06	8.05	5.17	7.19	9.21	6.65	8.70	10.75
(with HCM)	Eastern	3.17	4.95	6.73	3.46	5.25	7.04	4.41	6.22	8.03	5.67	7.51	9.34
Exxon Catalytic	Eastern	4.66	6.32	7.98	5.02	6.69	8.35	6.18	7.87	9.55	7.73	9.44	11.15
HYGAS (97% conv.)	Eastern	3.72	5.43	7.14	4.05	5.77	7.49	5.12	6.86	8.61	6.56	8.32	10.09
(97% conv.)	Western	2.91	4.37	5.83	3.18	4.65	6.12	4.07	5.56	7.04	5.26	6.77	8.27
(80% conv.)	Western	3.36	4.99	6.63	3.67	5.31	6.96	4.66	6.33	7.99	5.99	7.68	9.36
Shell Coal:*													
(with Shift)	Eastern	5.10	6.92	8.73	5.54	7.36	9.19	6.93	8.77	10.62	8.79	10.66	12.53
(with HCM)	Eastern	4.71	6.45	8.19	5.11	6.86	8.61	6.39	8.16	9.93	8.11	9.90	11.70
Texaco:*													
(50% slurry)	Eastern	6.14	8.26	10.41	6.70	8.85	10.99	8.50	10.68	12.85	10.92	13.12	15.32
(65% slurry)	Eastern	5.34	7.24	9.15	5.82	7.73	9.64	7.35	9.29	11.23	9.41	11.37	13.54
MCG (3000 MWt – 250 x 10^9 BTU/SD)													
Dry-ash Lurgi	Eastern	3.04	4.71	6.37	3.32	4.99	6.66	4.19	5.99	7.58	5.37	7.09	8.80
British Gas/Lurgi	Eastern	1.85	3.26	4.66	2.01	3.42	4.84	2.51	3.94	5.37	3.18	4.63	6.08
Shell Coal*	Eastern	2.52	3.80	5.08	2.68	3.97	5.26	3.19	4.50	5.80	3.88	5.20	6.53
Texaco*	Eastern	3.17	4.56	5.94	3.40	4.80	6.19	4.15	5.56	6.98	5.16	6.59	8.02
MCG (500 MWt – 40 x 10^9 BTU/SD)													
Dry-ash Lurgi	Eastern	4.34	6.00	7.67	4.76	6.43	8.11	6.11	7.81	9.50	7.93	9.65	11.37
British Gas/Lurgi	Eastern	2.76	4.17	5.57	3.01	4.43	5.84	3.82	5.25	6.68	4.90	6.35	7.80
Shell Coal*	Eastern	3.27	4.55	5.83	3.50	4.79	6.08	4.25	5.55	6.86	5.24	6.56	7.89
Texaco*	Eastern	4.05	5.44	6.83	4.37	5.77	7.16	5.41	6.82	8.24	6.80	8.23	9.67

Mid-1979 $
All data rounded

* No change from base-case

Table E4 Gas costs ($/GJ) – base case, 'no-tax' 150% base investment

DCF rate-of-return		3%			5%			10%			15%		
Coal cost ($/GJ)		**1**	**2**	**3**	**1**	**2**	**3**	**1**	**2**	**3**	**1**	**2**	**3**
SNG (3000 MWt – 250 x 10^9 BTU/SD)													
Dry-ash Lurgi	Eastern	6.31	8.23	10.15	6.89	8.82	10.75	8.74	10.70	12.65	11.24	13.22	15.10
	Western	4.97	6.49	8.00	5.43	6.95	8.48	6.91	8.45	9.99	8.89	10.46	12.02
BI-GAS	Eastern	4.98	6.50	8.03	5.42	6.96	8.49	6.86	8.41	9.96	8.79	10.36	11.93
	Western	5.37	7.01	8.64	5.86	7.51	9.15	7.45	9.11	10.78	9.58	11.27	12.95
British Gas/Lurgi													
(with Shift)	Eastern	5.76	7.55	9.35	6.27	8.07	9.87	7.91	9.73	11.56	10.10	11.95	13.80
(with HCM)	Eastern	5.01	6.61	8.21	5.45	7.06	8.66	6.85	8.47	10.10	8.72	10.37	12.01
Exxon Catalytic	Eastern	6.02	7.66	9.30	6.55	8.20	9.85	8.27	9.94	11.61	10.58	12.27	13.96
HYGAS (97% conv.)	Eastern	5.35	6.99	8.63	5.84	7.49	9.14	7.43	9.10	10.77	9.56	11.25	12.95
(97% conv.)	Western	4.34	5.81	7.18	4.84	6.23	7.61	6.16	7.56	8.96	7.93	9.35	10.76
(80% conv.)	Western	4.96	6.52	8.08	5.42	6.99	8.55	6.89	8.48	10.06	8.87	10.48	12.08
Shell Coal:													
(with Shift)	Eastern	6.62	8.44	10.25	7.26	9.09	10.91	9.33	11.17	13.02	12.10	13.97	15.85
(with HCM)	Eastern	6.11	7.85	9.59	6.70	8.45	10.20	8.61	10.38	12.15	11.16	12.96	14.75
Texaco:													
(50% slurry)	Eastern	8.12	10.25	12.38	8.95	11.10	13.24	11.63	13.80	15.97	15.24	17.44	19.64
(65% slurry)	Eastern	7.02	8.92	10.83	7.73	9.64	11.56	10.01	11.95	13.89	13.08	15.04	17.01
MCG (3000 MWt – 250 x 10^9 BTU/SD)													
Dry-ash Lurgi	Eastern	4.58	6.11	7.65	4.98	6.52	8.07	6.28	7.84	9.41	8.03	9.61	11.20
British Gas/Lurgi	Eastern	3.04	4.30	5.56	3.27	4.54	5.80	4.01	5.29	6.57	5.00	6.30	7.60
Shell Coal	Eastern	3.07	4.35	5.63	3.31	4.59	5.88	4.07	5.37	6.68	5.08	6.41	7.73
Texaco	Eastern	3.98	5.37	6.76	4.33	5.72	7.12	5.44	6.86	8.27	6.94	8.37	9.81
MCG (500 MWt – 40 x 10^9 BTU/SD)													
Dry-ash Lurgi	Eastern	6.39	7.93	9.46	7.02	8.56	10.10	9.03	10.59	12.15	11.73	13.31	14.90
British Gas/Lurgi	Eastern	4.28	5.54	6.80	4.65	5.92	7.18	5.85	7.13	8.41	7.44	8.74	10.04
Shell Coal	Eastern	4.07	5.35	6.63	4.41	5.70	6.99	5.51	6.81	8.12	6.98	8.31	9.63
Texaco	Eastern	5.17	6.56	7.95	5.65	7.05	8.44	7.19	8.61	10.02	9.26	10.69	12.12

Mid-1979 $
All data rounded

Table E5 Gas costs ($/GJ) – base case, 'no-tax' lower load-factor – 75%

DCF rate-of-return		3%			5%			10%			15%		
Coal cost ($/GJ)		1	2	3	1	2	3	1	2	3	1	2	3
SNG (3000 MWt – 250 x 10^9 BTU/SD)													
Dry-ash Lurgi	Eastern	5.29	7.21	9.14	5.73	7.67	9.60	7.15	9.12	11.08	9.06	11.05	13.05
	Western	4.16	5.68	7.20	4.51	6.04	7.57	5.64	7.19	8.74	7.16	8.73	10.31
BI-GAS	Eastern	4.19	5.71	7.24	4.53	6.07	7.60	5.63	7.19	8.74	7.10	8.68	10.26
	Western	4.50	6.13	7.77	4.87	6.52	8.17	6.09	7.76	9.43	7.71	9.41	11.11
British Gas/Lurgi													
(with Shift)	Eastern	4.86	6.66	8.46	5.26	7.06	8.87	6.51	8.35	10.18	8.20	10.06	11.92
(with HCM)	Eastern	4.25	5.85	7.45	4.59	6.20	7.81	5.66	7.29	8.92	7.09	8.75	10.41
Exxon Catalytic	Eastern	5.07	6.71	8.35	5.48	7.13	8.78	6.79	8.47	10.14	8.56	10.26	11.96
HYGAS (97% conv.)	Eastern	4.47	6.12	7.76	4.85	6.50	8.16	6.06	7.74	9.42	7.69	9.40	11.10
(97% conv.)	Western	3.71	5.09	6.46	4.03	5.41	6.79	5.03	6.44	7.84	6.38	7.81	9.23
(80% conv.)	Western	4.15	5.71	7.27	4.50	6.07	7.64	5.63	7.22	8.81	7.14	8.76	10.37
Shell Coal:													
(with Shift)	Eastern	5.48	7.29	9.11	5.97	7.80	9.63	7.55	9.40	11.26	9.66	11.55	13.43
(with HCM)	Eastern	5.06	6.80	8.54	5.51	7.26	9.01	6.96	8.74	10.52	8.92	10.72	12.52
Texaco:													
(50% slurry)	Eastern	6.62	8.76	10.90	7.26	9.41	11.56	9.31	11.49	13.67	12.06	14.27	16.48
(65% slurry)	Eastern	5.75	7.66	9.56	6.29	8.21	10.13	8.04	9.98	11.93	10.38	12.35	14.33
MCG (3000 MWt – 250 x 10^9 BTU/SD)													
Dry-ash Lurgi	Eastern	3.86	5.40	6.94	4.17	5.72	7.27	5.17	6.74	8.31	6.50	8.10	9.69
British Gas/Lurgi	Eastern	2.65	3.91	5.17	2.83	4.09	5.36	3.39	4.68	5.97	4.15	5.46	6.76
Shell Coal	Eastern	3.67	3.94	5.23	2.84	4.13	5.42	3.42	4.73	6.05	4.20	5.54	6.87
Texaco	Eastern	3.37	4.76	6.15	3.64	5.03	6.43	4.49	5.91	7.33	5.63	7.07	8.51
MCG (500 MWt – 40 x 10^9 BTU/SD)													
Dry-ash Lurgi	Eastern	5.31	6.85	8.39	5.79	7.34	8.88	7.33	8.89	10.46	9.39	10.98	12.58
British Gas/Lurgi	Eastern	3.66	4.92	6.18	3.95	5.22	6.49	4.87	6.15	7.44	6.09	7.40	8.70
Shell Coal	Eastern	3.50	4.78	6.07	3.76	5.06	6.35	4.61	5.92	7.23	5.74	7.07	8.40
Texaco	Eastern	4.36	5.75	7.14	4.72	6.12	7.52	5.90	7.32	8.74	7.49	8.93	10.37

Mid-1979 $
All data rounded

APPENDIX F FORMULAE FOR DCF CALCULATIONS

Gas costs were calculated using a development of the PRP computer program developed at Oak Ridge National Laboratory (27). Equivalent mathematical expressions can be derived for the various cases and these are shown here.

The derivation given is a sample calculation of a generalised gas cost equation for a 3000 MWt (250×10^9 BTU/SD) plant at a 10% DCF rate-of-return without depreciation or taxation. Operation is assumed to be at a load factor of 0.85 (ie 81.81 PJ/y). Some of the more important economic assumptions of the PRP program are as follows:

- annual time periods are used
- investments (including working capital) occur at the **start** of the year
- expenses (including start-up costs) are paid at the **end** of the year
- income is received at the **end** of the year
- plants operate at 50% of normal load factor during the first year of operation
- working capital is recovered intact at the end of the project life
- process royalties are paid at the start of the final year of construction

If the following terms are defined (all in $\$10^6$):

T=total plant investment
S=start-up costs
W=working capital (includes initial charge of catalysts and chemicals)
N_1=net operating cost in first year
N=net operating cost in subsequent years
R=annual revenue received
P=Process royalties

then the DCF calculation can be summarised as in Table F1.

From this table one can calculate the following:

$$\text{Total discounted cash flow} = -0.8474T - 0.7153P - 0.6209N_1 - 0.6209S - 0.5815W - 5.1939N + 5.5044R$$

The total discounted cash flow is zero at the required value of R, so that:

$$R = 0.1539T + 0.1365P + 0.1128(N_1 + S) + 0.1056W + 0.9436N$$

$$\text{As gas cost/unit} = \frac{R}{\text{annual production}}$$

$$\text{Gas cost/unit expressed in ¢/GJ for a 3000 MWt plant} = \frac{R \times 100}{81.81}$$

$$\text{Hence: Gas cost (¢/GJ)} = 0.188T + 0.167P + 0.138(N_1 + S) + 0.129W + 1.153N$$

Table F1 Calculation of discounted cash flow for 10% discount rate with no tax or depreciation

End year	Revenue ($ x 10^6)	Net operating cost ($ x 10^6)	Net income ($ x 10^6)	Cash flow ($ x 10^6)	Discount factor	Discounted cash flow ($ x 10^6)
0	—	—	—	−0.100T	1.0000	−0.1000T
1	0	0	0	−0.225T	0.9091	−0.2045T
2	0	0	0	−0.475T	0.8264	−0.3925T
3	0	0	0	−0.200 T − P	0.7513	−0.1503T − 0.7153P
4	0	0	0	−W	0.5830	−0.6830W
5	0.5R	$-N_1$	$0.5R - N_1$	$0.5R - N_1 - S$	0.5209	$0.3105R - 0.6209(N_1 + S)$
6	R	−N	R − N	R − N	0.5645	0.5645(R − N)
7	R	−N	R − N	R − N	0.5132	0.5132(R − N)
.	.	.	.	.	.	.
.	.	.	.	.	.	.
.	.	.	.	.	.	.
24	R	−N	R − N	R − N + W	0.1015	0.1015(R − N) + 0.1015W

Using the above methodology, formulae for other cases were derived (Tables F2 & F3)

Table F2 Formulae for discounted cash flow calculations – 3000 MWt gas plant

Rate of return (%)	Gas cost[1] (¢/GJ)
3	$0.0907\ T + 0.0875\ P + 0.0825\ (N_1 + S) + 0.0379\ W + 1.181\ N$
5	$0.114\ T + 0.107\ P + 0.0971\ (N_1 + S) + 0.0635\ W + 1.174\ N$
10	$0.188\ T + 0.167\ P + 0.138\ (N_1 + S) + 0.129\ W + 1.153\ N$
15	$0.289\ T + 0.241\ P + 0.182\ (N_1 + S) + 0.197\ W + 1.131\ N$

Note:

1. Definitions of T, P, N_1, S, W and N are as given previously

Table F3 Formulae for discounted cash flow calculations – 500 MWt gas plant

Rate of return (%)	Gas cost[1] (¢/GJ)
3	$0.554\ T + 0.534\ P + 0.503\ (N_1 + S) + 0.231\ W + 7.209\ N$
5	$0.694\ T + 0.654\ P + 0.593\ (N_1 + S) + 0.388\ W + 7.165\ N$
10	$1.149\ T + 1.018\ P + 0.842\ (N_1 + S) + 0.788\ W + 7.040\ N$
15	$1.762\ T + 1.479\ P + 1.114\ (N_1 + S) + 1.203\ W + 6.904\ N$

Note:

1. Definitions of T, P, N_1, S, W and N are as given previously

Using the equations given in the tables above, the cost savings of the different processes relative to the dry-ash Lurgi process can be expressed as a function of the coal cost. We will here consider only 10% DCF rate-of-return and 3000 MWt SNG plants operating on an Eastern coal.

Table F4 Data for discounted cash flow calculations – 3000 MWt SNG plant, Eastern US coal, 10% DCF rate-of return, 'no-tax'
C=coal cost (in $/GJ)

Process	T[3]	P	S[1]	W[1] (all in $x10^6$)	N_1[2]	N[2]
Dry-ash Lurgi	1530	38	15.1C+ 8.9	28.4C+60.0	77.7C+105.1	155.3C+126.4
British Gas/Lurgi (with HCM)	1146	29	12.5C+ 8.8	23.6C+49.0	64.6C+ 84.6	129.1C+105.3
Exxon Catalytic	1418	35	12.8C+10.1	24.2C+53.1	66.2C+109.8	132.5C+142.6
Shell Coal (with HCM)	1575	39	13.6C+ 7.3	25.7C+54.7	70.3C+110.1	140.6C+118.7
Texaco (65% slurry)	1889	47	14.9C+ 7.4	28.1C+67.6	77.0C+116.1	153.9C+131.7

Notes:

1. Approximate formulae only; calculated from data in Table D5
2. Includes export power revenue for Texaco and Shell Coal processes
3. Includes contingency (see Table C5)

Using the above data and the formulae given in Table F2 the equations shown in the following table can be derived for the approximate cost of SNG from the various processes under the stated conditions.

Table F5 Formulae for SNG cost for 3000 MWt plant – Eastern US coal, 10% DCF rate-of-return, 'no-tax'
C=coal cost (in $/GJ)

Process	Gas cost ($/GJ)
Dry-ash Lurgi	1.96C + 4.63
British Gas/Lurgi (with HCM)	1.63C + 3.61
Exxon Catalytic	1.67C + 4.60
Shell Coal (with HCM)	1.77C + 4.63
Texaco (65% slurry)	1.94C + 5.41

The percentage change in the cost of gas relative to the dry-ash Lurgi process is given in the following table. This table also shows the differential of this percentage change with respect to coal costs. As can be seen, all these differentials are a function of coal cost – which automatically implies that the percentage change in the cost of gas varies non-linearly with coal price. This can be seen in Figures 4 and 8, for example. A negative sign for the differential implies that the cost savings will **decrease** as the coal price increases.

Table F6 **Percentage savings in the costs of SNG relative to dry-ash Lurgi—3000 MWt plant, Eastern US coal, 10% DCF rate-of-return, 'no-tax'**

C=coal cost ($/GJ)

Process	Percentage savings	Differential
British Gas/Lurgi (with HCM)	100 x (1.02+0.33C)/(4.63+1.96C)	$-47.1/(4.63+1.96C)^2$
Exxon Catalytic	100 x (0.03+0.29C)/(4.63+1.96C)	$128.4/(4.63+1.96C)^2$
Shell Coal (with HCM)	100 x (0.19C)/(4.63+1.96C)	$88.0/(4.63+1.96C)^2$
Texaco (65% slurry)	100 x (−0.78+0.02C)/(4.63+1.96C)	$230.9/(4.63+1.96C)^2$

7. BIBLIOGRAPHY

(1) Eriksson S., Forrester R., Johnston R., Teper M.
'Economic and Technical Criteria for Coal Utilisation Plant.
Part I: Economic and Financial Conventions'
Report No. A1/77, Economic Assessment Service,
IEA Coal Research, London
December 1977

(2) Eriksson S., Forrester R., Johnston R., Teper M.
'Economic and Technical Criteria for Coal Utilisation Plant.
Part II: Gasification Processes'
Report No. A2/77, Economic Assessment Service,
IEA Coal Research, London
December 1977

(3) Eriksson S., Forrester R., Johnston R., Teper M.
'Economic and Technical Criteria for Coal Utilization Plant.
Part III: Liquefaction'
Report No. A3/77, Economic Assessment Service,
IEA Coal Research, London
December 1977

(4) Eriksson S., Forrester R., Johnston R., Teper M.
'Economic and Technical Criteria for Coal Utilisation Plant.
Part IV: Power Generation'
Report No. A4/77, Economic Assessment Service,
IEA Coal Research, London
December 1977

(5) Baker A., Prior M.
'The Economics of Electricity from Coal, Nuclear and Wind Energy'
Report No. H1/78, Economic Assessment Service,
IEA Coal Research, London
Summer 1980 (Revised)

(6) Hemming D.F., Johnston R., Teper M.
'The Economics of Coal-based Electricity Generation'
Report No. E1/79, Economic Assessment Service,
IEA Coal Research, London
November 1979

(7) Eriksson S , Prior M.
'Treatment of Liquid Effluents from Coal Gasification Plants'
Report No. B2/79, Economic Assessment Service,
IEA Coal Research, London
March 1979

(8) Prior M.
'The Supply of Energy to Industry'
Report No. H2/79, Economic Assessment Service,
IEA Coal Research, London
December 1979

(9) Fant B.T.
'EDS Coal Liquefication Process Development Phase III A – Exxon Donor Solvent Coal Liquefication Plant Study Design Interim Report'
Prepared by Exxon Research & Engineering Co. for US ERDA
FE-2353-13
January 1978

(10) Allen D.H., Page R.C.,
'The Predesign Estimation and Capital Investment for Chemical Plant'
Presented at the 3rd International Cost Engineering Symposium, London, England
October 1974

(11) Detman R.
'Factored Estimates for Western Coal Commercial Concepts Interim Report'
Prepared by C.F. Braun & Co. for US ERDA & AGA
FE-2240-5
October 1976

(12) Detman R.
'Factored Estimates for Eastern Coal Commercial Concepts Interim Report'
Prepared by C.F. Braun & Co. for US DOE & GRI
HCP/T2240-31
September 1978

(13) Schreiner M.
'Research Guidance Studies to Assess Gasoline from Coal by Methanol-to-Gasoline and Sasol-type Fischer-Tropsch Technologies'
Prepared by Mobil Research & Development Corporation for US DOE
FE-2447-13
August 1978

(14) Kimmel S., Neben E.W., Pack G.E.
'Economics of Current and Advanced Gasification Processes for Fuel Gas Production'
Prepared by Fluor Engineers and Constructors, Inc. for EPRI
EPRI AF-244
July 1976

(15) Chandra K., McElmurry B., Neben E.W., Pack G.E.
'Economic Studies of Coal Gasification Combined Cycle Systems for Electric Power Generation'
Prepared by Fluor Engineers and Constructors, Inc. for EPRI
EPRI AF-642
January 1978

(16) McElmurry B., Smelser S.
'Economics of Texaco Gasification – Combined Cycle Systems'
Prepared by Fluor Engineers and Constructors, Inc. for EPRI
EPRI AF-753
April 1978

(17) Chandra K., McElmurry B., Smelser S.
'Economics of Fuel Gas from Coal – An Update'
Prepared by Fluor Engineers and Constructors, Inc. for EPRI
EPRI AF-782
May 1978

(18) Holmes J., Smith M., Merrick D., Harrison J.S.
'Coal Gasification for Combined-Cycle Power Generation: A General Simulation Method'
Presented at 'Future Energy Concepts',
London, England
January 1981

(19) Van Cooten P., Steeman J.W.M., de Leeuw den Bouter J.A.
'Computer Simulation of Coal Gasification and Combined Cycle Electric Power Generation'
Presented at the 12th European Symposium on Computer Applications in Chemical Engineering,
Montreux, Switzerland
April 1979

(20) 'Conceptual Designs & Assessments of a Coal Gasification Demonstration Plant
Volume III – Texaco Process'
Prepared by C.F. Braun & Co for Tennessee Valley Authority
TVA/OGM/CG-81/3
October 1980

(21) Private Communications

(22) Lupa D.J., Kliesch H.C.
'Simulation of a Texaco Gasifier
Volume 1: A Steady-State Model'
Prepared by Texaco for EPRI
EPRI AF-1179 Volume 1
September 1979

(23) 'Phase I: The Pipeline Gas Demonstration Plant Design and Evaluation of Commercial Plant'
Prepared by Continental Oil Company for US DOE
FE-2542-10
June 1978

(24) Kalina T., Nahas N.C.
'Exxon Catalytic Coal Gasification Process Predevelopment Program Final Project Report'
Prepared by Exxon Research & Engineering Co. for US DOE
FE-2369-24
December 1978

(25) Euker C.A.
'Exxon Catalytic Coal Gasification Process Development Program Annual Technical Progress Report, 1 July 1978 - 30 June 1979'
Prepared by Exxon Research & Engineering Co. for US DOE
FE-2777-10
October 1979

(26) Detman R.F.
'Preliminary Econornic Analysis of New Gasification Processes'
Presented at 1st International Gas Research Conference Chicago, Illinois
June 1980

(27) Salmon R.
'PRP – A Discounted Cash Flow Program for Calculating the Production Cost (Product Price) of the Product from a Process Plant'
Prepared by the Oak Ridge National Laboratory for US ERDA
ORNL-5251
March 1977

(28) 'DOE & Great Plains ink £2-Billion Loan Guarantee for Coal-Gas Plant'
Inside Energy p. 4b-5
5 February 1982

(29) 'France finally settles with Algeria'
World Gas Report Vol. 3, No. 3, p. 1,11-12
5 February 1982

(30) 'Japanese LNG import prices rise, LPG prices decline'
World Gas Report Vol. 3, No. 3, p. 12
8 February 1982

(31) Bonfiglioli G., Carella R., Bergmann B., Carta G., Cima F.
'Tavola rotonda sul tema: Aspetti economici e prospettive del'SNG per l'Italia'
Presented at 'La Gassificazione del Carbone – Prospettive techno-economiche' Pugnochiuso, Italy
May 1981

(32) 'Engineering Construction Performance
Report of the Comparative Construction Performance Working Party'
Prepared by NEDO for Mech. & Elec. Eng. Construction EDC,
London, England
December 1976

(33) Serrurier R.
'Prospects for marketing coal gasification by-products'
Hydrocarbon Process. Vol 55, No. 9, p. 253-257
September 1976

(34) Dickenson R.L., Simbeck D.R.
'SNG plant by-products need attention'
Oil & Gas Journal Vol 77, No. 11, p. 65-68
12 March 1979

(35) Anson D.
'Availability Patterns in Fossil-Fired Steam Power Plants'
Prepared by EPRI
EPRI FP-583-SR
November 1977

(36) Walley K.H., Robinson S.J.Q.
'Effects of scale on the economics of olefin production - theory and reality'
Petroleum Review Vol 26, No. 11, p. 328-332
November 1972

(37) Schrodt J.T.
'Hot Gas Desulphurization'
Prepared by Dept. of Chemical Engineering, University of Kentucky, Lexington, Kentucky, for US DOE
DOE/ET/10463-T1
February 1981

(38) Kertamus N.G.
'Combined Shift-Methanation Processes'
Prepared by C.F. Braun & Co. for US DOE & GRI
FE-2240-97
September 1978

(39) Dybkjaer I.
'Carbon Monoxide Shift Catalysts and Carbonyl Sulfide Hydrolysis Catalysts'
Presented at the IGT Symposium 'Ammonia from Coal', Muscle Shoals, Alabama.
May 1979

(40) Happel J., Hnatow M.A.
'Direct Catalytic Methanation of Raw Synthesis Gas'
Presented at 1st International Gas Research Conference, Chicago, Illinois
June 1980

(41) Happel J., Hnatow M.A., Bajars L., Lee A.L.
'Direct Methanation of Raw Synthesis Gas'
Presented at 1981 International Gas Research Conference, Los Angeles, California
September-October 1981

(42) Koch B.J., Yoon H., Carter W.B.
'Application of Conoco's Super-Meth Combined Shift/Methanation Process to the BGC/Lurgi Slagging Gasifier'
Presented at 'Coal Technology '79', Houston, Texas
November 1979

(43) Hill R.F.
'Potential for Liquefaction in the U.S. Energy Market'
Presented at the IEA Coal Liquefication Workshop, Jülich, W Germany
September 1978

(44) Parker H.W.
'The Energy Component of Future Energy Costs'
Escoe Echo Vol. 3, No. 24, p. 1-3
19 November 1979

(45) Hoogendoorn J.C.
'Gas from Coal with Lurgi Gasification at Sasol'
Presented at the Clean Fuels from Coal Symposium I, Chicago, Illinois
September 1973

(46) 'Trials of American Coals in a Lurgi Gasifier at Westfield, Scotland'
Prepared by Woodall-Duckham Ltd. for US ERDA & AGA
FE-105
1974

(47) Sharman R.B., Lacey J.A., Scott J.E.
'The British Gas/Lurgi Slagging Gasifier - A Springboard into Synfuels'
Presented at 8th Annual Intl. Conference on Coal Gasification, Liquefaction and Conversion to Electricity, Pittsburgh, Pennsylvania
August 1981

(48) 'Operating Experience with the 170-MW STEAG Coal Gasification Combined Cycle Power Plant'
STEAG, Essen, W. Germany
October 1977

(49) Koch B.J.
'Market Study for Sale of the Coal Fines By-product from a Coal Gasification Plant'
Prepared by Continental Oil Co. for US DOE
FE-2542-8
1977

(50) DiFulgentiz R.A.
'Phase I: The Pipeline Gas Demonstration Plant. Coal Fines Briquetting Study'
Prepared by Continental Oil Co. for US DOE
FE-2542-11
1978

(51) Timmins C.
'The future role of gasification processes'
Gas Eng. Manage. Vol. 20, No. 2, p. 81-94
February 1980

(52) Hebden D., Brooks C.T.
'Westfield – the development of processes for the production of SNG from coal'
Presented at the 113th Annual General Meeting,
Institution of Gas Engineers, Edinburgh, Scotland
April 1976

(53) Aul E.F., Curran G.P., Fink C.E., Heunisch G.W., Spangler M.D., Sudbury J.D.
'Phase 1: The Pipeline Gas Demonstration Plant.
British Gas Corporation Westfield Development Centre,
Technical support program report'
Prepared by Continental Oil Co. for US DOE
FE-2542-13
1978

(54) Roberts G.F.I., Hebden D., Brooks C.T., Sudbury J.D.
'The application of slagging gasification to the production of SNG from coal'
Presented at 14th World Gas Conference, Toronto, Canada
May 1979

(55) Sharman R.B., Scott J.E.
'The British Gas/Lurgi Slagging Gasifier – What it can do'
Presented at 'Coal Technology '80', Houston, Texas
November 1980

(56) Sharman R.B., Lacey J.A., Scott J.E.
'The British Gas/Lurgi Slagging Gasifier'
Presented at Synfuels International Conference, Frankfurt, W Germany
May 1981

(57) Scott J.E.
'US Coal Test Program on BGC-Lurgi Slagging Gasifier'
Prepared by British Gas Corporation for EPRI
EPRI AP-1922
August 1981

(58) Fishlock D.
'British Gas Slagger now on the market'
Energy Daily p. 3-4
11 January 1982

(59) Tart K.R., Rampling T.W.A.
'Methanation key to SNG success'
Hydrocarbon Process. Vol. 60, No. 4, p. 114-118
April 1981

(60) Koch B.J., Schwartz H.H.
'Conoco's Methanation Processes: Ready for Synfuels Industry'
Presented at 'Coal Technology '80', Houston, Texas,
November 1980

(61) Houle W.E.
'The Exxon Process for Catalytic Coal Gasification'
Presented at 'Refining of Hard Coal and Lignite - Bergbau '81',
Düsseldorf, W Germany
June 1981

(62) Hirsch R.L., Gallagher J.E., Euker C.A.
'Exxon's Catalytic Coal Gasification Process'
Presented at 1981 International Gas Research Conference,
Los Angeles, California
September-October 1981

(63) Seipenbusch J., Ruprecht P.
'Die Aussichten der Kohlenstaub-Druckvergasung nach dem Texaco-Verfahren'
Energie Vol. 30, No. 6, p. 189-190
June 1978

(64) Cornils B., Ruprecht P., Langhoff J., Dürrfeld R.
'Stand der Texaco-Kohlevergasung in die Ruhrchemie/Ruhrkohle-Variante'
Stahl Eisen Vol. 100, No. 7, p. 388-392
April 1980

(65) Cornils B., Specks R.
'Experiences with the Texaco Process of Coal-Dust Pressure Gasification Using the Ruhrchemie/Ruhrkohle Technical Version'
Presented at 'Synthetic Fuels – Status and Directions',
San Francisco, California
EPRI WS-79-238
October 1980

(66) 'Coal Gasification: Ruhrkohle-Ruhrchemie's adaptation of the Texaco Process'
EPRI J. Vol. 6, No. 5, p. 29-31
June 1981

(67) Reed T.L.
'Preliminary Design Study for an Integrated Coal Gasification Combined Cycle Power Plant'
Prepared by Southern California Edison Company for EPRI with Ralph M. Parsons Company as sub-contractor.
EPRI AF-880
August 1978

(68) Grace R.J.
'Development of the BI-GAS Process'
Presented at the Clean Fuels from Coal Symposium I, Chicago, Illinois
September 1973

(69) Maize K.
'Bi-Gas Back on Its Feet; Other Gasifier Vendors Tout Their Wares'
Energy Daily Vol. 9, No. 150, p. 2
6 August 1981

(70) Meyer J.P., Wells J.W., Cox J.R., Belk J.P., Frazier G.C.
'Mathematical Model of the HYGAS Pilot Plant Reactor'
Presented at the AIChE Meeting, Houston, Texas
CONF-790405-11
April 1979

(71) 'Pipeline gas from coal – Hydrogenation (IGT Hydrogasification Process)
Annual Report, 1 July 1978 – 30 June 1979'
Prepared by IGT for US DOE
FE-2434-50
May 1980

(72) Detman R.
'Factored Estimates for Lignite Commercial Concepts
Interim Report'
Prepared by C.F. Braun & Co. for US DOE & GRI
FE-2240-98
September 1978

(73) 'Coronach Coal Gasification Study'
Prepared by Lummus Co. Canada for Saskatchewan Power Corporation.
October 1977

(74) 'Studies of Advanced Electric Power Generation and Coal Gasification
Based on the Use of Hat Creek Coal'
Prepared by Intercontinental Consultants, EPD Consultants, Shawinigan
Engineering Co., Lummus Co. Canada for BC Hydro and Power, EMR
Canada
1976

(75) Rudolph P.F.H.
'Coal Gasification'
Energiespectrum p. 311-321
November 1977

(76) 'Coal Gasification: A Technical Description'
Western Gasification Company, Farmington, N.M.
Revised January 1977

(77) Jones F.L.
'The Great Plains Gasification Associates Project'
Presented at the 5th Annual Intl. Conference on Coal Gasification, Liquefaction, and Conversion to Electricity, Pittsburgh, Pennsylvania
August 1978

(78) 'Fuel Gas from Coal'
Lurgi Kohle und Mineralöltechnik,
Frankfurt, W. Germany
January 1980

(79) Rudolph P.F.H., Bierbach H.H.
'Lurgi Coal Gasification and how it can contribute to our future energy supply'
Presented at Coal Gasification Symposium, Delft, Netherlands
September 1980

(80) Rudolph P.F.H., Herbert P.K.
'Conversion of Coal to High Value Products'
Presented at Symposium on Coal Gasification, Liquefaction and Utilization, Pittsburgh, Pennsylvania
August 1975

(81) 'Feasibility Study for the Production of Intermediate BTU Fuel Gas from Coal at Edmonton, Alberta'
Prepared by SNC Tottrup for Shell Canada,
1977

(82) Moe J.M.
'SNG from coal via the Lurgi Gasification Process'
Presented at the Clean Fuels from Coal Symposium I,
Chicago, Illinois
September 1973

(83) Rudolph P.F.H., Hafke C., Herbert P.K.
'Lurgi Coal Gasification'
Presented at 'Synthetic Fuels – Status and Directions',
San Francisco, California
EPRI WS-79-238
October 1980

(84) Hoelen O.E.J.J.M.
'Kohlenvergassingsproject van N.V. Nederlandse Gasunie'
Gas Vol. 100, No. 5, p. 226-238
May 1980

(85) Mujadin M.J.
'Great Plains Gasification Associates Coal Gasification Project'
Presented at Symposium 'Advances in Coal Utilization Technology'
Louisville, Kentucky
May 1979

(86) Gallagher J.E., Euker C.A.
'Catalytic Coal Gasification for SNG Manufacture'
Presented at 6th Annual Intl. Conference on Coal Gasification, Liquefaction and Conversion to Electricity
Pittsburgh, Pennsylvania
July-August 1979

(87) Fant B.T., Euker C.A.
'Exxon's Catalytic Coal Gasification Process'
Presented at 1st International Gas Research Conference,
Chicago, Illinois
June 1980

(88) Völkel H.K.
'Der Shell-Koppers Prozess zur Vergasung von kohle unter Druck'
Presented at 14th World Gas Conference, Toronto, Canada
May 1979

(89) McCullough G.R., van der Burgt M.J., Waller J.
'Shell Coal Gasification Process'
Presented at 8th Annual Intl. Conference on Coal Gasification, Liquefaction and Conversion to Electricity,
Pittsburgh, Pennsylvania
August 1981

(90) Vogt E.V., Weller P.J., van der Burgt M.J.
'The Shell Coal gasification process (SCGP)'
Contribution for The Handbook of Synfuels Technology,
McGraw-Hill, New York, N.Y.
1982

(91) Cornils B., Hibbel J., Ruprecht P., Dürrfeld R., Langhoff J.
'RCH/RAG's version of Texaco Coal Gasification'
Hydrocarbon Process. Vol. 60, No. 1, p. 149-156
January 1981

(92) Cornils B., Hibbel J., Ruprecht P., Langhoff J. Dürrfeld R.
'Raw Materials and Energy from Coal Gasification: The Ruhrchemie/Ruhrkohle Demonstration Plant Based on Texaco's Coal-Gasification Process'
Chem. Econ. Eng. Rev. Vol. 12, No. 6-7, p. 7-11
June/July 1980

(93) Konkol W., Ruprecht P., Cornils B., Dürrfeld B., Langhoff J.
'Autothermal coal gasification'
Hydrocarbon Process. Vol. 61, No. 3, p. 97-102
March 1982

(94) Alves G.W., Waitzmann D.A.
'TVA Ammonia from Coal Project – 1981 Update'
Presented at 8th Energy Technology Conference, Washington, D.C.
March 1981

(95) Tarman P.B.
'The HYGAS Process – Pipeline Gas from Coal'
Presented at 1st Intl. Gas Research Conference, Chicago, Illinois
June 1980

(96) 'BI–GAS Pilot Plant Gasifier Operation
Tests G–3 through G–3G'
Prepared by BCR and Phillips Petroleum Co. for US DOE
FE–1207–T22
October 1979

(97) 'BI–GAS Pilot Plant Operation
Quarterly Technical Progress Report, 1 July 1980 - 30 Sept 1980'
Prepared by Stearns-Roger Inc. for US DOE
DOE/ET/14705–15
1980

(98) Winton J.M.
'Plant Sites 1978'
Chemical Week p. 49-60
14 December 1977

(99) Kohn P.M.
'CE cost indexes maintain 13-year ascent'
Chemical Engineering Vol. 85, No. 11, p. 189-190
8 May 1978

(100) Arnold T.H., Chilton C.H.
'New Index Shows Plant Cost Trends'
Chemical Engineering Vol. 70, No. 4, p. 143-152
18 February 1963

(101) Musgrove R.E., Maifield D.L.
'Considerations in Sizing Coal Gasification Plants'
Prepared by C.F. Braun & Co. for US DOE & GRI
FE-2240-10
September 1978

(102) Williams R.
'Standardisation: cost data and process equipment'
Chemical Engineering Vol. 54, p. 102
June 1947 and ibid p. 124, December 1947

(103) Chilton C.H.
'Six-tenths factor applied to complete plant costs'
Chemical Engineering Vol. 57, p. 112
April 1950

(104) Cran J.H.
'The effect of scale on chemical plant costs'
Process Engineering p. 154-161
September 1978

(105) Taylor J.H., Craven P.J., Richards D.
'The Economics of Scale in Chemical Manufacture'
Presented at the Fifth Intl. Cost Engineering Conference,
Utrecht, Netherlands
October 1978

(106) Burgert W.
'Cost Structure Analysis – A Flexible Method of Investment Cost Estimating'
Presented at the Fifth Intl. Cost Engineering Conference,
Utrecht, Netherlands
October 1978

(107) Seward W.H.
'Process Alternatives for Sulfur Management Overview Report'
Prepared by C.F. Braun & Co. for US DOE & GRI
FE-2240-41
January 1978

(108) Chia W.S., Todd F.A.
'Sulfur Recovery in a Coal Gasification Plant'
Prepared by C.F. Braun & Co. for US DOE and GRI
FE-2240-50
August 1978

(109) Zawacki T.S., Duncan D.A., Macriss R.A.
'Process optimized for high pressure gas clean-up'
Hydrocarbon Process. Vol. 60, No. 4, p. 143-149
April 1981

(110) Drnevich R.F., Ecelbarger E.J., Portzer J.W.
'Industrial Oxygen Plants – A Technology Overview for Users of Coal Gasification – Combined-Cycle Systems'
Prepared by Union Carbide Corp. for EPRI
EPRI AP-1674
January 1981

(111) Baker C.R.
'Low purity O_2 saves energy in coal conversion'
Hydrocarbon Process. Vol. 60, No. 7, p. 75-80
July 1981

(112) Lohmann C., Langhoff J.
'Ruhr 100 – Development Work on the Pressurized Lurgi Gasifier in Dorsten'
Presented at 'Synthetic Fuels – Status and Directions',
San Francisco, California
EPRI WS-79-238
October 1980

REPORTS PUBLISHED BY THE ECONOMIC ASSESSMENT SERVICE

Report		Published	Price
	Economic & technical criteria for coal utilisation plant		
A1/77	Part I : economic & financial conventions	Dec 77	£20
A2/77	Part II : gasification processes	Dec 77	£20
A3/77	Part III : liquefaction	Dec 77	£20
A4/77	Part IV : power generation	Dec 77	£20
B1/77	The control of sulphur oxides emitted in coal NB: This report is now out of print	Dec 77	£20
B2/79	Treatment of liquid effluents from coal gasification plants	Mar 79	£20
C1/77	Published plans & projections for coal production, trade & consumption	Dec 77	£20
D1/78	The long-run economics of the ocean transport of coal	Dec 78	£20
D2/79	The future economics of coal transport	Jul 80	£20
E1/79	The economics of coal-based electricity generation	Nov 79	£20
E2/80	The economics of gas from coal	Jan 83	£80
E4/82	Methanol production from natural gas or coal	Dec 82	£50
G1/80	Inflation and the real cost of energy	Dec 80	£20
G2/81	Market aspects of an expansion of the international steam coal trade	Aug 81	£20
G3/82	Constraints on international trade in coal	Dec 82	£50
H1/78	The economics of electricity from coal, nuclear and wind energy (revised 1980)	Sept 80	£20
	The supply of energy to industry		
H2/79/1	Volume I : executive summary	Sept 79	)£20
H2/79/2	Volume II : main report	Aug 79	)the set
H3/82	The future economics of coal-based energy in residential market	Feb 83	£50

END OF PAPER

38. Table

UCG

DOE/MC/19865-1674
(DE85001966)

FOSSIL ENERGY

FLAG
A COMPUTER CODE MODEL FOR FLUIDIZED BED COAL GASIFICATION REACTORS

Volume I - Technical Document

By
Dr. Allen Goldman

April 1984

Work Performed Under Contract No.: DE-AC21-82MC19265

For
U.S. Department of Energy
Office of Fossil Energy
Morgantown Energy Technology Center
Morgantown, West Virginia

By
The BDM Corporation
McLean, Virginia and Albuquerque, New Mexico

TECHNICAL INFORMATION CENTER
OFFICE OF SCIENTIFIC AND TECHNICAL INFORMATION
UNITED STATES DEPARTMENT OF ENERGY

DOE/MC/19265-1674
(DE85001966)
Distribution Category UC-90c

FLAG
A COMPUTER CODE MODEL FOR FLUIDIZED BED COAL GASIFICATION REACTORS

Volume I - Technical Document

By
Dr. Allen Goldman

April 1984

Work Performed Under Contract No.: DE-AC21-82MC19265

For
U.S. Department of Energy
Office of Fossil Energy
Morgantown Energy Technology Center
P.O. Box 880
Morgantown, West Virginia 26505

By
The BDM Corporation
7915 Jones Branch Drive
McLean, Virginia 22102

FOREWORD

This report, BDM/A-84-013-TR, was prepared for the U.S. Department of Energy by The BDM Corporation, McLean, Virginia and Albuquerque, New Mexico, in compliance with the requirements of Contract DE-AC21-82MC19265. The principal author of this document is Dr. Allen Goldman.

TABLE OF CONTENTS

List of Figures

List of Tables

Chapter I
Introduction

This is the first volume in a three volume set which will explain various aspects of the FLAG code. This volume sets forth the basic differential equations used to model a reacting fluid-particle system and then presents the numerical procedures used to solve the differential equations. The basic philosophy employed has been to simply state what has been programmed in the FLAG code. For a number of points just showing an equation provides everything necessary to understand what has been done. However, for other aspects of the code an equation presented outside the context of the development has little meaning. In these instances enough of the development is given to make the equations meaningful, but the full detailed step by step development which produced the equation is not given. That level of detail is left to the references.

A second point to keep in mind is that the coding in FLAG does not necessarily have a one to one correspondence to the equations given here. For example, equation (1.1-1) shows calculation of a variable composed of the sum of three quantities

$$q = q_1 + q_2 + q_3 \qquad (1.1\text{-}1)$$

Within FLAG the quantities q_1, q_2 and q_3 may each be created in different subroutines and with a variable name different from that shown in (1.1-1). Therefore, FLAG may contain three FORTRAN statements of the form

$$q = q + r \qquad (1.1\text{-}2)$$

rather than the one equation given by (1.1-1). Thus, the equations coded in FLAG are not always recognizable as those shown in this volume.

Exactly how equations are implemented is discussed in Volume III. There for example equation (1.1-1) is given and then the details of where within FLAG each of the terms on the right hand side are created and how they are assembled to produce the variable q. In general Volume I answers the question of what are the mathematical models of the system, what are the numerical models and what methods have been used to solve the numerical equations. On the other hand Volume III answers the questions on the details of how the numerical equations and techniques have been combined to produce FLAG.

Volume II details the information required to make the code run, and the information which the code produces as output. This volume is meant to be a stand alone source of information. What is presented therein is sufficient to run FLAG as configured. Volumes I and III is the information needed to reconfigure the code.

Finally, there are some general comments which need to be made concerning FLAG. The presentation of equations as given in this volume does not truly convey the complexity of the code. The code is complex for a number of reasons. First, FLAG has not been designed from the ground up, rather, it was built on the skeleton of a similar code called FLAME. The result is that FLAG has been bent to fit a structure designed around a solution philosopy different from FLAG. In fact parts of the FLAG code are never accessed and appear to relate only to the earlier code.

However, the major factor contributing to the complexity is the poor programming style used through the code. Most of the rules for creating code, as set forth in basic programming texts, have been violated. Control parameters are hardwired, the x-y coordinate directions are interchanged from subroutine to subroutine, and not all the code contained in FLAG is actually used. This adds up to a code which seems to be more in a state of development than a finished product. Furthermore making

changes within the code will require a good deal of effort and time. In fact it is highly recommended that Volume I and III be thoroughly read and understood before any attempts are made to modify the code.

Lastly, a word of warning must be given. The sole purpose of this work is to set forth the various equation and techniques which taken together form FLAG. This should not be interpreted as an endorsement of the correctness of either the mathematical model or the numerical techniques. FLAG, like any code, must be run for a number of well documented problems in order to determine the accuracy of the code. Until this is done, any results produced by the code should be regarded with sus; icion.

Chapter II
Mathematical Formulation of Model

2.1 Gas Equations

Creation of a set of equations to model a gas-particle system involves the same two step process standard to a simple fluid system. The first step is a control volume analysis on a small element of the gas-particle system. The element chosen should contain both particles entirely enclosed within the control surface and particles in the process of crossing the control surface. The control volume is large compared to the mean particle separation, but small compared to the characteristic dimensions of the system. The second step in the proce s is to convert all surface integrals to volume integrals. With the exception that the volume may not become so small as to enclose only one component, the volume is arbitrary. This allows the integral equations to be converted to differential equations. Details of the general technique are given in reference (1). The full set of fluid equations is given below. Care must be taken with these equations. Although they appear in the standard form, the quantities which look like velocities are actually fluxes, i.e., if u is the velocity in the axial direction, ρ is the fluid density, and ϵ is the void fraction, then the axial momentum is given by

$$U = \rho \epsilon u$$

After each equation a parameter list is given: it is important that each parameter be correctly understood before proceeding on.

Mass Continuity Equation

$$\frac{\partial(\rho\epsilon)}{\partial t} + \frac{\partial U}{\partial x} + \frac{1}{r}\frac{\partial rV}{\partial r} = r_m \qquad (2.1\text{-}1)$$

where

ϵ = Volume averaged void fraction
ρ = Gas density
u = Axial gas velocity
U = Volume averaged axial momentum density = $\rho\epsilon u$
v = Radial gas velocity
V = Volume averaged radial momentum density = $\rho\epsilon v$
x = Axial distance
r = Radial distance
t = Time
Γ_m = Mass source term

Axial Momentum Equation

$$\frac{\partial U}{\partial t} + \frac{\partial(\alpha UU)}{\partial x} + \frac{1}{r}\frac{\partial(r\alpha UV)}{\partial r} = -\epsilon\frac{\partial P}{\partial x} \qquad (2.1\text{-}2)$$

$$-\frac{g}{\alpha} + \frac{\partial}{\partial x}\left(\Gamma\frac{\partial \alpha U}{\partial x}\right) + \frac{1}{r}\frac{\partial}{\partial r}\left(r\Gamma\frac{\partial \alpha U}{\partial r}\right)$$

$$-F_{DU} + S_u$$

where

U = Volume averaged radial momentum density = $\rho\epsilon u$
ϵ = Volume averaged void fraction
ρ = Gas density
u = Axial velocity
α = Inverse of gas density = $1/\epsilon\rho$
x = Axial distance
r = Radial distance
V = Volume averaged radial momentum density = $\rho\epsilon v$

Γ = Gas density times diffusion coefficient

P = Gas pressure

g = Gravitational acceleration

F_{DU} = Drag force in axial direction

S_u = Axial force per unit volume = $\alpha U r_m$

t = Time

Radial Momentum Equation

$$\frac{\partial V}{\partial t} + \frac{\partial(\alpha U V)}{\partial x} + \frac{1}{r}\frac{\partial(r\alpha V V)}{\partial r} - \frac{\alpha W W}{r} = \quad (2.1\text{-}3)$$

$$-\epsilon\frac{\partial P}{\partial r} + \frac{\partial}{\partial x}\left(\Gamma\frac{\partial \alpha V}{\partial x}\right) + \frac{\partial}{\partial r}\left(\frac{\Gamma}{r}\frac{\partial r\alpha V}{\partial r}\right)$$

$$-F_{DV} + S_v$$

V = Volume averaged radial momentum density = $\rho\epsilon v$

W = Volume averaged swirl momentum density = $\rho\epsilon w$

v = Radial velocity

w = Swirl velocity

F_{DV} = Drag force in radial direction

S_v = Radial force per unit volume = $\alpha V r_m$

Swirl Momentum Equation

$$\frac{\partial W}{\partial t} + \frac{\partial(\alpha U W)}{\partial x} + \frac{1}{r}\frac{\partial(r\alpha V W)}{\partial r} + \frac{\alpha V W}{r} = \quad (2.1\text{-}4)$$

$$\frac{\partial}{\partial x}\left(\Gamma\frac{\partial \alpha W}{\partial x}\right) + \frac{\partial}{\partial r}\left(\frac{\Gamma}{r}\frac{\partial r\alpha W}{\partial r}\right) - F_{DW} + S_w$$

where

W = Volume averaged swirl momentum density = $\rho \epsilon v$

F_{DW} = Drag in swirl direction

S_w = Swirl force per unit volume = $\alpha W r_m$

Energy Equation

The energy equation is in a slightly different form than usual. Normally, the dependent variable is some form of energy, i.e., total energy, internal energy, or enthalpy, or the related quantity of temperature. However, the energy equation has been cast in terms of pressure and forms the foundation of the ICE method [reference (11)]. It is a variation of the ICE method whichis used in FLAG. A complete derivation of this equation is given in Appendix I. The equation given below has been slightly modified over and above making the pressure the dependent variable. The equation has been modified by scaling to reference thermodynamic values. In reality this does not change the equations since the reference quantities are constants and the derivative of a constant is zero. Nevertheless, it does produce an equation with a unique appearence.

Energy Equation:

$$\frac{\partial \delta P}{\partial t} + \frac{\gamma R}{\epsilon}\left[\frac{\partial [U(T_B+\delta T)]}{\partial x} + \frac{1}{r}\frac{\partial [rV(T_B+\delta T)]}{\partial r}\right] = \tag{2.1-5}$$

$$\frac{\gamma R}{\epsilon}\left[\frac{\partial}{\partial x}\left(\Gamma \frac{\partial T}{\partial x}\right) + \frac{1}{r}\frac{\partial}{\partial r}\left(r\Gamma \frac{\partial T}{\partial r}\right)\right]$$

$$+ \frac{(\gamma-1)}{\epsilon}\left[\alpha\epsilon U \frac{\partial P}{\partial x} + \alpha\epsilon V \frac{\partial P}{\partial r} + C_p T r_m\right.$$

$$\left. - \sum_{i=1}^{N} \frac{\partial (h_i C_i)}{\partial t} + S_{RAD} + S_{COND}\right] + \frac{\gamma P}{R}\frac{\partial R}{\partial t} - \frac{\gamma P}{\epsilon}\frac{\partial \epsilon}{\partial t}$$

where

P_B = Base pressure = constant

δP = Difference between total pressure and base state pressure = $P - P_B$

T = Gas temperature = $P\alpha/R$

S_{RAD} = Radiation heat transfer

S_{COND} = Conduction heat transfer

C_p = Specific heat at constant pressure

h_i = Specific enthalpy of species i

C_i = Bulk-averaged concentration of species i

$\sum \frac{\partial (h_i C_i)}{\partial t}$ = Change in gas energy from homogenous chemical reactions.

The final equations which close the set are the species equation and the equation of state; these are

Species Equation:

$$\frac{\partial C_i}{\partial t} + \frac{\partial(\alpha U C_i)}{\partial x} + \frac{1}{r}\frac{\partial(r\alpha V C_i)}{\partial r} = \frac{\partial}{\partial x}\left(\Gamma \frac{\partial \alpha C_i}{\partial x}\right) \quad (2.1\text{-}6)$$

$$+ \frac{1}{r}\frac{\partial}{\partial r}\left(r\Gamma \frac{\partial \alpha C_i}{\partial r}\right) + S_i$$

C_i = Volume averaged concentration of species i

S_i = Production of species i

Equation of State

The derivation of the equations as given in reference 1 is carried out in terms of volume averaged quantities. This leads to an equation of state of the form

$$\langle P \rangle \alpha = RT \quad (2.1\text{-}7)$$

where the volume averaged pressure is related to the point presure by

$$\langle P \rangle = \epsilon P$$

Equation (2.1-7) is the basic definition of the equation of state. However, the pressure shown in equations (2.1-2) through (2.5-5) and the pressure used in FLAG is the point pressure. This means that when the equation of state is used to evaluate, for example, temperature, what is coded in FLAG is,

$$T = \frac{P\epsilon\alpha}{R} .$$

The difference between the point and volume pressure is emphasized because pressure is the one major variable given in equation (2.1-2) through (2.1-5) as a point value rather as a volume average quantity. The basic equations could of course be changed so that all variables are either point or volume quantities. This has not been done here because the equations as shown are what is coded in FLAG.

2.2 Particles

There are two basic approaches to evaluating particle dynamics. The first is to treat the particles as a fluid which is handled as one component of a multi-component fluid. The other approach is a Lagrangian formulation where the particle is continuously tracked as it moves throughout the system. It is the latter formulation which is used in FLAG. However, rather than actually following each and every particle the formulation uses macroparticles. The macroparticle is composed of a number of identical microparticles (the microparticle is the actual solid particle) distributed over a region in space. Thus, the movement of the macroparticle represents the motion of a large number of actual particles and therby reduces the resources needed to evaluate particle motion. The following description shows single particle equations, but it should be kept firmly in mind that macroparticles are being used rather than microparticles.

One other point needs to be made before starting the particle discussion. Regardless of what is stated on comment cards within the code, FLAG, as it is presently configured, does not consider agglomeration. The subroutine which controls particle calculations is PMONIT. PMONIT in turns calls a subroutine named COLIDE which refers to various calculations concerning agglomeration. Within COLIDE as presently configured, agglomeration is not considered. There is, however, a second version of COLIDE based on the JAYCOR agglomeration model, written by a

group at West Virginia University which does account for agglomeration. The basics of the agglomeration model will be given in this chapter but a discussion of the numerical techniques used in the code is left to reference 3.

The basic equations used in FLAG to describe particle motion are derived directly from Newton's law. The particle velocity and position are determined by

$$m_p \frac{d\vec{V}_p}{dt} = m_p \vec{g} - D_p(\vec{V}_g - \vec{V}_p) \tag{2.2-1}$$

and

$$\frac{d\vec{X}_p}{dt} = \vec{V}_p \tag{2.2-2}$$

where m_p is the mass of the macroparticle, $\vec{V}_g$ and $\vec{V}_p$ are the gas and particle velocities respectively ($\vec{V}_g - \vec{V}_p$ is the relative velocity) and D_p is the drag coefficient. The drag term is examined in more detail in section 2.6. The energy equation is

$$\frac{\partial(m_p C_p T_p)}{\partial t} = -\sum r_g(T_p) H_g(T_p) + S_{RAD} + S_{COND} \tag{2.2-3}$$

where

r_g = Rate of production of component g ($kg\text{-}sec^{-1}$) at particle temperature T_p

H_g = Specific enthalpy of gas component g
$r_g H_g$ = Heat release from chemical reactions
S_{rad} = Conduction transfer
S_{cond} = Conduction transfer.

These terms are considered in greater detail in section 2.4.

2.3 Chemistry

The equations presented in section 2.1 and 2.2 are sufficient to determine the state of the system if the various components do not undergo chemical reactions. With no reaction the S_i term in equation (2.1-6) is zero and the set of equations may be solved. However, if the components do react, S_i, the net production of the i^{th} species, is no longer zero. This section describes the reaction model used to determine S_i. There are two basic types of reactions which must be determined, heterogeneous and homogeneous reactions. The homogeneous reactions are chemical changes which occur throughout the entire volume of the fluid where as the heterogeneous reactions occur at the surface of the particles. It is assumed that as a coal particle is introduced into the reactor devolatization takes place immediately producing H_2O, CO, CO_2, N_2 and CH_4 with the solid assumed to be carbon and ash. The system can also contain O_2 as a component of the fluidizing gas. These components will produce the following reaction

R1: $C + 1/2\ O_2 \longrightarrow CO$
R2: $C + H_2O \longrightarrow CO + H_2$
R3: $C + CO_2 \longrightarrow 2CO$

} Hetrogeneous Reactions

R4: $CO + 1/2\ O_2 \longrightarrow CO_2$
R5: $H_2 + 1/2 O_2 \longrightarrow H_2O$
R6: $CO + H_2O \rightleftharpoons CO_2 + H_2$

} Homogeneous Reactions

Reaction (R6) is assumed to be at equilibrium and reactions R4 and R5 are assumed to go to completion instantaneously. The process of hydrogasification ($C + 2H_2 \rightarrow CH_4$) is neglected because it is negligibly slow compared to other char reactions. FLAG does contain a CH_4 concentration equation, but the production term has been set to zero. Therefore, the concentration of CH_4 varies throughout the reactor by advection and diffusion, but not by chemical reaction.

The chemistry package contained within FLAG is consistent with the reactions given above. FLAG, however, contains three subroutines which are extraneous. These routines are CALCSI, CALSI and CUBERT. These routines were part of the FLAME code, but are not part of FLAG.

The following set of reaction rates are used to describe the set of chemical reactions

R1: $C + 1/2\ O_2 \rightarrow CO$ (2.3-1)

$r_1 = k_1\ C_{O_2}$ kg-mol-C/m^2-s (external area)

$k_1 = 3.007 \times 10^5 \exp(-17966/T_p)$ (m/sec)

The steam gasification and CO_2 gasification rate constants are stated as fitting reaction rate data for Western Kentucky char.

R2: $C + H_2O \rightarrow CO + H_2$ (2.3-2)

$r_2 = k_2\ C_{H_2O}$

$k_2 = 95.5 \exp(-17594.4/T_p)$

R3 $C + CO_2 \rightarrow 2CO$ (2.3-3)

$r_3 = k_3\ C_{CO_2}$

$k_3 = 6.25 \times 10^5 \exp(-29491/T_p)$

R6 Water-gas shift equilibrium (2.3-4)

$CO + H_2O \rightleftharpoons CO_2 + H_2$

$\text{Log}_{10}K = -1.6945 + 1855.6/T_g$

where T_p is particle temperature and T_g is gas temperature.

The final part of the chemistry package describes the change in the particle due to the reactions. The dependence of the reaction rates on the amount of carbon present in the char particle is accounted for by a shrinking core approximation function ϕ, where

$$\phi = (1-X)^{2/3} \tag{2.3-5}$$

and

$$X = \frac{\text{carbon gasified}}{\text{initial carbon content of particle}} \tag{2.3-6}$$

The basic idea of the shrinking core model [reference (2)] is that the particle is composed of a porous ash sphere containing carbon. At the beginning of a reaction the carbon is uniformly distributed throughout the ash sphere. As the reaction proceeds, the size of the particle does not vary, rather it is the region containing carbon within the particle which varies. It is further assumed that the carbon containing region is always spherical and the reaction only occurs on the surface of this carbon containing region . This region of course shrinks in size as the carbon is consummed. This leads to the relationship

$$X = 1 - \left(\frac{r}{R_o}\right)^3 \tag{2.3-7}$$

where r = radius of carbon containing part of particle

R_o = particle radius. This is the radius of the ash particle left when all carbon is consummed.

The mass balance for species i at particle surface is given by

$$-k_g (C_i - C_{i,s}) = \sum_j \alpha_{i,j} r_j \phi \qquad (2.3\text{-}8)$$

where

r_j = specific rate of reaction j
$\alpha_{i,j}$ = stoichiometric coefficient of i^{th} species, j^{th} reaction
k_g = mass transfer coefficient
$C_{i,s}$ = concentration of i^{th} species at particle surface
C_i = concentration of i^{th} species in bulk fluid

The mass transfer coefficient, k_g, is obtained from an empirical relationship. The relationship used is

$$Sh = \frac{2k_g d}{\mathcal{D}} = 2 + .654\ Re^{1/2}\ Sc^{1/3} \qquad (2.3\text{-}9)$$

where

Sh = Sherwood No.
Sc = Schmidt No. = $\mu/\rho\mathcal{D}$
Re = Reynolds No.
$\mathcal{D}$ = Molecular diffusion coefficient
d = particle diameter

The diffusion coefficient appears to be from the Chapman-Enskog diffusion equation and is given in FLAG as

$$\mathcal{D} = 1.265*10^{-8} \frac{(T_g)^{3/2}}{P}$$

where T_g is the gas temperature in °K and P is in atmosphere. However, two things have been done in FLAG. First, a minor change was to change .654 to .60. This is a minor point because reference (4) recommends the coefficient be set to .60 whereas reference (5) recommends .654. Therefore, the coefficient used is acceptable, but confusing since it is different from the stated value.

The second point, however, needs further investigation. The last two terms in equation (2.3-9) can be rewritten as

$$Re^{1/2}\, Sc^{1/3} = \left(\frac{Ud}{\mathcal{D}} \right)^{1/2}\, Sc^{-1/6} \qquad (2.3\text{-}10)$$

The Schmidt number usually takes on values form .5 to 1.0 so that $Sc^{-1/6}$ is between 1.12 and 1.0. What has been done in FLAG is to set Sc = 1 so the equation evaluated is

$$Sh = 2.0 + .60 \left(\frac{Ud}{\mathcal{D}}\right)^{\frac{1}{2}}. \qquad (2.3\text{-}11)$$

Considering all of the approximations involved in creating FLAG, this probably has little effect on the results, but this should be investigated further.

Finally the rate of change of the particle mass is given by

$$\frac{dM}{dt} = -12 A_s \sum r_j \Phi \qquad (2.3\text{-}12)$$

where A_s is the surface are of the particle,

$$A_s = 4 \pi R_o^2$$

The rate of conversion is given by

$$\frac{dX}{dt} = \frac{36}{\rho_o W_o R_o} \sum r_j \phi \qquad (2.3\text{-}13)$$

The numerical form of these equations as programmed in FLAG are given in Chapter IV.

2.4 Heat Transfer

The two source terms, S_{cond} and S_{rad}, in the energy equation represent the energy transfer between particles and fluid by virtue of contact between the two components and energy transfer through out the system by radiation. Specification of S_{cond} is fairly easy by assuming this component can be modeled as convective heat transfer to a sphere.

Then

$$S_{COND} = 2\lambda_h d\, Nu\, (T_g - T_p) \qquad (2.4\text{-}1)$$

where

Nu = particle Nusselt Number = hd/k
λ_h = Empirical heat transfer coefficient
h = heat transfer coefficiet
d = particle diameter

This term is evaluated in subroutine COND where a DATA statement sets

λ_h = .1 (J /(sec-m-k))
Nu = 2.0

The evaluation of the radiation source term is more complicated. A radiation model is developed by treating the energy as photons rather

than electromagnetic waves. The change from a wave to a particle view point allows photon movement to be evaluated in the same manner as neutron transport in a reactor. The later process is well documented and may be found in reference (6), and when coupled to the assumption that the radiation field is at steady state produces a diffusion equation for the energy flux

$$-\nabla\cdot\left|\frac{\lambda_{AS}}{3}\nabla\mathcal{U}\right| + \frac{\mathcal{U}}{\lambda_{AS}} = S \qquad (2.4\text{-}2)$$

where

$\mathcal{U}$ = Radiant energy flux in direction Ω $(W\text{-}m^2)$

S = Radiation source term

λ_{AS} = Absorption and scattering mean free path

FLAG contains a DATA statement that sets

$$1/\lambda_{AS} = 15.$$

The radiation source term in equation (2.4-2) has two parts, a particle source

$$S_p = 4\epsilon_p \sigma T_p^4 n_p \pi r_p^2 \qquad (2.4\text{-}3)$$

and a gas source

$$S_g = 4K_g \sigma T_g^4 \qquad (2.4\text{-}4)$$

where

σ = Stephen-Boltzman Constant
n_p = particle number density
r_p = particle radius
T_p = particle temperature
T_g = gas temperature
K_g = $1/\lambda_{AS}$
ϵ_p = emissivity

The particle emissivity is based on a mass averaged value for carbon and ash, i.e..

$$\epsilon_p = \frac{m_c}{m_T}\epsilon_c + \frac{m_a}{m_T}\epsilon_a$$

where

m_c = Mass of carbon
m_a = Mass of ash
$m_t = m_c + m_a$
ϵ_c = emissivity of carbon
ϵ_a = emissivity of ash

The same DATA statement used to set λ_{AS} is also used to set emissitivity at

$$\epsilon_a \quad .50 \quad \text{and} \quad \epsilon_c \quad .85$$

Equations (2.4-3) and (2.4-4) are substituted into equation (2.4-2) to evaluate $\mathcal{U}$. This is a straight forward process, the equation is finite differenced and the resulting algebraic equation solved with line successive over relaxation. Once $\mathcal{U}$ is known the gas heating per unit volume is calculated from

$$S_{RAD} = K_g(\mathcal{U} - 4\sigma T_g^4) \qquad (2.4\text{-}5)$$

2.5 Diffusion Coefficients

The diffusion terms in the momentum, energy and concentration equations require a diffusion coefficient, Γ, before they may be evaluated. The coefficient has a molecular contribution and a turbulent contribution and is assumed to be the same for all transport equations. The molecular part is evaluated using Sutherland's viscosity model

$$\frac{\mu}{\mu_0} = \left(\frac{T}{T_0}\right)^{3/2} \frac{T_0 + S_1}{T + S_1} \tag{2.5-1}$$

Both μ_0 and T_0 are reference quantities and S_1 is a model constant, which for air is

$$S_1 = 110\ ^\circ K \tag{2.5-2}$$

Values for reference quantities have been chosen so that as used in FLAG equation (2.5.-1) is

$$\mu = \frac{1.5 * 10^{-6}\ T^{3/2}}{\alpha (T + S_1)} \tag{2.5-3}$$

The numerical coefficient of 1.5×10^{-6} is actually the value of kinematic viscosity at the reference temperature, thus α appears in equation 2.5-3 in oder to convert the equation back to absolute viscosity.

The turbulent contribution is evaluated using a Prandtl mixing theory. The turbulent diffusion, Γ_t, is given by

$$\Gamma_t = .15 \rho \ell_m (\overline{\nabla}'^2)^{1/2} \tag{2.5-4}$$

where ρ is the gas density and l_m is the mixing length and $(\overline{\nabla}'^2)^{1/2}$ is the rms velocity fluctuations, and is given by

$$(\overline{\nabla}'^2)^{1/2} = .4 \ell_m \left[\left(\frac{\partial V_x}{\partial x} \right)^2 + \left(\frac{\partial V_y}{\partial y} \right)^2 \right]^{1/2} \tag{2.5-5}$$

The value of l_m is not fixed in the code, but is an input variable. Adding together equation (2.5-3) and (2.5-4) produces the diffusion coefficient required for the momentum, energy, and concentration equations

$$\Gamma = \mu + \Gamma_t \tag{2.5-6}$$

Two other estimates of the diffusion coefficient are made beside the value of Γ_t as shown above. The first value is based on viscosity necessary to maintain the cell Reynold's number below a certain level. A DATA statement in subroutine TURB sets this limit at $Re_{Lim} = 50$. Using the definition of Reynolds number, two values of viscosity are evaluated

$$\nu_x = \frac{U \delta x}{Re_{Lim}} \tag{2.5-7a}$$

and

$$\nu_y = \frac{V \delta y}{Re_{Lim}} \tag{2.5-7b}$$

Now from the values calculated, Γ_t, ν_x, ν_y choose the largest value.

Next, choose the smaller cell dimension, i.e., δx or δy. This can be viewed as a characteristic length scale for the energy dissipation eddies in turbulent flow and may be used to create a diffusion coefficient as

$$\nu_c = \frac{1/4\ \delta\ell}{\delta t}$$

where $\delta\ell$ is the characteristic dimension and δt is the time step. The value of ν_c is compared to the value of the coefficient chosen in the first step with Γ_t defined as the smaller of the values.

There are two important points regarding this evaluation of Γ. This variable is calculated in subroutine TURB. Within TURB are two statements which may be removed but if left inplace negate the evaluation of equation 2.5-3 and 2.5-6. Immediately after calculating (2.5-3) a FORTRAN statement sets μ= .1, and immediately after evaluating (2.5-6) a statement sets Γ = .1; this value corresponds to an average value of the turbulent levels expected in a typical gasifier. FLAG has been run with different values of Γ ranging from .05 to .25 and as would be expected, the larger value tend to stabilize the calculations. Exactly how useful is the model and what are the effects of varying the mixing length need to be further investigated.

2.6 Drag Coefficient Model

The gas-particle drag term is evaluated from a curve fit to experimental data. Figure 1 taken from reference (7) shows a series of

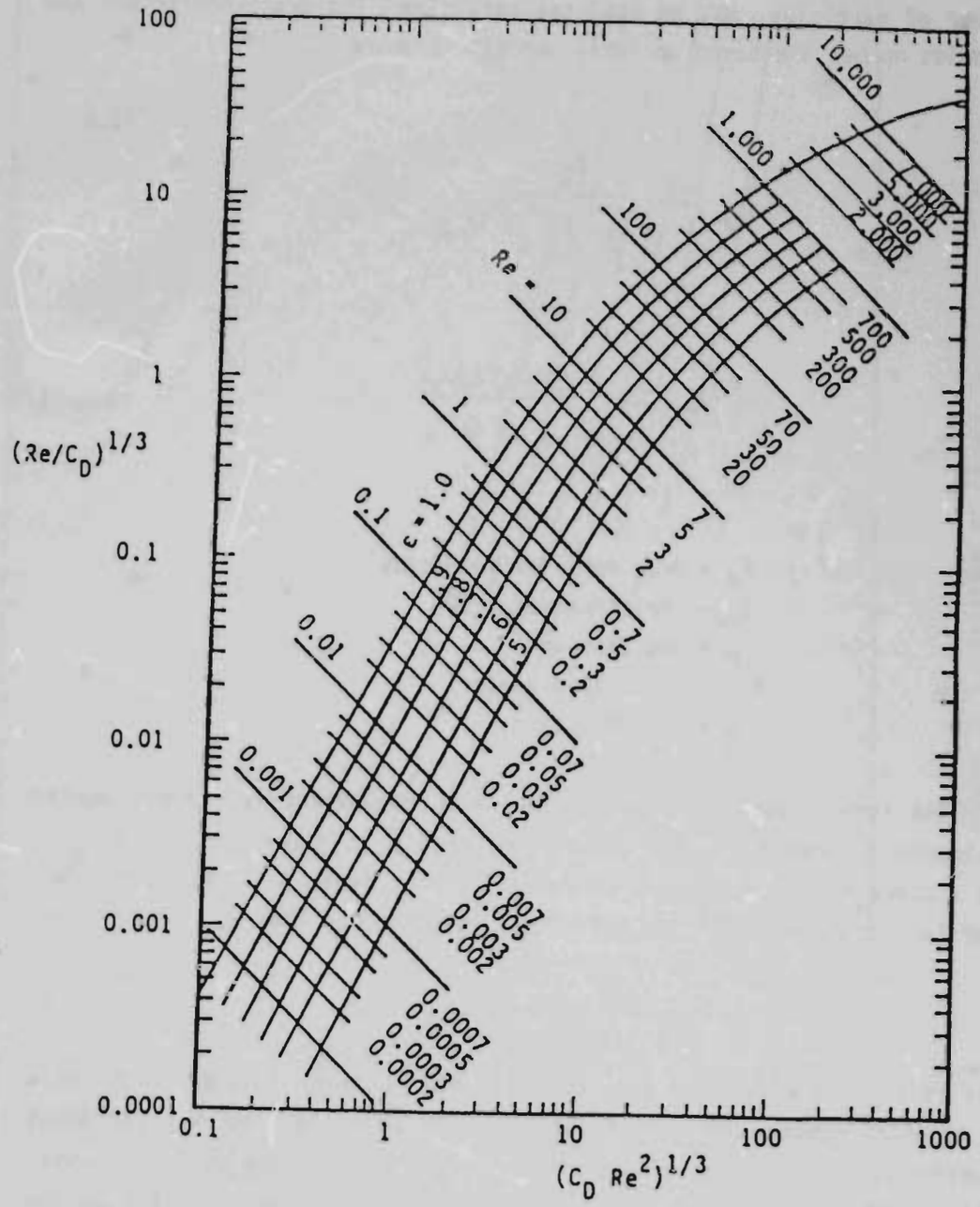

Figure 1 Coefficient of drag over particle cluster - Reference 7

curves taken from experiments done for a range of voidage, particle size, and Reynolds numbers. The force is for a fluid flowing over a large number of particles, not an isolated particle. The drag coefficient and Reynolds number are based on local quantities where

$$C_D = \frac{F_D}{\frac{\pi}{8}\rho\epsilon^2 d^2 U_{rel}} \tag{2.6-1}$$

and

$$Re = \frac{d\rho\epsilon U_{rel}}{\mu} \tag{2.6-2}$$

where

F_d = Drag force on particles
U_{rel} = Relative velocity
ρ = gas density
d = particle diameter
ϵ = void fraction

The curves shown are not in the most convenient form for computer evaluation. Therefore, the curves are recast as shown in Figure 2 and a curve fit of this plot is used in FLAG. Table 1 shows the data used for the curve fit. The functional relationship used is

$$C_D = \frac{C_1}{(Re)^{C_2}} \tag{2.6-3}$$

This is a piece wise curve fit, i.e., C_1 and C_2 vary from cycle to cycle in Reynolds number and void fraction. The point to keep in mind about equation (2.6-3) is that it represents only points on the curves. Linear interpolation is used to find C_D for void fractions not directly on the curves.

The procedure is to first find the Reynolds number range and then

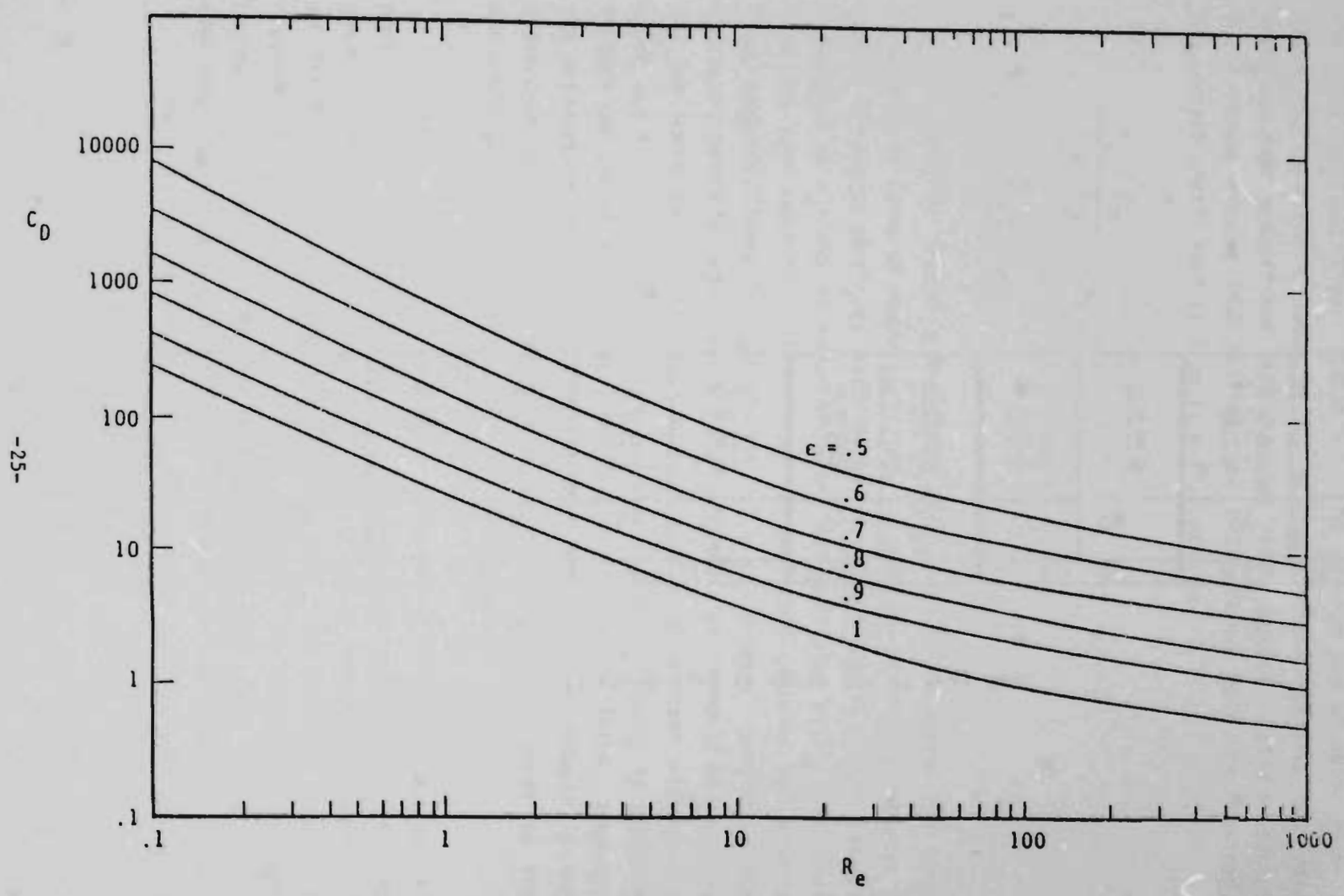

Figure 2 Reformat of Figure 1

Table 1 Coefficient used in curve fit of drag data

ReNo	ε = .5		ε = .6		ε = .7		ε = .8		ε = .9		ε = .10	
	C_1	C_2	C_1	C_2	C_1	C_2	C_1	C_2	C_1	C_2	C_1	C_2
.10	730	1.03	340	1.00	150	1.03	80	1.02	43.5	1.00	27.0	.98
1.0	730	.96	340	.87	150	.83	80	.77	43.5	.78	27.0	.81
10.0	310	.59	190	.625	90	.61	59	.64	28.0	.59	22.0	.72
100.0	140	.414	51.8	.340	18	.25	13.6	.32	6.54	.27	2.46	.24

the void fraction range. Table 1 is entered and equation (2.6-3) isused to generate a value of C_p at the correct Reynolds but void fractions just greater and less than the value desired. Using subscript U for values greater than desired, and L for values less than desired, the correct coefficient of drag is evaluated from

$$\frac{C_D - C_{DL}}{C_{DU} - C_{DL}} = \frac{\epsilon - \epsilon_L}{\epsilon_U - \epsilon_L}$$

2.7 Particle Collisions

In order to create a tractable problem particle motion has been formulated in terms of macro particles. Each macro particle represents a number of micro particles distributed throughout space. This can be visualized as a cloud of particles where all particles within the cloud have the same velocity. If any computational cell contains two or more macro particles there is a possibility of a collision . However, since the macro particle represents a cloud of particles it would be possibie for one macro particle to pass completely through another without one being aware of the existance of the other. This difficulty is overcome through the use of a statistical formulation for the collision. However, the explanation of the collision process is more understandable if the discussion starts by examining solid particles and then moves to the discussion of the interaction of the macroparticles.

Figure 3 shows one computational cell in the flow containing six particles. At the start of a time step the particles are positioned as shown. The arrow attached to each particle shows the particle velocity and the dotted line indicates the particle path. A three step process is required to determine if a collision occurs. The first step in the process is to determine if the particle paths intersect. If they do, then there exists the possibility of a collision. As shown in Figure 3 there is the potential for a collision of particle one with

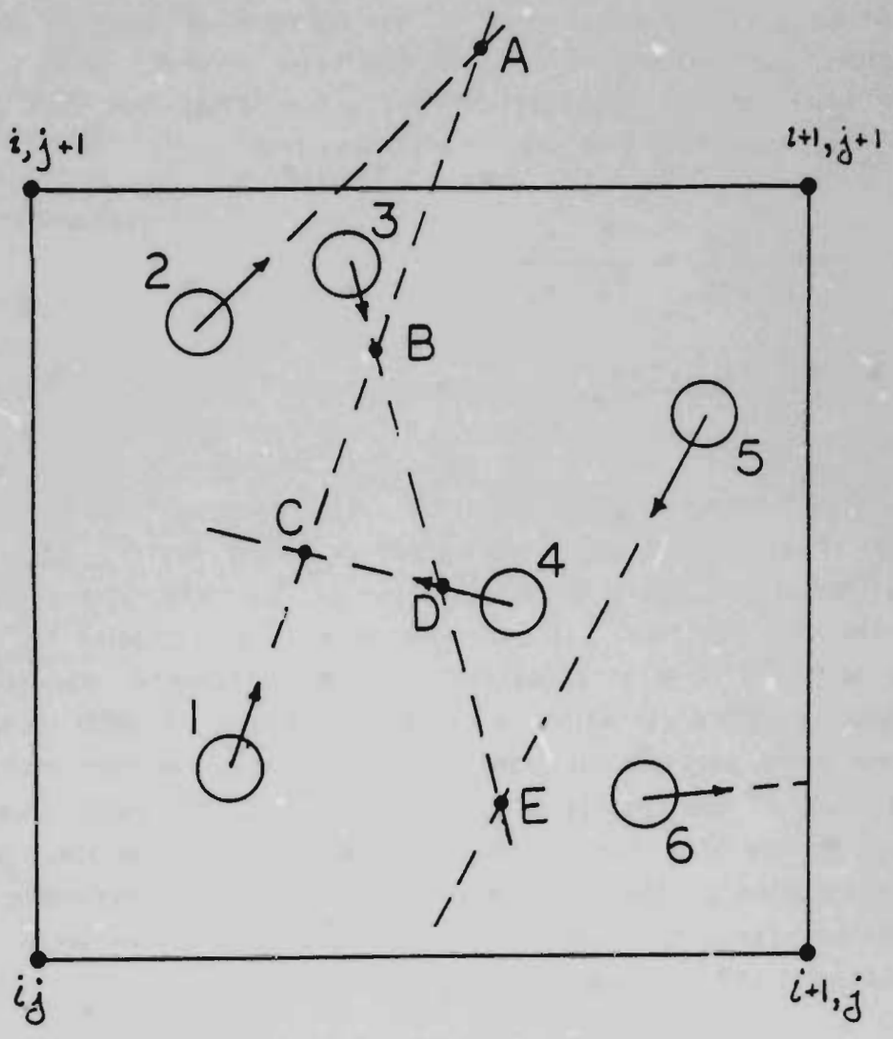

Figure 3 Possible particle collisions

particles two, three and four at points A, B, and C respectively. There is also the possibility that particle three collides with four or five at D and E respectively. At the end of this step those particle combinations which do not have intersecting pathlines are eliminated from further consideration. Also eliminated are those collisions such as between particles one and two because the interaction at point A is outside the boundaries of the computational cell.

The first step identifies the possible collisions, but if a collision is to actually occur there is a second requirement, the particles must be at the intersection point at the same time. The time is calculated based on particle velocity and distance from particle to intersection point. For example, let l_{3E} be the distance from particle 3 to intersection point E and let l_{5E} be the distance from particle 5 to point E. The time for each particle to arrive at point is then

$$\delta t_{3E} = \frac{l_{3E}}{|V_3|}$$

and

$$\delta t_{5E} = \frac{l_{5E}}{|V_5|}$$

Now, if

$$\delta t_{3E} = \delta t_{5E}$$

a collision occurs, but if they are not equal, no collision occurs. The intersection times are calculated for the various particle combinations and those combinations with incorrect intersection times are eliminated from further consideration. This leaves only those particle combinations

where the particles are at the same point in space at the same time. However, this does not mean that every collision indicated actually occurs. For example, two collisions are indicated if

$$\delta t_{1C} = \delta t_{4C}$$

and

$$\delta t_{1B} = \delta t_{3B}$$

But it is clear that a collision between particles one and four alters the path of particle one so that the collision with particle three does not take place. The collision which occurs is the one associated with the shortest intersection time. Again, for the example under consideration

$$\delta t_{1c} < \delta t_{1B}$$

and so the collision is between particles one and four.

Normally, the number of particles within a cell is large enough so that a particle will collide many times before leaving the cell. Consideration of all particles and all collisions establishes the average distance a particle moves before colliding with another particle. This average distance, λ, is called the mean free path. Any individual particle can travel an arbitrary distance before a collision, but on the average, the collision distance is λ. This idea is embodied in a probability distribution function, P(S). The probability distribution function [reference (6)] states that the probability a particle suffers a collison before moving a distance, S, is given by

$$P(s) = \int \frac{e^{\int_0^{s'} \frac{ds''}{\lambda(s'')}}}{\lambda(s')} ds' \qquad (2.7\text{-}1)$$

where λ is again the mean free path. If λ is a constant, equation (2.7-1) may be integrated to produce

$$P(s) = 1 - e^{-s/\lambda} \qquad (2.7\text{-}2)$$

Notice that P(S) is not evenly distributed with S, i.e., the probability of a collision before moving a distance equal to one mean free path is 63% but the probability of a collision before moving five mean free path is 99%.

Looking at Figure 3 if $l_{1C} = .5\lambda$ and $l_{1B} = 5\lambda$ the probability of the particle undergoing a collision before arriving at point C is 39% whereas the probability of a collision occuring before the particle arrives at point B is 99%. The key is that something happens which prevents the particle form reaching a particular point. Since the probabilty of something happening to prevent the particle reaching point C is lower than the probability of something happening which prevents the particle reaching B, it is far more likely that a collision occurs at point C than at point B.

It is important to understand that there are two separate issues at hand. The first is that a collision at point C between particles one and four has in fact occured. The second issue is that without actually following the individual particles on a statistical basis there was a 39% probability tht something would happen which prevented the particles from reaching point C. It is this two stage view point which is extended to the macroparticle description.

The macroparticles represent a large number of microparticles, uniformly distributed throughout the cell, all with the same velocity and identity. In other words the macroparticle is a cloud of microparticles. From this view point two macroparticles could pass through one another without any effect of one on the other. However, what is done in FLAG is to choose a collision distance for each particle pair. The important point is that the collision paths be constant with the collision

probability function. By this it is meant that there should be a large number of collision paths on the order of one mean free path, but only a small number of paths on the order of 5 mean free paths. These collision distances are created using the random number generator on the computer as follows. Each particle is assigned a number ξ which has equal probability in the range 0 to 1 , i.e. ξ is uniformaly distributed over the range zero to one. A second number χ is generated according to

$$\chi = -\ln(\xi) \tag{2.7-3}$$

If equation (2.7-3) is inverted so that

$$\xi = e^{-\chi} \tag{2.7-4}$$

and compared to equation (2.7-2) it is seen that ξ as a function of χ is distributed in the same way as P(S) as a function of (S/λ). Thus uniformly distributed random numbers ξ are used to generate collision distances, χ , which are non uniformly distributed consistent with the collision probability function, equation (2.7-2).

Now, the macroparticles can be viewed in the same way as the individual solid particles first discussed. Each particle has a collision distance and this distance is consistant with the probability distribution function. At this point the macroparticle collision distances must be viewed in the same fashion as the solid particle collision distances. Again, referring to the example of solid particles, particle one has a collision distance with particle three and particle four, but only the first collision involving minimum collision time actually occurs. The same thing must be done for the macroparticles; from all of the collisions which the macroparticle can undergo, one must be chosen to be the actual collision. This is accomplished by assigning each particle a second random number which serves the function of collision time. This second random number is again created using the

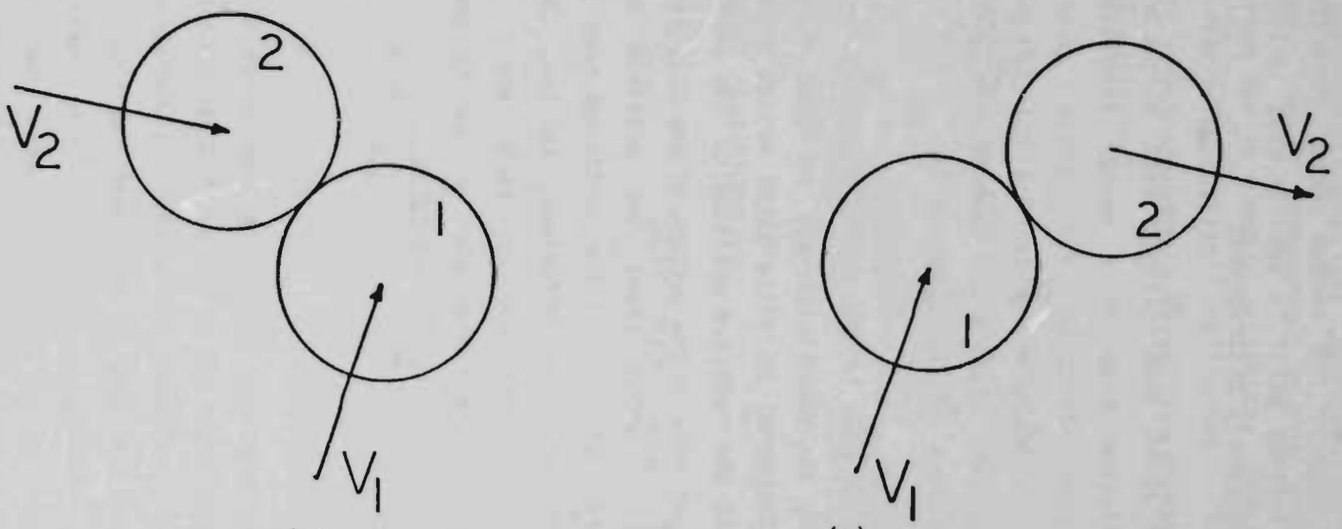

Figure 4 Two possible collisions for one set of velocity vectors

random number generator, but there is no further transformation as with equation (2.7-3). This is because the random number generator picks numbers from a uniform distribution which is exactly what is required to simulate time since time is uniformly distributed.

The procedure outlined above thus assigns each particle pair a collision distance and collision time in a manner consistant with the probability distribution function for solid point mass particles. All of these calculations are carried out in subroutine COLIDE. Section 4.4 of this report details the computational expressions which appear in COLIDE to implement collision mechanics.

There is, however, one more step in the collision process which must be taken into account. The macroparticles are assigned a non zero diameter, i.e., they are considered as distributed masses rather than point masses. This means that the relative position of the particles at time of impact plays an important role in the outcome of the collision. This can be seen in Figure 4 which shows two possible collision configurations. In both a and b of Figure 4 the particles have the same velocities, but the point of impact is different, so that the final velocities after impact will be different for each case. This is accounted for by generating a random number used to specify the impact point. This process is carried out in subroutine COLVEL.

2.8 Agglomeration

As mentioned above, FLAG does not contain any mechanism to account for agglomerations, however, a separate set of subroutines has been developed at West Virginia University to implement the JAYCOR agglomeration model. The model is presented here and the code to implement the model is given in detail in reference (3). Basically, there are three parts to the model. First, the determination of whether or not two colliding particles agglomerate, second, the final velocity if agglomeration occurs and third, the final velocity if no agglomeration occurs.

Figure 5 shows the configuration for two spheres undergoing a collision. Model development starts with a description of particle deformation for an elastic collision. The equations are then modified to account for viscocoelastic collisions. This produced equation (2.8-1) which is a relationship between the approach distance verses time from start of collision.

$$\frac{d^2\alpha}{dt^2} = -\frac{\frac{8}{3} r_c^{1/2} \alpha^{3/2}}{\frac{1}{G_c} + \frac{t}{\eta_c}} + F_B H(t-t_m) \qquad (2.8\text{-}1)$$

The initial conditions are:

$$\alpha(0) = 0 \quad \text{and} \quad \frac{d\alpha}{dt} = V_n$$

where

$m = \frac{m_1 m_2}{m_1 + m_2} m_i$ = mass of particle i

$\alpha = r_1 + r_2 - r$ r = distance between centers

$$r_c = \frac{r_1 r_2}{r_1 \quad r_2}$$

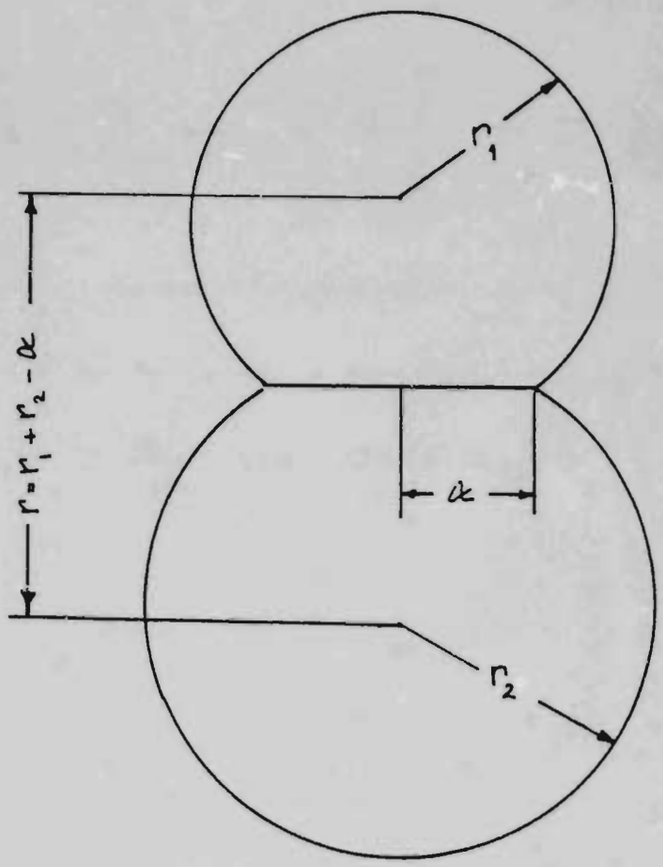

Figure 5 Collision of two particles: agglomeration

$G_c = \frac{g_1 g_2}{g_1 + g_2}$ g_i = shear modulus of particle i

$\eta_c = \frac{\eta_1 \eta_2}{\eta + \eta}$ η_i = viscosity of particle i

F_b = binding force

H = Heaviside step function $H(t) = \begin{cases} 0 & t \leq 0 \\ 1 & t > 0 \end{cases}$

t_m = time at which maximum deformation occurs

V_n = initial normal component of approach velocity (relative velocity)

The first step in determining agglomeration is to integrate equation 2.8-1. The integration starts at time equals zero with the given initial conditions. Figure 6 shows a typical curve, where the maximum point on the curve defines a time t_m. At this time α is a maximum and for values of time less than this, the last term in (2.8-1) is zero. After t_m the Heaviside function is set to one and integration continues until time t_f. Time t_f corresponds to the point on the curve where $d^2\alpha/dt^2 = 0$; at this time integration stops. The system kinetic energy is

$$E_{k_f} = \frac{m V_f^2}{2} \qquad (2.8\text{-}2)$$

where

$$V_f = \left.\frac{d\alpha}{dt}\right|_{t=t_f} \qquad (2.8\text{-}3)$$

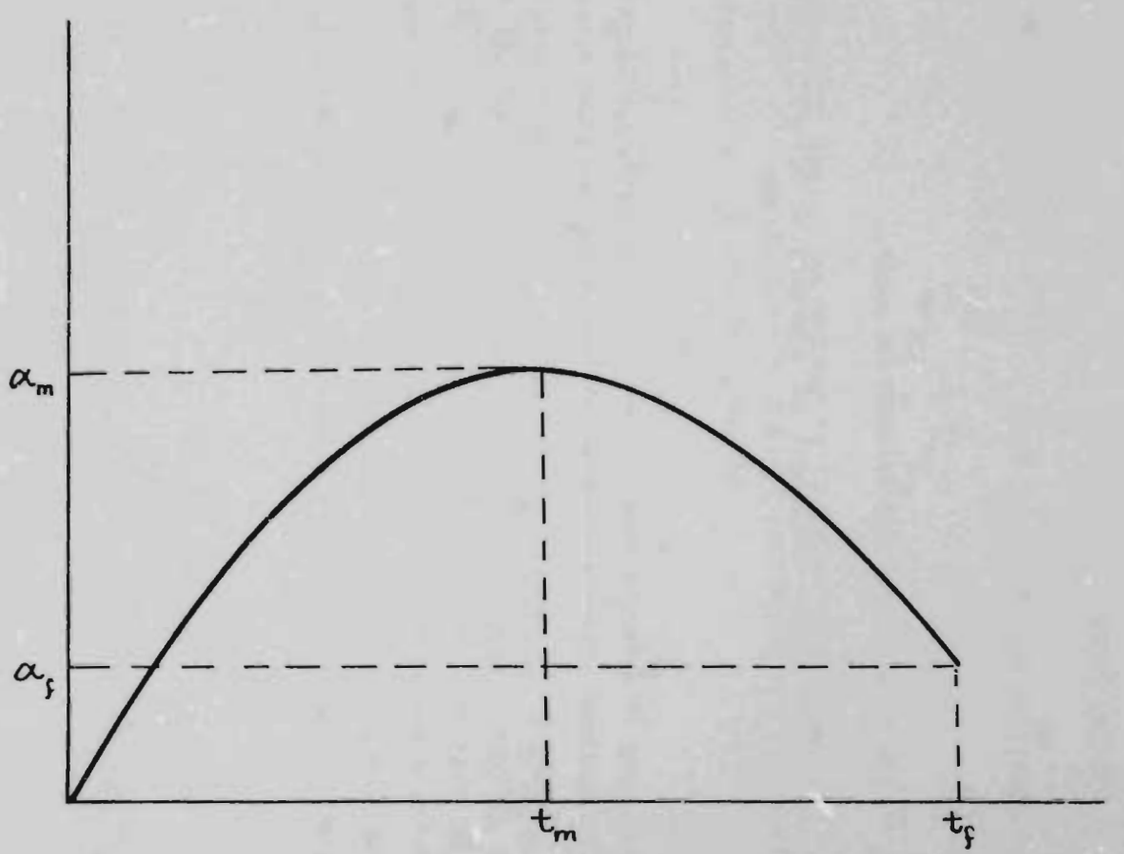

Figure 6 Deformation curve for colliding particles

and the binding energy is

$$E_{b_f} = F_b \alpha_f \tag{2.8-4}$$

where

$$\alpha_f = \alpha \text{ when } t = t_f \tag{2.8-5}$$

Agglomeration occurs when

$$E_{k_f} < E_{k_b} \tag{2.8.-6}$$

The next step in the process is to determine particle velocity after collision. If agglomeration occurs the particles stick together to form one new particle with velocity given by

$$\vec{V}_{ac} = \frac{m_1}{m_1+m_2}\vec{V}_1 + \frac{m_2}{m_1+m_2}\vec{V}_2 \tag{2.8-7}$$

The subscript "ac" indicates velocities after collision. If agglomeration does not occur the velocities after collision are

$$\vec{V}_{1_{ac}} = \vec{V}_1 + \pi\sigma^2[B]\frac{m_2}{m_1+m_2}\left|\vec{V}_2-\vec{V}_1\right|(\vec{V}_2-\vec{V}_1)(1+e)\delta t/2 \tag{2.8-8}$$

and

$$\vec{V}_{2_{ac}} = \vec{V}_2 + \pi\sigma^2[A]\frac{m_1}{m_1+m_2}\left|\vec{V}_2-\vec{V}_1\right|(\vec{V}_2-\vec{V}_1)(1+e)\delta t/2 \tag{2.8-9}$$

where

σ = collision radius

[A] = number density of Particle A

[B] = number density of Particle B

e = coefficient of restitution

$\vec{V}_1$ = velocity of particle 1 (Vector quantity)

$\vec{V}_2$ = velocity of particle 2 (Vector quantity)

It should be noted that the particle velocities after collision must be calculated regardless of whether or not agglomeration occurs. The set of subroutines which make up the agglomeration package does not contain a subroutine to calculate the final velocities. These calculations are carried out in a subroutine called COLVEL which is the FLAG subroutine used to calculate the velocities for nonagglomerating particles. This would be perfectly acceptable if everything within COLVEL is correct. Unfortunately, the equations given in COLVEL are not consistent with (2.8-8) and (2.8-9); COLVEL is discussed in greater detail in section 4.2.

Chapter III
Grid System

The grid system implemented in FLAG is a rectangular-staggered mesh system as shown in Figure 7. This is termed a staggered system because thermodynamic variables such as pressure, temperature, and density are defined at the center of each cell, but the velocities are defined at the cell interfaces. This is shown more clearly in Figure 8. The lower left hand corner of the cell is denoted by point (i,j) with i increasing in the x-direction and j increasing in the y-direction. As depicted the x-axis is the center line of an axisymmetric flow entering at the left and exiting on the right, i.e., this is the axial flow direction. Thus, the y-axis is the radial flow direction with the container wall in the upper part of the grid. This orientation is maintained throughout this report. Unfortunately, the notation in several of the FLAG subroutines interchange the i and j indices so that the axial velocity, U, is along the y-axis and moves in the direction of increasing j. If FLAG is modified the first step in the process is to determine whether increasing i or increasing j corresponds to the flow direction. Regardless of the orientation or indexing, U is always in the axial direction.

One other point needs to be made concerning the correspondence of variables as shown in Figure 7 and the quantities found in the computer code. The integer and fractional nature of the subscripts clearly indicates that the quantities are not evaluated at the same point in the flow field. Computer languages do not allow fractionally subscripts which results in $X_{i,j}$, $U_{i,j+\frac{1}{2}}$, $V_{i+\frac{1}{2},j}$ and $P_{i+\frac{1}{2}j+\frac{1}{2}}$ being denoted by X(I,J), U(I,J), V(I,J) and P(I,J). To the unwary the fact that the values of I and J are the same for all the variables leads to the incorrect belief that the variables are all evaluated at the same point in space. Determining the point at which a quantity is evaluated is fairly easy, velocities are always evaluated at cell boundaries as shown in Figure 8 and all other quantities are evaluated at the center of the cell.

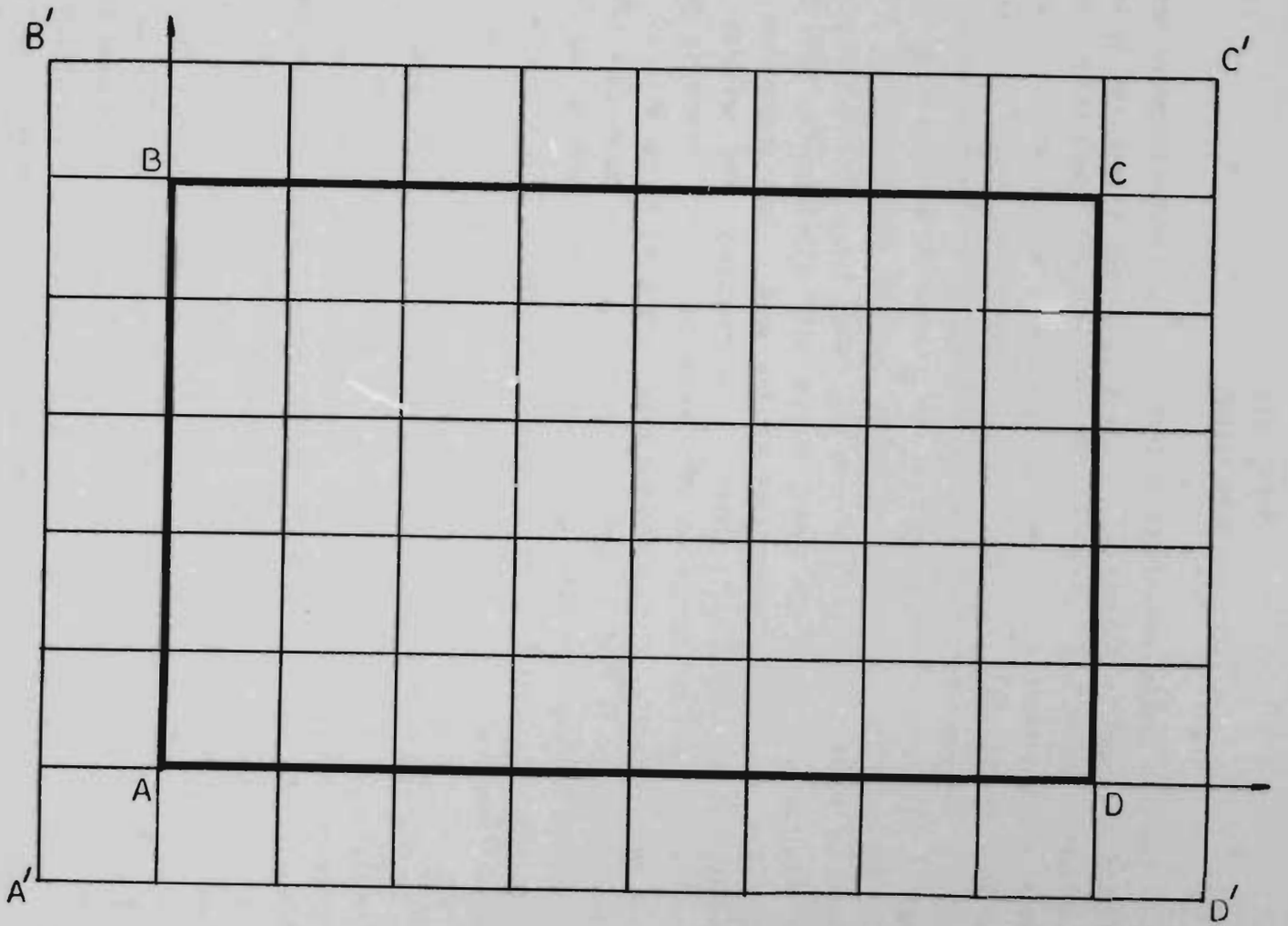

Figure 7 Uniform Grid System

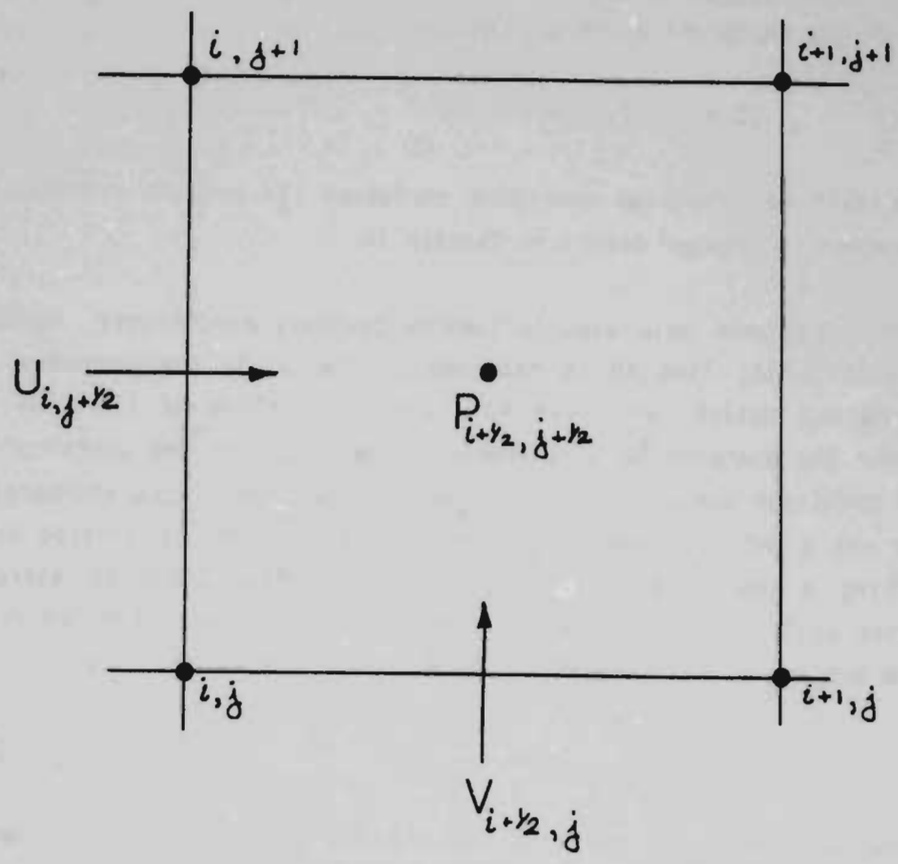

Figure 8 Typical interior cell

If there is a need to produce a variable at some point other than the point of definition, surrounding values are averaged. For example, the axial velocity at the cell center is

$$U_{i+\frac{1}{2},j+\frac{1}{2}} = \frac{1}{2}\,(U_{i,j+\frac{1}{2}} + U_{i+1,j+\frac{1}{2}}) \qquad (3.1\text{-}1)$$

or as it may appear in a computer code

```
UC = ½(U(I,J)+U(I+1,J))
```

In variable mesh systems averaging variables can present problems, this is examined in greater detail in Chapter IV.

The staggered grid also influences boundary conditions. Again look at Figure 3.3-1; line AB is the inlet, line BC is the container wall, line CD the outlet, and line AD is the centerline of the flow. Now consider the standard no slip boundary conditions on the container wall. These condition specify U_w=0 and V_w=0, but because of the staggered grid U_w is not a defined quantity. The correct boundary is created by constructing a row of cells outside the true flow field to mirror the interior cells adjacent to the boundary. Now, the wall velocity is given by the average of the velocities above and below the wall, i.e.

$$U_{i,jw} = \frac{1}{2}(U_{i,jw-\frac{1}{2}} + U_{i,jw+\frac{1}{2}}). \qquad (3.1\text{-}2)$$

But the wall velocity is zero, which means $U_{i,jw+\frac{1}{2}} = -U_{i,jw-\frac{1}{2}}$. Boundary conditions are thus met by including the appropriate values in the fictitious cells. The grids, A' B' C' D', shown in Figure 7 is the flow region, ABCD, plus a row of fictitious boundary cells. The complete set of boundary conditions is examined in more detail in Chapter IV.

The FLAG code allows a maximum of 40 points in the axial direction and 10 points in the radial direction. The 40 x 10 grid includes the

fictitious boundary cells leaving a 37 x 7 cell flow field interior to the container. There is no guarantee that 7 cells between the centerline and wall can always resolve the flow field. Poor results may be obtained if the center of the cell immediately adjacent to the wall is completely outside the boundary layer. The FLAG code was configured to allow variable mesh grids. This would allow concentrating node points in high gradient regions and also allow for non rectangular containers. This is a capability which must be used with extreme care. This is also a topic covered in greater depth in the next chapter.

Chapter IV
Method of Solution

4.1 Difference Formula

The form taken by finite difference operators is determined by such factors as whether a uniform or variable mesh is used, what order of accuracy is desired, and the type solvers at hand. Therefore, particular operators may be chosen just because the algebraic equations generated are of a type solvable by a package already in hand. The first step in the solution process, the choice of finite difference operators is thus determined by the last step in the process, the solver package. This is somewhat true of the flow routines in FLAG. The finite difference formulation used in FLAG is the standard second order accurate central difference scheme. But the manner of implementation and point of implementation are intimately related to ICE solution philosphy. Thus, to understand the flow code more is necessary than just knowing the form of the difference operators; the basics of the ICE method must also be understood. Two examples are given to provide this knowledge. The first example is for a constant grid system and the second for a variable mesh system. The finite difference operators and the flow equations as used in FLAG are presented in the appendix.

Before proceeding to the development of the equations used in FLAG it is worth while to quickly review a few concepts. There are a number of ways in which the solution to the governing equations can be formulated. The first, and simplest is an explicit formulation. For this formulation the time derivative is evaluated as a function of all the other terms evaluated at time level n, i.e.

$$\frac{\partial q}{\partial t} = Q\left(q^n, \frac{\partial q^n}{\partial x}, \frac{\partial^2 q^n}{\partial x^2}, \cdots\right) \qquad (4.1\text{-}1)$$

A simple forward difference in time replaces the left hand side of the equation, thus

$$q_\beta^{n+1} = q_\beta^n + \delta t\, Q\left(q_\beta^n, \frac{\partial q_\beta^n}{\partial x}, \ldots\right) \tag{4.1-2}$$

Normally, the time step, δt, must be very small for the process to be stable.

A second, more complex method, is a predictor-corrector method, for example MacCormack's method. The process again starts with equation (4.4-1), but the result obtained in (4.1-1) is considered a temporary estimate of the new value and not the correct final value of the quantity at level n+1. If the result generated by (4.4-1) is given as q^{n+1} then the correct value at n+1 is given by

$$q_\beta^{n+1} = q_\beta^n + \delta t\, Q'\left(\bar{q}_\beta^{n+1}, \frac{\partial \bar{q}_\beta^{n+1}}{\partial x}, \ldots\right) \tag{4.1-3}$$

where Q in equation (4.1-3) is not the same as Q in (4.1-2). This may be strictly a two step process, i.e., the calculations are advanced from one time level to another by first applying (4.1-2) then (4.1-3). However, this need not be the case. Equation (4.1-3) represents the correction to the estimate of the value at the new time level and may be applied recursively. This means that the result obtained by one application of (4.1-3) maybe viewed as a new estimate to be corrected by a second application of (4.1-3). This procedure is continued until two successive estimates are within some predetermined distance of each other. Thus, q^{n+1} is estimated k times before the flow is actual advanced one time step. It is assumed k is small and t relatively large so that to reach any time

level, the total number of calculations will be less than if a purely explicit method is used.

The third technique is a purely implicit technique. Here, all the terms in the differential equation are evaluated at time level n+1. This produces a problem with N equations in N unknowns which is solved by a matrix inversion technique. It is assumed that t may be made large enough that regardless of the work required to invert a matrix, the total work will still be less than in either of the first two methods.

The equations generated for use in the FLAG code are semi-implicit. What this means is that more than one term in the differential equation is evaluated at time level n+1, but not all of the terms. All of the remaining terms use an estimate of the n+1 quantities. This will become more understandable as the development proceeds. However, what is being done is to combine the second and third techniques given above to produce a stable method with a large time step that will require less calculations than either technique.

The equation which forms the foundation of the flow code in FLAG will now be developed. The idea is to first write the energy and two momentum equations in a finite difference form, then replac the velocities in the convection terms of the energy equation with velocities obtained by analytically solving the momentum equation.

The analysis will focu on the cell shown in Figure 9 with point (i,j) at the lower left hand corner. The idea is to expand the energy equation around the pressure at the center of the cell, point $(i+\frac{1}{2}, j+\frac{1}{2})$.

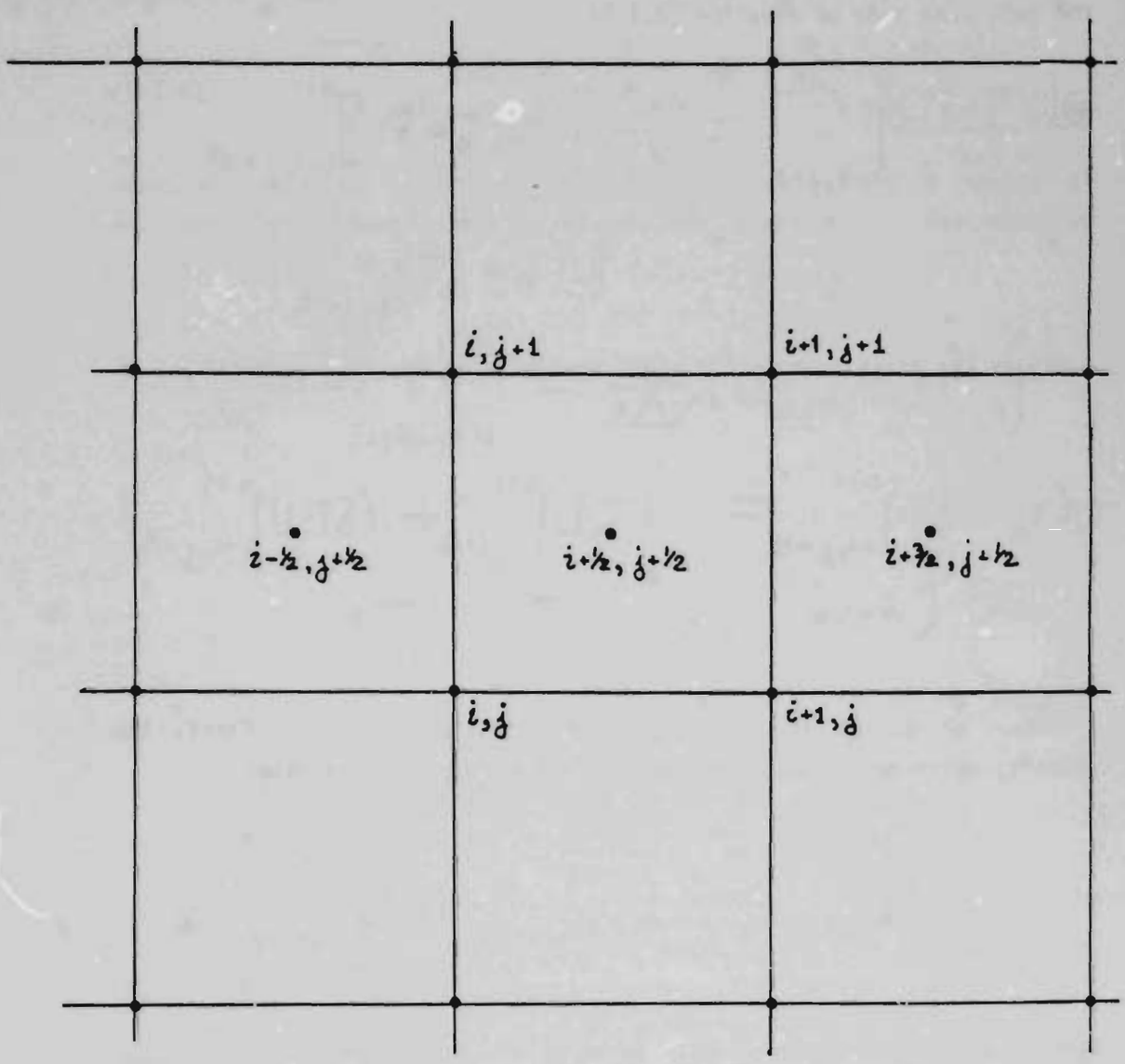

Figure 9 Uniform grid: interior cell

The start of the process is to form a centered finite difference for the axial convection term in the energy equation, i.e., the second term on the left hand side of equation (2.1-5).

$$\left.\frac{\partial[U(T_B+\delta T)]}{\partial X}\right|_{i+1/2,\,j+1/2} = \frac{1}{\Delta X}\left\{\left[U(T_B+\delta T)\right]^{n+1}_{i+1,\,j+1/2} - \left[U(T_B+\delta T)\right]^{n+1}_{i,\,j+1/2}\right\} \tag{4.1-4}$$

Consider the first term on the right hand side of equation (4.1-4).

$$U(T_B+\delta T)^{n+1}_{i+1,\,j+1/2} = (T_B\cdot U)^{n+1}_{i+1,\,j+1/2} + (\delta T\cdot U)^{n+1}_{i+1,\,j+1/2} \tag{4.1-5}$$

A number of things are done to modify equation (4.1-5). First, the velocity which muliplies T_B is replaced by a time averaged value

$$U^{n+1}_{i+1,\,j+1/2} \rightarrow \left(U^{n+1}_{i+1,\,j+1/2} + U^{n}_{i+1,\,j+1/2}\right)/2$$

This is a standard Crank-Nicolson formulation, and the value of $U^{n+1}_{i+1,\,j+1/2}$ is considered unknown. Secondly, the remaining two terms on the right hand side of the equation are replaced by the latest estimate of these values, thus

$$(\delta T\cdot U)^{n+1}_{i+1,\,j+1/2} = (\delta\overline{T})_{i+1,\,j+1/2}\;\overline{U}_{i+1,\,j+1/2}$$

where the overbar indicates the average between the n and last estimate of the n+1 values.

$$\overline{U}_{i,j+1/2} = \left(U^{n}_{i,j+1/2} + U^{n\,1}_{(k)\,i,j+1/2} \right) 1/2$$

Remember, this is an iterative process and there are a number of estimates made for the quantities at time level n+1. Now equation (4.1-4) is

$$\left.\frac{\partial[U(T_B+\delta T)]}{\partial x}\right|_{i+1/2,j+1/2} = \frac{T_B}{2\Delta x}\left(U^{n+1}_{i+1,j+1/2} - U^{n+1}_{i,j+1/2}\right) \qquad (4.1\text{-}6)$$

$$+ \frac{T_B}{2\Delta x}\left(U^{n}_{i+1,j+1/2} - U^{n}_{i,j+1/2}\right)$$

$$+ \frac{1}{\Delta x}\left[\left(\delta T \cdot U\right)_{i+1,j+1/2} - \left(\delta T \cdot U\right)_{i,j+1/2}\right]$$

Or, in a more compact form

$$\left.\frac{\partial[U(T_B\ \delta T)]}{\partial x}\right|_{i+1/2,j+1/2} = \frac{T_B}{2\Delta x}\left(U^{n+1}_{i+1,j+1/2} - U^{n+1}_{i,j+1/2}\right) \qquad (4.1\text{-}7)$$

$$+ C_{i+1/2,j+1/2}$$

The momentum densities at $(i+1,j+\frac{1}{2})$ and $(i,j+\frac{1}{2})$ will be replaced by an expression derived from the momentum equation.

As with the energy equation not all of the terms in equation (2.1-2) are evaluated at time level (n+1). Appendix II presents the equations shown in complete detail. Here, the momentum equation is presented with the various terms gathered together by time levels. Thus

$$\frac{\partial U}{\partial t}^{n+1} = -\epsilon \frac{\partial P}{\partial x}^{n+1} - KU^{n+1} + R_u \tag{4.1-8}$$

The convection terms, diffusion terms and source terms are evaluated using values at time level n or the last estimate of the quantity at level n+1. All of these terms have been collected into the last term, R_u. The second term on the right hand side of (4.1-8) results from the drag term. Details of the generation of this term are given in section 4.3. Finally the pressure term is modified as follows.

$$\frac{\partial P}{\partial x} = \frac{\partial (P - P_B + P_B)}{\partial x} = \frac{\partial (\delta P + P_B)}{\partial x} = \frac{\partial \delta P}{\partial x} \tag{4.1-9}$$

since P_B is a constant.

Equation (4.1-8) is now finite differenced and solved to provide the values of $U^{n+1}_{i+1,j+1/2}$ and $U^{n+1}_{i,j+1/2}$. Thus equation (4.1-8) becomes.

$$U^{n+1}_{i+1,j+1/2} = U^{n}_{i+1,j+1/2} - \frac{\epsilon \delta t}{\Delta x}\left(\delta P^{n+1}_{i+3/2\, j+1/2} - \delta P^{n+1}_{i+1/2\, j+1/2}\right) \quad (4.1\text{-}10)$$

$$- \delta t\, K_{i+1,j+1/2}\, U^{n+1}_{i+1,j+1/2} + \delta t\, R_{U_{i+1,j+1/2}}$$

Solving (4.1-10) for the velocity at the n+1 time level produces.

(4.1-11)

$$U^{n+1}_{i+1,j+1/2} = \frac{1}{(1+\delta t\, K_{i+1,j+1/2})}\left[U^{n}_{i+1,j+1/2}\right.$$

$$\left. - \frac{\epsilon_{i+1,j+1/2}\, \delta t}{\Delta x}\left(\delta P^{n+1}_{i+3/2,j+1/2} - \delta P^{n+1}_{i+1/2,j+1/2}\right) + \delta t\, R_{U_{i+1,j+1/2}}\right]$$

Similarly

$$U^{n+1}_{i,j+1/2} = \frac{1}{(1+\delta t\, K_{i,j+1/2})}\left[U^{n}_{i,j+1/2} - \frac{\epsilon_{i,j+1/2}\,\delta t}{\Delta x}\left(\delta P^{n+1}_{i+1/2,j+1/2} - \delta P^{n+1}_{i-1/2,j+1/2}\right) - \delta t\, R_{U_{i,j+1/2}}\right] \quad (4.1\text{-}12)$$

Equations (4.1-11) and (4.1-12) are substituted into equation (4.1-7) to produce

$$\frac{\partial[U(T_B+\delta T)]}{\partial x} = -\frac{T_B\,\delta t\,\epsilon_{i+1,j+1/2}}{2\Delta x^2(1+\delta t\, K_{i+1,j+1/2})}\delta P^{n+1}_{i+3/2,j+1/2} \quad (4.1\text{-}13)$$

$$+\frac{T_B\,\delta t}{2\Delta x^2}\left(\frac{\epsilon_{i+1,j+1/2}}{1+\delta t\, K_{i+1,j+1/2}} + \frac{\epsilon_{i,j+1/2}}{1+\delta t\, K_{i,j+1/2}}\right)\delta P^{n+1}_{i+1/2,j+1/2}$$

$$-\frac{T_B\,\delta t\,\epsilon_{i,j+1/2}}{2\Delta x^2(1+\delta t\, K_{ij+1/2})}\delta P^{n+1}_{i-1/2,j+1/2} - \frac{T_B}{2\Delta x}\left[\left(\frac{U^{n}_{i+1,j+1/2}}{1+\delta t\, K_{i+1,j+1/2}} - \frac{U^{n}_{i,j+1/2}}{1+\delta t\, K_{i,j+1/2}}\right) + \left(\frac{R_{U_{i+1,j+1/2}}}{1+\delta t\, K_{i+1,j+1/2}} - \frac{R_{U_{i,j+1/2}}}{1+\delta t\, K_{i,j+1/2}}\right)\right]$$

$$+ C_{U_{i+1/2,j+1/2}}$$

Remember, the energy equation is being expanded around the pressure at point $(i+\frac{1}{2}, j+\frac{1}{2})$. Thus, in Figure 9 the pressure at $(i+3/2, j+1/2)$ is to the right of the expansion point and the pressure at $(i-1/2, j+1/2)$ is to the left. This allows a more convenient representation of equation (4.1-13) as

$$\frac{\partial[U(T_B+\delta T)]}{\partial x} = -AR'_{i+1/2\,j+1/2}\,\delta P^{n+1}_{i+3/2,\,j+1/2} + ACU'_{i+1/2\,j+1/2}\,\delta P^{n+1}_{i+1/2,\,j+1/2} - AL'_{i+1/2\,j+1/2}\,\delta P^{n+1}_{i-1/2,\,j+1/2} + B'_{U_{i+1/2,\,j+1/2}} \tag{4.1-14}$$

With equation (4.1-14) as a guide, it is easy to see that the radial convection term in the energy equation is given by

$$\frac{1}{r}\frac{\partial[rV(T_B+\delta T)]}{\partial r} = -AT'_{i+1/2\,j+1/2}\,\delta P^{n+1}_{i+1/2,\,j+3/2} + ACV'_{i+1/2\,j+1/2}\,\delta P^{n+1}_{i+1/2,\,j+1/2} - AB'\,\delta P^{n+1}_{i+1/2,\,j-1/2} + B'_{V_{i+1/2,\,j+1/2}} \tag{4.1-15}$$

In each equation the center coefficient is the sum of the surrounding coefficients, i.e.

$$ACU'_{L+1/2,J+1/2} = AR'_{L+1/2,J+1/2} + AL'_{L+1/2,J+1/2} \quad (4.1\text{-}16a)$$

and

$$ACV'_{L+1/2,J+1/2} = AT'_{L+1/2,J+1/2} + AB'_{L+1/2,J+1/2} \quad (4.1\text{-}16b)$$

Also notice that B_u and B_v are known quantities because they are entirely evaluated in term of quantities specified at time level n or the last estimate of quantities at time level n+1. Equations (4.1-14) and (4.1-15) are now substituted into the left-hand side of the energy equation (2.1-5) to produce

$$\frac{\delta P^{n+1}_{L+1/2,J+1/2} - \delta P^{n}_{L+1/2,J+1/2}}{\delta t} + \frac{\gamma R}{\epsilon}\Big[- AR'_{L+1/2,J+1/2}\, \delta P^{n+1}_{L+3/2,J+1/2} \quad (4.1\text{-}17)$$

$$- AL'_{L+1/2,J+1/2}\, \delta P^{n+1}_{L-1/2,J+1/2} - AT'_{L+1/2,J+1/2}\, \delta P^{n+1}_{L+1/2,J+3/2}$$

$$- AB'_{L+1/2,J+1/2}\, \delta P^{n+1}_{L+1/2,J-1/2} + (ACU'_{L+1/2,J+1/2} + ACV')\, \delta P^{n+1}_{L+1/2,J+1/2}$$

$$+ B'_{U_{L+1/2,J+1/2}} + B'_{V_{L+1/2,J+1/2}}\Big] = LHS$$

This defines the left hand side of equation (2.1-5). Now, attention is focused on the right hand side of the equation. These terms are reproduced below

$$RHS = \left\{\frac{(\gamma-1)}{\epsilon}\left[\alpha\epsilon U\frac{\partial P}{\partial x} + \alpha\epsilon V\frac{\partial P}{\partial r} + C_p T r_m - \sum\frac{\partial(h_i C_i)}{\partial t}\right]\right.$$
$$+\left[\frac{\gamma P}{R}\frac{\partial R}{\partial t} - \frac{\gamma P}{\epsilon}\frac{\partial \epsilon}{\partial t}\right] + \frac{\gamma R}{\epsilon}\left[\frac{\partial}{\partial x}\left(\Gamma\frac{\partial T}{\partial x}\right) - \frac{1}{r}\frac{\partial}{\partial r}\left(r\Gamma\frac{\partial T}{\partial r}\right)\right]\Bigg\}$$
$$+ \frac{(\gamma-1)}{\epsilon}\left(S_{RAD} + S_{COND}\right)$$

Clearly, there are a number of different ways to evaluate the individual terms. Within FLAG the decision was made to evaluate the first three terms from known data at n or the last estimate at n+1, and the last two terms are evaluated at (n+1). Thus,

(4.1-18)

$$RHS = D_{L+1/2,\,J+1/2} - K_1\,\delta P^{n+1}_{L+1/2,\,J+1/2} - K_2\,\delta P^{n+1}_{L+1/2,\,J+1/2}$$

Evaluation of K_1 and K_2 is considered in detail in section 4.3. Equation (4.1-18) is now substituted into equation (4.1-17) to produce equation (4.1-19).

$$\frac{\delta P^{n+1}_{i+\frac{1}{2},j+\frac{1}{2}} - \delta P^{n}_{i+\frac{1}{2},j+\frac{1}{2}}}{\delta t} + \frac{\gamma R}{\epsilon}\Big[- AR'_{i+\frac{1}{2},j-\frac{1}{2}}\, \delta P^{n+1}_{i+\frac{3}{2},j+\frac{1}{2}}$$

$$- AL'_{i+\frac{1}{2},j+\frac{1}{2}}\, \delta P^{n+1}_{i-\frac{1}{2},j+\frac{1}{2}} - AT'_{i+\frac{1}{2},j+\frac{1}{2}}\, \delta P^{n+1}_{i+\frac{1}{2},j+\frac{3}{2}} \qquad (4.1\text{-}19)$$

$$- AB'_{i+\frac{1}{2},j+\frac{1}{2}}\, \delta P^{n+1}_{i+\frac{1}{2},j-\frac{1}{2}} + \left(ACU'_{i+\frac{1}{2},j+\frac{1}{2}} + ACV'\right) \delta P^{n+1}_{i+\frac{1}{2},j+\frac{1}{2}}$$

$$+ B'_{U_{i+\frac{1}{2},j+\frac{1}{2}}} + B'_{V_{i+\frac{1}{2},j+\frac{1}{2}}} \Big] =$$

$$D_{i+\frac{1}{2},j+\frac{1}{2}} - K_1\, \delta P^{n+1}_{i+\frac{1}{2},j+\frac{1}{2}} - K_2\, \delta P^{n+1}_{i+\frac{3}{2},j+\frac{1}{2}}$$

Equation (4.1-19) is put into a more compact form by first multiplying through by δt, moving all terms involving δP^{n+1} to the left hand side of the equation, moving all known quantities to the right hand side of the equation, and finally absorbing the factor $\gamma R \delta t/\epsilon$ into the coefficients of the pressure terms. This produces equation (4.1-20).

(4.1-20)

$$-AR_{i+\frac{1}{2},j+\frac{1}{2}}\, \delta P^{n+1}_{i+\frac{3}{2},j+\frac{1}{2}} - AL_{i+\frac{1}{2},j+\frac{1}{2}}\, \delta P^{n+1}_{i-\frac{1}{2},j+\frac{1}{2}} - AT_{i+\frac{1}{2},j+\frac{1}{2}}\, \delta P^{n+1}_{i+\frac{1}{2},j+\frac{3}{2}}$$

$$- AB_{i+\frac{1}{2},j+\frac{1}{2}}\, \delta P^{n+1}_{i+\frac{1}{2},j-\frac{1}{2}} + AO_{i+\frac{1}{2},j+\frac{1}{2}}\, \delta P^{n+1}_{i+\frac{1}{2},j+\frac{1}{2}} =$$

$$\delta P^{n}_{i+\frac{1}{2},j+\frac{1}{2}} + \delta t\, D_{i+\frac{1}{2},j+\frac{1}{2}} - \frac{\gamma R \delta t}{\epsilon}\left(B'_U + B'_V\right)_{i+\frac{1}{2},j+\frac{1}{2}}$$

where

$$AO = 1 + K_1 + K_2 + AR + AL + AT + AB.$$

The pressure obtained as the solution of equation (4.1-20) is the major element of FLAG. This pressure drives the flow, and requires further inspection.

Some of the terms on the right hand side originate in the u and v momentum equations, some orginate in the pressure equation, and others are created as a result of using the Crank Nicolson formulation. Some of these terms are of course numerically larger than others, and perhaps the smaller terms may be neglected. However, it is important to understand that as solved in FLAG, most of the terms on the right hand side of equation (4.1-21) have been set to zero. If these terms are small, then little error results by setting them to zero. However, there is nothing to indicate these terms can be neglected and until proven otherwise this assumption should be viewed with caution. Appendix II contains the complete pressure equation in terms of all flow parameters and lists the terms retained.

The above development provides the basic ideas on how the flow code was created. As used in FLAG the various terms must be modified to account for variable spacing. The modifications are explained below and the basic finite difference equations as used in FLAG are given in the appendix.

Variable Mesh Grid System

The preceding development was carried out for a uniform grid system. In this section the finite differencing methods for a variable mesh system are developed. One important key in the development is to realize that terms in the energy equation are expanded about the center of the cell, but terms in the momentum equations are expanded about the cell interface. A review of equations (4.1-3) - (4.1-12) show two types of terms which must be evaluated, the convection terms which are first derivatives, and the diffusion terms which are second derivatives. First consider the convection terms for the energy equation. Figure 10 shows the formulation of a term as expanded about the center of a cell.

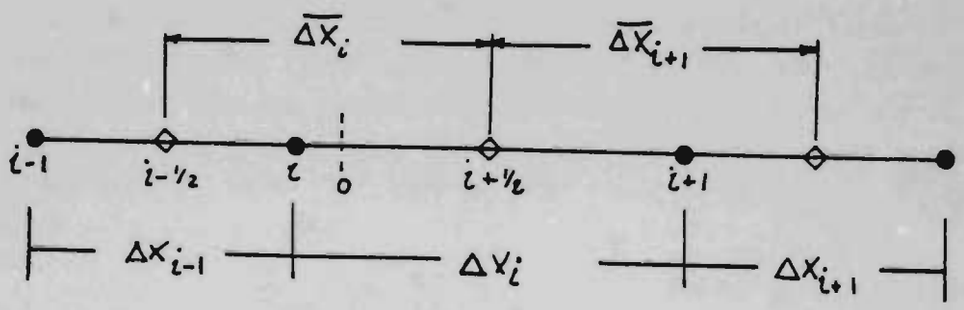

Figure 10 Variable grid mesh

$$\frac{\partial TU}{\partial x} \qquad \frac{(TU)_{i+1} - (TU)_i}{\Delta x_i} \tag{4.1-21}$$

This is a centered difference about the cell center. There is no difficulty in providing values of the velocity because velocity is defined at the cell interfaces (i) and (i+1). On the other hand the temperatures are defined at the center of the cell and are obtained by taking a simple average i.e., $T_i = \frac{1}{2}(T_{i+\frac{1}{2}} + T_{i-\frac{1}{2}})$. This assumes a linear variation between cell centers, but is correct only for a uniform mesh. If mesh spacing does not greatly vary this introduces a small but acceptable error. However, for large variations from cell to cell the error maybe sustantial.

The second type of term evaluated at the cell center is the second derivative

$$\frac{\partial}{\partial x}\left(\Gamma \frac{\partial T}{\partial x}\right)_{i+1/2} \tag{4.1-22}$$

This is evaluated in a two step process. First set

$$q_f = \Gamma \frac{\partial T}{\partial x} \tag{4.1-23}$$

so that what is being evaluated is

$$\left.\frac{\partial q}{\partial x}\right|_{i+1/2} \tag{4.1-24}$$

This is given by a central difference

$$\frac{q_{i+1} - q_i}{\Delta x_i} \tag{4.1-25}$$

The second step is to evaluate q_i and q_{i+1}, again a centered difference formula is used.

$$\Gamma \left.\frac{\partial T}{\partial x}\right|_i = \Gamma_i \frac{T_{i+1/2} - T_{i-1/2}}{\Delta x_i} \tag{4.1-26}$$

Therefore

$$\frac{\partial}{\partial x}\left(\Gamma \frac{\partial T}{\partial x}\right) = \frac{1}{\Delta x_i}\left[\Gamma_{i+1} \frac{T_{i+3/2} - T_{i+1/2}}{\Delta x_{i+1}} - \Gamma_i \frac{T_{i+1/2} - T_{i-1/2}}{\Delta x_i}\right] \tag{4.1-27}$$

Again a variable step size is used, but the formulation is strictly correct only for a constant step size.

Now consider the momentum equation, which requires the evaluation of

(4.1-28)

$$\left.\frac{\partial \alpha U^2}{\partial x}\right|_i \quad \text{and} \quad \left.\frac{\partial}{\partial x}\left(\Gamma \frac{\partial U}{\partial x}\right)\right|_i$$

These terms are evaluated similiarly to those given above, i.e., central differences are taken about the expansion point, x_i.

(4.1-29)

$$\left.\frac{\partial \alpha U^2}{\partial x}\right|_i = \frac{(\alpha U^2)_{i+\frac{1}{2}} - (\alpha U^2)_{i-\frac{1}{2}}}{\Delta x_i}$$

Both ρ and U are easy to specify. The former is a thermodynamic variable and as such is defined at the center of the cell. The velocity is required at the cell center and is easily specified as

$$U_{i+1/2} = (U_{i+1} + U_i)/2$$

This is always correct regardless of step size because the average is only over the individual center. The temperature average given above required information from two cells. Nevertheless, equation (4.1-30) is a central difference equation over the interval between $(i+\frac{1}{2})$ and $(i-\frac{1}{2})$ and actually represents the expansion around point o and not point i. Point o is the point midway between $(i-\frac{1}{2})$ and $(i+\frac{1}{2})$. Notice, the momentum equation also contains the pressure gradient, which is given as

$$\left.\frac{\partial P}{\partial x}\right|_i \qquad \frac{P_{i+1/2} - P_{i-1/2}}{\Delta x_i} \tag{4.1-30}$$

Again the two values of pressure are exactly specified because they are defined at these points; but, as with the convection term this is actually expanded about point o and not point i.

The last type of term evaluated in the momentum term is the stress term. The same general procedure is used here as was used to evaluate the second derivative in the energy equation.

$$q = \Gamma \frac{\partial U}{\partial x}$$

$$\frac{\partial}{\partial x}\left(\Gamma \frac{\partial U}{\partial x}\right)_i = \frac{\partial}{\partial x}\left(q\right)_i = \frac{q_{i+1/2} - q_{i-1/2}}{\Delta x_i} \qquad (4.1\text{-}31)$$

where

$$q_{i+1/2} = \Gamma_{i+1/2} \frac{U_{i+1} \quad U_i}{\Delta x_i} \qquad (4.1\text{-}32)$$

Therefore

$$\frac{\partial}{\partial x}\left(\Gamma \frac{\partial U}{\partial x}\right)_i = \frac{1}{\Delta x}\left[\Gamma_{i+1/2} \frac{U_{i+1} - U_i}{\Delta x_i} - \Gamma_{i-1/2} \frac{U_i - U_{i-1}}{\Delta x_{i-1}}\right] \qquad (4.1\text{-}33)$$

Again equation (4.1-32) is the standard second order central difference expansion about point i + 1/2, but equation (4.1-33) is the expansion about point o, not the point i.

Another point about the formulation is that in many of the terms point values are not used, rather values are averaged over a number of cells. Equation (4.1-34) shows the formulation for the x-momentum axial advection term.

(4.1-34)

$$\frac{\partial(\alpha U U)}{\partial x} = \frac{\langle\langle\bar{\alpha}\rangle\bar{U}\rangle_{i+\frac{1}{2},j+\frac{1}{2}}\langle\bar{U}\rangle_{i+\frac{1}{2},j+\frac{1}{2}} - \langle\langle\bar{\alpha}\rangle U\rangle_{i-\frac{1}{2},j+\frac{1}{2}}\langle\bar{U}\rangle_{i-\frac{1}{2},j+\frac{1}{2}}}{\Delta x_i}$$

where the overbar is a time average given by

$$\overline{A} = \frac{A^{n+1} + A^n}{2} \qquad (4.1\text{-}35)$$

and the angle brackets are space averages given by

$$\langle A\rangle_{ij} = \frac{A_{i+\frac{1}{2},j} + A_{i-\frac{1}{2},j}}{2} \qquad (4.1\text{-}36)$$

When (4.1-36) is used to evaluate quantities, the result is to smear out the gradient over a larger number of cells than just the two cells indicated by the variable subscripts.

4.2 Particles

There are three major calculations which must be to advance the particle velocities and particle positions in time. The first step made is evaluation of drag term, next is the determination of which particles undergo a collision, and finally if a collision occurs whether or not agglomeration occurs. The computational form of the drag equation is given in section 4.3 and the equations to determine collisions are given in section 4.4. The numerical formulation of agglomeration is detailed in reference (3) and will not be reproduced here.

The formulation used in FLAG is implicit, thus in finite difference form equation (2.2-1) becomes

$$\frac{\vec{V}_p^{n+1} - \vec{V}_p^{n}}{\delta t} = \vec{g} - \frac{D_p}{m_p}\left(\vec{V}_g - \vec{V}_p^{n+1}\right) \qquad (4.2\text{-}1)$$

or solving for $\vec{V}_p$

$$\vec{V}_p^{n+1} = \frac{\vec{V}_p^{n} + \frac{\delta t\, D_p}{m_p}\vec{V}_g + \vec{g}\,\delta t}{\left(1 + \frac{\delta t\, D_p}{m_p}\right)} \qquad (4.2\text{-}2)$$

Having determined $\vec{V}_p$ at (n+1) the new position is obtained from (2.2-2) as

$$\vec{X}_p^{n+1} = \vec{X}_p^{n} + \frac{\delta t}{2}\left(\vec{V}_p^{n} + \vec{V}_p^{n+1}\right) \qquad (4.2\text{-}3)$$

Notice, both equation (4.2-2) and (4.2.-3) are vector equations. The actually coding provides separate equations for the axial and radial components.

Once the velocity and positions are known other advanced time variables may be evaluated. The new particle positions provide the new particle mass distribution which allows evaluation of cell void fractions by

$$\epsilon_{ij} = 1 - \frac{\pi}{6\Delta V_{ij}} \sum_{p} N_p d_p^3 \qquad (4.2\text{-}4)$$

where ΔV_{ij} is the cell volume. The summation is over all macro particles within cell (i,j) where N_p is the number of micro particles of diameter d which comprise the macro particle.

Similarly, the drag force per unit volume on the gas from the particles is

$$\vec{F}_{ij} = -\frac{1}{\Delta V_{ij}} \sum_{p} N_p D_p (\vec{V}_g - \vec{V}_p) \qquad (4.2\text{-}5)$$

Equation (4.2-5) is the defining formulation for drag in FLAG.

At the end of PMONIT a set of terms is calculated which is labeled drag, but does not look like equation (4.2-5). These are the drag terms, but they have been transformed as required for incorporation into the coefficients of the pressure equation. If there is any desire to change the drag model used in FLAG the terms must be reviewed to insure that they are consistant with the new model and the coefficients of the pressure equation.

Two other models within PMONIT need to be examined. The first is the equation used to determine particle velocities after a collision. Figure 4.2-1 shows two particles with arbitrary velocities, V_1 and V_2, undergoing a collision. Equations (4.2-6a) and (4.2-6b) are found in

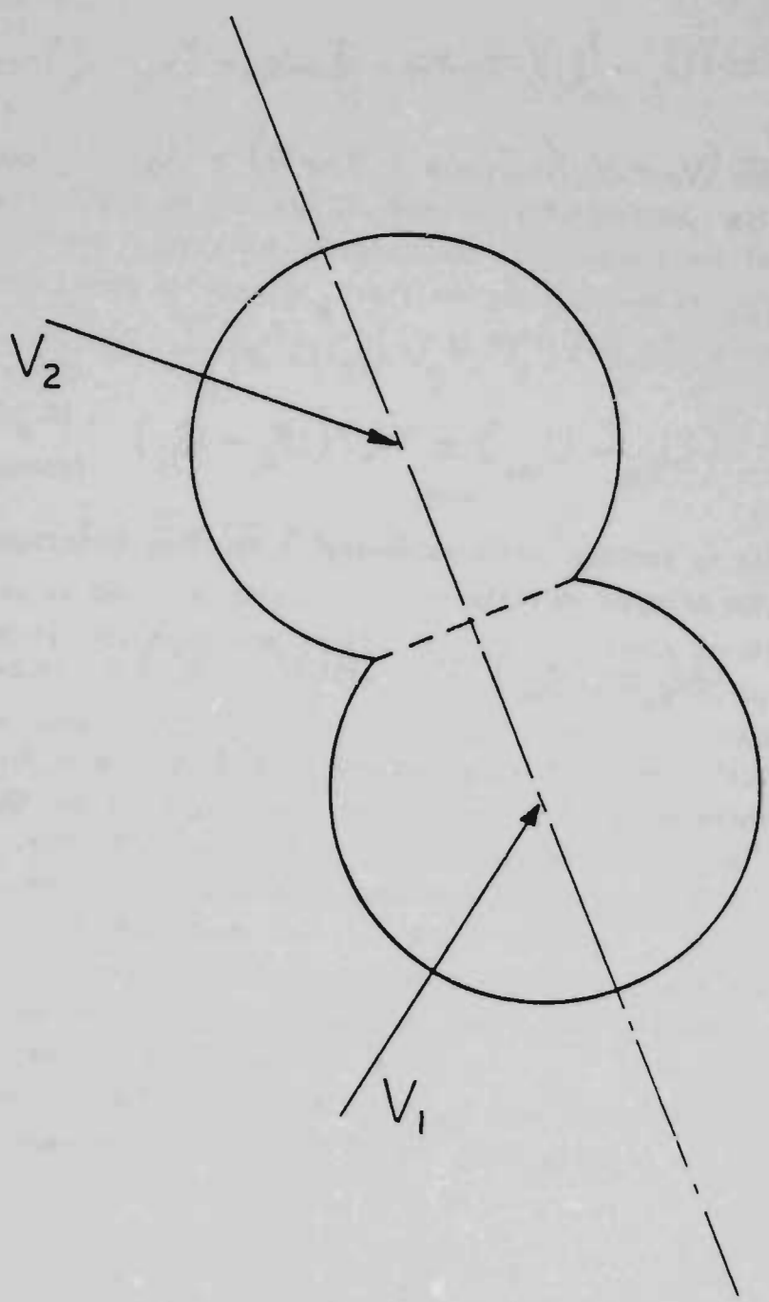

Figure 11 Particle Collision

subroutine COLVEL. Equation (4.2-6) is used to calculate the relative velocities based on the initial geometry and initial relative axial and radial velocities into the collision.

$$(U_{2ac} - U_{1ac}) = (U_{2i} - U_{1i})(-.7\cos^2\theta + .8\sin^2\theta) - (V_{2i} - V_{1i})\cos\theta\sin\theta \quad (4.2\text{-}6a)$$

$$(V_{2ac} - V_{1ac}) = (V_{2i} - V_{1i})(-.7\cos^2\theta + .8\sin^2\theta) - (U_{2i} - U_{1i})\cos\theta\sin\theta \quad (4.2\text{-}6b)$$

The two numerical coefficients, -.7 and .8, are set in a DATA statement at the start of the subroutine. Now, consider two cases. The first case is for two particles moving along the x-axis in opposite directions. The relative velocity after collision is

$$(U_{2ac} - U_{1ac}) = -.7(U_{2i} - U_{1i}) \quad (4.2\text{-}7)$$

The second case is for two particles moving in opposite directions along the y-axis. The relative velocity is

$$(V_{2ac} - V_{1ac}) = .8(V_{2i} - V_{1i}) \quad (4.2\text{-}8)$$

There is actually no difference between case 1 and case 2. Both represent a head on collision, and the results should be the same. Nevertheless, as can be seen, they are not the same. Further, comment cards within FLAG state these equations were developed to describe an elastic collision. Equation 4.2-7 is consistent with an inelastic collision where the .7 coefficient is the coefficient of restitution. On the other hand equation 4.2-8 does not seem consistent with momentum or energy conservation at all. Therefore, subroutine COLVEL needs further investigation to determine what has actually been programmed and what is the effect on the results, when the coefficients in the equations are varied.

4.3 Implicitization of Drag, Conduction, and Radiation

As shown earlier, the drag terms in the momentum equations and conduction and radiation terms from the energy equation have been made implicit. The particle drag force is evaluated in rearranging equation 2.6-1 to obtain

$$F_D = \frac{\pi}{8} \rho \epsilon^2 d^2 C_D U_{REL}^2 \qquad (4.3\text{-}1)$$

where

$U_{REL} = V_g - V_p$ relative velocity between fluid and particles.

or

$$F_D = \frac{\pi}{8} \rho \epsilon^2 d^2 C_D (V_g - V_p)^n (V_g - V_p)^{n+1} \qquad (4.3\text{-}2)$$

which becomes

$$F_D = K_{1D} V_g^{n+1} - K_{2D} \qquad (4.3\text{-}3)$$

This is the basic scheme to implicitize the drag term. Notice that K_1 is a velocity dependent quantity because it depends on the coefficient of drag, C_D. The scheme used evaluates C_D at time level n, which makes K_1 an n level variable. This is an important point because K_1 is a strong function of velocity and may dominate the term. Thus, the scheme used does not make the more important part of the drag implicit, and in fact may do little over evaluating the entire term at the n^{th} time level.

The two heat transfer terms in the energy equation are also made implicit with the same method used for both. The term to be made implicit is multiplied and divided by pressure; the pressure in the denominator is taken at time level n and the pressure in the numerator at level n+1. The procedure for the conduction term is

$$S_{cond} = hA(T_p - T_g) \tag{4.3-4}$$

or $$S_{cond} = hAT_p - hAT_g \frac{p^{n+1}}{p^n} = K_{1_C} p^{n+1} + K_{2_C}$$

Similarly radiation is

$$S_{rad} = \sigma\epsilon A(T_p^4 - T_g^4) = \sigma\epsilon AT_p^4 - \sigma\epsilon AT_g^4 \frac{p^{n+1}}{p^n} \tag{4.3-6}$$

or $$S_{rad} = - K_{1_R} p^{n+1} + K_{2_R} \tag{4.3-7}$$

Each term involving p^{n+1} is moved to the left hand side of the energy equation and the coefficients K_{1_C} and K_{1_D} are incorporated in AC of equation 4.1-19.

Now consider a different method of making 4.3-4 implicit

$$S_{cond} = hA \left(\frac{T_p}{T_g} - 1\right) T_g = hA \left(\frac{T_p}{T_g} - 1\right) \frac{P\mathcal{M}}{R}$$

where all terms are evaluated at level n except P which is evaluated at level (n+1). Compare equations (4.3-5) and (4.3-8) for the case where $T_p = T_g$. In equation (4.3-8) the source term is zero and AC is unchanged. However, even if the temperature is uniform the K_{1_C} coefficient is not zero and AC is thus modified by the amount. A procedure similar to (4.3-8) can be used for the radiation term with the same result; i.e..

$$S_{RAD} = \epsilon\sigma A(T_g^4 - T_p^4) = \epsilon\sigma A\left(\frac{T_p}{T_g} - 1\right)\left(T_p^3 + T_p^2 T_g + T_p T_g^2 + T_g^3\right) T_g$$

where the term is zero for uniform temperature. What this means is that these term assume an influence out of proportion to their actual importance. These terms are not counter balanced by the other terms K_{2_C} and K_{2_R} because both terms appear on the right hand side of the energy equation, which as pointed out above, has been set to zero.

It should be firmly kept in mind that the flow is driven by the pressure which is determined by the energy equation. If the various terms in the energy equation are distorted in importance, the pressure solution is also distorted, and in turn the flow field. Thus, the general implicitization scheme should be viewed with caution.

4.4 Probability of Two Particles Colliding

In order to determine which pair of macro particles collide the following procedure is carried out. First a collision cross-section is assigned for each possible collisions. The cross section for particle i colliding with particle j is

$$\sigma_{ij} = \pi (r_i - r_j)^2 \frac{|V_i - V_j|}{|V_i|} \qquad (4.4\text{-}1)$$

where

r_i, r_j = the radii of the micro particles within macro particles i and j.

$|V_i - V_j|$ = relative velocity between particles

The mean free path for macro particle i colliding with macro particle j is

$$\lambda^{-1} = n_j \sigma_{ij} \tag{4.4-2}$$

where

n_j = number density of j.

The total mean free path is given by

$$\lambda_i = \sum_{j=1}^{N} \lambda_{ij} \tag{4.4-3}$$

This is summed of all the particles within a cell.

Each particle has already been assigned a random number using equation (2.7-4). At each time step the following test is made

$$\sum_{j=1}^{n-1} \left(\frac{S_j}{\lambda_j}\right) < \chi < \sum_{j=1}^{n} \left(\frac{S_j}{\lambda_j}\right) \tag{4.4-4}$$

The summation is taken over time steps. If (4.4-4) is true a collision occurs between i and j. Next generate

$$\Omega_j = \frac{n_j \sigma_{ij}}{\sum_j n_j \sigma_{ij}} \tag{4.4-5}$$

where the summation is overall the particles which have collided according to equation (4.4-4). Finally a second uniformly distributed random number on the interval (0,1) is picked and the largest k is found for

$$\sum_{j=1}^{k} \Omega_j < \xi_2 \qquad (4.4\text{-}6)$$

Particle i collides with particle k.

4.5 Solution Algorithm

The pressure equation is solved using the optimized "block-implicit relaxation" (BIR) technique [reference (8)]. This technique is easier to understand if compared to the ADI method. ADI [reference (9)] can be termed a two step method for solving multi-dimensional problems. The first step is to formulate the multi dimensional problem in terms of a series of one dimensional problems. The second step is to solve the one dimensional problems using the an efficient 1-D solver. Thus, ADI is a technique of utilizing a method of solution which would otherwise not be applicable to the problem at hand.

The idea behind the BIR method is very similar to ADI, it is to divide a large two dimensional problem into a number of smaller two dimensional problems (blocks) with a efficient 2-D solver to evaluate the small problems. The 2-D solver used has been termed error vector propagation (EVP) [reference (9)] method or the generalized sweepout method (GSM). This metnod is not directly used to solve the pressure equation because the GSM technique is restricted to problems of less than a specific size. The maximum problem size for which the GSM method works

is normally much smaller than the size of the pressure problem. Thus, in the spirit of ADI, the BIR method utilizes a very efficient method which is otherwise not applicable to the problem at hand. The following discussion summarizes first the GSM method, then explains its block by block application to complete the BIR technique.

Equation (4.5-1) presents a fairly general second order partial differential equation. Equation 4.8-2 is the finite difference form of the equation where second order accurate centered differencing was used to replace derivatives.

$$\nabla^2 \phi + \vec{A}(x,y) \cdot \vec{\nabla} \phi + B(x,y)\phi = S(x,y) \qquad (4.5\text{-}1)$$

$$AR_{ij}\,\phi_{i+1,j} + AL_{ij}\,\phi_{i-1,j} + AT_{ij}\,\phi_{i,j+1} + AB_{ij}\,\phi_{i,j-1} - AC_{ij}\,\phi_{ij} = S_{ij} \qquad (4.5\text{-}2)$$

Now solve for $\phi_{i,j+1}$ in terms of the other quantities

$$\phi_{ij+1} = \frac{1}{AT_{ij}}\left(S_{ij} - AR_{ij}\,\phi_{i+1,j} - AL_{ij}\,\phi_{i-1,j} - AB_{ij}\,\phi_{ij-1} + AC_{ij}\,\phi_{ij}\right) \qquad (4.5\text{-}3)$$

If the values of ϕ along the row immediately adjacent to the boundary row are known equation (4.5-3) could be used to sweep out the rest of the interior points. However, if the first row of points is a guess, application of equation (4.5-3) produces results which differ from the true values by some error, i.e.,

$$\phi_{ij} = \phi'_{ij} + e_{ij} \qquad (4.5\text{-}4)$$

ϕ_{ij} = true solution
ϕ'_{ij} = solution obtained from guessed values
e_{ij} = error

Equation (4.5-4) is true for all points, including the top boundary. This is important because along the top boundary $\phi_{i,j_{max}}$ is the boundary condition, which is known. Therefore along the top the true value of the error, e, is known. There is linearly relationship between the error at the boundary and the error of the values guess along row 2 given by

$$e_{i,j_{max}} = [C]\, e_{i,2} \tag{4.5-5}$$

Creation of the [C] matrix is described below. Now, by inverting equation (4.5-5) errors along row 2 are known. Remember, the ϕ's input to start the problem were guesses. Therefore the corresponding e's were unknown. Once the errors have been determined equation (4.5-4) is used to calculate the true solution along the second row, which in turn is used in equation (4.5-3) to calculate the true values for all interior points.

The process does not actually start by evaluation e as indicated above. Rather, ϕ' as given in equation (4.5-4) is substituted into equation (4.5-3). Then the equation is grouped in terms of ϕ and e. The group of terms with ϕ and s adds to zero; this is because it is the true solution. The remaining terms define an equation for the error.

$$e_{i,j+1} = \frac{1}{AT_{ij}}\left(-AR_{ij}\, e_{i+1,j} - AL_{ij}\, e_{i-1,j} - AB_{ij}\, e_{i,j-1} + AC_{ij}\, e_{ij}\right) \tag{4.5-6}$$

Equation (4.5-6) is the actual starting point and is used with the following procedure.

(1) Starting at point (2,2) set $e_{2,2} = 1$ and $e_{i,2} = 0$.

(2) Sweep all errors using (4.5-6) to generate an error along upper boundary $e_{i,jmax}$.

(3) This row of errors is the 1st column of the (c) array shown in equation (4.5-5).

(4) Repeat steps 1,2,and 3 (IMAX-2) times. Each time through set $e_{m,2} = 1$ and all other $e_{i,2} = 0$, and create an error

This is one column in the (C) array

$$C_{\ell,m-1} = F_\ell$$

(5) Invert (C) to obtain $(C)^{-1}$

(6) Guess solution along row 2, $\phi'_{i,2}$.

(7) Sweep array to generate interior ϕ'_{ij}.

(8) Create error vector along top boundary

$$e_{i,jmax} = \phi'_{i,jmax} - \phi_{i,jmax}$$

where $\phi_{i,jmax}$ is the known boundary condition.

(9) Evaluate error along row 2 from

$$e_{i,2} = C^{-1}_{m,\ell}\, e_{i,jmax}$$

(10) Generate correct solution along row 2

$$\phi_{i,2} = \phi'_{i,2} \quad e_{i,2}$$

(11) The values of $\phi_{i,2}$ generated in step 11 and the boundary condition are used in equation (4.5-3) to evaluate the solution at all interior points.

So far the boundary conditions have been alluded to but have not been specifed. There are four boundaries to consider, the inlet, exit, wall, and center line. The first two are easy to specify, FLAG reads in the inlet pressure and internally sets the exit pressure at one atmosphere. Both values are held constant throughout the calculations. The wall and centerline are treated in the same way, i.e., it is assumed

$$\left.\frac{\partial P}{\partial y}\right|_{\substack{\text{Wall or}\\ \text{Center line}}} = 0 . \qquad (4.5\text{-}7)$$

Equation (4.5-7) is finite differenced and the resulting equation is solved for the presure in the fictitious cells. It is easy to see that the pressure in the row of fictitious cell is just equal to the pressure in the adjacent cells in the actual flow region. This means that unlike the inlet and outlet conditions which are fixed at some specified values the wall and center line boundaries must evolve along with the flow in the interior cells. Because of this the wall and center line boundary conditions are part of the solution algorithm and are thus automatically evaluated by the code. The user does not specify these boundary

conditions, in fact, extensive code modification is necessary to remove these boundary conditions from the general algorithms and make them user controllable.

A second important point about equation (4.5-7) is that it is essentially a boundary layer approximation. This approximation is accurate when the boundary cells are submerged within the boundary layer, but there is no guarantee this approximation is valid if the boundary layer is completely enclosed by the boundary cell. Another complicating factor is that equation (4.5-7) does not take into account the presence of particles in the flow. The particles may make equation (4.5-7) a good approximation even through for the same flow velocities without particles equation (4.5-7) is a poor approximation, however, this is not a certainty.

The major difficulty with this technique is that roundoff and truncation error destroys the solution. Thus, error associated with the computer word length limits the use to problems smaller than some maximum limit, perhaps a 10 x 10 problem. The BIR technique divides a large problem into a number of small blocks where the small problems can be evaluated with the GSM.

Figure 12 shows a 14 x 14 grid divided into nine 6 x 6 blocks. Boundary conditions are given along ABCD. The process starts by guessing values along the even numbered lines. Next block 1, bounded on the top by line 6 and on the right by line 2 is evaluated using GSM. This step creates new values within block 1, but more importantly it creates values along line 1 which serve as boundary conditions for block 2.

Block 2 with vertical boundaries 1 and 4 and top boundary, line 6, is evaluated next. This produces values along line 3 which serve as boundary conditions for block 3. This process continues until all of the subblocks have been evaluated. The only requirement is that blocks overlap so interior points of one block form boundary points for adjacent blocks.

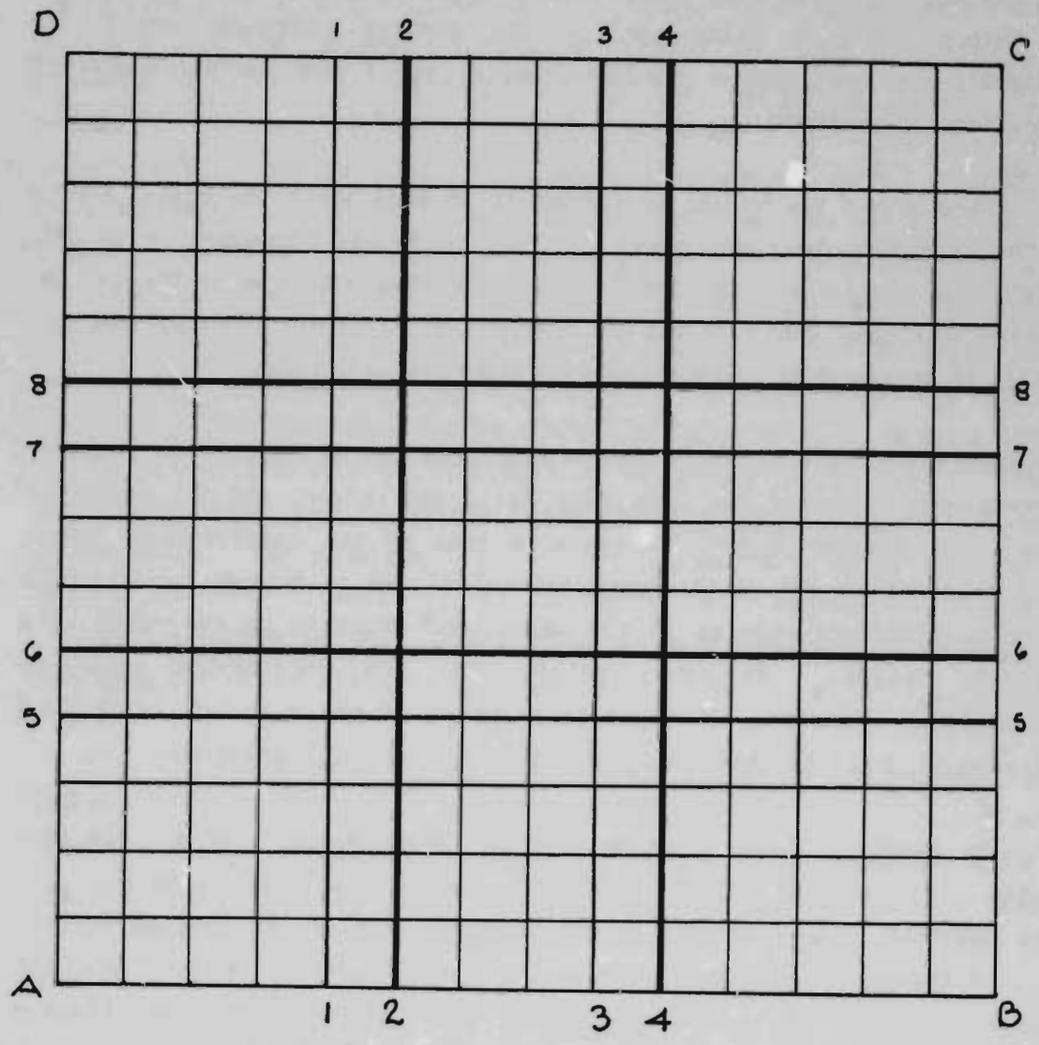

Figure 12 Overlapping grid used in BIR method

This is an iterative process. The initial boundary values for the blocks were guesses. Sweeping through all the blocks improves the values, but one sweep does not resolve the problem. Thus, the relaxation in "Block Implicit Relaxation". The process continues until the residuals are less than a preset value, or until some maximum number of iterations is exceeded.

There are a few points that need to be made about the actual coding of the technique described above. First, the usual procedure is to calculate the coefficients of the finite difference equation in the calling routine and pass these values to the solver routine. This allows the solver to be replaced without changing the calling program.

Unfortunately, in FLAG the flow program does not calculate the required coefficients. Rather the flow code calls the solver, and the solver in turn calls another routine to evaluate some of the coefficients. But, only a subset of the coefficients are calculated . This is because only those coefficients related to the individual block being evaluated are actually needed. To save storage only the one needed block is calculated. Therefore, if there is a desire to use a solver other than BIR more is involved than simply changing the solver subroutines

The finite difference equation which forms the heart of the BIR subroutine is equation (4.5-3). Notice, the only difference between the form equation (4.5-3) and the error equation (4.5.-6) is the source term S_{ij}. Although S_{ij} has been termed a source it is actually the right hand side of the pressure equations. Rather than reproduce these equations a number of times, only one equation, (4.5-7), is coded

$$H_{ij} = RECUR_{ij}\left(RQ \cdot TQ_y - AR_{ij} H_{i+1,j} - AL_{ij} H_{i-1,j} - AB_{ij} H_{i,j-1} + AC_{ij} H_{ij}\right) + (1 - RECUR_{ij}) H_{ij} \qquad (4.5\text{-}8)$$

Equation (4.5-8) is given in terms of the variables used in FLAG. In this equation RECUR is used to preserve the exterior boundary condition, i.e., values on ABCD in figure 12 . Along these points RECUR is set to zero, and for interior points it is set to one. Evaluation of equation 4.5-8 is accomplished by calling subroutine SWEEP. The arguments used in the call determine whether equation (4.5-8)is interperated as the solution of the pressure equation, or the solution to the error equation. To evaluate error set RQ=0, and use the error as the argument in the call. To evaluate pressure set RQ=1, and use pressure in the argument. The user is not required to actually set these quantities. A DATA statement in the solver routine initializes two variables D =0 and D1 = 1. When subroutine SWEEP is used to evaluate errors. D is contained in the argument list and sets the value of RQ to zero in SWEEP. Similarly when pressure is evaluated D1 is in the SWEEP to one. Thus, the calculations are correctly made without the necessity of user intervention. The quantity, TQ, is the right hand side of the energy equation as given in section 4.2. Presently TQ is evaluated in the flow routine and passed to the solver, which in turn passes it to subroutine SWEEP along with the pressure, and the value of RQ.

Finally, there needs to be a word about the solver in general. The references cited provide a guide to the method, but the algorithm programmed does not appear in the open literature. As presented above a trial solution is created by starting on one boundary and sweeping across to the opposite boundary. However, here the trial solution is generated by simultaneously starting at both boundaries and sweeping to the interior. What effect this has is unknown, it may or may not decrease the error. Whatever it does, is not documented in the open literature. This strongly suggests that the BIR method as implemented in FLAG be used to solve a simple problem, i.e., a transient conduction problem, so that what the algorithm actually does can be better understood.

4.6 Chemistry

The reactions set forth in section 2.3 require slightly different handling depending on whether or not the concentration of oxygen in a computational zone is zero or greater than zero.

Case 1: Concentration for $O_2 \neq 0$ (combustion zone)

Mass balances for O_2 and CO_2 at the particle surface produce

$$k_g (C_{O_2} - C_{O_2,S}) = (k_1 C_{O_2,S} + k_2 C_{H_2O,S} + k_3 (C_{CO_2,S}) \quad (4.6\text{-}1)$$

$$k_g (C_{CO_2,S}) = -(k_1 C_{O_2,S} + k_2 C_{H_2O,S} + k_3 C_{CO_2,S}) \quad (4.6\text{-}2)$$

There is no net production of consumption of H_2O

$$C_{H_2O,} = C_{H_2O} \quad ((4.6\text{-}3)$$

Equation 4.6-1, 4.6-2 and 4.6-3 can be solved to produce

$$C_{O_2,S} = \frac{k_g C_{O_2} - \phi k_2 C_{H_2O} - k_3 \phi (C_{O_2} + C_{CO_2})}{(k_g + \phi k_1 - \phi k_3)} \quad (4.6\text{-}4)$$

and

$$C_{CO_2,S} = C_{O_2} + C_{CO_2} - C_{O_2,S} \quad (4.6\text{-}5)$$

Now rate of conversion is

$$\frac{dX}{dt} = \frac{36}{\rho_o W_o R_o} (k_1 C_{O_2,S} + k_2 C_{H\,O} + k_3 C_{CO_2,S}) \phi \quad (4.6\text{-}6)$$

and the production rates are

$$S_{O_2} = \sum_{k=1}^{NP_i} - \left[(k_1 C_{O_2,S} + k_2 C_{H_2O} + k_3 C_{CO,S}) \phi 4\pi R_0^2\right]_k - \frac{1}{2}(N_{H_2} + N_{CO}) \tag{4.6-7}$$

$$S_{CO_2} = \sum_{k=1}^{NP_i} \left[(k_1 C_{O_2,S} + k_2 C_{H_2O} + k_3 C_{CO_2,S}) \phi 4\pi R_0^2\right]_k - N_{CO} \tag{4.6-8}$$

The summation is over all particles in a cell and N_{H_2} and N_{CO} are inflow rates of these components into the cell.

If all the oxygen within the cell is consumed in a time step the cell becomes a gasification zone in the next time step.

Case 2: Concentration of O_2 = 0 (Gasification zone)

In the absence of oxygen the reactions which take place are R2, R3, and R6 are defined in section 2.3. For this case mass balances on the components produce

$$C_{H_2O,S} = \frac{k_g C_{H_2O}}{(k_g + k_2\phi)} \tag{4.6-9}$$

and

$$C_{CO_2,S} = \frac{k_g C_{CO_2}}{(k_g + k_3\phi)} \tag{4.6-10}$$

The particle conversion is

$$\frac{dX}{dt} = \frac{36}{\rho_o w_o R_o}(k_2 C_{H_2O,S} + k_3 C_{CO_2,S})\phi \qquad (4.6\text{-}11)$$

and the production rates are

$$S_{H_2O} = \sum_{k=1}^{NP_i} -(\phi 4\pi d^2 k_2 C_{H_2O,S})_k + 2N_{O_2} - r_6 \qquad (4.6\text{-}12)$$

$$S_{CO_2} = \sum_{k=1}^{NP_i} -(\phi 4\pi d^2 k_3 C_{CO_2,S})_k - r_6 \qquad (4.6\text{-}13)$$

$$S_{CO} = \sum_{k=1}^{NP_i} 4\pi\phi d^2 (k_2 C_{H_2O,S} + 2k_3 C_{CO_2,S})_k - r_6 \qquad (4.6\text{-}14)$$

$$S_{H_2} = \sum_{k=1}^{NP_i} (\phi 4\pi d^2 C_{H_2O,S})_k - 2N_{O_2} + r_6 \qquad (4.6\text{-}15)$$

where r_6 is the rate for the water-gas shift reaction, R6. Equations ((4.6-12) thru (4.6-15) specifies the S_i term in the concentration equation, (2.3-1). However, the rate term $_6$ comes from the water-gas shift reaction, a reaction assumed to be in equilibrium. This means that rather than knowing the reaction rate $_6$, the parameter which describes the water-gas shift is the equilibrium constant K,

$$K = \frac{C_{CO_2} C_{H_2}}{C_{H_2} C_{CO,}} \qquad (4.6\text{-}16)$$

where

$$\log_{10} K = 1.6945 + 1855.6/T_g \qquad (4.6\text{-}17)$$

knowing K rather than r_6 causes a round about technique for evaluating the gas concentrations. The first step in the process is to set $r_6 = 0$ in equations (4.6-12) thru (4.6-15) and use the resulting values of S_i in

equation (2.3-1). The resulting values of the species concentrations will of course be incorrect because r_6 in general is not actually zero. But it is assumed that incorrect values may be used in conjunction with equation (4.6-16). This is accomplished as follows, equation (4.6-16) is rewritten as

$$\frac{(B_3 - X)(B_2 - X)}{(B_1 + X)\,X} = K$$

where

$$B_1 = C'_{H_2O} - C'_{CO} \qquad (4.6\text{-}18a)$$
$$B_2 = C'_{H_2} + C'_{CO} \qquad (4.6\text{-}18b)$$
$$B_3 = C'_{CO_2} + C'_{CO}. \qquad (4.6\text{-}18c)$$

where the concentration in (4.6-18) are the newly calculated, but incorrect value, and X in (4.6-17) is the correct, but unknown concentration of CO. Equation (4.6-17) is rearranged to produce a quadratic equation

$$Ax^2 + Bx + C = 0$$

where

$$A = (1 - K)$$
$$B = -(B_3 + B_2 + KB_1)$$
$$C = B_2 + B_3$$

Equation (4.6-19) is solved to produce two roots x_1 and x_2. These roots are fractionalized with respect to the total concentration and then the particular root between zero and one is the root which corresponds to the correct concentration of CO. Once the true CO concentration i known equation 4.6-18 is used to evalute the true concentrations of the other species, for example

$$C_{H_2O} = C'_{H_2O} - C'_{CO} + X,$$

where the unprimed concentration is the true value and the primed concentrations are the same incorrect values which were used to begin the procedure.

4.7 Overall Structures

The information given below outlines the methodology for advancing the flow field in time. However, a number of comments need to be made. First concerns the time step used in the calculations. The algorithm used in FLAG is semi-implicit, which means that the equations will diverge if the time step is too large. Unfortunately, what is too large is not known before hand. One way to make an estimate of the maximum time step is to consider the equation written in a completely explicit form and do a standard stability analysis, reference (12), to find the maximum stable time step. However, one of the reasons for using an implicit or semi-implicit formulation is the ability to use time step larger than the explicit time step and still have a stable solution. FLAG contains a subroutine called NEWDT which attempts to optimize the time step so that largest stable time step may be used. Unfortunately, NEWDT does not calculate the theoretical maximum time step for an explicit formualtion then adjust the time step on this basis. Rather, what is done is to look at the percent change over a time step of the density and U and V momentum densities. If the percentage change is less than 8% the time step is increased to a user specified maximum. If the percentage change of the major variable is greater than 8% the time step is decreased to some user specified minimum.

Be sure to understand that the user supplies the time step to start the calculations and the maximum and minimum time steps. Although FLAG will vary the time step there is really nothing within the code which prevents unstable time steps from being created and used. The responsibility for avoiding this situation lies entirely with the user. The code does, however, provide some information which may be helpful in deciding what to do. A subroutine called UVWP calculates the right and left hand sides of density, momentum, and energy equations and compares the results. When the true flow field has been found the right and left hand side of the equations must be equal. Conversely, if the correct flow field has not been established the equations will not balance. It

is this imbalance which is calculated by UVWP. Again, it must be emphasized that no control decisions within FLAG are based on this information. If this information is used and how it is used is totally the responsibility of the individual using the code.

One last word about the algorithm listed below. The major reason for the way it is structured is that when a chemical reaction takes place the enthalpy strongly influences the pressure, which of course drives the flow. The algorithm has thus been structured to provide the best estimates possible for the enthalpy. As can be seen this requires making estimates of variables at time levels $t+\delta t/2$, $t+\delta t$, and $t+3\delta t/2$, which as expected is a time consuming process. But the algorithm is locked into the computer code. Thus, non reacting flows are evaluated in the same way as reacting flows. Therefore, it should not be expected that the total CPU time needed to solve a non reacting problem will be markedly different than the CPU time required for a reacting flow. Keeping all the points listed above in mind, the basic FLAG algorithm is now presented.

(1) Initialize all fields, including prescribed inflow conditions.

(2) Calculate individual gas species <u>fluxes</u> at $t = t_0 + \delta t$, using the gas velocity at $t = t_0 + \delta t$ and species concentrations at staggered time levels $t = t_0 + 1/2\ \delta t$ and $t = t_0 + 3/2\ \delta t$. The latter are the most recently iterated values or extrapolated initial estimates. Calculate temporary values for species concentrations at $t = t_0 + 3/2\ \delta t$, using concentrations at $t = t_0 + 1/2\ \delta t$, fluxes at $t = t_0 + \delta t$, and PG species sources at $t_0 + 1/2\ \delta t$, and assuming no gas phase reactions.

(3) Starting with the temporarty species concentrations at $t = t_0 + 3/2\delta t$, as calculated in step (2), calculate the species concentrations resulting after a time increment δt with gas phase reactions, assuming no fluxes or species sources from particles.

(4) By leapfrogging around $t = t_0 + \delta t$ (using the gas velocity at $t = t_0 + \delta t$ to calculate the particle drag terms), update the particle velocities and positions to $t_0 + 3/2\ \delta t$. This scheme is trapezoidal with

respect to particle positions and velocities when converged.

(5) Update particle termperature and composition. The particle energy equation includes radiation, conduction, and particle chemistry effects. Particle chemistry uses gas concentrations C_i at $t_o + 3/2\ \delta t$ as initial conditions.

(6) Gas quantities and concentrations are interpolated to $t = t_o + 1/2\delta t$ and $t = t_o + \delta t$ and extrapolated to $t = t_o + 3/2\ \delta t$ and $t = t_o + 2\delta t$.

(7) Start inner gas iteration loop by averaging gas fields (G) between old time level, at $t = t_o + 1/2\ \delta t$, and most recently iterated or extrapolated initial estimates at $t = t_o + 3/2\ \delta t$ to get the values at the intermediate time, $t = t_o + \delta t$.

(8) Calculate the intermediate gas velocity by dividing the gas mass flux calculated in (7) by the gas density.

(9) Calculate the turbulent eddy transfer coefficients, using a modified Prandtl mixing length model.

(10) Calculate gas momentum and energy fluxes and pressure work terms at the intermediate time, $t = t_o + \delta t$, using the results from (7), (8), and (9).

(11) Substitute the fluxes and pressure work terms (calculated in step (10), and sources from particles, gas phase chemistry, and radiation (calculated in steps (3)-(5)) into the gas energy and momentum equations.

(12) Solve the coupled semi-implicit (compression wave terms) gas energy and momentum equations for the new pressure, at $t = t_o + 3/2\ \delta t$.

(13) Calculate the new gas mass flux components from the momentum conservation equations, using the new pressure.

(14) Using the new gas mass flux components and the mass sources from the particles, calculate the new gas density from the gas mass continuity equation.

(15) Using the new pressure, density, and mean molecular weight fields, calculate the new gas temperature from the equation of state.

(16) Return to step (7) if fewer than NLIM (a prescribed parameter) inner iterations have been completed within the time step. NLIM = 2 or NLIM = 3 is used in practice.

(17) Return to step (2) if fewer than MAXITF (a prescribed parameter) time steps have been completed.

REFERENCES

1. Anderson, T. B., and Jackson, R., "A Fluid Mechanical Description of Fluidized Beds." I & EC Fundamentals, Vol 6, No. 4, (1967)

2. Wen, C. Y., "Noncatalytic Hetrogeneous Solid Fluid Raction Models," Ind Eng Chem, Vol 60, No 9, Sept 1968

3. Mosely, J. L., O'Brien, T. J., Nicoletti, P., "Implementation of the JAYCOR Model for Agglomeration." DOE/METC83-62 (DE83011366)

4. Rohsenow, W. M., Hartnett, J. P., Handbook of Heat Transfer, McGraw-Hill (1973)

5. Bird, R. B., Stewart, W. E., Lightfoct, E. N., Transport Phenomena, Wiley (1960)

6. Bell, G.I., Glasstone, S., Nuclear Reactor Theory, Van Nostrand Reinnold (1970)

7. Zenz, F. A., "Fluidized-Bed Reactors: Design Scale-up Problem Areas.", AIChE Today Series, (1974)

8. McDonald, H., Briley, W.R., "On the Structure of Linearized Block Implicit Schemes.", Journal of Computational Physics 34 (1980)

9. Douglas, J. "Alternating Direction Methods for Three Space Variables.", Numerische Mathematik, Vol 4 (1962)

10. Roache, P. J. "Marching Methods For Elliptic Problems: Part I", Numerical Heat Transfer, vol 1 (1978)

11. F. H. Harlow and A. A. Amsden, "A Numerical Fluid Dynamics Calculations Method for All Flow Speeds," J. Computational Phys. 18, (1971)

12. Roache, P. J. "Computational Fluid Dynamics," Hermosa Publishers, 1972

Glossary

d = Diameter (m)

g = Gravitational acceleration (m/s^2)

h = Convective heat transfer coefficient (W/M^2-K)

h_i = Specific enthalpy (J/kg or J/mole when referring to species i)

k_g = Mass transfer coefficient (m/s)

l_m = Turbulent mxing length (m)

m_p = Particle mass (kg)

n_a = Number density for particle A.

n_p = Particle number density

r = Radial space coordinate (m)

r_m = Mass source from particles (kg/m^3-s)

r_i = Hetrogeneous chemical reaction rate of i^{th} chemical spaces ($knol/m^3$-s)

t = Time (s)

u = Velocity in axial direction (m/s)

v = Velocity in radial direction (m/s)

w = Swirl velocity (m/s)

x = Axial space coordinate (m)

A = Number density of particle type A

B = Number density of particle type B

C = speed of light (m/s)

C_D = coefficient of drag

C_i = Volume averaged concentration of species i ($kmol/m^3$)

d = Diameter (m)

g = Gravitational acceleration (m/s^2)

h = Convective heat transfer coefficient (W/M^2-K)

h_i = Specific enthalpy (J/kg or J/mole when referring to species i)

k_g = Mass transfer coefficient (m/s)

l_m = Turbulent mxing length (m)

m_p = Particle mass (kg)

n_a = Number density for particle A.

n_p = Particle number density

r = Radial space coordinate (m)

r_m = Mass source from particles (kg/m^3-s)

r_i = Heterogeneous chemical reaction rate of i^{th} chemical spaces ($knol/m^3$-s)

t = Time (s)

u = Velocity in axial direction (m/s)

v = Velocity in radial direction (m/s)

w = Swirl velocity (m/s)

x = Axial space coordinate (m)

A = Number density of particle type A

B = Number density of particle type B

C = speed of light (m/s)

C_D = coefficient of drag

C_i = Volume averaged concentration of species i ($kmol/m^3$)

C_p = Specific heat at constant pressure (J/kg-K)

C_v = Specific heat at constant volume (J/kg-K)

C_1, C_2 = Dimensionless coefficients used in curve fit of drag data

CO = Symbol of carbon monoxide

CO_2 = Symbol for carbon dioxide

$\mathcal{D}$ = Coefficient of diffusion (m^2/S)

D_P = Particle drag (N-s/m)

F_D = Total drag force (N)

F_{DU} = Drag force in axial direction (N)

F_{DV} = Drag force in radial direction (N)

F_{DW} = Drag force in swirl direction (N)

H = Gas heating rate (W/m^3)

H_g = Specific enthalpy of gas component g (J/kmol)

H_2 = Symbol for hydrogen

H_2O = Symbol for water

M = Mass (kg)

Nu = Nusselt number = hd/λ_h

P = Pressure (N/m^2)

$\langle P \rangle$ = Volume averaged pressure (N/m^2)

P_B = Reference or base pressure (N/m^2)

R = Gas constant (J/kmol-K)

Re = Reynolds number = $\rho Ud/\mu$

S = Distance between particle collisions (m)

Sc = Schmidt number = $\mu/\rho\mathcal{D}$

Sh = Sherwood no = $2\ k_g d/\mathcal{D}$

S_{COND} = Conductive heat transfer source (W/m^3)

S_i = Production rate of species i ($kmol/m^3$-s)

S_{rad} = Radiation heat transfer source (W/m^3)

S_u = Axial force per unit volume = Ur_m (N/m^3)

S_v = Radial Force per unit volume = Vr_m (N/m^3)

S_w = Swirl force per unit volume = Wr_m (N/m^3)

T = Temperature (K)

U = Volume average axial momentum density = U (kg/m^2-s)

UREL = Relative velocity = (Vg - Vp) (m)

V = Volume averaged radial momentum density = V (kg/m^2-s)

V_f = Final velocity of colliding particle (m/s)

V_g = Gas velocity (vector quantity: m/s)

V_p = Particle velocity (vector quantity: m/s)

W = Volume averaged swirl momentum density = W (ky/m^2-s)

X = Carbon conversion function

Xp = Particle position (Vector quantity: m)

α = Inverse of gas density = $1/(\epsilon\rho)$ (m^3/kg)

γ = Ratio of specific heats = C_p/C_v

δP = Pressure difference ($P - P_B$) (n/m^2)

ϵ = Volume average void fraction

ϵ_p = Particle emissivity

λ = Mean free path between particle collisions (m)

λ_h = Heat transfer coefficient (J/sec-m-K)

λ_{AS} = Absorption and scattering mean free path (m)

μ = Molecular viscosity

μ_o = Reference value of molecular viscosity

ξ = Random number

ρ = Gas density (kg/m^3)

$\langle\rho\rangle$ = Volume averaged gas density (kg/m^3)

σ = Stephen-Boltzmann constant ($w/m^2\text{-}K^4$)

ϕ = Shrinking core function

χ = Random number

Γ = Gas density times diffusion coefficient

Appendix I

The energy equation as used in FLAG is derived from a system statement of the First Law of Thermodynamics for a simple compressible substance. In terms of intensive properties the First Law is

$$dq_b = de + P dv \qquad \text{(A.1-1)}$$

where

q_b = heat transfer
e = internal energy
v = specific volume = $1/\rho$
P = pressure

Additionally, the internal energy is taken as a function of only the temperature

$$de = C_v dT \qquad \text{(A.1-2)}$$

where

T = temperature
C_v = specific heat at constant volume, function of temperature only

Equation (A.1-1) is converted to a rate form and the entire equation is multiplied by $\rho\epsilon$ where ϵ is the void fraction. This produces

$$\rho\epsilon\left(C_v \frac{dT}{dt} + P\frac{dv}{dt}\right) = \dot{Q} \qquad \text{(A.1-3)}$$

The right hand side of (A.1-3) is considered later, for the time being, attention is focussed on the left hand side of the equation.

The next step in the process is to change from the Lagrangian to the Eulerian viewpoint. Equation (A.1-3) becomes

$$\rho\epsilon C_v\left(\frac{\partial T}{\partial t} + \vec{V}\cdot\vec{\nabla}T\right) + \rho\epsilon P\left(\frac{\partial v}{\partial t} + \vec{V}\cdot\vec{\nabla}v\right) = \dot{Q} \qquad \text{(A.1-4)}$$

where

$$\vec{\nabla} = \text{gradient operator} = \frac{\partial}{\partial x}\underline{i} + \frac{\partial}{\partial y}\underline{j} + \frac{\partial}{\partial z}\underline{k}$$

Each of the terms within brackets will be changed in the same way. This is accomplished as follows

$$\frac{\partial(\rho\epsilon T)}{\partial t} + \vec{\nabla}\cdot(\rho\epsilon\vec{V}T) = \rho\epsilon\left(\frac{\partial T}{\partial t} + \vec{V}\cdot\vec{\nabla}T\right) + T\left(\frac{\partial \rho\epsilon}{\partial t} + \vec{\nabla}\cdot(\rho\epsilon\vec{V})\right) \quad \text{(A.1-5)}$$

The last term in brackets on the right hand side is seen to be the continuity equation. From Chapter II

$$\frac{\partial(\rho\epsilon)}{\partial t} + \vec{\nabla}\cdot(\rho\epsilon\vec{V}) = r_m$$

Therefore

$$\rho\epsilon\left(\frac{\partial T}{\partial t} + \vec{V}\cdot\nabla T\right) = \frac{\partial(\rho\epsilon T)}{\partial t} + \vec{\nabla}\cdot(\rho\epsilon\vec{V}T) - Tr_m \quad \text{(A.1-6)}$$

The second term in brackets in (A.1-4) may similarly be evaluated, and then (A.1-4) may be written as

$$C_v\left(\frac{\partial \rho\epsilon T}{\partial t} + \vec{\nabla}\cdot(\rho\epsilon\vec{V}T)\right) + P\left(\frac{\partial \rho\epsilon}{\partial t} + \vec{\nabla}\cdot(\rho\epsilon v\vec{V})\right) = \dot{Q} + C_v T r_m + P v r_m \quad \text{(A.1-7)}$$

Noting that $Pv = RT$, $\rho v = 1$

and $$C_v + R = C_v + (C_p - C_v) = C_p$$

equation (A.1-7) is rewritten as

$$C_v\left(\frac{\partial \rho\epsilon T}{\partial t} + \vec{\nabla}\cdot(\rho\epsilon\vec{V}T)\right) + P\frac{\partial \epsilon}{\partial t} + P\vec{\nabla}\cdot(\epsilon\vec{V}) = \dot{Q} + C_p T r_m \quad \text{(A.1-8)}$$

Now replace ρT by (P/R) in the first term, expand and collect like terms.

Furthermore

$$\frac{C_v}{R} + 1 = \frac{C_p}{R} \quad , \qquad \gamma = \frac{C_p}{C_v}$$

and let

$$\vec{U} = \rho\epsilon\vec{V} \tag{A.1-9}$$

which allows equation (A.1-8) to be written as

$$\frac{\partial P}{\partial t} + \frac{R}{\epsilon}\vec{\nabla}\cdot(T\vec{U}) = \frac{(\gamma-1)}{\epsilon}\left[\dot{Q} + C_p T r_m - P\vec{\nabla}\cdot(\epsilon\vec{V})\right] + \frac{P}{R}\frac{\partial R}{\partial t} - \frac{\gamma P}{\epsilon}\frac{\partial \epsilon}{\partial t} \tag{A.1-10}$$

Now, consider

$$\vec{\nabla}\cdot(\epsilon\vec{V}) = \vec{\nabla}\cdot\left(\rho\epsilon\frac{\vec{V}}{\rho}\right) = \vec{\nabla}\cdot\left(\frac{RT\vec{U}}{P}\right) = \frac{R}{P}\vec{\nabla}\cdot(T\vec{U}) + T\vec{U}\cdot\nabla\left(\frac{R}{P}\right)$$

Substituting this into (A.1-10) creates

$$\frac{\partial P}{\partial t} + \frac{\gamma R}{\epsilon}\vec{\nabla}\cdot(T\vec{U}) = \left(\frac{\gamma-1}{\epsilon}\right)\left[\dot{Q} + C_p T r_m - PT\vec{U}\cdot\nabla\left(\frac{R}{P}\right)\right] + \frac{P}{R}\frac{\partial R}{\partial t} - \frac{\gamma P}{\epsilon}\frac{\partial \epsilon}{\partial t} \tag{A.1-11}$$

Now expand

$$\nabla\left(\frac{R}{P}\right) = \frac{\nabla R}{P} - \frac{R}{P^2}\nabla P$$

and substitute this into equation (A.1-11) to get

$$\frac{\partial P}{\partial t} + \frac{\gamma R}{\epsilon}\vec{\nabla}\cdot(T\vec{U}) = \frac{(\gamma-1)}{\epsilon}\left[\dot{Q} + C_p T r_m - T\vec{U}\cdot\nabla R + \frac{RT\vec{U}}{P}\cdot\vec{\nabla}P\right] + \frac{P}{R}\frac{\partial R}{\partial t} - \frac{\gamma P}{\epsilon}\frac{\partial \epsilon}{\partial t} \tag{A.1-12}$$

The quantity RT/P is replaced by $1/\rho$ and a quantity α is defined as

$$\alpha = 1/(\rho\epsilon) \tag{A.1-13}$$

and is substituted into the equation. Recalling equation (A.1-9), the R term may be grouped to provide

$$\frac{\partial P}{\partial t} + \frac{\gamma R}{\epsilon}\vec{\nabla}\cdot(T\vec{U}) = \frac{(\gamma-1)}{\epsilon}\left[\alpha\epsilon\vec{U}\cdot\vec{\nabla}P + C_p T r_m + \dot{Q}\right] - \frac{\gamma P}{\epsilon}\frac{\partial \epsilon}{\partial t} + \frac{P}{R}\left(\frac{\partial R}{\partial t} + \vec{V}\cdot\nabla R\right) - \frac{\gamma P}{R}\vec{V}\cdot\vec{\nabla}R \tag{A.1-14}$$

The quantity R is the gas constant, therefore

$$\frac{\partial R}{\partial t} + \vec{V}\cdot\vec{\nabla}R = 0 \tag{A.1-15}$$

which also gives

$$\vec{V}\cdot\vec{\nabla}R = -\frac{\partial R}{\partial t}. \tag{A.1-16}$$

This information is put int equation (A.1-14) to produce

$$\frac{\partial P}{\partial t} + \frac{\gamma R}{\epsilon}\vec{\nabla}\cdot(T\vec{U}) = \frac{(\gamma-1)}{\epsilon}\left[\alpha\epsilon\vec{U}\cdot\vec{\nabla}P + C_p T r_m + \dot{Q}\right] - \frac{\gamma P}{\epsilon}\frac{\partial \epsilon}{\partial t} + \frac{\gamma P}{R}\frac{\partial R}{\partial t}. \tag{A.1-17}$$

Equation (A.1-17) is the basic energy equation as used in FLAG. The last step in creating the complete energy equation is to specify the heat transfer terms which constitute $\dot{Q}$.

There are four components of the heat transfer. Two of these components are the radiation heat transfer between the various elements inside the reactor, and the heat transfer between the particles and the gas. These are specified as S_{RAD} and S_{COND} respectively, and are given in detail in section 4.3. The third source of heat transfer is the conduction heat transfer through out the gas. This is given by Fourier's Law of Conduction as

$$\frac{\partial}{\partial x}\left(\Gamma \frac{\partial T}{\partial x}\right) + \frac{1}{r}\frac{\partial}{\partial r}\left(r\Gamma \frac{\partial T}{\partial r}\right) \qquad \text{(A.1-18)}$$

The last component of the heat Transfer is due to the energy released during a chemical reaction. Since there are a number of reactions going on at the same time, this component is the summation of all the reactions.

$$\sum \frac{\partial (h_i C_i)}{\partial t} \qquad \text{(A.1-19)}$$

Substituting the above terms into equation (A.1-17) produces the energy equation as given in Chapter II.

$$\frac{\partial P}{\partial t} + \frac{\gamma R}{\epsilon}\vec{\nabla}\cdot(T\vec{U}) = \frac{(\gamma-1)}{\epsilon}\left[\alpha\epsilon\vec{U}\cdot\vec{\nabla}P + C_p T r_m\right. \qquad \text{(2.1-5)}$$

$$\left. + \frac{\partial}{\partial x}\left(\Gamma\frac{\partial T}{\partial x}\right) + \frac{1}{r}\frac{\partial}{\partial r}\left(r\Gamma\frac{\partial T}{\partial r}\right) - \frac{\partial(h_i C_i)}{\partial t} + S_{RAD} + S_{COND}\right]$$

$$+ \frac{\gamma P}{R}\frac{\partial R}{\partial t} - \frac{\gamma P}{\epsilon}\frac{\partial \epsilon}{\partial t}$$

Appendix II

Listed below are the finite difference approximations for the various terms on the momentum and energy equations. It should be firmly kept in mind that these equations may appear substantially different within FLAG because they were transformed to be consistent with the philosophy of coding style used. Nevertheless, the equations within FLAG started with the approximations given below.

All of the terms in the finite difference approximations are averaged in one way or another. The three possible averages are:

Time average

$$\bar{A} = \left(\frac{A^{n+1}(t) + A^{n}}{2} \right) \qquad \text{(A.2-1)}$$

x-space average

$$\langle A \rangle_{ij} = \left(\frac{A_{i+\frac{1}{2},j} + A_{i-\frac{1}{2},j}}{2} \right) \qquad \text{(A.2-2)}$$

y-space average

$$\{ A \}_{i,j} = \left(\frac{A_{i,j+\frac{1}{2}} + A_{i,j-\frac{1}{2}}}{2} \right) \qquad \text{(A.2-3)}$$

$$\frac{\partial U}{\partial t} = \frac{U^{n+1}_{i,j+1/2} - U^{n}_{i,j+1/2}}{\delta t}$$

$$\frac{\partial(\alpha U U)}{\partial x} = \frac{\langle\langle\bar{\alpha}\rangle\bar{U}\rangle_{i+1/2,j+1/2}\langle\bar{U}\rangle_{i+1/2,j+1/2} - \langle\langle\bar{\alpha}\rangle\bar{U}\rangle_{i-1/2,j+1/2}\langle\bar{U}\rangle_{i-1/2,j+1/2}}{\Delta x_i} \quad \text{(A.2-4)}$$

$$\frac{1}{r}\frac{\partial(r\alpha U V)}{\partial r} = \frac{r_{j+1}\langle\{\bar{\alpha}\}\bar{V}\rangle_{i,j+1}\{U\}_{i,j+1} - r_j\langle\{\bar{\alpha}\}\bar{V}\rangle_{i,j}\{U\}_{i,j}}{r_{j+1/2}\,\Delta r_{j+1/2}}$$

$$\frac{\partial}{\partial x}\left(\Gamma\frac{\partial\alpha U}{\partial x}\right) = \frac{1}{\Delta x_i}\left[\Gamma_{i+1/2,j+1/2}\ \frac{\langle\bar{\alpha}\rangle_{i+1,j+1/2}\bar{U}_{i+1,j+1/2} - \langle\bar{\alpha}\rangle_{i,j+1/2}\bar{U}_{i,j+1/2}}{\Delta x_{i+1/2}}\right. \quad \text{(A.2-5}$$

$$\left. - \Gamma_{i-1/2,j+1/2}\ \frac{\langle\bar{\alpha}\rangle_{i,j+1/2}\bar{U}_{i,j+1/2} - \langle\bar{\alpha}\rangle_{i-1,j+1/2}U}{\Delta x_{i-1/2}}\right]$$

$$\frac{1}{r}\frac{\partial}{\partial r}\left(r\Gamma\frac{\partial\alpha U}{\partial r}\right) = \frac{1}{r_{j+1/2}\,\Delta r_{j+1/2}}\left[r_{j+1}\Gamma_{i,j+1}\ \frac{\langle\bar{\alpha}\rangle_{i,j+3/2}\bar{U}_{i,j+3/2} - \langle\bar{\alpha}\rangle_{i,j+1/2}\bar{U}_{i,j+1/2}}{\Delta r_{j+1}}\right.$$

$$\left. - r_j\Gamma_j\ \frac{\langle\bar{\alpha}\rangle_{i,j+1/2}\bar{U}_{i,j+1/2} - \langle\bar{\alpha}\rangle_{i,j-1/2}\bar{U}_{i,j-1/2}}{\Delta r_j}\right] \quad \text{(A.2-6}$$

$$\varepsilon\frac{\partial P}{\partial x} = \langle\varepsilon\rangle_{i+1/2}\left[\frac{P^{n+1}_{i+1/2,j+1/2} - P^{n+1}_{i-1/2,j+1/2} + P^{n}_{i+1/2,j+1/2} - P^{n}_{i-1/2,j+1/2}}{2\,\Delta x_i}\right] \quad \text{(A.2-}$$

$$\frac{\partial V}{\partial t} = \frac{V^{n+1}_{i+1/2,j} - V^{n}_{i+1/2,j}}{\delta t} \qquad \text{(A.2-8)}$$

$$\frac{\partial \alpha U V}{\partial x} = \frac{\{\langle\bar{\alpha}\rangle \bar{U}\}_{i+1,j}\langle\bar{v}\rangle_{i+1,j} - \{\langle\bar{\alpha}\rangle \bar{U}\}_{i,j}\langle\bar{v}\rangle_{i,j}}{\Delta x_{i+1/2}}$$

$$\frac{1}{r}\frac{\partial (r \alpha V V)}{\partial r} = \frac{r_{j+1/2}\{\{\bar{\alpha}\}\bar{v}\}_{i+1/2,j+1/2}\{\bar{V}\}_{i+1/2,j+1/2} - r_{j-1/2}\{\{\bar{\alpha}\}\bar{v}\}_{i+1/2,j-1/2}\{\bar{V}\}_{j-1/2}}{r_j \Delta r_j} \qquad \text{(A.2-9)}$$

$$\frac{\alpha' W V'}{r} = \frac{\{\overline{\alpha W}\}_{i+1/2,j}\{\bar{w}\}_{i+1/2,j}}{r_j} \qquad \text{(A.2-10)}$$

$$\frac{\partial}{\partial x}\left(\Gamma \frac{\partial \alpha V}{\partial x}\right) = \frac{1}{\Delta x_{i+1/2}}\left[\Gamma_{i+1,j}\frac{\{\bar{\alpha}\}_{i+3/2,j}\bar{V}_{i+3/2,j} - \{\bar{\alpha}\}_{i+1/2,j}\bar{V}_{i+1/2,j}}{\Delta x_{i+1}}\right. \qquad \text{(A.2-11}$$

$$\left. - \Gamma_{i,j}\frac{\{\bar{\alpha}\}_{i+1/2,j}\bar{V}_{i+1/2,j} - \{\bar{\alpha}\}_{i-1/2,j}\bar{V}_{i-1/2,j}}{\Delta x_i}\right]$$

$$\frac{1}{r}\frac{\partial}{\partial r}\left(r\Gamma\frac{\partial \alpha V r}{\partial r}\right) = \frac{1}{r_j \Delta r_j}\left[\frac{\Gamma_{i+1/2,j+1/2}}{r_{j+1/2}}\frac{\{\bar{\alpha}\}_{i+1/2,j+1}\bar{V}_{i+1/2,j+1}\bar{r}_{j+1} - \{\bar{\alpha}\}_{i+1/2,j}\bar{V}_{i+1/2,j}r_j}{\Delta r_{j+1/2}}\right.$$

$$\left. - \frac{\Gamma_{i+1/2,j-1/2}}{r_{j-1/2}}\frac{\{\bar{\alpha}\}_{i+1/2,j}\bar{V}_{i+1/2,j}r_j - \{\bar{\alpha}\}_{i+1/2,j-1}\bar{V}_{i+1/2,j-1}r_{j-1}}{\Delta r_{j-1/2}}\right] \qquad \text{(A.2-12)}$$

$$\varepsilon\frac{\partial P}{\partial r} = \{\varepsilon\}_{i+1/2,j}\left[\frac{P^{n+1}_{i+1/2,j+1/2} - P^{n+1}_{i+1/2,j-1/2} + P^{n}_{i+1/2,j+1/2} - P^{n}_{i+1/2,j-1/2}}{2\Delta r_j}\right] \qquad \text{(A.2-13}$$

Energy equation reformated in terms and pressure - Main equation in FLOW

$$-AR_{L+1/2\,J+1/2}\,\delta P_{L+3/2\,J+1/2} - AL_{L+1/2\,J+1/2}\,\delta P_{L-1/2\,J+1/2} - AT_{L+1/2\,J+1/2}\,\delta P_{L+1/2\,J+3/2} \quad \text{(A.2-}$$

$$-AB_{L+1/2\,J+1/2}\,\delta P_{L+1/2\,J-1/2} + ACO_{L+1/2\,J+1/2}\,\delta P_{L+1/2\,J+1/2} =$$

$$\left[\frac{RHS}{1 - GAMMAI\,(CSCOND + CSRAD)}\right]_{L+1/2\,J+1/2}$$

$$AR = AR' * ZZ \qquad AL = AL' * ZZ \qquad AT = AT' * ZZ \qquad AB = AB' * ZZ$$

$$ACO = 1 + AR + AL + AT + AB$$

$$ZZ = \frac{1}{1 - GAMMAI\,(CSCOND + CSRAD)} \qquad \text{(A.2-15}$$

CSCOND = Implicit conduction term
CSRAD = Implicit radiation term
GAMMAI = $\delta t(\gamma - 1)/\varepsilon$

$$AR'_{L+1/2\,J+1/2} = \frac{\delta t\,\gamma RT_B}{2\Delta x_{L+1/2}\,\varepsilon_{L+1/2\,J+1/2}}\,AR''_{L+1/2\,J+1/2} \qquad \text{(A.2-1E}$$

$$AL'_{L+1/2\,J+1/2} = \frac{\delta t\,\gamma RT_B}{2\Delta x_{L+1/2}\,\varepsilon_{L+1/2\,J+1/2}}\,AL''_{L+1/2\,J+1/2} \qquad \text{(A.2-17}$$

$$AT^{\bullet}_{i+1/2,\,j-1/2} = \frac{\delta t\,\gamma R T_B}{2\Delta r_{j-1/2}\, r_{j-1/2}\, \varepsilon_{i+1/2,\,j-1/2}}\, AT^{\bullet\bullet}_{i+1/2,\,j-1/2} \qquad \text{(A.2-18)}$$

$$AB^{\bullet}_{i+1/2,\,j-1/2} = \frac{\delta t\,\gamma R T_B}{2\Delta r_{j-1/2}\, r_{j-1/2}\, \varepsilon_{i+1/2,\,j-1/2}}\, AB^{\bullet\bullet}_{i+1/2,\,j-1/2} \qquad \text{(A.2-19)}$$

$$AC^{\bullet} = 1 + AR^{\bullet} + AL^{\bullet} + AT^{\bullet} + AB^{\bullet}$$

$$AR^{\bullet\bullet}_{i+1/2,\,j-1/2} = \frac{\delta t\, F_{DU_{i+1,\,j-1/2}} \langle \varepsilon \rangle_{i+1,\,j-1/2}}{2\Delta x_{i-1}} \qquad \text{(A.2-20)}$$

$$AL^{\bullet\bullet}_{i+1/2,\,j-1/2} = \frac{\delta t\, F_{DU_{i,\,j-1/2}} \langle \varepsilon \rangle_{i,\,j-1/2}}{2\Delta x_{i}} \qquad \text{(A.2-21)}$$

$$AT^{\bullet\bullet}_{i+1/2,\,j-1/2} = \frac{\delta t\, F_{DV_{i+1/2,\,j+1}} \langle \varepsilon \rangle_{i+1/2,\,j+1}\, r_{j+1}}{2\Delta r_{j+1}} \qquad \text{(A.2-22)}$$

$$AB^{\bullet\bullet}_{i+1/2,\,j-1/2} = \frac{\delta t\, F_{DV_{i+1/2,\,j}} \langle \varepsilon \rangle_{i+1/2,\,j}\, r_{j}}{2\Delta r_{j}}$$

F_{DU} = Implicit axial drag (A.2-23)

F_{DV} = Implicit radial drag

$$RHS = \left.\frac{\partial UT_B}{\partial x}\right|^n + \left.\frac{1}{r}\frac{\partial (rVT_B)}{\partial r}\right|^n \qquad (A.2\text{-}24)$$

The formal development of equation A-14 produces a large number of terms in RHS. However, as explained in Chapter IV all the terms except the two listed above have been dropped from the equation.

*U. S. GOVERNMENT PRINTING OFFICE: 1985-544-063/10495

END OF PAPER